REVIEWS OF
MODERN PHYSICS

VOLUME 9 JULY, 1937 NUMBER 3

Nuclear Physics

C. Nuclear Dynamics, Experimental*

M. STANLEY LIVINGSTON AND H. A. BETHE†
Cornell University, Ithaca, New York

TABLE OF CONTENTS

XV. Experimental Methods

IN this discussion of experimental methods the field will be divided into three sections, dealing respectively with the sources of nuclear projectiles, the properties of nuclear radiations and the detecting and recording instruments and methods.**

§92. Sources of Nuclear Projectiles

Artificial disintegration of elements was first accomplished by Rutherford in 1919 using the high speed alpha-particles from Ra C′ as projectiles, and more than 10 years passed before any other projectiles were considered. By 1930 several laboratories were working on the development of high voltage apparatus to produce high speed ions artificially. It was expected that energies sufficient to penetrate the force fields of nuclei would be required, i.e., several million volts, and the proton was considered the most likely possibility as a projectile. At this stage Gamow (G7) and Condon and Gurney (C32) introduced the quantum mechanical interpretation of natural α-decay according to which there exists a certain probability of penetration of a potential barrier by particles with considerably less energy than required to go over the top of the barrier. Cockcroft and Walton (C18) realized that this might make disintegrations possible with relatively low energy protons and performed the first successful experiment resulting in the disintegration of Li (C19). Lawrence, Livingston and White (L11) immediately checked these observations with the 1 MV protons then available with the magnetic resonance accelerator, and others soon followed, some using much lower proton energies and proving the validity of the hypothesis.

At the present time the projectiles that have been successfully used for nuclear disintegration are: the *alpha-particle*, artificially accelerated *protons* and *deuterons*, *neutrons* occurring as products of other nuclear reactions, *gamma-rays* and accelerated ions of *He* and *Li*.

A. Natural radioactive sources

Alpha-particles are obtained from high intensity prepared sources of many radioactive materials. Of considerable importance has been the use of polonium (Ra F) since this material can be electrochemically separated from parent materials which are beta- and gamma-active, has no radioactive product and very weak gamma-radiation, and so supplies a pure source of alphas. They have a mean range of 3.805 cm at 15°C and 76 cm Hg pressure and a corresponding energy of 5.303 MV (R23). Higher energy alphas, such as those from Ra C′ with a mean range of 6.87 cm and an energy of 7.6802 MV (B60) have been used for much of the work on disintegration. Lower energies can be obtained by the use of absorbing material, either in the form of thin foils or as gases. The range-energy relations for alpha-particles are well known, both experimentally and theoretically (§95), and also the straggling after absorption (§97), so that the homogeneity of the alpha-beam is known for all energies. The ranges have been measured accurately with ionization chambers (L23) and the energies by magnetic analysis (B60, R23). In addition, alpha-particles have been used in experiments on nuclear scattering (Chap. XII), the results of which can be interpreted to show the extent and something of the character of the nuclear force fields.

The advantages due to the simplicity of naturally radioactive sources are unmistakable but the technique has always been handicapped by the low intensities available. Sources have seldom been used which yield more than 1.8×10^9 alphas/second (equivalent to 500 millicuries of radon), and observations must be made on small numbers of disintegration particles over extended times.

The *gamma-radiation* from naturally radioactive materials has been, up to a very recent date, the only source of photons of energies

* Part A of this report ("Stationary States of Nuclei," by H. A. Bethe and R. F. Bacher) appeared in these Reviews in the issue of April, 1936; part B ("Nuclear Dynamics, Theoretical") in the April, 1937 issue. The present part contains also the references to part B while part A contains its own reference section.

† The authors are greatly indebted to Drs. E. J. Konopinski and M. E. Rose for help in computing tables, drawing figures and especially for a critical revision of the manuscript.

** The descriptive material of this chapter is of necessity limited to include only a few of the many experimental devices and techniques now in use in nuclear physics laboratories. The discussion deals with those considered to be the most representative and those which have been most productive of experimental data.

greater than 1 MV. The commonly known radium source has a radiation consisting of many lines with an average energy of 1.5 MV and so is considerably less useful than Th C″ which has a single strong line of 2.62 MV and relatively small intensities of other energies. Other radioactive materials have their characteristic rays, although in general with less intensity due to the small amounts of radioactive material concentrated in units.

Natural gamma-ray energies have been accurately measured through the β-ray lines due to internal conversion (cf. §88). Unfortunately this method cannot be applied to the gammas from disintegration processes in light elements and other techniques are required. In §93 these methods are discussed in some detail.

As disintegrating agents natural gamma-rays have been successful for only two targets, H^2 (C9) and Be^9 (S28), requiring energies of greater than 2.20 and 1.74 MV in the two cases. Similar disintegrations of other elements require higher energies than are available from natural sources (see §103). Certain disintegration processes produced with high speed ions in apparatus to be described later yield gamma-rays with energies up to 17.5 MV, usually either monochromatic or having a definite line structure. Another promising source is from certain of the induced radioactive materials, such as Na^{24}, in which the ejected electron is accompanied by gamma-radiation of about 3 MV, and already produced with intensities equal to weak radioactive sources. X-rays of about 1.5 to 2.0 MV energy have been used to produce disintegration of Be (B49), but higher energies are not easily obtained.

Neutrons are emitted as disintegration products of certain light elements such as Be^9, Li^7 and B^{11} on alpha-particle bombardment. They are also ejected from H^2 and Be^9 by gamma-radiation. In fact the discovery of the neutron occurred as a result of the studies of the highly penetrating radiations from Be on alpha-bombardment. The neutrons from this reaction have a wide spread of energies ranging up to 13.0 MV for Rn alphas and with an intensity maximum at about 4.8 MV (D20) (see §99). A standard type of radioactive neutron source is a sealed capsule containing finely divided Be and Rn gas, which is alpha-active with a half-life of 3.8 days. With 1 millicurie of Rn about 27,000 neutrons per second are obtained (A11) and this yield varies roughly with the 3/2 power of the energy of the alpha if obtained from other sources than Rn. Gamma-rays from the Rn decay products accompany the neutrons from this source and it must be properly shielded in experiments where such gamma-rays would bias the interpretation of the results. Po is sometimes used where such radiation is disadvantageous. For many experiments the small size of such a source makes observations exceedingly simple and effective due to the large solid angle available for targets.

Alphas on B produce neutrons of a different energy distribution, in this case with a maximum intensity at <1 MV and an upper limit of 4.2 MV (M34). Sources of neutrons of different energies are valuable for analyzing certain processes and especially in determining reaction cross sections as a function of energy. The inhomogeneity of neutron energies from the reactions noted is of considerable disadvantage, and in order to avoid this use has been made of neutrons from other processes in which energies are homogeneous. Chief of these is the reaction of deuterons on deuterium, to be discussed in detail later.

B. Condenser-rectifier voltage multiplier

Of the several types of high voltage ion sources in use for nuclear research at present the first to produce disintegrations and explore the field of proton-produced reactions was that of Cockcroft and Walton (C22) in the Cavendish Laboratories, where earlier Rutherford had opened the door to such research with his alpha-produced disintegrations. It has undergone many improvements since 1932 but still embodies the voltage-multiplier circuit originally used. In this design the "voltage doubling" principle of charging condensers in parallel and discharging in series across a load has been extended to triple the voltage output from a transformer of standard design supplying about 250 kv of 60 cycle alternating current. The use of rectifier tubes as switches provides the method with a means of charging the condensers 60 times a second and supplies an essentially constant direct potential of about 800 kv across the final bank of 3 condensers. The condensers are mounted on suitable

insulating supports. The rectifier tubes are of special design and are continuously pumped, with the filaments heated by insulated transformers. In operation the transformer charges a feeding condenser through a pair of rectifiers which are conducting during one half-cycle. In the succeeding half-cycle these rectifiers are nonconducting and the feeding condenser divides its charge with another through a second set of rectifiers, and so on until all condensers are fully charged.

The high voltage discharge tube in which the ions are accelerated is in two sections for voltage distribution. (Single sections have never been operated satisfactorily with potentials above 400 kv.) The tube was originally built of large glass cylinders but these have been replaced with porcelain (C25); joints are sealed with wax and the chamber is continuously pumped. Canal-ray sources of hydrogen ions are placed at the high potential end of the tube and the ions are accelerated through large tubular electrodes and strike a target placed at the grounded end. The original source produced up to 10 microamperes of ions at 800 kv but recent improvements (C25) have increased this yield to 100 microamperes. Voltages are determined with sphere-gap sparking measurements and although calibration details are not published they are probably accurate to better than 5 percent. A magnetic deflection chamber has been added (C27) to separate the H^1 and H^2 focal spots of the ion beam and these measurements are used to check the sphere gap voltage calibration. Fluctuations in the supply voltage are less than 20 kv, introducing an error of 2.5 percent. The focal spot on the target is 1 cm in diameter and with the magnetic deflecting field the ion energies can be considered as essentially homogeneous.

C. Cascade transformer

The development of high voltage transformers for transmission line testing and as power sources for deep therapy x-ray tubes led to the "cascade transformer" potential source used by Lauritsen and Crane and their collaborators (L9) at the Kellogg Radiation Laboratory of the California Institute of Technology in Pasadena. Three transformers are used, each producing about 350 kv. They are arranged in "series"; the primaries of the second and third transformers are activated from low voltage tertiaries at the high potential ends of the high voltage windings of the first and second transformers respectively. The second and third transformers are mounted on platforms of porcelain insulators so they may be operated at 350 and 700 kv above ground potential. This yields a 60-cycle voltage of about 1.0 MV root mean square between ground and the high end of the third transformer. The alternating character of the voltage gives potentials both positive and negative with respect to ground and so can be used to accelerate either electrons or positive ions, depending on the type of source used. The source supplies the rectification and when used with positive ions the stray electrons accelerated in the odd half-cycles give a small intensity of x-rays from the target.

The discharge tube is in two sections, using two standard conical transformer bushings of porcelain of the type used on commercial 220 kv transformers and having a 750 kv sparkover limit. The porcelains are sealed end on end with wax to metal plates which also support the interior accelerating tubes, and are evacuated with high speed pumps. The accelerating electrodes are tubular and re-entrant so that the porcelain wall is protected from discharge originating in the ion beam. The intermediate electrode is connected to the mid-point of the voltage supply for distribution of potential. Ions are supplied by a hydrogen discharge tube at the high potential end of the accelerator and are focused by the accelerating voltage to a spot of less than 1.2 cm diameter on the target. Steady currents of as much as 20 microamperes of hydrogen ions are obtained up to 900 kv, and 100 microamperes have been obtained for short time intervals synchronized with a cloud chamber for certain observations. It is to be expected that different types of ions, such as H^1, H_2 and H^2 will be accelerated simultaneously and that a spread of energies will result due to the sinusoidal character of the voltage supply. Magnetic focusing is not used but tests indicate that there is a considerable predominance of high energy ions, and that with proper care in purity of gases entering the source the light and heavy hydrogen beams can be kept relatively pure.

Maximum ion energies are determined by spark gap measurements of voltage, based on the Westinghouse high voltage calibrations and are subject to some criticism. Corona from terminals and wires at this high potential (easily visible) introduces fluctuations estimated to be about 5 percent at 900 kv but considerably less for lower voltages. Data of Hafstad and Tuve (H2) on the resonance values of proton energies in the "simple capture" by C do not check with similar values given by Lauritsen, showing a discrepancy between the voltage calibrations of the two laboratories by as much as 30 percent. Many experiments, however, do not require an accurate voltage calibration, and such is the case for much of the published data from this laboratory. Most voltage excitation functions of nuclear processes are steeply-rising curves with increasing voltage and the experimenters take advantage of this fact by subtracting out the small effects due to ions of less energy or of complex character.

The target is ideally located at the end of a long tube through which the focused ion beam travels, and can readily be shielded with lead or paraffin. Due to the method of locating the target this type of apparatus has been used more successfully than other types for measurement of emitted gamma-radiation.

A recent installation by Crane (C52) yields 1 MV in 5 sections and with an ion intensity of 250 microamperes.

D. Electrostatic generator

A simplified method for the production of high electrostatic voltages involving a large sphere charged by a rapidly moving belt was developed by Van de Graaff from a small apparatus capable of delivering a few microamperes at 80,000 volts (V4) to the present Round Hill installation (V1) yielding several milliamperes at 5 MV. During this time a paralleling development of the application of this method to discharge tubes has been carried on by Tuve, Hafstad and Dahl (T16) in the Bureau of Terrestrial Magnetism of the Carnegie Institution at Washington. They have placed the emphasis on the development of a discharge tube and other operational details with the result that positive ion currents of 20 microamperes at energies up to 1.2 MV have been available for experiments. With this technique a large sphere, or rather a cylinder with spherical caps over the ends, of 2 meters diameter, is charged by means of a belt on which charge is sprayed by a high voltage rectifier unit. Insulation for the high potentials is achieved by mounting the sphere on Textolite supports. The multiple-section discharge tube contains about 14 hollow cylindrical electrodes supported at equal intervals along the length of the glass tube wall and each equipped with an external doughnut-shaped corona shield. These shields are varied in curvature and points are adjusted between them where needed to distribute the sphere voltage uniformly between the electrodes. This design protects the discharge tube and the voltage limit is set by the corona from the surface of the sphere or by sparks down the belt or across the gaps of minimum clearance.

When used to accelerate positive ions the source is placed in the sphere which is maintained at a high positive potential by spraying positive charge on the belt. Since it is possible to utilize the interior as well as the exterior curvature of the sphere for field distribution a smaller sphere is mounted concentric with and inside the 2 meter one and is maintained at a positive potential with respect to it. Two accelerating sections are placed between the two shells and by means of corona points which are variable by means of long insulating strings the potentials between these two sets of electrodes can be varied to adjust the focusing of the ion beam. The hydrogen discharge tube used as a source of ions is inside the central sphere where gas flow and potentials are also regulated by strings. A generator to supply the power for operation of the discharge is driven by an auxiliary belt.

The focusing of the ions is determined chiefly by the first two accelerating stages mentioned above, and is maintained down the long column of electrodes by the accelerating fields between them. This produces a focal spot at the target of 3 to 4 mm in diameter. A magnetic field deflects the beam, analyzes it into the component ions and maintains the energy to within a maximum spread of 20,000 volts. Both H^1_2 and H^2 ions reach the target when the mass 2 spot is in focus and so a subtraction technique is required to

analyze results for mixed gases. Due to irregularities in the corona discharge and other conditions the high voltage itself has a fluctuation of about 20,000 volts, and this varies greatly with changing atmospheric conditions.

Proton energies were at first determined by direct range measurements on the primary beam for energies above 500 kv. The ions passed through a thin foil and out into air where the range was measured visually or electrically. In the first instance the blue ionization glow was found to have a relatively sharp terminus, enabling estimates of range to within 1 or 2 mm. The voltage fluctuations of the source resulted in a flicker of intensity in the last few mm of range. A shallow (1 mm deep) ionization chamber and electrometer were used to measure the range electrically, but due to the straggling of the ions and the extreme sensitivity of the electrical method a range was observed of some 2 mm greater than the visual one. Due to doubts as to the reliability of the then existing range-energy relations an assumed (H4) 10 mm range for 500 kv and 36 mm for 1200 kv protons was chosen in stating ion energies up to August, 1935. More exact range-energy relations are given in §95 and where used later in this discussion the data from this laboratory are corrected by the proper factors. A fair estimate of the probable error in the measurement of proton ranges is 2 mm, equivalent to 50 kv at 1 MV and 80 kv at 500 kv. Below 500 kv sphere gap readings were used to calibrate voltages and possible errors in estimating the potential between inner and outer spheres result in an error which may be as high as 50 kv. A recent advance (H5) (June, 1936) in the accuracy of voltage calibration has resulted from current measurements through standard high resistances. The present calibrations, which check closely with the range-energy curves of §95 are 23 mm for 1.0 MV and 29 mm for 1.2 MV protons.

A modification by Herb, Parkinson and Kerst (H28) consists of the use of higher pressures to increase the voltage limits of the electrostatic generator. The cylindrical generator is mounted inside a tank 20 ft. long and $5\frac{1}{2}$ ft. in diameter which contains air at 7 atmospheres pressure. Ions have been obtained of up to 2.16 MV energy through a discharge tube extending longitudally along the cylinder. The success of this method suggests that it will be of importance for future high voltage experiments.

E. Low potential-high intensity discharge tubes

Certain disintegration reactions in light elements such as the disintegration of Li by protons can be studied with relatively low energy ions if sufficient intensity is available. Several laboratories have developed low voltage techniques for this purpose, of which that of Oliphant (O2) and his collaborators is an example. An intense discharge tube source yields 100 microamperes of protons or deuterons which are accelerated to 200 kv in a single stage tube supplied by a voltage doubler circuit and a 100 kv transformer. A 90° magnetic analyzer separates ions of different masses and energies. The voltage standard is a calibrated spark-gap, checked by the magnetic deflection of the ions, and is accurate to better than 1 percent. The voltage output was later raised to 400 kv by changes in the apparatus (O7) and the intensity increased to 200 microamperes.

The value of this type of apparatus lies in the accuracy with which the energies of the bombarding projectiles can be determined. A 1 percent error at 100,000 volts represents only 0.000001 mass units, negligible in comparison with other errors. So reaction energies can be obtained to within the accuracy of the measurements of the energies of the ejected particles. An added virtue is the freedom from scattered primary ions due to their very short range, which means that very short range groups of product particles can be detected. The method is of considerable importance in accurate studies of reaction energies. It is also valuable as a means of obtaining the neutrons of homogeneous energy resulting from the reaction $H^2+H^2\rightarrow He^3+n^1$. An apparatus developed by Ladenburg, *et al.* (L1), produces as many neutrons as a 260 mC Rn-Be source, at 200 kv and 100 microamps. Zinn and Seeley (Z2) use 4 milliamperes of ions at 60 kv to get neutrons equivalent to 500 mC of Rn and Be.

Extremely low voltage disintegration of lithium has been realized by Traubenberg, *et al.* (T12) who observed disintegrations by protons of as low as 13 kv, using ion currents of 1 milli-

ampere. Burhop (B68) has disintegrated Li and H^2 with 8 kv ions.

Zeleny (Z1) and his associates at Yale University have accelerated Li ions to such energies (240 kv) that they yield alphas when bombarding hydrogen. This is the same reaction as is observed when protons bombard a lithium target, and yields can be calculated from the relative velocities of the two ions.

F. The magnetic resonance accelerator

The highest energies obtained by artificial acceleration of ions have been achieved with the magnetic resonance accelerator or "cyclotron" of Lawrence and Livingston (L14) of the Radiation Laboratory of the University of California. In this method ions are brought to high energies not by high voltages but by many successive small accelerations in a low voltage, high frequency field with which they are in resonance. The ions revolve in a series of increasing semi-circles in a large and uniform magnetic field and receive an increment of energy each time they cross a diametral gap between two semi-circular hollow electrodes on which the high frequency is impressed. The angular velocity of ions moving in a uniform magnetic field is constant for all energies, which means that the time for the traversal of a circular path is constant, regardless of the radius of the path. If the magnetic field is such that this time interval is the period of the imposed high frequency oscillations the ions remain in "resonance" until they achieve an energy determined only by the strength of magnetic field and the radius of the final path. Ions are produced near the center of the chamber in hydrogen or deuterium gas by an electron beam from a filament. The magnetic field collimates the electron beam so that it is concentrated on the region between the electrodes where the source is desired. The ions receive about 100 to 200 accelerations of 30 to 60 kv each to reach the final energy, which is about 6 MV for H^2 atomic ions (deuterons). The normal intensities are 10 to 20 microamperes (L18), but recent changes involving increased electrode aperture have resulted in as much as 50 microamperes at somewhat lower energy (4 to 4.5 MV). A magnetic analysis of mass and velocity of the ions is inherent in the resonance principle, so only ions having the same e/m can be accelerated. H_2 and H^2 ions have the same e/m but widely different mean free paths, and if the gas pressure in the chamber is high enough all the molecular ions will be absorbed and only deuterons will reach the collector, so purity of gases is not essential. The energy spread is equal to twice the voltage between the electrodes and can be made as small as desired at the expense of beam intensity. In practice this spread is usually less than 2 percent of the ion energy. This condition is obtainable only with small sources and uniform magnetic fields; without these features much wider energy distributions are sometimes observed and must be corrected by "shimming" (see below).

Energies are calculable from the resonance value of magnetic field and the radius of the final path and are accurate to the limits stated above only if the ion paths are concentric about the center of the chamber. Iron "shims" near the periphery are used to increase the region of uniformity of the magnetic field. They also help to correct for any asymmetrical properties of the magnetic field which would result in a migration of the ion paths and so a lower final energy. Due to this feature energies are usually determined by the range of the ion beam in air, which involves a possible error of about 2 mm. In the original arrangement the focal spot was about 4 by 6 mm and targets were located opposite a large observation port just inside the edge of the magnetic field. For experiments on induced radioactivity the re-entrant observation port was placed deep enough to allow the ions to pass inside through a foil mounted on the side of the port; targets were activated at atmospheric pressure and removed for observation.

Recent improvements in the accelerating chamber (L18) allow the ion beam to be brought out tangentially by means of electrostatic deflecting fields. The beam passes through a thin window and emerges into the air where it can be observed visually as a blue ionization glow having a range of some 26 cm (6 MV). Still further development (A6) has resulted in bringing a fraction of this beam through an evacuated tube to a point 6 feet from the cyclotron.

Several other installations are now completed

or in progress. Small compact models yielding 1 to 2 MV are in operation at Cornell University (L31) and the University of Illinois (K26). A record high voltage of 6.7 MV has been obtained at the University of Michigan and results of several experiments have been reported (C36). Preliminary experiments using cyclotrons have recently been reported from the University of Rochester (B4a) and Princeton University (W13a, D29). Several other cyclotrons in this country and abroad are nearing completion.

Very intense yields of neutrons are obtained from high voltage apparatus by bombarding Li, Be, B, etc., by high speed deuterons. These processes have probabilities proportional to the intensity of the deuteron beam but varying approximately with the 3/2 power of the energy above a characteristic threshold value in each case, so the most intense neutron sources have been obtained with the magnetic accelerator. An estimate made by Lawrence of the total number of neutrons is 10^9 to 10^{10} per second.[1]

G. Other sources—general

Several other types of apparatus for accelerating ions have been successful in disintegration experiments to some extent, and others are at present under development. The "linear accelerator" of Sloan and Coates (S13) produced 2.8 MV Hg^+ ions by a radiofrequency resonance method similar to that of the magnetic accelerator, but no disintegrations were observed. An application of this method to Li ions by Kinsey (K13) has resulted in the observation of the $Li^7+H^1 \rightarrow He^4+He^4$ reaction. Van Atta, *et al.* (V2) are at present engaged in developing a discharge tube for the large Van de Graaff generator (V3). A surge generator supplying a low vacuum discharge tube developed by Brasch, *et al.* (B48) yields great intensities of a variety of ions but has not been brought under control except for disintegrations by x-rays as previously indicated. Beams and Trotter (B6) have accelerated protons to over a million volts energy in an apparatus utilizing transmission lines to supply the accelerating electrodes, but intensities are still too small for experiments. The "resonance transformer" x-ray tube, developed by Sloan (S14, S24) has been applied by Livingood and Snell (L25) to the search for radioactivity produced by 0.8 MV electrons with no positive results.

§93. Properties of Nuclear Radiations

A. Alpha-particles

The methods whereby alpha-particles are used as projectiles for disintegration experiments have been discussed in §92. When occurring as products of nuclear reactions they are detected through the dense ionization they produce. Several instruments such as the cloud chamber and the pulse amplifier utilize this property and are sufficiently sensitive to detect individual particles (§94).

The specific ionization varies with velocity (the Bragg curve); about 2500 ion pairs/mm being formed by alphas having a residual range of 5 cm and 7000 ion pairs/mm at 3 mm from the end of the range. Alphas have been observed having ranges from a few mm to 14 cm in air at standard conditions. The range-energy relation is known to great accuracy (see Figs. 29(a)(b), §95), especially in the region calibrated by alphas of known energy from natural sources. Observations are usually made on the extrapolated range and are reduced to mean range for energy determinations (§97).

B. Protons

Protons produce less ionization along their tracks than alphas, about 32 percent of the specific ionization of the alpha at the maxima of the Bragg curves and 25 percent for residual ranges of more than 2 cm. This results in the cloud chamber in a fainter track, and is observed in the ionization chamber as a smaller current pulse for the same depth of penetration, making it possible to distinguish the two particles.

[1] It seems important to point out to prospective experimenters in the field that these intensities of neutrons are sufficient to produce harmful biological effects. The high concentration of hydrogen makes the body an unusually efficient absorber of neutrons and the ionization produced by recoil atoms has already been shown to have biological effects similar to those from gamma-radiation. Quantum-for-quantum the neutrons are more effective than gammas. The neutrons obtained from the magnetic accelerator are found to have the biological effectiveness of 100 g of radium. Thick baricades of hydrogenous materials are required to reduce neutron intensities materially (6 cm of paraffin absorbs about $\frac{1}{2}$ the fast neutrons), and the experimenter should arrange to stay at considerable distances from the apparatus.

Groups of protons are separated by observing only the stronger pulses in the amplifier, equivalent to counting only those protons which have the maximum of the Bragg curve within the ionization chamber. Protons have much longer ranges than alphas, those observed ranging from a few cm to as much as 200 cm in air, which last is equivalent to 13.65 MV. The range is again usually observed as the extrapolated value; see §97 for the relation between mean and extrapolated ranges. The range energy relation, as inferred from the alpha-particle curve, is given in Figs. 30(a)(b)(c) of §95. Accurate experimental determinations are scarce, but the evidence that does exist indicates that the relation is essentially correct.

C. Deuterons

Deuterons are of chief interest as projectiles, being accelerated to high speeds by several types of apparatus, as discussed in §92. In the one reaction yielding deuterons as products ($Be^9+H^1 \rightarrow Be^8+H^2$) they could not be separated from alphas in deflection experiments due to their having the same e/m. Identification came through the observation of their lower specific ionization. The specific ionization is about 4/3 that for protons and about 1/3 that for alpha-particles for the same residual range. The range of a deuteron of energy E is twice that for a proton of half the energy. Using this relation deuteron energies can be determined from the proton range-energy curves of §95. (Figs. 30(a) (b) (c).)

D. Neutrons

Neutrons, having no charge, produce no effects in electrical counting instruments. They are detected either through recoil with atoms to form charged ions or through the disintegrations they produce.

Recoil protons from hydrogen have energies ranging up to the full neutron energy, depending upon the angle of projection. Only those projected in the direction of the incident neutrons are satisfactory for measurements, since neutrons may be scattered through large angles by adjacent heavy materials and yet retain a large share of their energy. Such neutrons, on recoil, will give high energy protons which, if interpreted as coming from nonscattered neutrons, will indicate excessively high energies. This feature is no doubt responsible for many erroneous measurements indicating high neutron energies. When care is taken on this point the recoil distribution-in-range curves show definite group structure and reasonably sharp endpoints, but with somewhat less resolution than equivalent curves for a proton beam. In hydrogen or methane-filled cloud chambers the direction of the individual protons may be ascertained and this condition fulfilled.

With a paraffin layer in front of a shallow ionization chamber about 3.7 protons are projected from the surface per 1000 neutrons of 5 MV energy. The efficiency is approximately proportional to the energy; 0.35 proton results from 1000 neutrons of 0.5 MV energy. The paraffin should be equal in thickness to the equivalent range of the protons produced, for highest intensity; for best resolution of groups the paraffin should be thin compared to the proton range.

An alternative method of measuring neutron energies is through recoil with other atoms, such as C, O or N (F8). This is seriously handicapped by the uncertain range-energy relations for such particles, and data will probably serve best as calibrations of such relations when neutron energies are better known.

The other general property through which neutrons are observed and measured is the disintegration of certain target elements to yield observable radiations. Three types of disintegration serve this purpose; the n-α reaction is known to occur with slow neutrons only in Li and B, the n-p type reaction is endoergic except for N, while the simple capture reaction is always exoergic and often results in induced radioactivity.

The cross section for the $Li^6+n^1 \rightarrow He^4+H^3$ reaction is about 900×10^{-24} cm^2, that for the $B^{10}+n^1 \rightarrow Li^7+He^4$ process is 3000×10^{-24} cm^2. The range of the H^3 from Li is about 6 cm, and the He^4 from B only 0.8 cm, so the number of observable disintegrations from a solid target are about the same in the two cases. These substances are used to line the inside of ionization chambers in which the disintegration products are recorded (C14). With layers essentially equal

to the range of the product particles, the number of particles entering the chamber far enough to be recorded is about 7/1000 neutrons for B and 10/1000 neutrons for Li. A still more efficient technique is the use of large ionization chambers filled with a B gas (C30). With BF_3 at atmospheric pressure in a chamber about 20 cm deep 200 counts/1000 incident neutrons are recorded if the neutrons are assumed to travel parallel to the axis of the chamber; the efficiency varies with the geometry of source and ionization chamber.

The simple capture reaction induces electron activity in many substances and may be used as a detector of neutrons through observation of these activities. Average cross sections are in general smaller than those mentioned for the particle processes but the simplicity of the technique and the recording devices (counters, electroscopes, etc.) have made this a useful alternative. With pressure ionization chambers (in which a large share of the electron ionization is observed) and sensitive electrometers Fermi and his group at Rome have been able to get sensitivities nearly as good as those obtained from counters, and better accuracies due to the more constant background.

Neutrons may be classified as fast or slow, on the basis of their widely different cross sections for the capture process. Slow neutrons may be further subdivided into those of thermal energies and of energies in the "resonance" region (see §60). Fast neutrons are slowed down by elastic and inelastic impacts with the nuclei in their paths. In hydrogenous materials they have, on the average, an energy $1/e^n$ of their initial energy after n collisions. Relatively few impacts are required to reduce neutron energies to the thermal range (about 20), and in the process they pass through the region of resonance energies (from 0.1 to 1000 volts). In paraffin the mean free path for a 5 MV neutron is about 5 cm; this rapidly decreases as the energy becomes lower until it reaches the value of 3 mm for those of thermal energy. So a paraffin sphere of about 6 cm radius results in a maximum density of slow neutrons near its surface. Thicker paraffin absorbs the fast neutrons in an exponential manner, resulting in a reduced number of slow neutrons. Fink (M21) has designed a slow neutron "howitzer" which, by taking advantage of the back scattering of neutrons starting away from the target and by reducing the absorption of those neutrons directed toward the target, produces slow neutron intensities of 3 to 5 times the intensity obtainable from a sphere of paraffin.

Certain simple capture reactions resulting in stable rather than radioactive products have very large cross sections, observed as absorption of slow neutrons. Cd, for example, has a cross section of 3000×10^{-24} cm^2, while Sm has the largest known value, of 9000×10^{-24} cm^2. Such substances are valuable as absorbers of slow neutrons; a layer of 0.5 mm of Cd is sufficient to remove all thermal neutrons from a beam. This makes it possible to study the disintegrations due to neutrons of "resonance" energies (see §60).

Thermal neutrons have an undirected motion resulting in diffusion through the paraffin. They pass and repass many times through a target immersed in the paraffin, which feature assists in producing the large efficiencies of slow neutron processes. This diffusion has been utilized in certain experiments in which the neutrons are "piped" through paraffin to a more distant point or around corners (H36). It makes it possible to shield targets or detecting instruments from the gamma-radiation of a Rn source with lead blocks, in which case the slow neutrons diffuse around the lead to the target (R3). The slow neutrons are finally absorbed, after covering a region of influence of about 3.5 cm radius, with the emission of photons following the reaction:

$$H^1+n^1\rightarrow H^2+h\nu.$$

E. Gamma-radiation

The absorption of gamma-radiation by matter is a complex phenomenon, involving three processes of absorption. The photoelectric absorption effect, prominent for low energy x-rays, still persists but is relatively unimportant for energies above 1 MV (in lead). The absorption is known to follow an exponential law: $I/I_0=ce^{-\tau x}$, where x is the thickness of material and τ is the photoelectric absorption coefficient, for a monochromatic beam of gamma-rays. Hulme, McDougall, Buckingham and Fowler (H38a) have

calculated the magnitude of this coefficient and the variation with energy. The result is in accord with an empirical relation of Gray (G21). The second process, predominant for energies between 0.6 and 2.5 MV (in lead) is the "Compton" absorption, in which recoil electrons and scattered quanta are produced. The absorption coefficient, σ, is given by the equation of Klein and Nishina (K19). Both coefficients decrease with increasing energy, τ much more rapidly than σ. The third process is the absorption due to the formation of electron pairs and involves the transformation of part of the gamma-ray energy into the mass of the electrons. It does not occur for energies less than $2\ mc^2$ (electron mass), which corresponds to about 1.0 MV, and rises with increasing energy in a manner predicted by the theoretical work of Bethe and Heitler (B9) and others. In lead the absorption coefficient for this process, κ, is essentially equal to σ at 2.5 MV, and in aluminum at 10–12 MV. This leads to a minimum in the total absorption coefficient near these energies and means that an observed coefficient may indicate one of two energies, one greater and one less than the value at the minimum. Even though the measurement of the absorption in different materials gives a unique value of the energy (a technique used by certain experimenters (Mc4)) the variation of the coefficient with energy near the minimum is so slow that accurate results are not possible.

The three processes mentioned above involve different types of reduction of the energy, τ resulting in complete absorption of the quantum, σ producing only partial transformation into beta-rays and yielding scattered quanta of degraded energies while κ results in the production of positrons which, on annihilation, produce photons of 0.5 MV. Equilibrium of these secondary radiations with the primary gammas will be achieved only after considerable thickness of absorber, so thickness is an additional complicating factor, and the absorption is not truly exponential.

The most accurate method of measuring gamma-ray energies in the disintegration of light elements is through the observation of the high energy limit of the secondary electrons, or through measuring the total energy of pairs. Energies are measured through the curvatures of the electron paths in magnetic fields. The cloud chamber, equipped with Helmholtz coils, has been used most successfully for the observations, but magnetic spectrographs with coincidence counters have also been satisfactory. From the energy and momentum relations of the Compton effect it is found that the electron can have a maximum energy just 0.25 MV less that the energy of the gamma-quantum. Photoelectrons acquire essentially the full energy of the gamma-ray (less the K ionization limit of the element in which they are absorbed). The theory of pair production indicates that the gamma-quantum is completely absorbed, so the sum of electron and positron energies plus their mass (1.02 MV) is a measure of the initial energy. The thickness of absorber in which the secondaries are produced determines the resolution of the technique; gamma-ray energies are determined from the extrapolated upper limits of electron energy distributions.

F. Electrons and positrons

Nuclear electrons (β-particles) and positrons are observed with maximum energies ranging from 0.3 to 12 MV. An electron-active substance emits electrons having a distribution in energy from zero to a poorly defined maximum energy in each case—the characteristic continuous β-ray spectrum. Even monokinetic electrons do not have a well-defined range as do the heavier particles, but are strongly scattered in passing through an absorber, so that there is no distinct extrapolated range. Absorption of the electrons of a β-spectrum results in an almost exponential absorption curve, having no unique characteristic. Measurements of the half-value thickness (thickness of absorber to reduce intensities to half) have been used by certain experimenters as a measure of the electron energy. This can only be approximate since the distribution curves are not identical.

Magnetic analysis, as used for measurements of secondary electrons from gamma-rays, is at present the best technique for energy measurements. Beta-ray spectrographs and cloud chambers are used for this purpose, and only recently have there been reports of satisfactory measurements. The shape of the β-spectrum involves the theoretical problem of explaining the apparent loss of energy and has resulted in the hypothesis

of the neutrino. Only the upper limit of the spectrum has any significance in the energy measurements, and attempts to explain the shape of the distribution and predict this end-point have met with only partial success (§105).

§94. Instruments for Detection and Observation

The first recorded physical evidence of nuclear radiations was the photographic effect of certain uranium salts, which led Becquerel, in 1896, to the discovery of natural radioactivity in this mineral. The electrical method of observation with an ionization chamber was initiated by Mme. Curie in 1898, and with electroscope and electrometer recording such instruments are still in use. In 1903 Sir William Crookes and also Elster and Geitel discovered that alpha-rays are capable of producing brilliant luminosity of a fluorescent screen, and led to the use of the scintillation technique for individual particles. Rutherford and Geiger, in 1908, developed the forerunner of the Geiger-Müller tube counter, now in wide use. With the development of the Wilson cloud expansion chamber starting from 1912 the tracks of individual ions have been observable. A most valuable development has followed from the use of vacuum tube amplifiers by Wynn-Williams to record the ionization of single charged particles.

A. The scintillation method

Although it has nearly outlived its usefulness in view of later developments of apparatus for recording individual high speed ions the scintillation screen was for years the most sensitive instrument for making such observations. Its use must necessarily be dependent on an observer and so introduces human fallibility and fatigue to some degree. It was successful, at least in the hands of the Cavendish Laboratory group, in yielding all the essential information about alpha-particle disintegration and scattering. Only high speed, heavy, charged ions are observable, such as the alpha-particle and the proton. In its usual form the screen consists of a thin layer of zinc sulphide or some other fluorescent salt mounted on a glass plate and observed on a dark field by a low power microscope. Observers must have their eyes dark-adapted and attempt observations only for relatively short periods to avoid errors due to fatigue. The scintillations are distinct and unmistakable with the eye in proper focus; the optimum size of field and frequency of counts are determined for the individual observer. As the end of the alpha-article range is approached the intensity of the scintillations fades gradually. Rutherford states that alphas of velocity $V=0.15\,V_0$ (V_0 is the initial velocity of the Ra C′ alpha) are not detectable, so that ranges obtained with this method are subject to variations between observers and are in general short. A thorough discussion of the technique and applications is contained in the book by Rutherford, Chadwick and Ellis (R21).

B. The cloud expansion chamber

Since its inception by Wilson (W19) the "cloud chamber" has undergone many modifications and at present exists in a variety of forms, each adapted to some special purpose. In general, a volume of gas containing a saturated vapor is adiabatically expanded to give a short interval of supersaturation. During this interval the ions produced along the paths of alpha-particles, protons or electrons traversing the chamber act as condensation nuclei for the vapor and under suitable illumination sharp tracks of droplets of liquid are observable.

The improvement of illumination and photographic technique has resulted in essentially perfect recording of these tracks. Stereoscopic photography, introduced by Wilson, makes it possible to calculate ranges and directions of the tracks, or they can be directly observed and measured by reprojection through the two films onto a suitably oriented translucent screen. A modification by Kurie (K27) replaces the two cameras with a single camera and lens system equipped with mirrors and a prism to take the two stereoscopic views on motion picture film. As a source of illumination the carbon arc is usually used, with an arrangement whereby a resistance in the power line can be momentarily shorted out to give an instant of intense illumination. Capillary mercury arcs (D1) and exploded wires are also satisfactory. For dense tracks (alphas or protons) "photoflood" or overvoltage lamps are successful. Recent improve-

ments in technique have made this method satisfactory for electron tracks as well.

Mechanically the expansion is achieved in a variety of ways. A reciprocating piston to compress the gas slowly and expand it rapidly can be operated by a cam, by an electromagnet or by changing pressure in the chamber under the piston. Sylphon bellows may take the place of the piston and have their length altered suddenly by valving air under pressure. Rubber diaphragms with similar pressure regulation provide another satisfactory method. Excessive turbulence is avoided by maintaining a geometrical simplicity in the design, and with fine-mesh screens just below the active portion of the chamber. This region is usually several cm deep and, depending on the use, from a few inches to 20 inches in diameter. Most installations are operated cyclically by clockwork or pendulum and arranged to repeat the cycle at regular intervals, so spaced that temperature equilibrium is maintained.

With high pressures and large diameters the particle range observable in the chamber can be increased to include the whole of even the fastest proton tracks. The use of low pressures (down to a few cm of Hg) of gas inverts the results so that particles of small energy such as heavy atom recoils from disintegration or scattering processes can be observed. Ranges come directly from the known gas density and constitution and can be measured to a reasonable accuracy, depending upon the density of track, etc. The expansion ratio is determined from the known constants of the gas and vapor in the chamber which produce supersaturation. It is usually determined experimentally to give the sharpest definition of tracks. For water vapor in air this ratio is in the region 1.25 to 1.38, but is much lower for other vapors such as propyl alcohol, or in other gases such as He or A.

The cloud chamber has been used with great success in cosmic-ray studies by Anderson and by Blackett, and much of the technique developed for this work is directly applicable to disintegration studies. The use of the chamber to observe and measure the charged particle products of disintegration is obvious. When the gas in the chamber contains the target substance and the bombarding projectile enters the chamber the complete disintegration reaction is recorded. Neutron produced reactions are distinguishable as sharp angle tracks, often with definite differences in the density to indicate the particle and the recoil atom, and neutron energies and directions are calculable from the momenta of the particle tracks. There is still, however, insufficient knowledge of the range-energy relations for the recoil nuclei, and this handicaps the accuracy of the observations. Blackett and Lees (B25) and Feather (F8) have made attempts to evaluate these but more experimental work is required.

For the observation of the secondary electrons from gamma-rays a magnetic field is superimposed by the use of a pair of Helmholtz coils, and the curvatures of the electron tracks in this field can be used to calculate gamma-energies. This technique has been highly developed by Lauritsen and his collaborators (C51). The same principle is applied to the measurement of the radioactive betas and positrons from induced radioactive materials. The chief difficulty in these experiments is the excessive number of photographs required to give sufficient data for an exact statistical value of the electron energy distribution. These workers have also initiated a method for measuring gamma-radiation by observing the energies of both the positive and negative electrons of pairs and adding to this sum the 1 MV equivalent of the mass of the electrons. The pairs are formed in the walls of the chamber or laminae inserted in the chamber and so may have been partially absorbed, but if sufficiently thin laminae are used a relatively few pairs are sufficient to determine the gamma-ray energy.

C. Ionization chamber and pulse amplifier

The most satisfactory method of measuring the ranges of individual charged particles is in the shallow ionization chamber and with the use of the linear pulse amplifier, originally developed by Greinacher (G22), as a recording instrument. The amplifier has been perfected by Ward, Wynn-Williams and Cave (W2) and by Dunning (D22) and others with the addition of control features and the reduction of the background or noise level. With the instruments in use at present a chamber 2 mm deep suffices to give alpha-particle pulses large enough in comparison with

the background to make accurate measurements possible. The voltage pulse due to the individual alpha-particle in the chamber is amplified by 3 or 4 stages of resistance-capacity coupled vacuum tube amplifiers, and is made to operate an oscillograph or electrical counter. The theory of the amplifying circuits and the resolving time of the instrument has been worked out by Ortner and Stetter (O13) and by Johnson and Johnson (J3). The resolving time is usually smaller than that of the mechanical counter used to record the counts. The chamber is usually constructed of two parallel electrodes, one a wire grid or thin foil through which the particles enter and upon which a suitable saturation voltage is applied; the other a plate connected to the grid of the first amplifier tube (near ground potential). The microphonic sensitivity of the instrument requires vibrationless supports for the chamber and at least the first tube of the amplifier. This also limits the use of thin metal foils as defining walls for the chamber, since such a foil records sound vibrations in the air as a condenser microphone.

In such shallow chambers electrons do not yield sufficient ionization to record and so protons and alpha-particles are observable even when accompanied by rather intense beta- or gamma-radiation. Protons and other light nuclei recoiling from fast neutrons are readily detected. If the chamber walls are coated with lithium or boron energetic alpha-particles are emitted in neutron disintegration processes and will be recorded by the amplifier. These reactions are greatly increased in probability with slow neutrons, and so this method constitutes one of the best methods of observing them.

With a properly constructed instrument the natural contamination alpha-particle background is less than one count per minute. The background due to the minimum "shot effect" of the individual thermionic electrons in the amplifier tubes and the "Johnson effect" of electron currents in the resistances in the circuits define the ultimate amplification possible with such an instrument. Careful shielding of the amplifier in iron and copper boxes has made it possible to reduce the extraneous effects nearly to this limit, and the background to approximately 1/50 of the amplitude of the alpha-particle pulse in a 2 mm chamber. The amplitude of this background fluctuation determines the minimum depth of the chamber, and a "bias" voltage must be applied to the output to prevent such fluctuations from operating the recording instruments. The "thyratron" or grid controlled relay tube is often used for this purpose. Here the grid is biased to any desired value and only those pulses of greater amplitude than this bias will operate the tube, which in turn operates a mechanical counter. The thyratron "scale of 8" counter (W23) is often used to increase the rate of recording. With such an instrument operating a high speed counter as many as 5000 counts/min. statistically distributed in time can be recorded with small error.

Due to the different specific ionizations of protons and alpha-particles these two ions will give pulses of different amplitudes and can be separated in the counting with the use of the bias voltage mentioned above. Also some success has been achieved in the use of the "differential ionization chamber," essentially two equivalent chambers with opposite applied potentials through which the ions pass. This makes it possible to obtain no counts from particles which cross both chambers, but only from those stopping after crossing one chamber. By this means short ranges of particles can be counted, even though longer range particles are traversing the chamber. A somewhat similar effect is obtained with the single chamber if sufficiently high bias is applied to allow the recording of only those ions which have their maximum specific ionization in the chamber. Due to the variation of the specific ionization with velocity (the "Bragg" curve) this means that only those ions near the end of their range will be counted.

D. Integrating ionization chambers

Electroscopes and integrating ionization chambers in general have been the basic instruments in the experimental development of natural radioactivity. They are the simplest of all sensitive electrical instruments and in their present form still supply the best values of ionization intensities. Background effects due to electrical leakage, cosmic rays and contamination of radioactive materials give a steady rate of discharge which can be subtracted from observations to give very accurate results. Where the nature of the radiation is known and the chamber is de-

signed for proper absorption of that radiation the results are unique and nearly as sensitive to small intensities as individual counting methods. For the observation of the induced beta or positron radioactivity in various elements the standard techniques are immediately adaptable since decay periods can be measured directly.

A rather large chamber with several atmospheres pressure of CO_2 which has a thin aluminum window is used by Fermi and his group (S9) for the measurement of neutron induced activities. A sensitive electrometer is the observing instrument. It is accurately calibrated for sensitivity and background effects and is peculiarly adapted to the study of relatively long-lived materials.

A modification of the electroscope, designed by Lauritsen (L7) uses a small metalized quartz fiber whose deflections are observed by a small microscope focused on the tip. Fibers of about 5 microns diameter and about 6 mm long are stable for any orientation of the instrument. The low capacity of this small fiber gives a high charge sensitivity. It is charged and deflected electrically and the rate of discharge is observed in the microscope. It has the advantage of small size and can be used to measure any radiation observable above the background. Its chief value is for studies of induced radioactivity and as a qualitative instrument for the detection of γ's and n's. It has been used in certain experiments in which interchangeable lead and Cellophane walls make it differentially sensitive to neutron and gamma-radiations. The ionization is largely due to absorption of radiation in the walls of the chamber, the volume of air being small, and this absorption is a function of the wall materials.

E. Tube and point counters

The Geiger-Müller tube counter and its contemporary the Geiger point counter have been used for the detection of all types of radiations. In fact, this universal sensitivity constitutes its chief disadvantage since all kinds of radiations are identically recorded. It responds to cosmic rays and radioactive contaminations so that a natural background is always present. Many workers have studied the physical and electrical conditions influencing the action of the counters and in the hands of a relatively few, proper conditions of stability have been achieved. In such hands it has been a valuable and consistent instrument, and due to its extreme sensitivity it has been successful in certain exploratory observations where other instruments would have failed. It consists of a system of electrodes between which a steady potential is applied which is just under that for which a continuous discharge occurs. The tube counter has a cylindrical cathode with a central thin wire anode. The materials should be of low photoelectric sensitivity and free from contaminations. A tungsten or iron wire of 1- to 10-thousandths of an inch with a copper or nickel cylinder of 1 to 5 cm diameter would represent a typical instrument, although different workers recommend widely different specifications. The potential range in which the counter is sensitive is a rather narrow one, requiring a carefully regulated supply of from 1000 to 1800 volts determined by the construction.

The point counter consists of a cylindrical anode with a central cathode terminating in a point located at a distance from the end of the anode about equal to the radius of the cylinder. The end is usually closed with a thin metal foil to define the active region. The point counter can be operated at atmospheric pressure (which makes it valuable for certain experiments) while the tube counter has its greatest sensitivity for a few cm of Hg pressure. The type of gas in the counter is also a function of the experimenter, involving variations with purity of gas which are not easily explainable. The tube counter has a wider range of voltage for the sensitive condition and is not so readily disturbed by discharge.

A relatively few ions formed in the chamber by an ionizing radiation produce what is essentially a cumulative ionization resulting in a discharge. Proper adjustment of external circuit constants extinguishes the discharge within a very short time interval and reestablishes the sensitive condition. A simple one- or two-stage tube amplifier is sufficient to amplify the voltage pulse for recording.

For gamma-rays thick walled chambers may be used, although the practice is to keep the amount of material at a minimum in order to reduce the contamination background. Secondary electrons released chiefly from the metal tube

walls produce the discharge. When intended for the detection of beta-particles or positrons either thin windows or thin chamber walls are used to admit the radiation. Constructed in this way the chamber is sensitive to gamma-radiation and is shielded with lead when necessary. Heavy particles such as alphas or protons are most readily observed with the point counter which may have thinner chamber walls due to operation at atmospheric pressure. With somewhat lower operating voltages the instrument will respond only to heavy particles—the "proportional counter." When filled with hydrogen the chamber records neutrons, but not efficiently enough to make it valuable for this purpose.

Coincidence methods with two or more counters, such as are used for cosmic-ray experiments, are also available. Such techniques have been used by Rasetti (R3) to measure the secondary electrons from the gamma-rays emitted by the absorption of slow neutrons in various materials, following earlier experiments by Bothe. The method also serves to determine the association of different radiations emitted from a reaction simultaneously but in different directions and recorded as coincidences. Bothe and Baeyer (B45) used a central counter with 8 others surrounding it and from the duplicate coincidences (requiring the central counter and two others to discharge simultaneously) concluded that one gamma-ray is emitted with each beta-particle from Ra E.

F. Photographic effects

Microscopic examination of suitably sensitized photographic plates shows a linear arrangement of developed grains in the emulsion along the track of an alpha-particle or proton. Such tracks are not as dense as those in a cloud chamber and due to the questionable estimates of density and nature of the emulsion, range measurements, obtained with a micrometer microscope, are not as accurate as from other methods. Neutrons give recoil protons which can be observed, but electron tracks are not dense enough to measure. The chief value is in the spatial orientation of tracks, as with the cloud chamber. Taylor and Goldhaber (T1) have been successful in showing that in the disintegration of boron by slow neutrons two particles (straight tracks in the emulsion) resulted and so the reaction was identified. The one peculiar advantage of the technique is that the records are permanent and cumulative so that long exposures with weak sources will give observable effects.

G. Chemical separations

As in the development of experimental results on natural radioactivity the studies of the new induced radioactivities have been materially assisted by the use of certain standard chemical separation techniques. A good guess as to the nature of a disintegration reaction makes it possible to separate the possible products and by observing in which of the separated residues the activity lies the chemical nature of the element can be determined. It is usually accomplished by using a radioactively inert element of the kind to be separated, as a carrier, in order to have a sufficient quantity to work with. It was introduced for alpha induced radioactivity by Curie and Joliot (C53) and for neutron processes by Fermi (F13). Positron radioactivity obtained by deuteron bombardment has been studied in like manner (Mc6).

A valuable modification was initiated by Szillard and Chalmers (S27). They realized that chemical bonds would be broken by the recoil of the activated atom and so the free element would be released from a chemical compound. Radioactive iodine can thus be separated from an iodine compound by reduction of the free iodine. Precipitation of the radioactive material from a large sample used as a target concentrates the activity into a small sample which can be brought close to the recording instrument, and so increases the observable intensity.

XVI. Auxiliary Data for the Evaluation of Experiments

§95. The Range-Energy Relation

Practically in all experiments on nuclear transmutations, the energy of the emitted particle is deduced from its range. Thus the relation between range and energy is of paramount importance for the determination of nuclear reaction energies. By "range" we understand in this section the mean range in air of 15°C temperature and 760 mm pressure. The relation between mean range and extrapolated range will be discussed in §97.

A. Experimental determinations

The ranges and energies of most of the natural α-ray groups emitted from radioactive sources have been measured with extremely great accuracy, by Rutherford, Wynn-Williams, Lewis and Bowden (R23, L23), by Briggs (B58–60) and by Rosenblum (R12, R14, R14a). The energy was measured by magnetic deflection of the particles, the error was in some cases as small as 1 in 10,000 for energy as well as range. The energies of the α-particles for which such precision measurements are available, extend from 5.3 MV (polonium) to 10.5 MV (long range α-particles from Ra C′ and Th C′). In this energy region we can therefore regard the range-energy relation for α-particles as absolutely certain.

For lower energies, careful measurements have been carried out by Mano (M4, M5). Mano measured the magnetic deflection of α-particles from Th C′ and Th C after these particles had traversed measured thicknesses of air. The accuracy claimed is about 1 in 1000 which is sufficient to determine α-particle energies from their range to about 5 kv. The main difficulty as compared to the measurements mentioned before is the straggling of the energy of the α-particles (cf. §97). While the α-particles emerging from the source all have exactly the same energy (for a given radioactive substance and given α-group!), the energies of α-particles which have traversed stopping material will be distributed over a more or less broad energy band. Mano chose consistently the most probable energy as significant.

Mano's measurements extend from 8.8 MV down to about 2.1 MV energy. They agree well with the data obtained from natural α-rays in the region from 5 to 8 MV. For energies below 5 MV, Mano's measurements seem internally consistent, following a smooth curve with the possible exception of the two lowest energies (2.1 and 2.5 MV) for which the ranges obtained seem to be too large as compared to the other measurements.

Earlier measurements by Briggs (B56), also based on magnetic deflection of partially stopped α-particles, gave ranges considerably higher than those found by Mano. Moreover, Briggs found a range of 3.93 cm for α-particles of 5.30 MV energy, which is the energy of natural α-particles from polonium. The observed range of Po α-particles is only 3.805 cm (R23). This discrepancy is found in spite of the fact that Briggs' ranges have been multiplied by 6.87/6.90 in order to bring his range of natural α-particles from Ra C′ (6.90 cm) into agreement with the now accepted range (6.870 cm). There can thus be no doubt that Briggs' values are too high throughout. For energies below 2 MV, the energies obtained by Briggs for a given range, should be increased by about 9 percent in order to obtain the energy values accepted in Section C.

A point at lower energies may be obtained from disintegration data, using the reaction

$$Li^6+H^1=He^4+He^3 \qquad (746a)$$

which was studied carefully by Neuert (N4). The He^3 particles were found to have a (most probable) range of 1.19 cm, the He^4 particles of 0.82 cm. These figures should be corrected for the penetration of the protons into the Li target. The protons used had an energy of 0.16 MV. Following the procedure of §97, we find that the most probable range corresponds to a penetration of the protons of about 0.03 cm. Thus the true ranges of the particles would be 1.22 and 0.85 cm, respectively. Now a He^3 particle of energy E has a range 3/4 times as great as that of an α-particle of energy 4/3 E (cf. Section B). Interpolating between Mano's experimental points, we find that the energy of an α-particle of $4/3 \cdot 1.22 = 1.62_7$ cm range would be 2.90 MV. The energy of the He^3 is therefore $3/4 \cdot 2.90 = 2.17_5$ MV. From the conservation of momentum, it follows that the He^4 produced in the reaction (746a)

receives an energy equal to 3/4 times the energy of the He^3, i.e., 1.63 MV. A correction for the momentum of the incident proton lowers this figure to 1.62 MV. Thus we conclude that an α-particle of range 0.85 cm has an energy of 1.62 MV. This value was used in the accepted range-energy relation.

The region of *very low energies* was investigated by Blackett and Lees (B25). The production of such slow α-particles by slowing down fast (natural) alphas is very inconvenient because of the large straggling which prevents accurate measurements. Blackett and Lees therefore used *collisions* to reduce the energy of the α-particles: The "close" collisions of α-particles near the end of their range with helium nuclei were photographed in a cloud chamber. From the angle of deflection, the ratio of the energies after and before the collision can be obtained (§70). The energy before the collision can be found from the fraction of the range between α-particle source and collision; this procedure is safe because the incident α-particle has a fairly high energy so that the straggling of ranges is relatively not so important. The range of the scattered α-particle (from the point of collision) can be measured directly.

Unfortunately, Blackett and Lees had to use Briggs' range-energy relation for determining the energy of the incident α-particle, no other determination being available at the time. Assuming that in most cases the energy of the incident α-particle was less than 2 MV, the Briggs energies may be expected to be 9 percent low, so that we may expect the same error in Blackett and Lees' values. For ranges up to 0.4 cm (energies up to 0.66 MV) we have used the experimental energy values of Blackett and Lees, plus nine percent, for constructing our final range-energy curve (Fig. 29).

Blackett and Lees have also measured the ranges of *slow protons* produced by collisions of α-particles with hydrogen nuclei. The ranges were measured in a cloud chamber filled with a mixture of hydrogen and air, and the energies calculated from that of the incident α-particle in the same way as before. The proton ranges were reduced to those in pure air using approximate values for the stopping power of hydrogen relative to air.

It was found that slow protons have much smaller ranges than α-particles of the same velocity. On the other hand, for velocities greater than about $6\cdot10^8$ cm sec.$^{-1}$, the range of α-particles and protons increases by the same amount for a given increase in velocity, both theoretically (Section B) and experimentally (B26). According to the experiments of Blackett and Lees, we have

$$R_H(v)=R_\alpha(v)-0.2\text{ cm} \tag{747}$$

for $v>6\cdot10^8$ cm/sec. This relation (or the more accurate one, (760), (760a)) is used for calculating the ranges of faster protons (Section C). The difference of 0.2 cm is purely empirical.

B. Theory

The energy loss of charged particles when passing through matter is mainly due to ionization and excitation of the atoms of the substance traversed. The probability of these inelastic collisions with the atoms depends on velocity and charge of the particle. At not too low energies (>1 MV for α-particles, >0.1 MV for protons) it is safe to assume that α-particles are doubly, protons singly charged. When the particles have been slowed down sufficiently, they will capture electrons: Thus, e.g., an α-particle of 0.8 MV is found to be singly ionized about as often as doubly ionized (R21a). The probability of single ionization increases with decreasing energy, until finally neutral atoms appear. This reduction of the average charge of a particle was studied by Kapitza (K1, cf. B) for α-particles in H_2 and by various authors for canal rays of H and He (R18). The reduction of charge will tend to decrease the energy loss of slow particles. On the other hand, the process of capture and loss of electrons itself will use up some energy so that the stopping is not reduced as much as would be expected from the decrease of the average charge.

The theory of the energy loss by inelastic collisions has been given by Bethe (B8), on the basis of Born's approximate treatment of collision processes. Bethe's formula is valid only if the velocity of the incident particle is large compared to the velocities of the electrons in the atom, in other words if

$$E\gg(M/m)E_{el}, \tag{748}$$

where E is the energy of the incident particle,

E_{el} the ionization potential of the electrons, and M and m the masses of incident particle and electron. Under these conditions, the energy loss per cm path is

$$-\frac{dE}{dX}=\frac{4\pi e^4z^2}{mv^2}NB \tag{749}$$

with $$B=Z\log(2mv^2/I). \tag{749a}$$

Here v is the velocity and ez the charge of the incident particle, N the number of atoms per cm^3 of the material, Z the nuclear charge and I the average excitation potential of the atom (cf. Section C). B is a convenient dimensionless quantity proportional to the stopping power, we call it the "stopping number."

A relativistic treatment by Bethe (B19) and Møller (M25) showed that a term

$$-\log(1-\beta^2)-\beta^2 \tag{750}$$

had to be added to the log in (749a). For small $\beta=v/c$, (750) is proportional to β^4 and is therefore negligible for the velocities occurring in nuclear processes (less than $5\cdot10^9$ cm sec.$^{-1}$).

On the basis of classical mechanics, Bohr (B33a) derived a formula for the stopping power which contained essentially an additional factor $\hbar v/e^2$ in the argument of the logarithm in (749a). Bloch (B29) has investigated the reasons for this discrepancy between classical and quantum theory. By taking into account approximately the perturbation of the wave functions of the atomic electrons by the incident particle, he arrived at a formula which contains the quantum theoretical formula (749a) and the classical formula of Bohr's as limiting cases for high and low velocities, respectively. Bloch's correction is negligible when

$$v\gg e^2z/\hbar. \tag{751}$$

The right-hand side is the velocity of an electron moving around the incident particle in a 1s-orbit. This velocity is, in all practical cases, *much smaller* than the velocity of a K electron in the atoms of the stopping material—except, of course, if the stopping material has smaller nuclear charge than the incident particle. Now the calculations of Bloch, as well as those of Bethe, were made with the assumption that the particle velocity is greater than the velocity of all electrons in the atoms constituting the stopping material. Therefore the Bloch correction is always negligible in the domain of validity of Bloch's formula. It should therefore *not* be included in calculations of the stopping power, contrary to the procedure adopted by Mano (M4) and by Bloch himself (B31) for calculating range-energy relations.

The condition (748) is quite a serious restriction of the validity of the stopping formula (749). For oxygen, e.g., the ionization potential of the K shell is about 540 volts, and therefore the right-hand side of (748) is almost 4 MV for α-particles. This means that the condition (748) is never very well fulfilled for α-particles, even with a stopping substance as light as oxygen. While we may expect the stopping due to L electrons of oxygen (valence electrons!) to be correctly represented by (749) down to quite low energies (less than 1 MV for α-particles), this will not be the case for the stopping by the K electrons. If the theoretical formula for the stopping is to be used for obtaining a range-energy relation of any precision, the stopping by the K electrons must be taken into account more accurately.

Fortunately, it can be shown that *the general principles of Born's approximation method can be applied to the collisions of heavy particles with atoms down to velocities much lower than that of the atomic electron*, and that only some minor approximations made in deriving (749) are no longer justified. The validity of Born's approximation was first proved by Mott (M33). He points out first that the motion of the incident heavy particle (proton, α-particle etc.) may be treated by classical mechanics since its wavelength is very small compared to atomic dimensions. The incident particle will then be equivalent to a perturbing potential whose center moves with constant velocity. Mott then shows that the transitions caused by such a potential are exactly the same as those found by the Born method provided the incident particle (if considered stationary at a given place inside the atom) does not distort greatly the wave functions of the atomic electrons. This condition will be fulfilled when the charge of the incident particle is small compared to that of the atomic nucleus, i.e., in all cases when the velocity of the K electrons of the atom is high. Thus we get the

somewhat paradoxical result that the Born method as such is the better justified the less condition (748) is fulfilled.

The same result was obtained by Henneberg (H26) using a more analytical argument. Henneberg also calculated the probability of ionization of atoms in the K shell by slow protons and α-particles and found good agreement with experimental data of Gerthsen and Reusse (G14) and of Bothe and Fränz (B44). More recent experiments of Livingston, Genevese and Konopinski (L34), using higher intensities, also agree well with Henneberg's theory.

According to the Born method, the contribution to the "stopping number" B (cf. (749a)) due to excitation of the two K electrons is (cf. B16).

$$B_K=\int_{\vartheta}^{\infty}\epsilon d\epsilon\int_{Q_0(\epsilon)}^{\infty}\frac{dQ}{Q}\varphi(\epsilon, Q). \tag{752}$$

Here ϵ is the energy given to the atomic electron divided by $Z^2_{\text{eff}}Ry$ where Ry is the ionization potential of the hydrogen atom and $Z_{\text{eff}}\approx Z-0.3$ the effective nuclear charge in the K shell. The kinetic energy of the ejected K electron is thus

$$E_{\text{kin}}=\epsilon Z^2_{\text{eff}}Ry-E_K=(\epsilon-\vartheta)Z^2_{\text{eff}}Ry, \tag{753}$$

where E_K is the (observed) ionization potential of the K shell

$$\text{and}\qquad \vartheta=E_K/Z^2_{\text{eff}}\,\text{Ry} \tag{753a}$$

is the ratio of E_K to the "ideal ionization potential" in the absence of "outer screening," Z^2_{eff} Ry (cf. B16, p. 478). Q is defined by

$$Q=(\mathbf{p}-\mathbf{p}')^2/(2mZ^2_{\text{eff}}Ry), \tag{754}$$

where $\mathbf{p}$ and $\mathbf{p}'$ are the momenta of the incident particle before and after collision. $Q_0(\epsilon)$ is the smallest value of Q possible for a given energy transfer ϵ; from energy and momentum considerations one finds easily

$$Q_0(\epsilon)=\epsilon^2/4\eta \tag{754a}$$

$$\text{with}\quad \eta=mv^2/2Z^2_{\text{eff}}Ry=Em/MZ^2_{\text{eff}}Ry. \tag{754b}$$

φ is the transition probability from the K shell to a state of energy (753), *viz.*

$$\varphi(\epsilon, Q)=Q^{-1}\left|\int\psi_K(\mathbf{r})\psi_\epsilon(\mathbf{r})\exp\left(i(\mathbf{p}-\mathbf{p}')\cdot\mathbf{r}/\hbar\right)d\tau\right|^2, \tag{755}$$

where ψ_K and ψ_ϵ are the wave functions of a K electron and an electron of energy (753), respectively. For not too low nuclear charge (a condition which we have always assumed to hold), Coulomb wave functions may be taken for ψ_K and ψ_ϵ and we find

$$\varphi(\epsilon, Q)=\frac{2^7(Q+\frac{1}{3}\epsilon)}{[(q+k)^2+1]^3[(q-k)^2+1]^3}\times\frac{\exp\left(-(2/k)\arctan 2k/(q^2-k^2+1)\right)}{1-e^{-2\pi/k}} \tag{755a}$$

$$\text{with}\qquad q=Q^{\frac{1}{2}},\quad k=(\epsilon-1)^{\frac{1}{2}}. \tag{755b}$$

For a given value of the energy of the incident particle (or of η, (754b)), the energy loss (752) can be calculated by numerical integration. The result is given in Fig. 28, for $\vartheta=0.7$ (cf. (753a)) which is very nearly correct for all elements from about carbon to aluminum. For high energies ($\eta\gg 1$), it is convenient to write

$$B_K(0.7, \eta)=1.81\log 3.63\eta-C_K(\eta), \tag{756}$$

where C_K approaches zero as η increases. 1.81 is the "effective number of K electrons," or, more accurately, the total oscillator strength of all optical transitions from the K shell into the continuous spectrum (and to the unoccupied discrete levels). This value was checked by calculating the oscillator strength corresponding to the transition to the $2p$ shell using the Hartree wave functions for oxygen (H16). An oscillator strength of 0.15_5 was found for the transition of *one* K electron to the $2p$ shell. Since 4 of the 6 substates of the $2p$ shell are occupied by electrons, this means an oscillator strength of $(4/6)\cdot 2\cdot 0.15_5=0.21$ for the transitions to the occupied states, leaving $2-0.21=1.79$ for the transitions to unoccupied discrete and continuous levels, in close agreement with the value of 1.81 obtained by integrating (752).

The argument of the log in (756) is

$$3.63\eta=\frac{2mv^2}{1.103Z^2_{\text{eff}}Ry}. \tag{756a}$$

Therefore, for high energies ($C_K=0$), (756) takes the same form as (749a), with the average excitation potential of the K shell being given by

$$I_K=1.103Z^2_{\text{eff}}Ry. \tag{757}$$

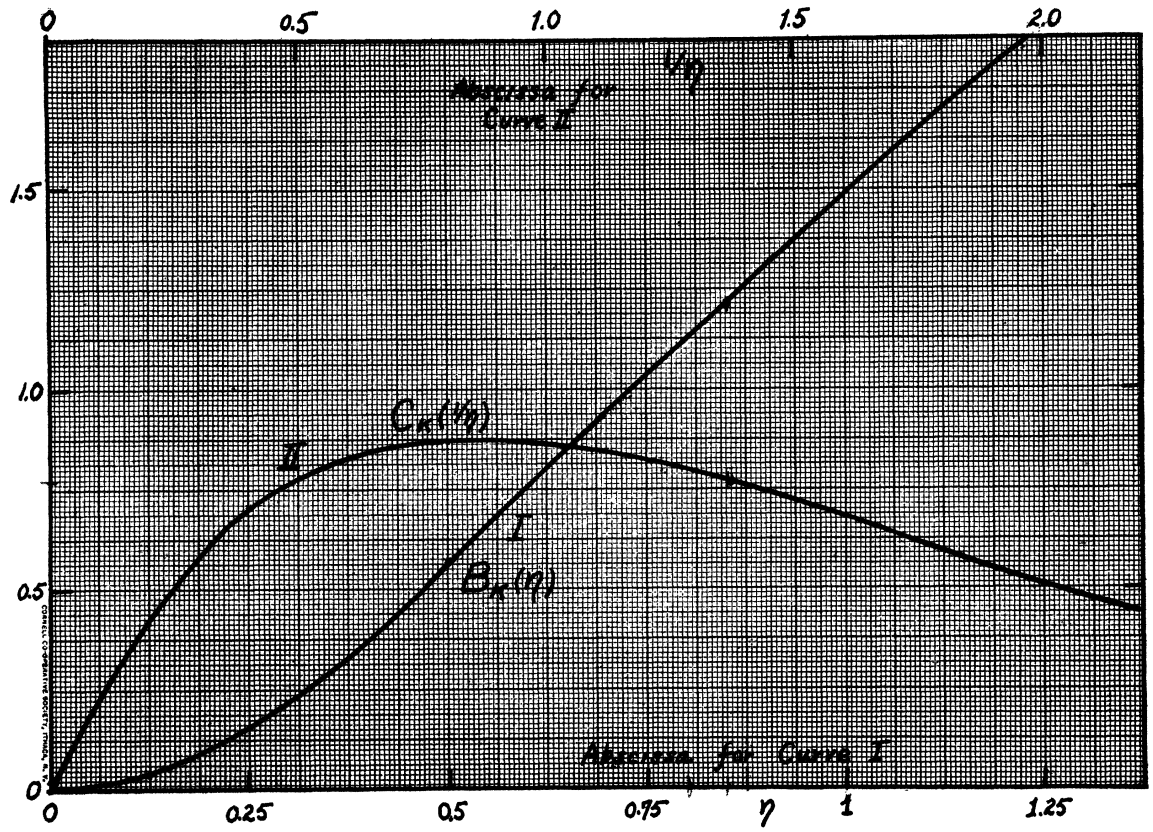

FIG. 28. Curve I: Contribution B_K of the K shell to the "stopping number" B (cf. (749a)). Abscissa: η = (velocity of the incident particle/velocity of a K electron)^2 = (electron mass × energy of the incident particle)/(particle mass × "ideal" ionization potential $Z^2\,Ry$ of the K shell). Curve II: Correction C_K to the high energy stopping number for K electrons against $1/\eta$. From C_K, the stopping number of K electrons can be obtained using (756), or the stopping number of the complete atom from (758).

If we denote the average excitation potential of the electrons outside the K shell by I', we can write the total stopping number

$$B=(Z-1.81)\log(2mv^2/I')+B_K, \quad (757a)$$

where $Z-1.81$ is the "effective" number of electrons outside the K shell. Using (756), we find

$$B=Z\log(2mv^2/I)-C_K, \quad (758)$$

where the average ionization potential of the whole atom is given by

$$\log I=(1-1.81/Z)\log I'+(1.81/Z)\log I_K. \quad (758a)$$

[redacted]een from Fig. 28, C_K is positive for high [redacted]. This means that the K electrons are less [redacted]in stopping than would be expected fr[redacted]mple formula (749), (749a). The deficiency stopping power C_K increases as the energy decreases down to about 1.5 times the "critical energy" $(M/m)Z^2_{\text{eff}}Ry$, then remains almost constant down to 0.8 times the critical energy and decreases from then on. For very low energies ($\eta\ll 1$), the stopping B_K due to K electrons becomes negligibly small. It will, of course, never become negative. This point has not been taken into account in previous calculations. For $\eta\ll 1$, the stopping number B is simply given by the first term in (757a), i.e., the effective number of stopping electrons as well as the average excitation potential are smaller than for high energies.

C. Determination of constants in stopping power formula

It is not easy to determine the average excitation potential I purely theoretically with any accuracy. An early attempt of Bethe (B8) in this

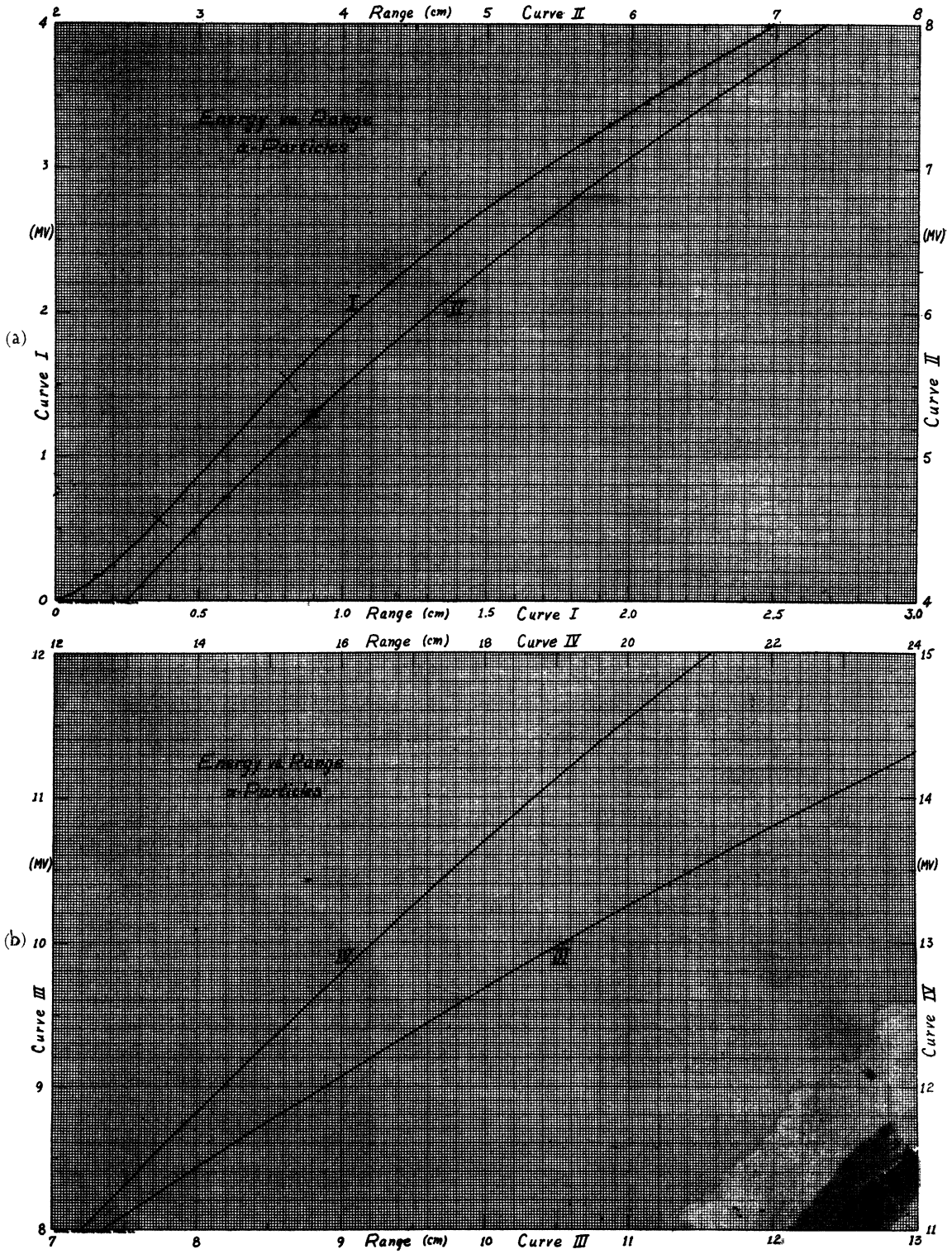

FIG. 29. Range-energy relation for α-particles. Abscissa: Range in air of 15°C and 760 [illegible]re in cm. Ordinate: Energy in MV. (a) From 0 to 8 MV. (b) From 8 to 15 [illegible]

direction gave much too low values for I. Therefore I must be determined from the experimental data on stopping. This procedure was first suggested by Blackett (B26) and later also adopted by Duncanson (D18) and Mano (M4). Blackett and Duncanson used the simple Bethe formula (749), (749a) and regarded Z as well as I as an adjustable parameter. Mano used the formula of Bloch mentioned above. We have redetermined the constant I, using the more accurate formula (758).

The value of I for air was determined so that the difference between the ranges of a Th C′ long range α-particle and a Po α-particle agrees with experiment. This yielded $I=80.5$ volts for air. From (758a) we obtain then $I'=40.3$ volts, inserting for Z the value[2] 7.22. This is a reasonable value for the average excitation potential of the L shell of nitrogen and oxygen, since it must be expected that most optical transitions from states in the L shell lead to states of rather high energy in the continuous spectrum (Bethe, unpublished).

When I has been determined, the stopping power is known for all energies. In order to obtain the range for a given energy, (749) has to be integrated. The integration constant is fixed by making the range at a given energy agree with experiment. In our calculations, we chose the integration constant so that agreement was obtained *in the average* over the region in which measurements of natural α-ranges are available (5.3 to 11.5 MV). In order to achieve this, we had to make the "theoretical" range of Ra C′ α-particles equal to 6.865 cm instead of the observed value of 6.870 cm.

The agreement obtained with the observed ranges of natural α-particles was quite satisfactory, the maximum difference being 0.012 cm for Po and Th C′ (long) α-particles, in both cases the theoretical ranges are too high. In the final range-energy relation (Fig. 29), we adopted the experimental values which can at present not be equalled in accuracy by any theoretical calculation.

Between 2.5 and 5 MV, the agreement with Mano's observations is fairly satisfactory. However, as the differences seemed just outside the experimental error and since the theoretical calculations are less accurate at low energies, we adopted an empirical correction of the theoretical energies by -10, -25, -40, -60 and -65 kv, at 4, 3.4, 2.9, 2.3 and 1.5 MV respectively. With this correction our curve passes about midway between Mano's experimental points, being slightly higher than his points at 2.1 and 2.6 MV, slightly lower than his result at 3.0 MV. Our curve is also made to give a range of 0.85 cm for 1.62 MV as is required by the observations on the disintegration (746a).[3]

No attempt was made to continue the theoretical calculations to energies below 1 MV, because then capture and loss of electrons will become important and no adequate theory is yet available for dealing with this case. Instead, Blackett and Lees' experimental values, increased by 9 percent (cf. Section A), were adopted up to 0.7 MV. These values join to the theoretical curve above 1 MV very smoothly, which was taken as an indication of the reliability of the adopted range-energy relation even in the intermediate region.

The extension to velocities greater than those of natural α-particles is straightforward, using (749, 749a). The theoretical range-energy relation may be considered particularly reliable in this region because no corrections like that for diminished stopping due to K electrons or capture and loss of electrons need to be applied. It must only be kept in mind that $\frac{1}{2}Mv^2$ can no longer be identified with the energy of the particle, the relativistic correction amounting up to 2 percent for the velocities considered here. This was not taken into account by Duncanson (D18) who was the first to give a theoretical range-energy relation for very fast particles (protons). The relativistic correction is the main reason why our range-energy relation differs appreciably from Duncanson's at high energies (239.3 cm range against Duncanson's 230.6 cm for protons of 15.03 MV energy).

[2] $2Z$ was taken equal to the average number of effective electrons per molecule. For nitrogen and oxygen, $Z=7$ and 8, respectively. For argon, the two K electrons are not effective ($\eta \ll 1$, see Section B), leaving 16 effective electrons, i.e., $Z=8$. With 78 percent nitrogen and 1 percent argon, the average of Z is 7.22.

[3] It might be thought that the theoretical relation is useless if it has to be corrected so extensively. However, the theoretical relation is still useful in order to provide a simple and accurate way of interpolation between the observed points.

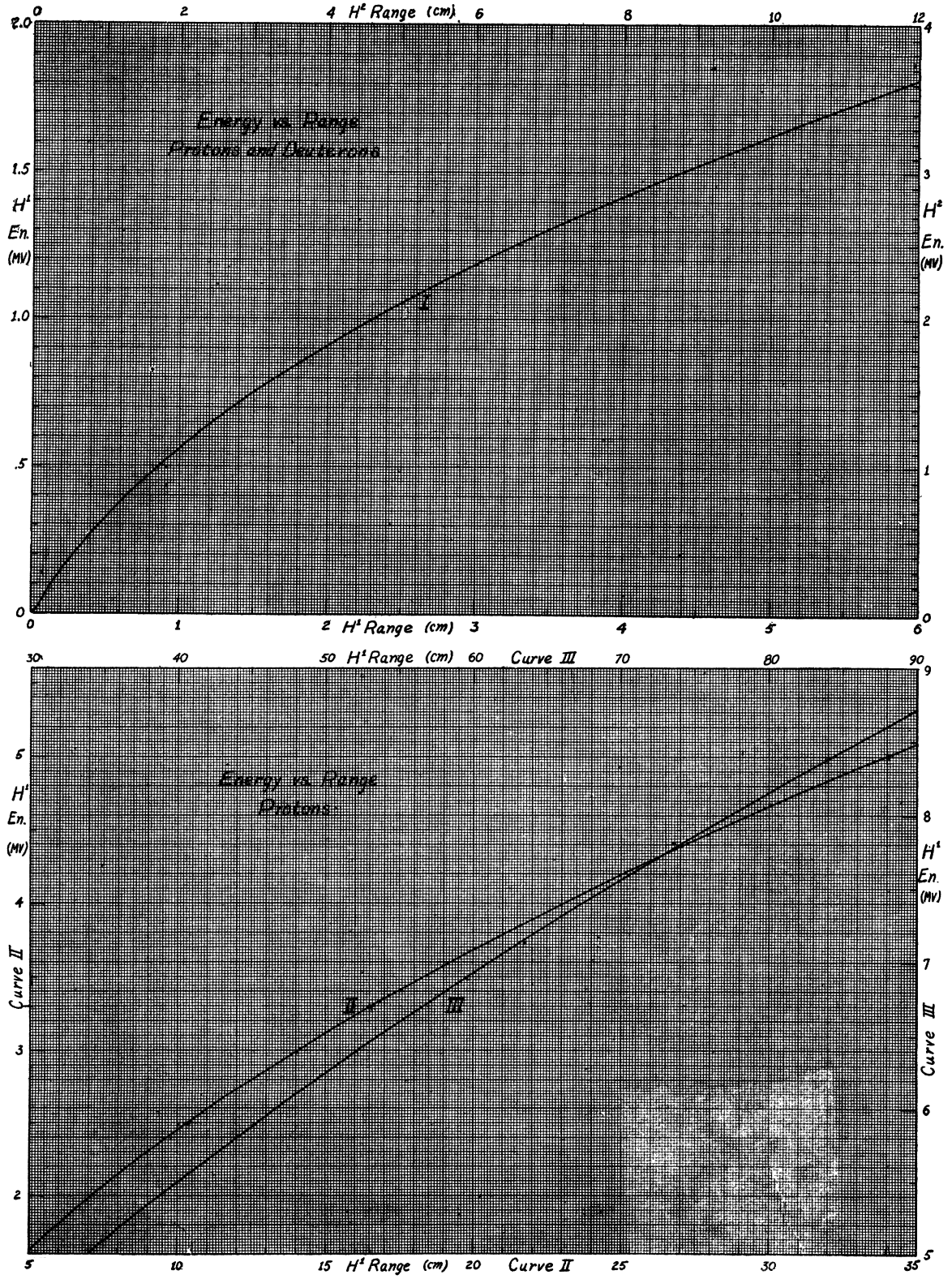
H² Range (cm)
Energy vs. Range
Protons and Deuterons
H¹ En. (MV)
H² En. (MV)
I
H¹ Range (cm)
Curve III
Energy vs. Range
Protons
Curve II
II
III
Curve III
H¹ Range (cm)
Curve II

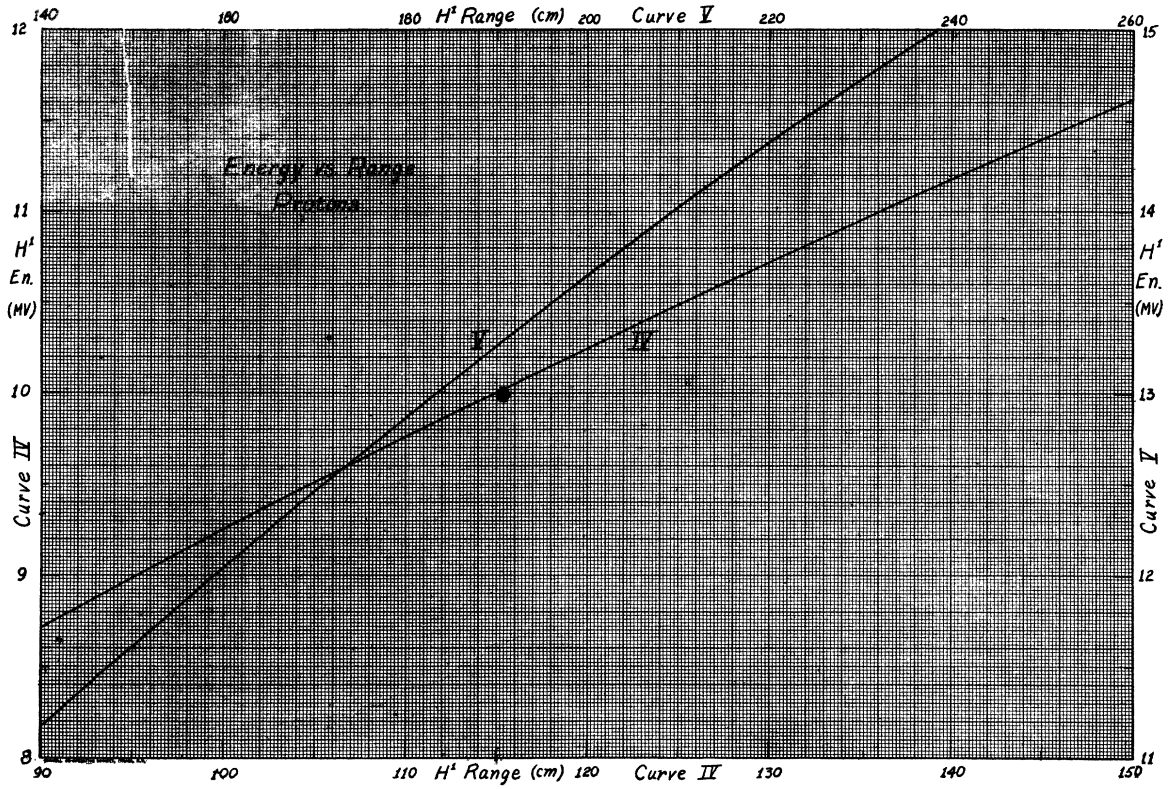

FIG. 30. (a) (b) (page 268) (c) (above) Range-energy relation for protons. (For deuterons, the ranges and the energies should be multiplied by 2.)

In the actual computation, the careful work of Duncanson was used as a starting point. The "stopping number" B was computed according to (758) with relativity corrections, and from Duncanson's formula. The percentage difference was calculated and Duncanson's ranges corrected accordingly. This saved the laborious computation of the integral exponential $Ei(x)$ which occurs in the integrated expression for the range (D18). Only at low energies (below 2.5 MV) Duncanson's calculation was found to be too much in error so that a completely new calculation was made.

For *protons* of high energy (i.e., high enough so that capture and loss of electrons is irrelevant) the energy loss per cm should be just one-quarter of that of an α-particle of the same velocity (cf. (749)), the energy loss being proportional to the square of the charge. Since E is, for a given velocity, proportional to the mass M of the particle, we should have generally

$$R(v, M, z) - R(v', M, z) = Mz^{-2}[f(v) - f(v')], \quad (759)$$

where v and v' are two velocities both large enough to minimize capture and loss of electrons, and f is a function of the velocity independent of mass and charge of the particle. From (759) it follows that

$$R_H(v) = (M_H/M_\alpha)(z_\alpha/z_H)^2 R_\alpha(v) - c, \quad (759a)$$

where c is a constant. With the known masses of hydrogen and helium, and with the constant c as determined experimentally by Blackett (Section A), we have

$$R_H(v) = 1.0072 R_\alpha(v) - 0.20 \text{ cm} \quad (760)$$

or

$$R_H(E) = 1.0072 R_\alpha(3.971E) - 0.20 \text{ cm}. \quad (760a)$$

The constant takes account of the capture and loss of electrons at low energies which affects α-particles more than protons. Its value (0.20

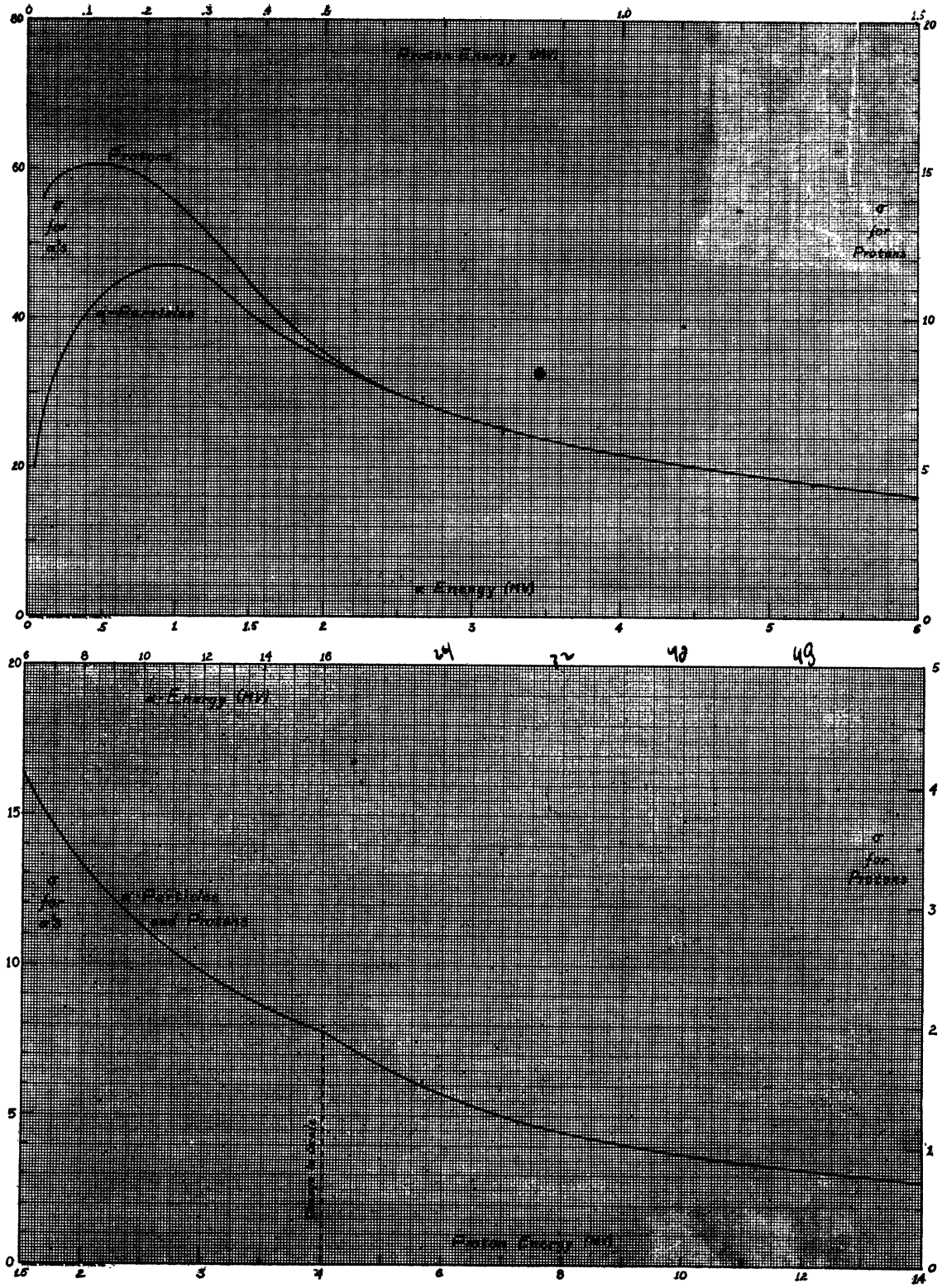

FIG. 31. Cross section for energy loss in 10^{-15} cm^2 volt. Scale for α-particles on left, for protons on right hand side. Abscissa: energy (different scale for protons and α-particles!). (a) (top) Up to 1.5 MV proton (6 MV alpha) energy. (b) (lower) From 1.5 to 14 MV proton energy, with a break of scale at 4 MV.

cm) is probably not very accurate. However, it is satisfactory that the range-energy relation for protons as obtained from (760a) passes very near two experimental points obtained by Cockcroft and Walton (C20). The lowest part of the curve (up to 0.3 MV) was again obtained from Blackett and Lees' experiments, with the energies increased by 9 percent. The rest of the curve is theoretical, with the same empirical corrections applied as for α-particles.

The range-energy relations for the ions of the other hydrogen and helium isotopes (H^2, H^3, He^3) may be obtained immediately from those of proton and α-particle, respectively. Capture and loss of electrons being the same for all hydrogen isotopes (or all helium isotopes) we have *exactly* (i.e., to a better approximation than (759a))

$$R_{z,M}(E)=(M/M_0)R_{z,M_0}(EM_0/M), \quad (761)$$

where $R_{z,M}(E)$ is the range of a particle of charge z, mass M and energy E.

The finally adopted range-energy relations for protons and α-particles are given in Figs. 29, 30. Experimental determinations are not indicated. We believe that our relation is accurate to 10 kv for α-particles between 5 and 10 MV, to about 30 kv between 2 and 5 MV and above 10 MV, to 50 kv between 0.5 and 2 MV and to 10 percent below $\frac{1}{2}$ MV. For protons, we estimate the accuracy to be about 10 percent below 0.2 MV and 20 or 30 kv above. However, more accurate experimental data are very much needed, particularly at low energies where the theoretical relation is least reliable.

D. Stopping cross section and range exponent

For some purposes, particularly for estimating disintegration cross sections from thick target experiments (cf., e.g., §81, 82) the "stopping cross section" is useful. This quantity is defined as the energy loss per cm, divided by the number of atoms per cm^3, or, according to (749):

$$\sigma=\frac{4\pi e^4z^2}{mv^2}B. \quad (762)$$

The dimension of σ is energy times area. The stopping cross section for protons and α-particles in air (per *atom*, not molecule) is given in Fig. 31 as a function of the energy. It is of the order of a few times 10^{-15} volt cm^2. The stopping cross section in other materials is of the same order of magnitude (section E).

For a number of corrections which must be applied to the observed range of particles (§96, 97) the logarithmic derivative of the range with respect to the energy is important. We define

$$n=2\ d\log R/d\log E. \quad (763)$$

For nonrelativistic energies,

$$n=d\log R/d\log v. \quad (763a)$$

If n were constant, R would be proportional to v^n. A relation of this type, with $n=3$, was first proposed by Geiger (G11) and is not very far wrong for natural α-particles. Actually, n varies considerably with energy, increasing from about 1.4 for slow α-particles and protons to over 3.6 for fast protons. For still higher energies, the "range exponent" n approaches 4.

E. Stopping power of substances other than air

According to (749a), the stopping number B (and therefore the stopping power per atom) will in general increase with increasing number Z of electrons in the atom. However, the stopping power increases more slowly than Z itself because the average excitation energy I which occurs in the log is also larger for high atomic number Z. Moreover, it follows immediately that the relative stopping power must be a function of the velocity of the particle. The stopping power of heavy atoms with high excitation potential will increase relatively with increasing particle energy.

The quantity customarily given is the stopping power relative to air,

$$s=B/B_{\text{air}}, \quad (764)$$

where B is the "stopping number" of the material as defined in (749a). The experimental data for s are rather conflicting, the more recent determinations giving consistently higher values for s than the older ones, at least for solid materials. This may be due to nonuniformity of the sheets used for the stopping in the older experiments. As it is most convenient to determine the reduction of the *extrapolated* range of the α-particles by passing through the sheet, the stopping power of the thinnest spot in the absorbing foil will be measured rather than an average. In the more recent experiments which are mainly due to Rosenblum

(R13), the *average* reduction in velocity was measured magnetically as a function of the thickness of the material.

Table XLVIII compares the older and the newer data for the relative stopping power. Part A of this table gives the thickness of various materials (in mg/cm²) equivalent to 1 cm air (1.22 mg/cm²) for the stopping of α-particles of initial range 6 cm, according to older measurements of Marsden and Richardson (quoted by Geiger, G12) and to the more recent ones of Rosenblum (R13). The latter are consistently about 6 percent lower. The old value for mica was obtained by Briggs, the new one calculated (see below). Part B of Table XLVIII gives the atomic stopping powers of various substances for "α-particles of medium velocity" according to Geiger's article in the *Handbuch der Physik* (old measurements) and according to Mano's tables which are based on newer measurements. Mano's values were taken for a velocity of $1.75 \cdot 10^9$ cm/sec. (energy about 6 MV); they are consistently about 10 percent higher for the heavier elements than Geiger's values, with the exception of the rare gases for which no error due to non-uniformity is possible.

TABLE XLVIII. *Relative stopping power of various materials for α-particles of about 6 MV.*

A. Thickness (in mg/cm²) equivalent to 1 cm of air

SUBSTANCE	MARSDEN AND RICHARDSON	ROSENBLUM
Al	1.62	1.51
Cu	2.26	2.09
Ag	3.86	2.71
Au	3.96	3.74
Mica	1.45*	1.43**

B. Atomic stopping power relative to air

SUBST.	GEIGER	MANO	SUBST.	GEIGER	MANO
$\frac{1}{2}H_2$	0.22	0.20	Cu	2.29	2.57
He	0.42	0.35	Kr	2.89	2.92
Li	0.53	0.50	Mo	2.75	3.20
$\frac{1}{2}N_2$	0.98	0.99	Ag	3.04	3.36
$\frac{1}{2}O_2$	1.10	1.07	Sn	3.19	3.59
Ne	1.24	1.23	Xe	3.94	3.76
Al	1.40	1.50	Au	4.02	4.50
A	1.92	1.94	Pb	4.25	4.43

* Briggs.
** Bennett.

In computing theoretical range-energy relations, it must be kept in mind that the innermost electrons can practically not be excited at all by the incident particle. Excitation is very improbable if $\frac{1}{2} mv^2 = mE/M$ is small compared to the ionization potential of the electron concerned. For α-particles of 8 MV energy, we have $mE/M = 1000$ volts, so that all electrons of more than 1000 volts (75 Rydberg) excitation potential will be ineffective in stopping. If we take, e.g., gold ($Z=79$), all the electrons in the K, L and M shells are to be excluded on this ground, i.e. 28 electrons altogether. However, this does not mean that the number of effective electrons is reduced to $79-28=51$, because the stopping effect of an electron is given (B8) by the oscillator strength of the optical transitions into the continuous spectrum. This oscillator strength is smaller than unity for inner, larger for outer electrons. It has been calculated by Hönl (H35) for the K and L shell; for Au the result is about 0.57 and 0.60 for each K and L electron, respectively. Assuming 0.65 for M electrons, the number of electrons effective for stopping would be $79-2\cdot 0.57-8\cdot 0.60-18\cdot 0.65=61.4$ in gold. In a similar way, this number may be determined for other substances.

Figure 32 shows the range-velocity relation for gold with $Z=61.4$ and $I=520$ volts. The agreement with the experimental points of Rosenblum (R13) is satisfactory, except for the last three points. This is understandable because at these low velocities the ionization potential of the N shell becomes comparable to $\frac{1}{2} mv^2$ so that a correction C_N, similar to C_K in (756) and whose exact form has not yet been calculated, should be applied. The curve marked "3.77 air" is obtained if it is assumed that 3.77 mg/cm² of gold are equivalent to 1 cm of air, i.e., that the stopping power of one gold atom is 4.42 times that of an air atom irrespective of the velocity of the particle. The deviations are considerable.

As an illustration of the dependence of the atomic stopping power (764) on the energy, we give in Table XLIX the stopping powers of some

TABLE XLIX. *Atomic stopping power for various velocities (semi-empirical, air = 1).*

v(10^9 cm/sec.)	1.0	1.5	2.0	2.5	3	4	5
E_α (MV)	2.07	4.66	8.3	12.95	18.6	33.2	51.9
E_H (MV)	0.52	1.17	2.09	3.26	4.70	8.36	13.06
$\frac{1}{2}H_2$	0.26	0.224	0.209	0.200	0.194	0.186	0.181
C	0.94	0.932	0.921	0.914	0.908	0.899	0.892
Al	1.45	1.51	1.53	1.54	1.55	1.57	1.59
Cu	(1.92)	2.41	2.62	2.73	2.80	2.89	2.95
Ag	(2.25)	3.08	3.43	3.64	3.76	3.93	4.04
Au	(2.42)	3.96	4.64	5.00	5.25	5.57	5.79

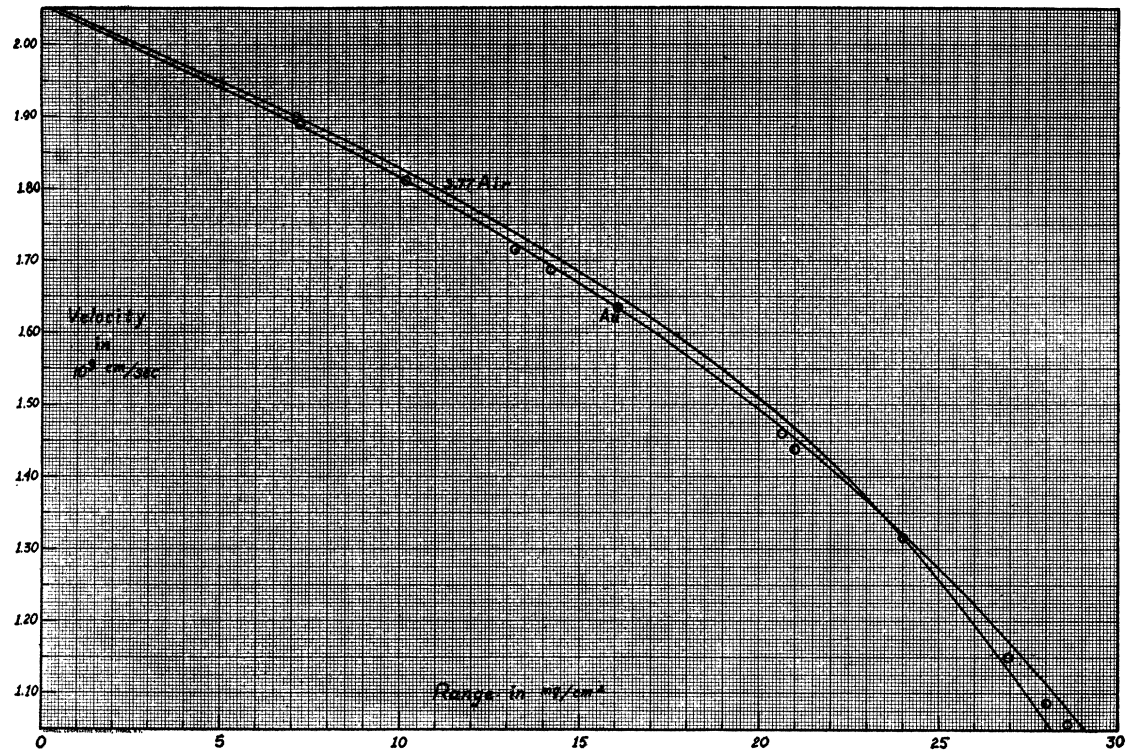

FIG. 32. Range-velocity relation of gold. Abscissa: thickness of gold absorber in mg/cm². Ordinate: velocity of α-particles in 10^9 cm/sec. The curve marked "Au" gives the theoretical range-velocity relation for Au. The curve marked "3.77 air" is computed assuming that 3.77 mg/cm² of Au are equivalent to 1 cm of air. The circles represent experimental points of Rosenblum. They fall closely on the Au curve except at the end where the N electrons of the Au will cease to follow the elementary theory of stopping. The figure shows the variation with velocity of the stopping power of gold relative to air.

elements as functions of the velocity (or energy) of the particle. The effective number of electrons used for Cu and Ag was 27.4 and 39.6, respectively. The average excitation potentials of Al, Cu, Ag and Au were determined so as to make the stopping power near $2 \cdot 10^9$ cm/sec. agree with Rosenblum's experiments. Since no correction was made for the electrons whose ionization potential is of the same order as $\frac{1}{2} mv^2$ (L, M and N electrons for Cu, Ag and Au, respectively), the value obtained for the lowest velocity ($1.0 \cdot 10^9$ cm/sec.) is probably considerably in error for Cu, Ag and Au; the correct value should be higher. For Al and C the correction C_K (Section B) was applied. The average ionization potential of carbon was estimated from that of N_2, O_2 and Ne (cf. Mano) by extrapolation, that of hydrogen was taken from Mano's experiments.

Because of the large variation of the relative stopping power with energy, it is not legitimate to use foils of heavy materials such as Au or Ag for the stopping of particles and to assume them to be equivalent to a given thickness of air. As the range-energy relation in these heavy materials is not yet accurately known either theoretically or experimentally, they should be avoided in range measurements.

For light elements the range-energy relation is sufficiently established to correct for the variation of stopping power with energy. In Fig. 33, we have given the stopping power per atom of hydrogen and carbon relative to air. Hydrogen and methane are frequently used as stopping gases in determinations of neutron energies (§94) by means of the proton recoils. The evaluation of a hypothetical experiment would go as follows: Proton range determined in methane of normal temperature (15°C) and pressure (760 mm) 64.3 cm. Estimated range in air (need not be accurate) 55 cm. For 55 cm, Fig. 33 gives for the stopping powers of C and H the values 0.903_2 and 0.189_1, respectively. Thus stopping power of half a mole-

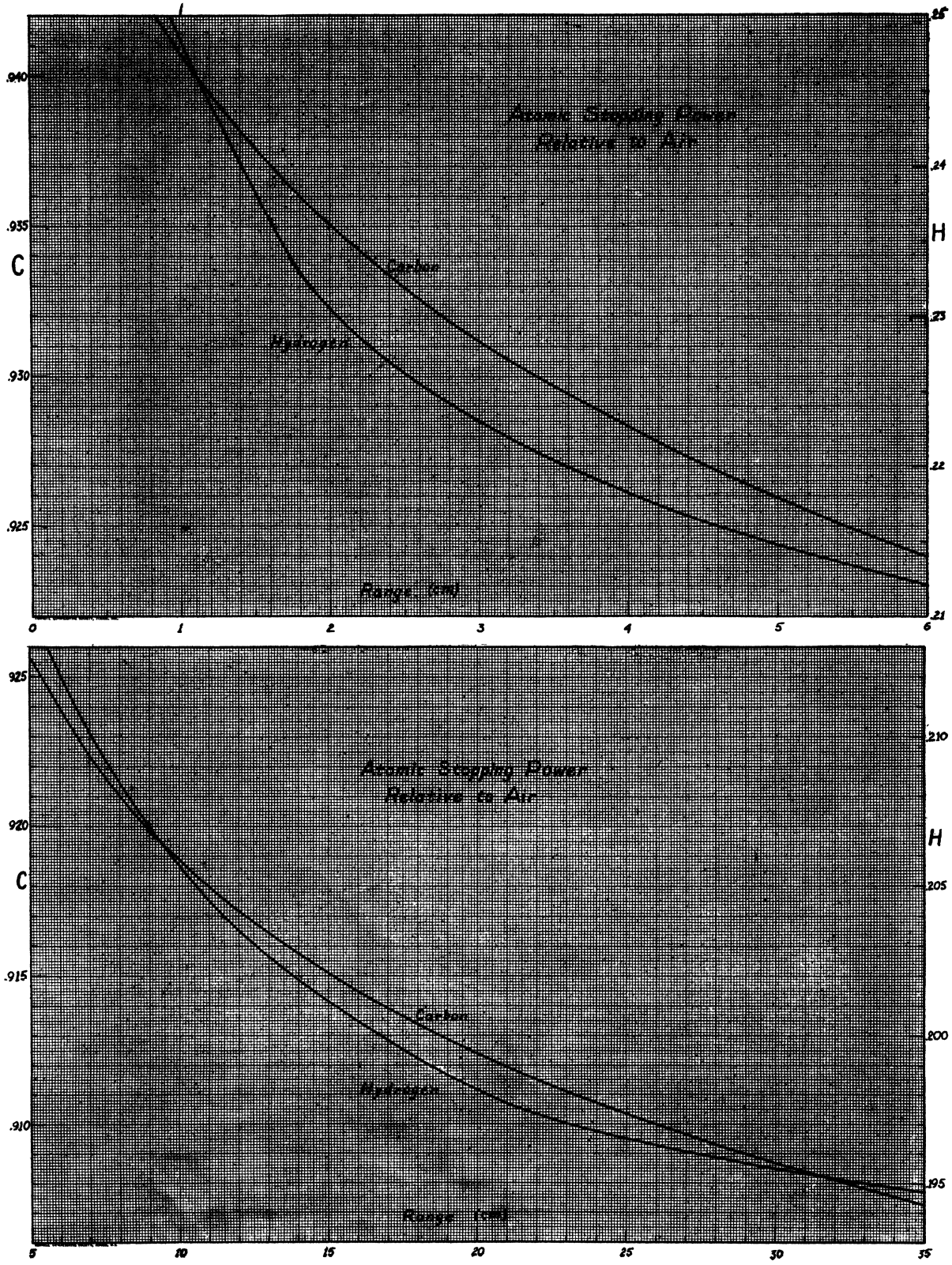
Atomic Stopping Power
Relative to Air
Carbon
Hydrogen
Range (cm)
.940
.935
.930
.925
C
H
.25
.24
.23
.22
.21
0
1
2
3
4
5
6
Atomic Stopping Power
Relative to Air
Carbon
Hydrogen
Range (cm)
.925
.920
.915
.910
C
H
.210
.205
.200
.195
5
10
15
20
25
30
35

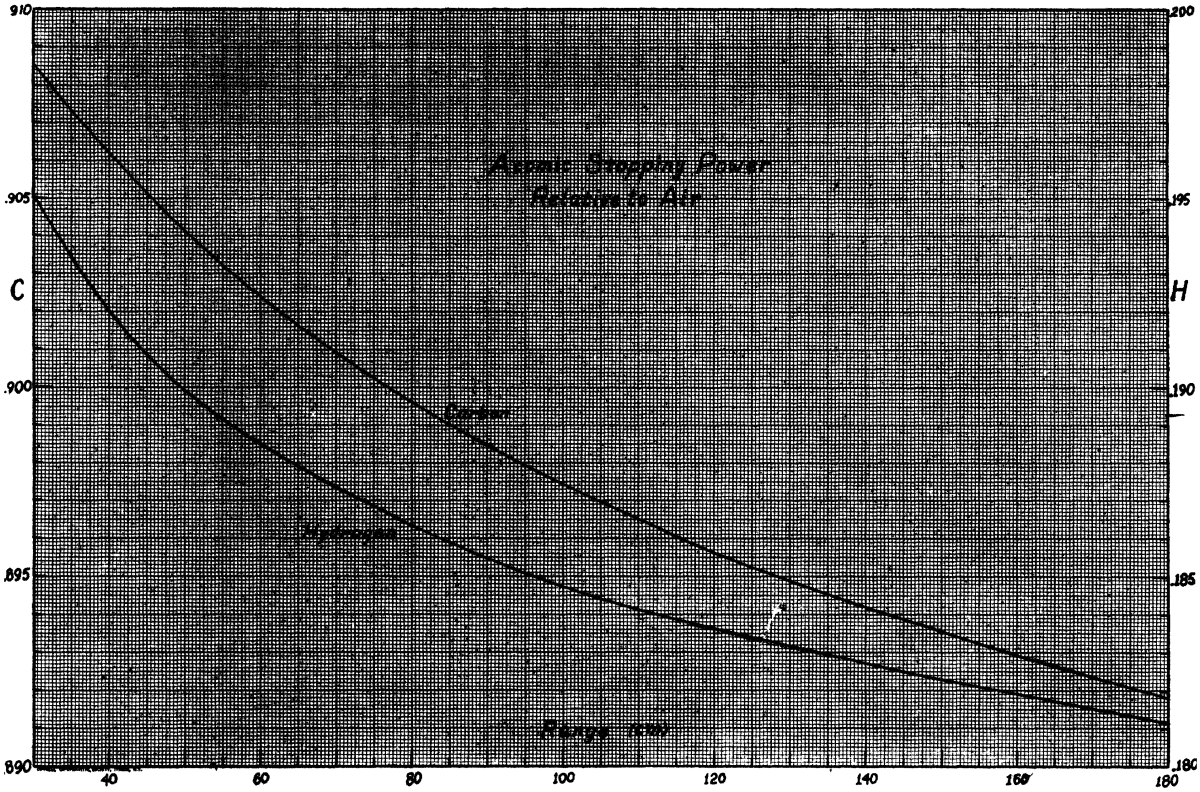

FIG. 33. (a) (b) (page 274) (c) (above) Stopping power of carbon and hydrogen. Abscissa: Range of particles in air. Ordinate: stopping power per atom relative to air. The curve is intended for the evaluation of experiments with hydrogen or methane filled cloud chambers. It is valid for α-particles and protons.

cule of $CH_4 = \frac{1}{2} \cdot 0.903_2 + 2 \cdot 0.189_2 = 0.830$. Therefore range in air $64.3 \cdot 0.830 = 53.3_7$ cm. (For this value of the range, the exact stopping power of methane would be 0.830_8, corresponding to a range in air of 53.4_2 cm. The difference is insignificant.)

For Al we have given the correction in a different form. As a first approximation, the stopping power of an Al atom may be put equal to 1.500. This means that 1.51_8 mg/cm^2 of Al are equivalent to one cm of air. With this reduction factor, the thickness of Al may be expressed in equivalent centimeters of air. To the "equivalent range" obtained in this way, a correction must be added which is given in Fig. 34 as a function of the equivalent range itself. The result is the range in air from which the energy is obtained in the usual way from Figs. 29, 30.[4]

In re-evaluating experimental data (Chapter XVII and XVIII) we have, therefore, not made any corrections for the absolute stopping power of mica. We have, however, corrected for the change of the stopping power with velocity by adding half the aluminum correction given in Fig. 34, corresponding to the fact that about half the stopping power of mica is due to the heavy atoms Al, Si and K, and half to oxygen and hydrogen.

F. Range of particles heavier than helium

Nuclei of Li and heavier elements are ordinarily only partially ionized at the velocities with which they are commonly produced in nuclear collisions. Since the dependence of the effective charge on the energy is unknown, no theoretical treatment of the range-energy relation is possible.

[4] Frequently, aluminum is only used for the first part of the stopping, the rest of the path being in air. In this case, the correction may also be read off Fig. 34. Suppose, e.g., the total range of an α-particle consists of 5.93 equivalent cm in Al and then 3.54 cm air, together 9.47 cm. The correction given in Fig. 34 for 9.47 cm is 0.041 cm, for 3.54 cm we find -0.026 cm. The total correction is the difference of these two figures, i.e. 0.067 cm, therefore the range in air 9.54 cm.

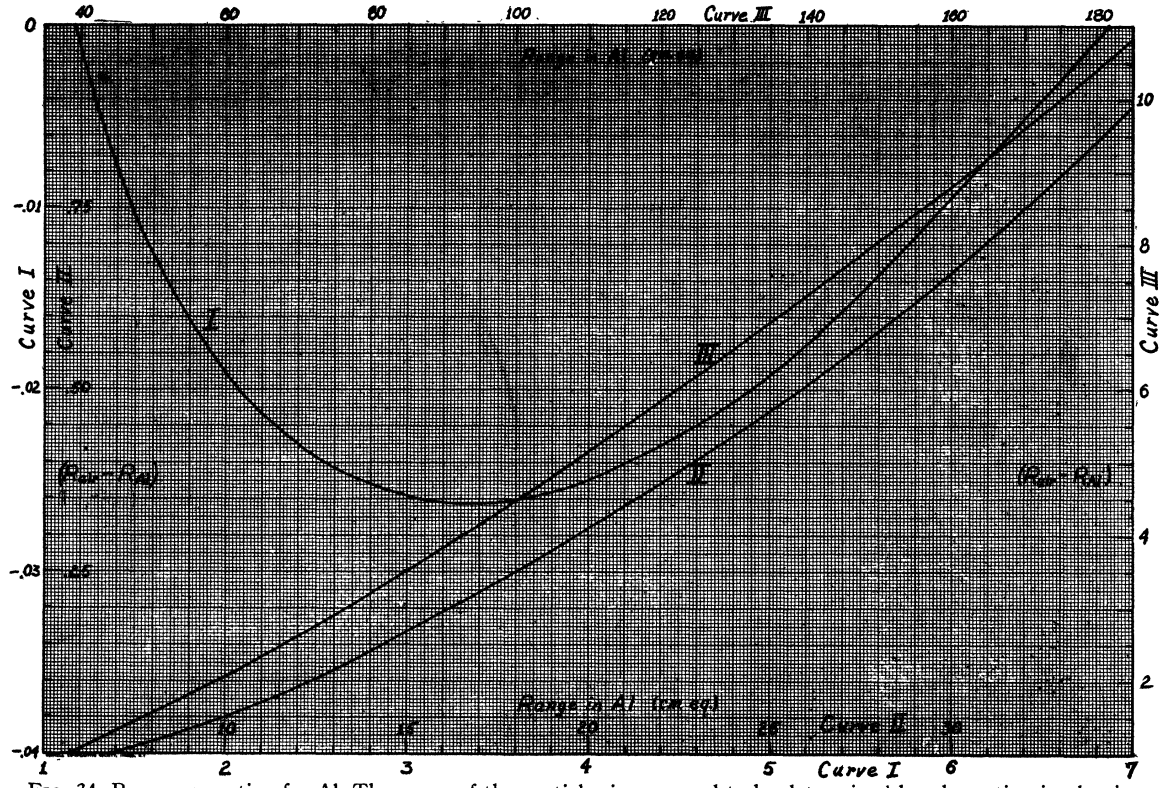

FIG. 34. Range correction for Al. The range of the particles is supposed to be determined by absorption in aluminum foils whose air equivalent has been measured beforehand using natural α-particles for calibration or using a suitable conversion factor (e.g., 1.52 mg/cm^2 Al = 1 cm air). For any value of the equivalent range in air thus obtained (abscissa), the curve gives the correction to be applied for the variation of the stopping power of Al with velocity (ordinate). For mica, one-half the correction should be applied. Curve valid for protons and α-particles.

Experimental data have been obtained by Blackett and Lees (B25) for N^{14}, O^{16}, O^{17} and A^{40} nuclei, by Feather (F7) for C^{12} and F^{19}. The method used was in all cases to observe, in a cloud chamber, the range of recoil atoms produced in collisions by α-particles of known energy. The range-energy relations obtained are rather irregular and the accuracy is quite small owing to the small number of recoil tracks measured. Therefore any experimental results which are based on the range-energy relations for heavy nuclei are very unreliable. This is true, e.g., for all measurements of disintegration energies in disintegrations produced by fast neutrons (§102) as has been pointed out by Feather (F8) and by Bonner and Brubaker (B41).

§96. Momentum Relations and Recoil Energy

In the most common type of nuclear reactions, we have two nuclei (initial nucleus and incident particle) in the beginning, which are transformed in the reaction into two other nuclei. Ordinarily, one of these resultant nuclei is light (mass 4 or less) the other heavier. The lighter one has ordinarily greater velocity and therefore longer range; it is therefore easier to observe. We call the particle which is actually observed in the experiments the "emitted particle" and the other nucleus produced in the reaction the "residual" or "recoil" nucleus. Our problem in this section is to determine the total energy Q evolved in the reaction when the range of the emitted particle is known. This is done by calculating the recoil energy of the residual nucleus from the law of conservation of momentum.

Let the subscript 0 refer to the initial nucleus, 1 to the incident particle, 2 to the produced particle and 3 to the residual nucleus. Let $M_0 \cdots M_3$ be the masses of the four nuclei, and $M = M_0 + M_1 = M_2 + M_3$ the total mass (mass of the compound nucleus). The kinetic energies of the particles

shall be denoted by $E_0 \cdots E_3$. The initial nucleus will in all practical cases be at rest so that $E_0=0$. The total energy evolution is

$$Q=E_2+E_3-E_1. \tag{765}$$

This quantity is the difference between the internal energies (masses) of the initial and final products of the reaction.

The law of conservation of momentum is

$$\mathbf{p}_3=\mathbf{p}_1-\mathbf{p}_2, \tag{766}$$

where $\mathbf{p}_i$ denotes the momentum of particle i, and $\mathbf{p}_0$ has been assumed to be zero (see above). We denote the angle between the directions of motion of incident and produced particle by ϑ. Using the relation[5]

$$p_i^2=2M_iE_i \tag{766a}$$

we obtain then

$$M_3E_3=M_1E_1+M_2E_2 -2(M_1M_2E_1E_2)^{\frac{1}{2}}\cos\vartheta. \tag{767}$$

Relation (767) gives the recoil energy E_3 if the angle ϑ is known. In most experiments, the geometrical arrangement is such that the produced particles leave the target perpendicularly to the incident beam ($\vartheta=90°$). Then (767) reduces to

$$E_3=(M_1E_1+M_2E_2)/M_3. \tag{767a}$$

Inserting this into (765), we obtain

$$Q=(M_2+M_3/M_3)E_2-(M_3-M_1/M_3)E_1. \tag{768}$$

Another arrangement often used in α-particle experiments is observation of the particles emitted *in* the direction of the incident beam ($\vartheta=0$). Then

$$E_3=(M_1^{\frac{1}{2}}E_1^{\frac{1}{2}}-M_2^{\frac{1}{2}}E_2^{\frac{1}{2}})^2/M_3. \tag{769}$$

In all cases, relative masses (atomic weights) may be used; and in almost all cases the exact atomic weights may be replaced by the mass numbers.

The formulae given have been widely used for calculating nuclear reaction energies. However, it must be pointed out that no experimental arrangement yet devised is geometrically so perfect that it is justified to put the angle ϑ exactly equal to 90° (or exactly equal to zero). In all practical cases, there will be a certain finite solid angle about the average of, say, 90° in which particles are observed. Since the recoil energy is very sensitive to the exact value of ϑ, corrections are necessary.

We assume an arrangement of the kind most commonly used (e.g. O8, C28) where the most direct path from target to detector is perpendicular to the incident beam but particles emitted in a rather wide solid angle may also reach the detector. According to (767), the recoil energy will be smaller if particle 2 is emitted in a more forward direction, and therefore the energy of particle 2 itself will be larger in this case. E_2 may be calculated as a function of ϑ if we express E_3 in (767) in terms of E_1E_2 and Q by (765). Solving for E_2, we obtain

$$ME_2^{\frac{1}{2}}=(M_1M_2)^{\frac{1}{2}}E_1^{\frac{1}{2}}\cos\vartheta +(MM_3Q+M_0M_3E_1-M_1M_2E_1\sin^2\vartheta)^{\frac{1}{2}}. \tag{770}$$

For small values of $\cos\vartheta$, this reduces to

$$E_2=E_2^0+2(M_1M_2E_1E_2^0)^{\frac{1}{2}}\cos\vartheta/M, \tag{770a}$$

where $$E_2^0=(M_3/M)Q+(M_3-M_1/M)E_1 \tag{770b}$$

is the energy of the emitted particle for emission at right angles to the incident beam.

The particles emitted in a more forward direction have, according to (770a), more energy and therefore longer range than those emitted at 90°. Since in most experiments the longest range is measured, the experimental determinations do not refer to emission at 90°. On the other hand, emission in the most forward direction possible geometrically is often not the most favorable case either, because then the particles have to

[5] Relativistic corrections need practically never be considered. The relativistically correct relation would be

$$p_i^2=2M_iE_i+E_i^2/c^2. \tag{A}$$

In the most important case $\vartheta=90°$ this gives a correction to the recoil energy

$$\delta E_3=(E_1^2+E_2^2-E_3'^2)/2M_3c^2, \tag{B}$$

where E_1 and E_2 are the measured energies of incident and emitted particle and E_3' the recoil energy calculated from the nonrelativistic formula (767). If the incident particle is slow compared to the emitted one, (B) reduces to

$$\delta E_3=\frac{E_2^2}{2M_3c^2}\frac{M_3^2-M_2^2}{M_3^2}. \tag{C}$$

As a typical example, we may choose the reaction $B^{10}+H^2 \rightarrow Be^8+He^4$. The energy E_2 of the emitted α-particles is about 12 MV, for small deuteron energy. Thus

$$\delta E_3=\frac{12^2}{2\cdot 8\cdot 930}\cdot\frac{3}{4}=0.007 \text{ MV}. \tag{D}$$

In most other cases, the relativistic correction is still smaller.

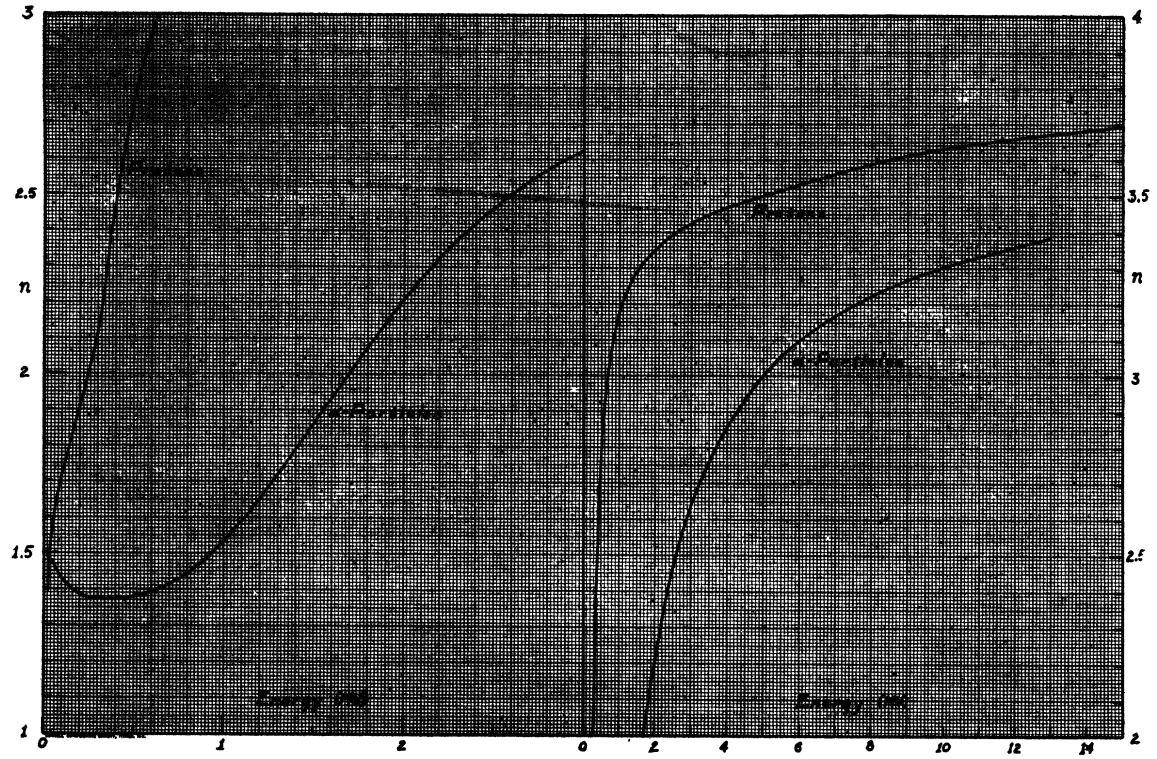

FIG. 35. Range exponent n for protons and α-particles. Over small regions, the range is proportional to the nth power of the velocity. Analytical definition: $n=2\ d\log R/d\log E$. The large deviations from Geiger's law ($n=3$) are apparent. The range exponent is important for thick target correction, angular straggling etc. (§§ 96, 97.)

traverse the material (air or absorbing foils) between target and detector obliquely. In general, there will be an optimum angle ϑ_0 for which the component x of the particle range R in the direction from target to detector is largest. We have

$$x=R\sin\vartheta\approx R(1-\tfrac{1}{2}\cos^2\vartheta). \qquad (771)$$

Furthermore, if R_0 is the range corresponding to emission at right angles ($\vartheta=90°$), and $n=2\ d\log R/d\log E$ (cf. §95 D and Fig. 35), we have

$$R=R_0[1+n(M_1M_2)^{\frac{1}{2}}M^{-1}(E_1/E_2{}^0)^{\frac{1}{2}}\cos\vartheta]. \qquad (771a)$$

According to (771), (771a), x has a maximum at ϑ_0 where

$$\cos\vartheta_0=n\frac{(M_1M_2)^{\frac{1}{2}}}{M}\left(\frac{E_1}{E_2{}^0}\right)^{\frac{1}{2}}. \qquad (772)$$

We may now distinguish two cases: "Good geometry," i.e., small aperture of the observing apparatus, and "poor geometry," i.e. large aperture. The condition for "poor geometry" is that particles emitted at an angle ϑ_0 may pass freely from target to detector. "Good geometry" means that all particles emitted in the direction ϑ_0 are prevented from reaching the detector. Both these cases are easy to treat; only the intermediate case would offer difficulties.[6] Fortunately, all of the more important experiments were made either with "good" or with "poor" geometry. We have, e.g., "good geometry" in the experiments of Oliphant, Rutherford and collaborators (O8, O9) and in those of Cockcroft and Lewis (C28, C29) "poor geometry" in the older experiments of Cockcroft and Walton (C23, C25) and in the older experiments of the California group (L16). The values of ϑ_0 vary widely: e.g., for α-particles from the reaction $Li^7+H^1=2He^4$, we have about $\cos\vartheta_0=0.13$ for $E_1=100$ kv, and $\cos\vartheta_0=0.4$ for $E_1=1$ MV. For protons from $Na^{23}+H^2=Na^{24}+H^1$, we would have $\cos\vartheta_0=0.08$ only for

[6] Therefore an improvement of the geometry is not always an advantage, unless the aperture can be reduced to decidedly less than $\cos\vartheta_0$.

$E_1=1$ MV. Thus it is fairly difficult to obtain "good geometry" for reactions with heavy nuclei, but in this case the recoil energy is not particularly important.

We treat now the two possible cases separately:

a. "*Poor geometry*" (aperture$\gg\cos\vartheta_0$). The most penetrating particles are those emitted in the direction ϑ_0. They penetrate through a thickness of material

$$x_0=R_0(1+\tfrac{1}{2}\cos^2\vartheta_0). \tag{772a}$$

If their energy is calculated from their "range" x_0, it is found to be

$$E_2^m=E_2^0\left(1+\frac{1}{n}\cos^2\vartheta_0\right) \tag{772b}$$

or, inserting (772)

$$E_2^m=E_2^0+n\frac{M_1M_2}{M^2}E_1. \tag{772c}$$

The reaction energy Q may now be expressed in terms of the "observed" energy E_2^m of the emitted particle by inserting the value of E_2^0 from (772c) into (768):

$$Q=\frac{M}{M_3}E_2^m+E_1\frac{M_1}{M_3}\left(1-n\frac{M_2}{M}\right)-E_1. \tag{773}$$

The term nM_2/M represents the correction for the forward emission of the particles. It often cancels or even over-compensates the term E_1M_1/M_3.

In the actual evaluation of experiments, it must be remembered that x_0 is only the effective range of the most penetrating particles but that we do not have a homogeneous group of particles of range x_0. If the direction of actual emission forms an angle χ with the "most favorable direction" (either because ϑ is larger or smaller than ϑ_0, or because of a sideways deviation from the plane defined by incident beam, target and detector, or both), the effective range will be $x=x_0\cos\chi$. Within certain limits given by the geometry, the number of particles emitted in the direction χ is proportional to $\sin\chi d\chi$. Therefore the number of particles of observable range between x and $x+dx$ is proportional to dx for all values of x below x_0 and above a certain lower limit x_1 given by the geometry. This will be of importance for determining the mean range from the extrapolated range (§97).

b. "*Good geometry*" (aperture$\ll\cos\vartheta_0$). The variation of the particle range because of the variation of ϑ will be slight. It may most conveniently be considered as a straggling of the ranges of the emitted particles which is added to the ordinary straggling arising from the process of stopping (§97A). We calculate this angular straggling assuming that the beam of emitted particles is defined by two circular openings of radius a at a distance b from each other ($b\gg a$). Such an arrangement has been used by Oliphant, Kempton and Rutherford (O8, O9) by Cockcroft and Lewis (C28, C29) and others.

A beam of particles which passes the first opening at an angle of χ with the normal, will be displaced by the amount

$$c=b\tan\chi \tag{774}$$

when it arrives at the second opening. The fraction of particles passing through this second circle is therefore proportional to the common area of two circles of radius a whose centers are a distance c apart. This area is, apart from the trivial factor a^2:

$$f(c)=2\varphi-\sin 2\varphi, \tag{774a}$$

where

$$\cos\varphi=c/2a. \tag{774b}$$

The function $f(c)$, although not a Gaussian function, may be approximated by one. This is convenient for comparison with the ordinary straggling due to stopping. As the best Gaussian function approximating $f(c)$, we may take that which gives the same value for the average of c^2. From (774a) we have

$$\frac{(c^2)_{Av}}{a^2}=\frac{4\int_0^{\pi/2}\cos^2\varphi(2\varphi-\sin 2\varphi)d\varphi}{\int_0^{\pi/2}(2\varphi-\sin 2\varphi)d\varphi}$$

$$=2\frac{\pi^2-8}{\pi^2-4}=0.637, \tag{774c}$$

so that the "best" Gaussian function is

$$g(c)=\exp(-c^2/1.274a^2). \tag{775}$$

The energy of the particles depends on the angle ϑ with the incident beam. We assume again that the direction of observation is approximately $\vartheta=90°$. Denoting by ψ the angle between

the direction of emission of a particle and the plane formed by the incident beam and the axis of the detecting system, we have since χ is small:

$$\tan^2\chi=\chi^2=\psi^2+(\cos\vartheta)^2. \qquad (775a)$$

The number of particles with a given ϑ detected is now proportional to

$$\int_{-\infty}^{\infty} g(c)d\psi\sim\exp(-b^2\cos^2\vartheta/1.274a^2). \qquad (775b)$$

The extension of the integration over ψ from $-\infty$ to $+\infty$ is allowable because of the rapid decrease of $g(c)$. Expressing $\cos\vartheta$ in terms of the range R of the particle by (771a), we find that the number of particles of range R observed will be proportional to[7]

$$g(R)=\exp(-\pi(R-R_0)^2/4\gamma^2), \qquad (776)$$

where
$$\gamma^2=\pi\frac{\pi^2-8}{\pi^2-4}\frac{a^2}{b^2}n^2R_0{}^2\frac{M_1M_2}{M^2}\frac{E_1}{E_2{}^0}. \qquad (776a)$$

The numerical factor is almost exactly unity, so that

$$\frac{\gamma}{R_0}=\frac{a}{b}n\frac{(M_1M_2)^{\frac{1}{2}}}{M}\left(\frac{E_1}{E_2{}^0}\right)^{\frac{1}{2}}. \qquad (777)$$

Since the geometry is "good," the ratio a/b is small. Also, in general the masses of incident and emitted particle, M_1 and M_2, are small compared to the total mass M, and the energy of the incident particle is small compared to that of the outgoing. Therefore the "angular straggling" γ is small compared to the range R. However, it is usually of the same order as the natural straggling due to stopping.

In this discussion of the case of good geometry, we have neglected entirely the *geometrical* effect of the obliquity of the particles on the apparent range which played a rather important rôle in the case of poor geometry. The apparent range of a particle moving at an angle χ with the axis of the detecting system is reduced by a factor

$$\cos\chi\approx 1-\tfrac{1}{2}\chi^2. \qquad (778)$$

With the distribution function (775), this gives in the average

$$(\cos\chi)_{Av}=1-a^2/\pi b^2. \qquad (778a)$$

[7] This form of the exponential is convenient for calculating the extrapolated range, §97.

In the experiments of Oliphant and collaborators (O8, O9), we have $a/b=1/12$, in those of Cockcroft and Lewis (C28, C29), $a/b=0.1125$. Thus the correction term in (778a) amounts to 0.22 and 0.40 percent, respectively, which is just noticeable when the reaction energies are given to 0.01 MV as is customary (cf. Tables LII ff).

However, the actual correction is even less than this. In the experiments of Oliphant, the ranges of the disintegration particles were compared to those of Th C″ α-particles. The latter are, of course, subject to the same obliquity correction as the former. Therefore, the obliquity correction should, in these experiments, only be applied to the *difference* between the particle range and the range of the Th C″ alphas. In a case like the α-particles from $Li^7+H^1=2He^4$, which have almost the same range as Th C″ alphas, the correction is therefore entirely negligible, and even for the long range alphas from $Li^6+H^2=2He^4$, it amounts only to 0.02 cm (=0.02 MV in Q). Therefore, we have applied this correction only to the best investigated reactions.

If the range is determined in mica or another substance whose stopping power must be measured before the actual experiment, no obliquity correction should be applied at all because the percentage correction is the same for the particles used for the calibration as for the disintegration particles themselves.

Besides the change of the average range, there is also a very small contribution to the angle straggling (776a) from the obliquity.

Three-particle disintegrations

Disintegrations leading to three product nuclei follow, according to the general theory (§85) the scheme

$$A+P\rightarrow C\rightarrow B^*+R;\qquad B^*\rightarrow D+S. \qquad (779)$$

The indices 0, 1, . . . 5 shall refer to the particles A, P, R, B, S and D, respectively. M_i denotes the mass, E_i the energy of particle i, $M=M_0+M_1$ is the mass of the compound nucleus C, Q_1 the energy evolution in the first part of the reaction, Q_2 the energy set free in the break-up of nucleus B^*. The velocity of the center of gravity is

$$v_0=(2M_1E_1)^{\frac{1}{2}}/M. \qquad (779a)$$

In the center of gravity system the energies of the particles are:

$$E_2'=[Q_1+(M_0/M)E_1]M_3/M, \qquad (780)$$

$$E_3'=[Q_1+(M_0/M)E_1]M_2/M, \qquad (780a)$$

$$[(E_3'M_4)^{\frac{1}{2}}-(Q_2M_5)^{\frac{1}{2}}]^2/M_3<E_4'<[(E_3'M_4)^{\frac{1}{2}}+(Q_2M_5)^{\frac{1}{2}}]^2/M_3 \quad (780b)$$

and E_5' correspondingly. The distribution of the values of E_4' between the limits indicated in (780b) is uniform if the direction of emission of the particles D and S is independent of the direction of motion of nucleus B.

The energy of any particle i emitted at an angle ϑ with the incident beam is in the *ordinary* coordinate system

$$E_i=E_i^0\left(1+2\frac{(M_iM_1)^{\frac{1}{2}}}{M}\left(\frac{E_1}{E_i^0}\right)^{\frac{1}{2}}\cos\vartheta\right), \quad (781)$$

where E_i^0 is the energy of a particle emitted at right angles to the incident beam:

$$E_i^0=E_i'-M_iM_1M^{-2}E_1, \quad (781a)$$

E_i' being the energy in the center of gravity system. Formulae (781, 781a) are valid for *any* type of disintegration and any mechanism (cf. (770a)). They show that the corrections for the deviation of the direction of emission from 90° are the same for three as for two particle disintegrations.

The energies of the particles emitted at right angles in the three-particle disintegration are, according to (780) to (781a):

Particle R: $E_2^0=Q_1M_3/M+E_1(M_3-M_1)/M.$ (781b)

Particle S: for $E_1\ll Q_1$ and Q_2, maximum and minimum energies:

$$(E_4)_{\min}^{\max}=\left[\left(Q_1\frac{M_2M_4}{MM_3}\right)^{\frac{1}{2}}\pm\left(Q_2\frac{M_5}{M_3}\right)^{\frac{1}{2}}\right]^2+\frac{M_4}{M^2}E_1\left[\frac{M_0M_2}{M_3}\left|1\pm\left(\frac{Q_2M_5M}{Q_1M_4M_2}\right)^{\frac{1}{2}}\right|-M_1\right]. \quad (781c)$$

With the help of (781b) and (781c), the reaction energies Q_1 and Q_2 can be deduced from the observations. This has been done, for the reaction $B^{11}+H^1\rightarrow 3He^4$, in §85.

Determination of reaction energies from the angular distribution of recoil nuclei

It has been suggested by Newson (N6) that the energy evolved in nuclear reactions can be determined from the angular distribution of the recoil nuclei. This can be conveniently done if the residual nucleus is radioactive.

Let χ denote the angle between the incident beam and the direction of motion of the recoil nucleus in the center of gravity system, φ the same angle in the ordinary coordinate system, v_0 the velocity of the center of gravity and v that of the recoil nucleus in the center of gravity system. Then in the ordinary coordinate system the velocity component parallel to the incident beam is $v_0+v\cos\chi$, the perpendicular component $v\sin\chi$, and therefore

$$\cot\varphi=\frac{v_0}{v\sin\chi}+\cot\chi. \quad (782)$$

We must distinguish two cases:

(a) $v_0<v$: Then, as χ goes from 0 to π, φ goes through the same interval.

(b) $v_0>v$: In this case, cot φ has a minimum for $\cos\chi=-v/v_0$.

At the minimum, we have

$$\cot\varphi_0=+(v_0^2/v^2-1)^{\frac{1}{2}}, \quad (782a)$$

$$\sin\varphi_0=v/v_0. \quad (782b)$$

This means that the recoil nuclei can only be emitted into a cone around the direction of the incident beam whose half-aperture φ_0 is less than 90°. By measuring the maximum angle at which recoil nuclei appear, v/v_0 can be found. This in turn determines Q; we have

$$v_0=(2M_1E_1)^{\frac{1}{2}}/M, \quad (783)$$

$$v=\left[\frac{2M_2}{MM_3}\left(Q+\frac{M_0}{M}E_1\right)\right]^{\frac{1}{2}}, \quad (783a)$$

$$Q=\frac{E_1}{M}\left[\frac{M_1M_3}{M_2}\left(\frac{v}{v_0}\right)^2-M_0\right]. \quad (783b)$$

The method is well applicable only in case (b), i.e., if $v_0>v$. Assuming that initial and resultant nucleus are heavy compared to incident and outgoing particle, this condition is equivalent to

$$M_1E_1>M_2(Q+E_1), \quad (783c)$$

$$Q<(M_1-M_2)E_1/M_2. \quad (783d)$$

If the incident particle is *lighter* than the outgoing, this requires a highly endoergic process. Therefore the method is practically never applicable to processes in which the emitted particle is an α-particle and the incident one a lighter particle (proton, neutron, deuteron). If the incident particle is heavier than the outgoing one, the condition requires that the process be not too exoergic. E.g., if the incident particle is a deuteron, the outgoing a proton or neutron, the condition is $Q<E_1$. In this case, the method is applicable when the incident particle is fast enough.

The angular distribution itself can be calculated if we assume that in the center of gravity system any direction of emission is equally probable. Then the number of particles per unit solid angle in the ordinary coordinate system is

$$N(\varphi)=\frac{\sin\chi d\chi}{\sin\varphi d\varphi}. \quad (784)$$

In case (a), this expression has the value

$$N(\varphi)\propto(1-\gamma^2\sin^2\varphi)^{-\frac{1}{2}}+2\gamma\cos\varphi, \quad (784a)$$

while in case (b):

$$N(\varphi)\propto(1-\gamma^2\sin^2\varphi)^{-\frac{1}{2}};\ \gamma=v_0/v. \quad (784b)$$

In this latter case, $N(\varphi)$ becomes infinite near the limiting angle φ_0 which should facilitate observation of this angle.

§97. Extrapolated and Mean Range, Corrections for Thick Target, etc.

A. Straggling of energy loss

Since the loss of energy by charged particles occurs in discrete amounts, the energy lost after a given length of path will show statistical fluctuations. It can be shown that the mean square fluctuation of the energy is given by

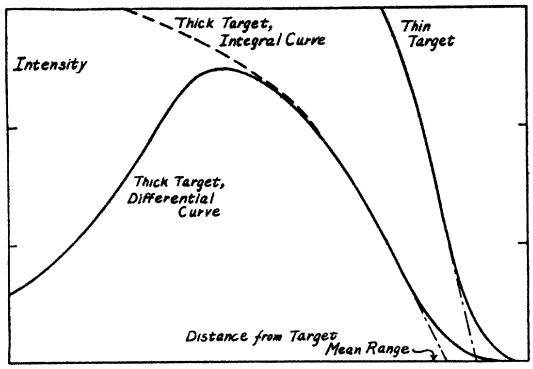

FIG. 36. Theoretical range distribution of disintegration products from a thin and thick target. For the thick target, the distribution is given (a) for a detector counting *all* particles ("integral" curve), (b) for a "differential detector" counting only particles near the end of their range. All curves are "extrapolated" along the steepest tangent. The extrapolated range for the thin target is seen to be much longer than for the thick target while for the latter it is practically independent of the type of detector used ("integral" or "differential"). The mean range is also indicated; the difference between extrapolated and mean range is much larger for the thin than for the thick target.

$$[(E^2)_{Av}-(E_{Av})^2]_X=N\int_0^X dx\sum_n E_n^2\sigma(E_n). \quad (785)$$

Here X is the amount of stopping material traversed, N the number of atoms per cm^3 in the material, E_n the excitation energy of the nth excited level of these atoms, and $\sigma(E_n)$ the cross section for the excitation of this level by the incident particle. $\sigma(E_n)$ is given by

$$\sigma(E_n)=\frac{2\pi e^4z^2}{mv^2}\int\frac{dQ}{Q^2}\times\left|\int\Psi_0\Psi_n^*\sum_j\exp\left(i(\mathbf{p}-\mathbf{p}')\cdot\mathbf{r}_j/\hbar\right)d\tau\right|^2, \quad (785a)$$

where $\mathbf{p}$ and $\mathbf{p}'$ are the momenta of the incident particle before and after collision, $\mathbf{r}_j$ the position of the electron j in the atom, Ψ_0 and Ψ_n the atomic wave functions of ground state and excited state, and

$$Q=(\mathbf{p}-\mathbf{p}')^2/2m, \quad (785b)$$

differing by a constant factor from the definition given in (754). σ is, of course, a function of the energy of the particle and therefore of the distance X traveled from the source.

Equation (785) may be evaluated by inverting the order of summation over n and integration over Q and using the completeness relation (cf. B8). In this way, an expression is obtained which involves only the wave function Ψ_0 of the ground state. We may then assume that Ψ_0 can be written as an antisymmetrical product (determinant) of wave functions of the individual electrons in the atom (Hartree-Fock approximation). Then we find

$$\frac{d}{dX}[(E^2)_{Av}-(E_{Av})^2]=\frac{2\pi e^4z^2N}{mv^2}\sum_k S_k, \quad (786)$$

where S_k is the contribution of the kth electron in the atom to the straggling (except for a constant factor). We have

$$S_k=\int_{Q_{\min}}^{Q_{\max}}dQ\left[1+\frac{4}{3}\frac{E_k-V_{ka}}{Q}-\frac{1}{Q^2}\sum_{l(\text{occ})}(E_l-E_k)^2\times\left|\int\exp\left(i(\mathbf{p}-\mathbf{p}')\cdot\mathbf{r}/\hbar\right)\psi_k\psi_l d\tau\right|^2\right]. \quad (786a)$$

Here E_k is the energy of the kth electron, V_{ka} its average potential energy in the atomic field so that E_k-V_{ka} is the average kinetic energy. The sum over l extends over all electronic states occupied by electrons in the atom in question; it takes account of the Pauli principle. ψ_k and ψ_l are the wave functions of the electronic states k and l. $Q_{\max}$ is the largest value which Q can take when momentum is conserved between the incident particle and the electron ejected from the atom,[8] *viz.*

$$Q_{\max}=2mv^2=(4m/M)E. \quad (786b)$$

$Q_{\min}$ is a suitable average of the quantity Q_0 defined in (754a); in sufficient approximation we may put

$$Q_{\min}=MI_k^2/4mE=I_k^2/2mv^2, \quad (786c)$$

where I_k is the average excitation potential of the kth electron defined similarly as in (749a). The contribution of small Q's to (786a) is small so that the exact value of $Q_{\min}$ does not matter.

For small values of $Q(<I_k)$, the second term in the square bracket in (786a) is partly compensated by the last term (sum over l), while the first term is comparatively small. For larger Q, the

[8] It is easy to show (B8) that for larger values of Q the expression (785*a*) becomes very small for any state n. (786*b*) corresponds to a velocity $2v$ of the ejected electron.

sum is negligible. Therefore we may write

$$S_k = Q_{\max} + \kappa'(E_k - V_{ka}) \log (Q_{\max}/Q_{\min}), \quad (787)$$

where κ' is between about 2/3 and 4/3. (For hydrogen, it is exactly 4/3.) The average potential energy V_{ka} would be equal to $2E_k$ for a pure Coulomb field (hydrogen) but is very much larger ($10E_k$ and more) for the outer electrons of heavy atoms. Thus $E_k - V_{ka}$ will in general be larger than the average excitation potential I_k. We may thus replace $\kappa'(E_k - V_{ka})$ by κI_k where κ is larger than κ', maybe about 4/3 or larger. Inserting (786b, c), this gives

$$S_k = 2mv^2 + 2\kappa I_k \log (2mv^2/I_k) \quad (787a)$$

and (786) becomes

$$\frac{d}{dX}[(E^2)_{Av} - (E_{Av})^2] = 4\pi e^4 z^2 N\left(Z' + \sum_n \kappa_n \frac{I_n Z_n}{mv^2} \log \frac{2mv^2}{I_n}\right). \quad (788)$$

Here Z' is the total number of effective electrons as defined in §95E, Z_n the number of electrons in the nth shell, I_n their average excitation energy and κ_n the respective value of the constant κ.

For high energies (788) reduces to

$$d[(E^2)_{Av} - (E_{Av})^2]/dX = 4\pi e^4 z^2 N Z'. \quad (788a)$$

This formula (only with Z' replaced by the actual number of electrons in the atom, Z) had been given in 1915 by Bohr on the basis of classical mechanics. For lower energies of the particle, the sum over n in (788) should be added. This sum may be fairly large, e.g., for α-particles of 5 MV in air the K electrons ($I_K \sim 700$ volts, $mv^2 \sim 1300$ volts, $\kappa_K \sim 4/3$, $Z \sim 1.8$) contribute about 1.7, the L electrons ($I_L \sim 40$, $\kappa_L \sim 4/3$, $Z_L = 5.4$) about 0.9, so that the second term in (788) is about 40 percent of the first ($Z' = Z = 7.2$). This shows that the straggling may, at lower energies of the particle, be considerably larger than Bohr's classical value (788a), in agreement with observation. However, the deviation from Bohr's value can certainly not be as large (100 percent) as earlier measurements by Briggs (B55) would indicate. The most recent measurements by Bennet (B6a) with 8 MV alphas in mica give 20 percent deviation, in satisfactory agreement with (788).

B. The extrapolated range for a homogeneous group of particles

Formula (788) gives the fluctuation of the energy of particles which have traversed a certain thickness of material. We are primarily interested in the reverse, *viz.* the fluctuation of the distance traveled by particles which have lost the same amount of energy. We have (cf. B34)

$$\frac{d}{dE}[(X^2)_{Av} - (X_{Av})^2] = \frac{d}{dX}[(E^2)_{Av} - (E_{Av})^2]\left(\frac{dE}{dX}\right)^{-3}. \quad (789)$$

Inserting (788) and integrating from the initial energy E_0 of the particle to zero, we obtain for the mean square fluctuation of the particle range:

$$(R - R_0)^2_{Av} = \int_0^{E_0} \frac{4\pi e^4 z^2 N Z'}{(dE/d\dot{X})^3} \times \left(1 + \sum_n \frac{\kappa_n I_n Z_n}{mv^2 Z'} \log \frac{2mv^2}{I_n}\right) dE. \quad (790)$$

From this relation the fluctuation in range may be calculated if the κ_k are known. For the actual calculations, we have put $\kappa = 4/3$ for both K and L shell of air. The dependence of all other quantities in (790) on the energy is known.

To a sufficient approximation, the distribution of the ranges of a homogeneous group of particles is given by a Gaussian distribution:

$$p(R)dR = \pi^{-\frac{1}{2}} \alpha e^{-\alpha^2 (R - R_0)^2} dR. \quad (791)$$

The range fluctuation is then

$$(R - R_0)^2_{Av} = \int p(R)(R - R_0)^2 dr = 1/2\alpha^2. \quad (791a)$$

From this equation and (790) α is determined.

Most of the important detecting devices (except the cloud chamber) measure the number of particles reaching a certain distance r from the source, in other words the particles whose range is greater than r, *viz.*

$$P(r) = \int_r^\infty p(R)dR = \tfrac{1}{2}[1 - \Phi(\alpha(r - R_0))]. \quad (792)$$

$P(r)$ is given in Fig. 36 (curve marked "thin target"). The mean range R_0 is that range which is reached by just one-half of the particles. This would seem to allow an easy determination of R_0. However, this method is restricted to a beam of particles perfectly homogeneous in the beginning. The material emitting the particles must be infinitely thin in order to provide no stopping of its own and its surface must be perfectly smooth. Even so, the beam will be homogeneous in energy only if emitted by a natural radioactive substance. The energy of the particles from artificial transmutations always depends on the angle of their emission (§96) which prevents complete homogeneity of the beam.

For an inhomogeneous beam the point at which the intensity is reduced to one-half has no particular significance. If, in particular, the inhomogeneity arises from a finite thickness of the source, the particles of larger range will be more significant as they come from the top layers of the source. For this reason it is in general preferable to measure the "extrapolated" range rather than the mean range. The extrapolated range is obtained by drawing the steepest tangent to the number-range curve (i.e., the experimental curve giving the number of particles detected as a function of the distance r from the source). The intersection of this tangent with the axis of abscissae gives the extrapolated range (cf. Fig. 36).

The range distribution function $P(r)$ for homogeneous particles has its steepest slope at $r=R_0$. We have

$$P(R_0)=\tfrac{1}{2};\quad P'(R_0)=-\alpha/\sqrt{\pi}. \tag{792a}$$

Therefore the extrapolated range is

$$R_{\text{extr}}=R_0-P(R_0)/P'(R_0)=R_0+\tfrac{1}{2}\sqrt{\pi}/\alpha. \tag{792b}$$

We denote by s the difference between extrapolated and mean range and obtain

$$s^2=\tfrac{1}{2}\pi(R-R_0)^2_{\text{Av}}, \tag{793}$$

$$\alpha=\tfrac{1}{2}\sqrt{\pi}/s, \tag{793a}$$

$$p(R)dR=\tfrac{1}{2}e^{-\pi(R-R_0)^2/4s^2}dR/s. \tag{794}$$

The difference s between mean and extrapolated range has been measured carefully for the α-particles from Th C′ (long), Ra C′ and Po, with the results 0.111, 0.075 and 0.043 cm, respectively. On the other hand, s may be calculated from (793) (790). The result of such a calculation for Po would be rather unreliable because the theory of stopping is known to be inaccurate at low energies. However, the difference between the values of s^2 for Po and the two other groups of α-particles should be comparable with the theoretical value. We have

	$s^2-s_{\text{Po}}^2$ (in 10^{-4} cm^2)	
	experimental	theoretical
Ra C′ α's	38	36
Th C′	105	121

The agreement is satisfactory, especially considering that s^2 is rather sensitive to small experimental errors in s. We are therefore justified in using the theoretical relation to calculate the "straggling" s for particles faster than Th C′ α-particles for which the theory should be even more accurate.

The result is given in Fig. 37 in which the straggling is given as a function of the range of the particles. The straggling of α-particles is about 1.2 percent of their range for energies around 4 MV, about 1.0 percent for 16 MV and would be about 0.85 percent for 50 MV energy.

The dependence of the straggling on the mass and charge of the particle can be found immediately from (790). The bracket $1+\cdots$ in (790) is a function of the velocity only. The energy loss dE/dx is (§95) proportional to z^2 times a function of the velocity. The energy E itself is $\frac{1}{2}Mv^2$. Therefore

$$s=M^{\frac{1}{2}}z^{-2}g(v), \tag{795}$$

g being another function of v. The straggling of particles of mass (atomic weight) M, charge z and range R can thus be expressed in terms of the straggling of protons of range z^2R/M, *viz.*:

$$(s/R)_{M,\,z,\,R}=M^{-\frac{1}{2}}(s/R)_{1,\,1,\,z^2M^{-1}R}. \tag{795a}$$

In this way, curve 37 which is given for protons may be used for any kind of particle.

C. Thick target

For reasons of intensity, most nuclear transmutation experiments are made in "thick" targets, i.e., targets thick compared to the range of the incident particles in the target material.[9]

[9] The use of thick targets is no disadvantage, as it can be easily corrected for. However, "medium thin" targets,

The particles produced in the reaction are therefore partly stopped in the target itself, so that their observable range is reduced. Only the particles produced in the surface layer of the material will have the full range. In order to determine this full range, *it is not sufficient to "extrapolate" the number-range curve along its steepest tangent* as described in the preceding section and to consider the extrapolated range so obtained as the extrapolated range for the particles produced in the top layer of the target. The reason why this leads to fallacious results is that the shape of the number-range curve is altered by the presence of the particles coming from greater depths of the target. We shall, in this section, derive a method for the determination of the mean range of the particles coming from the top layer of the target, from the measured number-range curve.

We assume that the incident beam strikes the target at an angle of 45°, and that the particles produced in the reaction are observed again at an angle of 45° with respect to the target, and at right angles with the incident beam. This arrangement is the most symmetrical and most commonly used; it means that the incident particles travel the same distance in the target as the produced ones. Generalization of the formulae to other arrangements is obvious.

Consider particles produced at a depth X in the target, X being measured along the path of the particle in cm air equivalent. Let $R(X)$ be the residual range of these particles after leaving the target. Then $R(X)$ will decrease with increasing depth X for two reasons: (1) because the part X of the particle range itself lies in the target, and (2) because the incident particles which have penetrated to the depth X have lost some energy, and therefore impart less energy to the produced particles. If the emitted particle is observed exactly at right angles to the incident beam, we have from (770b) for not too large X:

$$R(X)=R(0)-X\left[1+\frac{M_3-M_1}{M}\frac{(dE/dX)_1}{(dE/dX)_2}\right]. \quad (796)$$

The notations are the same as in §96, the indices 1 and 2 referring to incident and emitted particle, respectively. The stopping power dE/dX is proportional to the stopping cross section σ shown in Fig. 31. Alternatively we may write

$$\frac{(dE/dX)_1}{(dE/dX)_2}=\frac{\sigma_1}{\sigma_2}=\frac{E_1}{E_2}\frac{R_2 n_2}{R_1 n_1}, \quad (796a)$$

where R is the range and n the range exponent given in Fig. 35. The quantities E_1, R_1 etc., should be taken about at the depth $\frac{1}{2}X$. The first term in the square bracket in (796) is more important if the produced particle is heavy and slow, in the other cases the second term is usually more important.

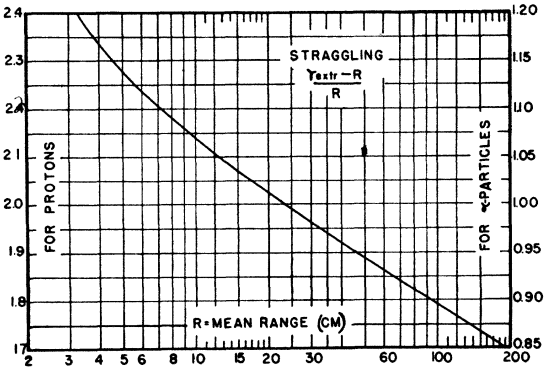

FIG. 37. Straggling of protons and α-particles. The difference between extrapolated and mean range, in percent of the latter, is given as a function of the mean range.

If the incident particle is charged (for neutrons cf. below), its efficiency in producing the nuclear reaction decreases approximately exponentially with X. Since we are only calculating a fairly small correction, it is sufficient to take the simple Gamow formula for the reaction probability (cf. §78, footnote 59), *viz.*

$$\varphi(v)\sim\exp\left(-2\pi\frac{zZe^2}{\hbar v}\right)=\exp\left(-0.99\frac{zZM_1^{\frac{1}{2}}}{E^{\frac{1}{2}}}\right), \quad (797)$$

where M_1 is the atomic weight of the incident particle and E its energy in MV at any point in the target. The number of particles produced at a depth X is thus

$$\varphi(X)dX\sim\exp\left[-\frac{1}{2}0.99\frac{zZM_1^{\frac{1}{2}}}{E_1^{3/2}}\left(\frac{dE}{dX}\right)_1 X\right]dX, \quad (797a)$$

where E_1 is a suitable average of the energy of the

of a thickness comparable to the range of the particles, are decidedly undesirable.

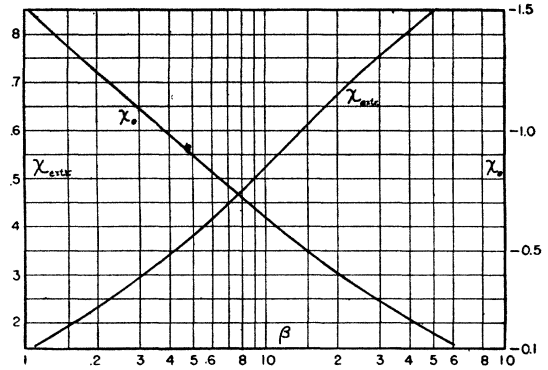

FIG. 38. Thick target correction. x_{extr} and x_0 as functions of the constant β which describes the depth of penetration into the target (cf. (798a)). To obtain the mean range from the most probable range, sx_0 should be added where s is the straggling (including angle straggling, see text). From the *extrapolated* range, the mean range is obtained by subtracting sx_{extr}.

incident particle in the target. The probability that the produced particle has a mean residual range r may be written

$$N(r)dr=(\beta/s)e^{-\beta(R_0-r)/s}dr, \tag{798}$$

where s is the straggling of a homogeneous group of particles as calculated in section B, R_0 is the mean range of the particles produced in the top layer of the target, and (cf. (796)–(798))

$$\beta=0.99zZ\left(\frac{M_1}{E_1}\right)^{\frac{1}{2}}\frac{s_2}{R_2}\left[\frac{R_1}{R_2}n_1+\frac{E_1}{E_2}\frac{M_3-M_1}{M}n_2\right]^{-1}. \tag{798a}$$

In this formula suitable average values should be inserted for energy and range of the incident particle. It is more convenient to use the approximate formula[10]

$$\beta=\left[zZ\left(\frac{M_1}{E_1}\right)^{\frac{1}{2}}+4\right]\frac{s_2}{R_2}\Big/\left[\frac{R_1}{R_2}n_1+\frac{E_1}{E_2}\frac{M_3-M_1}{M}n_2\right], \tag{799}$$

in which now E_1 and R_1 refer to the *initial* energy and range of the incident particle.

Formula (798) gives the number of particles with a *mean* range r which leave the target. For a given mean range, the number of particles having an actual range R is given by (794). Thus the number of particles with actual range R coming from a thick target is given by

$$t(R)dR=dR(\beta/2s^2)\int_0^{R_0}dr \exp\left(-\pi(R-r)^2/4s^2-\beta(R_0-r)/s\right). \tag{800}$$

We introduce the abbreviations

$$\frac{R-R_0}{s}=x; \qquad \frac{R_0-r}{s}=y \tag{800a}$$

and find

$$t(x)dx=\tfrac{1}{2}\beta e^{\beta(x+\beta/\pi)}\times\{1-\Phi(\tfrac{1}{2}\pi^{\frac{1}{2}}x+\pi^{-\frac{1}{2}}\beta)\}dx, \tag{801}$$

where Φ is the error integral.

The maximum of $t(x)$ lies always at a negative x, i.e., at a range smaller than the mean range of the particles emitted from the surface of the target. For large β (rapid decrease of the disintegration probability with the depth) the most probable range corresponds to

$$x_0=-1/\beta \tag{801a}$$

for small β (deep penetration) we have approximately

$$x_0=-2\pi^{-\frac{1}{2}}|\log 2\beta|^{-\frac{1}{2}}. \tag{801b}$$

For intermediate values of β, the most probable x_0 is given in Fig. 38. This quantity is important for the evaluation of cloud chamber measurements: The mean range of the particles emitted from the surface of a thin target is equal to the most probable range determined from experiment, plus $s|x_0|$.

The total number of particles reaching a given point x is given by

$$T(x)=\int_x^\infty t(\xi)d\xi=\tfrac{1}{2}[1-\Phi(\tfrac{1}{2}\pi^{\frac{1}{2}}x)]-\tfrac{1}{2}e^{\beta x+\beta^2/\pi}\cdot[1-\Phi(\tfrac{1}{2}\pi^{\frac{1}{2}}x+\pi^{-\frac{1}{2}}\beta)]. \tag{802}$$

A typical number-range curve of this type is shown in Fig. 36 (thick target, integral curve), together with the corresponding thin target

[10] This formula amounts to the assumption that the number of disintegrations produced by incident particles with energies between E and $E+dE$ is proportional to $\exp\left[-\frac{E_1-E}{E_1}\left(\frac{1}{2}zZ\left(\frac{M_1}{E_1}\right)^{\frac{1}{2}}+2\right)\right]$ where E_1 is the initial energy of the incident particle. For large $\frac{1}{2}zZ(M_1/E_1)^{\frac{1}{2}}$, this reduces to (797); in the opposite case, it gives for the *average* value of the energy of the incident particle just $\frac{1}{2}E_1$ as it should be.

curve. The extrapolated range is given by

$$x_{\text{extr}} = x_0 + T(x_0)/t(x_0), \qquad (802a)$$

where x_0 (cf. above) is the maximum of the function t, i.e., the point of steepest slope of the number-range curve. In the limiting cases we have

$$x_{\text{extr}} = 1 - \tfrac{1}{2}\beta \qquad \beta \gg 1, \qquad (802b)$$

$$x_{\text{extr}} = \beta(x_0^2 + \tfrac{1}{2}) \quad \beta \ll 1. \qquad (802c)$$

For intermediate values of β, x_{extr} is given in Fig. 38. For small β (deep penetration into the target), x_{extr} goes to zero, i.e., the *extrapolated range obtained* in the usual way *from* the *experimental* number-range curve *gives* directly the *mean range* of the *particles* coming *from* the *top layer* of the target. In the general case, the amount sx_{extr} should be subtracted from the experimental extrapolated range in order to obtain the mean range mentioned.

Many experiments have been carried out with "differentiating" detectors, especially with ionization chamber plus linear amplifier at high bias. In this case, only particles near the end of their range will be detected. The evaluation is the same as described above, provided the detection extends over a portion of the range large compared to the straggling s. An example is given in Fig. 36 (thick target, differential curve). It is seen that this curve coincides completely with that obtained from a nondifferentiating detector "thick target, integral curve" in the region important for the determination of the extrapolated range.

If the incident particle is a *neutron*, the number of produced particles emitted at a depth x is in first approximation independent of x. In this case we have to put $\beta = 0$ in the above theory. The number of particles of "range" x is then (cf. (801), divide first by β!)

$$t(x)dx = \tfrac{1}{2}[1 - \Phi(\tfrac{1}{2}\pi^{\frac{1}{2}}x)]dx, \qquad (803)$$

i.e., it reaches no maximum but remains constant for small ranges. Similarly, $T(x)$ increases linearly with decreasing range, *viz.*

$$T = (1/\pi)e^{-(\pi/4)x^2} - \tfrac{1}{2}x[1 - \Phi(\tfrac{1}{2}\pi^{\frac{1}{2}}x)]. \qquad (803a)$$

The determination of the extrapolated range causes no difficulty; it is, as already mentioned, equal to the mean range of the particles emitted from the surface of the target.

D. Evaluation of experiments with "good" geometry

As we have shown in §96, the spread in angle of emission is, in the case of "good" geometry equivalent to additional straggling. If s is the straggling due to the process of stopping as discussed in section B (range straggling), the total straggling s' is given by

$$s'^2 = s^2 + \gamma^2 = s_2^2 + n_2^2\left(\frac{a}{b}\right)^2 R_2^2 \frac{M_1 M_2}{M^2}\frac{E_1}{E_2^0}. \qquad (804)$$

Here γ is given in (777); the indices 1 and 2 refer again to incident and outgoing particle, a and b are radius and length of the cylindrical channel defining the beam; R is the range and n its logarithmic derivative with respect to the velocity. s' has to be used instead of s in the formula (799) for β.

We give an example of the determination of the reaction energy Q in the case of "good geometry." We choose the reaction

$$N^{14} + H^2 = C^{12} + He^4 + Q, \qquad (805)$$

which was studied by Cockcroft and Lewis (C28, C29). The beam of α-particles was defined by a channel of $a = 0.45$ cm radius and $b = 4$ cm length at right angles to the incident deuteron beam. The energy of the incident deuterons was $E_1 = 0.575$ MV; the observed extrapolated range of the α-particles 11.37 ± 0.1 cm. Without correction, this would correspond (Fig. 29) to $E_2 = 10.45$ MV. The criterion for "good geometry" is that $\cos\vartheta_0$ (cf. (772)) is greater than $a/b = 0.1125$. We have from (772):

$$\cos\vartheta_0 = 3.3 \cdot \frac{(2\cdot 4)^{\frac{1}{2}}}{16} \cdot \left(\frac{0.575}{10.45}\right)^{\frac{1}{2}} = 0.14.$$

Thus the condition of good geometry is just fulfilled. We have then:

(1) Correction because the range was measured in mica instead of air: Fig. 34 gives for Al and 11.4 cm range the correction 0.08 cm; the mica correction is one-half of this amount, i.e., +0.04 cm.

(2) Straggling: (*a*) Range straggling (according

to Fig. 37) $s=1.06$ percent (of the range) for α-particles of 11.4 cm range.

(*b*) Angle straggling (cf. (777). For α-particles of about 10.5 MV energy, Fig. 32 gives $n=3.32$. Therefore

$$\frac{\gamma}{R}=\frac{0.45}{4.0}\cdot 3.32\frac{(2\cdot 4)^{\frac{1}{2}}}{16}\cdot\left(\frac{0.575}{10.45}\right)^{\frac{1}{2}}=0.0154,$$

i.e. 1.54 percent.

(*c*) Total straggling $s'=(s^2+\gamma^2)^{\frac{1}{2}}=1.87$ percent of range.

(3) Thick target correction. For the incident deuterons ($E_1=0.575$ MV) Fig. 30 gives $R_1=0.86$ cm and Fig. 35 gives $n_1=2.1$. Therefore (799) gives

$$\beta=\frac{[1\cdot 7(2/0.575)^{\frac{1}{2}}+4]\cdot 0.0187}{2.1\cdot(0.86/11.37)+3.32(0.575/10.5)(10/16)}=\frac{17\cdot 0.0187}{0.160+0.11_4}=1.18.$$

From Fig. 38 we find that for $\beta=1.18$

$$x_{\text{extr}}=0.57.$$

Therefore the difference between extrapolated and mean range is

$$0.57s'=0.57\cdot 1.87\cdot 11.37/100=0.12.$$

Thus: Mean range $=11.37+0.04-0.12=11.29$ cm ± 0.15 cm. (Estimated error: 0.10 cm in measurement itself, 0.08 each in mica correction and straggling correction, total $(0.0100+2\cdot 0.0064)^{\frac{1}{2}}=0.15$.)

Energy of α-particle when emitted from top layer of target at 90° from Fig. 29 (corresponding to mean range of 11.29 ± 0.15 cm)

$$E_2=10.41\pm 0.08 \text{ MV}.$$

From (768) we then

$$Q=\frac{16}{12}\cdot 10.41-\frac{10}{12}\cdot 0.575=13.88-0.48,$$

$$Q=13.40\pm 0.11 \text{ MV}$$

$$=14.39\pm 0.12 \text{ milli-mass-units}.$$

E. Experiments with "poor" geometry

Let us suppose that particles from the target can enter the detector at all angles χ up to χ_0, where χ is the angle between the particle beam and the normal to the detector. If the target is thin, and if the straggling as well as the dependence of the particle energy on χ is neglected, the particles will all have the same true range, say, R_0. The apparent range (i.e., the range component normal to the detector) is then $X=R_0\cos\chi$. Since the number of particles emitted at an angle between χ and $\chi+d\chi$, is proportional to $\sin\chi d\chi$, the number of particles with an apparent range between X and $X+dX$, will be a constant times dX for X between $R_0\cos\chi_0$ and R_0. The total number of particles detectable at the distance X from the target, will then be

$$T(X)=\begin{cases}0 & \text{for } X>R_0\\ R_0-X & \text{for } R_0\cos\chi_0<X<R_0\\ R_0(1-\cos\chi_0) & \text{for } X<R_0\cos\chi_0,\end{cases}\qquad(806)$$

leaving out a constant factor.

The straggling will modify this distribution near the upper end $X\approx R_0$. If the straggling s is small compared to the region over which the apparent ranges are distributed, i.e., if[11]

$$s\ll R_0(1-\cos\chi_0)\qquad(806a)$$

the distribution function (806) is replaced by

$$T(X)=\tfrac{1}{2}\left(\frac{R_0-X}{s}\right)\{1-\Phi[\tfrac{1}{2}\pi^{\frac{1}{2}}(X-R_0)/s]\}+(1/\pi)\exp\left(-\frac{\pi}{4}(R_0-X)^2/s^2\right),\qquad(806b)$$

which goes over into the straight line $T(X)=(R_0-X)/s$ for $R_0-X\gg s$. The extrapolation of this straight line gives exactly the mean range R_0. This means that with a thin target and sufficiently poor geometry, the extrapolated range is equal to the mean range, just as for an infinitely thick target and good geometry (end of Section C).

The dependence of the energy on direction does not appreciably affect the range distribution. It merely changes the most favorable angle (i.e., the angle giving the longest extrapolated range) from $\chi=0$ to $\chi=\frac{1}{2}\pi-\vartheta_0$ (cf. 772). The extrapolated range R_0 becomes equal to the mean range of the particles emitted at the most favorable angle ϑ_0, times $\sin\vartheta_0$. If E_2^m is the energy cor-

[11] $s<\frac{1}{2}R_0(1-\cos\chi_0)$ is in general sufficient.

responding to the measured extrapolated range, Q follows from (773).

With a thick target and poor geometry, the number of particles increases faster than linearly with decreasing range X, since a linear decrease is already obtained from a thin target. It is therefore *impossible to find an extrapolated range by linear extrapolation.* The most suitable procedure seems to be to plot the square root of the number of counts as a function of the thickness of stopping material between detector and target, and to extrapolate *this* curve along the steepest tangent.

Since the experiments with poor geometry are never very accurate, it was not felt worth while to calculate the exact relation between the "penetration constant" β (cf. (799)) and the extrapolated range obtained from the extrapolation of the square root curve as described above. The relation was only determined in the limiting case of large and small β. We use again the abbreviation

$$x_{\text{extr}}=(R_{\text{extr}}-R_0)/s, \tag{807}$$

where R_{extr} is the experimental extrapolated range and R_0 the required mean range for the most favorable direction ϑ_0. Then we have

(*a*) for large β: $x_{\text{extr}}=1.21-1/\beta$, (807a)

(*b*) for small β: $\dfrac{x_{\text{extr}}}{1+2/(\pi x^2_{\text{extr}})}=\dfrac{6}{\pi}-\beta$. (807b)

Examples for "poor" geometry are very rare in the more recent experimental literature. In order to explain the principles of evaluation, we discuss the old experiments of Cockcroft and Walton (C25) on the reaction

$$C^{12}+H^2=C^{13}+H^1, \tag{808}$$

which have since been superseded by the more recent experiments of Cockcroft and Lewis (C29) with "good" geometry. The energy of the incident deuterons was 0.50 MV, the approximate range of the protons 13.7 cm, corresponding to an energy of 2.95 MV and to $n_2=3.4$ (Fig. 35). Thus (cf. (772))

$$\cos\vartheta_0=3.4\cdot\frac{(1\cdot 2)^{\frac{1}{2}}}{14}\cdot\left(\frac{0.50}{2.95}\right)^{\frac{1}{2}}=0.14.$$

The aperture of the detecting apparatus is not stated, but was apparently wide, so that particles with $\cos\vartheta=0.14$ could enter freely. This is sufficient for "poor" geometry.

When a plot of the square root of the number of particles observed is plotted against the apparent range, the extrapolated range turns out to be about 13.72 ± 0.20 cm. The straggling of protons of this range (Fig. 37) is $s=2.1$ percent. With $R_1=0.73$ cm and $n_1=2.0$ for the incident deuterons, (799) gives

$$\beta=\frac{[6\cdot(2/0.5)^{\frac{1}{2}}+4]\cdot 0.021}{\frac{0.73}{13.7}\cdot 2.0+\frac{0.50}{2.95}\cdot\frac{11}{14}\cdot 3.4}$$

$$=16\cdot 0.021/(0.106+0.454)=0.60.$$

Therefore we have approximately $x_{\text{extr}}=0.42$ (cf. curve 38, which, however, is not directly applicable to "poor" geometry). Thus straggling $\approx 0.42\cdot 2.1\%=0.88\%$ of the range $=0.12$ cm, giving for the mean range

$$R_0=13.60\pm0.2 \text{ cm}.$$

The corresponding energy is $E_2^m=2.94\pm0.04$ MV. From (773) we obtain then

$$Q=\frac{14}{13}\cdot 2.94+\frac{2}{13}\cdot 0.50\left(1-\frac{3.4\cdot 1}{14}\right)-0.50$$

$$=2.72\pm0.05 \text{ MV}.$$

The newer experiments of Cockcroft and Lewis give 2.71 ± 0.05 MV.

F. Measurement of neutron energies by proton recoil

The most exact measurements of neutron energies (B37, B38, B40) are based on measurements of the range of recoil protons produced by the neutrons in hydrogen gas or hydrogenic substances. The energy of the neutrons depends on their direction of emission ϑ, and on the depth in the target at which they are produced, just as with charged particles. The only difference is that the "range" of the neutrons is essentially infinite so that the first term in the denominator of (799) is absent. For s_2/R_2 in (799), the values for the recoil protons should be inserted.

If only the recoil protons emitted exactly

forward (i.e., in the direction of the neutron motion) are counted, the evaluation is the same as for charged particles. The quantity a/b in (777) should be replaced by one-half the angle subtended by the cloud chamber (or other detecting apparatus for neutrons) at the middle of the target. s' is then found from (804), s being the natural range straggling of the recoil protons. β is calculated from (799) as described above, x_{extr} or x_0 found from Fig. 38, and the mean range of the recoil protons found from their extrapolated or from the most probable range as usual. The corresponding proton energy gives immediately the energy of neutrons emitted at right angles to the incident beam.

If recoil protons within an angle χ_0 of the neutrons are taken into consideration, s' should be replaced by

$$s''=\left(s'^2+\frac{n^2}{48}R_2^2\chi_0^4\right)^{\frac{1}{2}}, \tag{809}$$

where R_2 is again the proton range and n the "range exponent" for the proton (Fig. 35). The evaluation of the "mean" proton range and the corresponding energy should then be carried out as before, but the result should be increased by

$$\tfrac{1}{2}E_2\chi_0^2. \tag{809a}$$

XVII. Results of Disintegration Experiments

(Closed July 1, 1937)*

§98: Notation

In the following sections (§§99 to 105) the results of disintegration experiments will be discussed in some detail. Attempts to organize the voluminous material in this field have necessitated subdivision of the subject matter. It would be wasteful of space to describe the techniques used by the various experimenters for each process. Accordingly, the experimental techniques most commonly employed are discussed in a separate chapter (Chap. XV), and only brief mention made of these techniques in discussing the results of experiment.

In the discussion of disintegration results general subdivisions into type reactions have been found valuable for the purpose of grouping the results into a form suitable for correlations. A shorthand terminology has been devised for identifying these reactions. The projectiles which have been successfully used for nuclear disintegration are: *alpha-particles*, *protons*, *deuterons*, *neutrons* and *gamma-rays*, denoted, respectively, by the symbols: α, p, d, n, γ. All of these radiations are observed as products of disintegrations as well, and in addition many product nuclei are formed which decay radioactively with emission of electrons (e^-) and positrons (e^+). The reactions produced by one projectile and releasing a common product may be designated by the corresponding symbols, in order. For instance alpha particle disintegrations yielding protons may be symbolized as reactions of the α-p type; neutron bombardment resulting in alpha-particle emission as the n-α type, etc. Under each type reaction the individual processes may be specified by prefixing the chemical symbol of the target, i.e.: B^{10}-α-p, Li^6-n-α, etc. The identity of the resultant products is then obvious from the requisite balance of nuclear charge and mass; in the two instances above they are C^{13} and H^3. A more complete symbolism for such type reactions is to write out the generalized reaction in the usual manner using Z for nuclear charge of the target element and A for its mass number. Using this method of grouping under type reactions we find experimental evidence for the 16 types of primary reactions and 2 radioactive decay processes listed in Table L.

In Table L the number of individual reactions falling under each type reaction is given in the column on the right. There are found to be 385 primary reactions, followed by 220 radioactive decay processes produced through various of the primary ones, giving a total of 605 observed to date (July 1937). Included in the list are those of unusual type which result in more than the usual

* The experimental material presented in this chapter covers publications received prior to July 1, 1937. In addition the Physical Review issues up to Aug. 1 have been included.

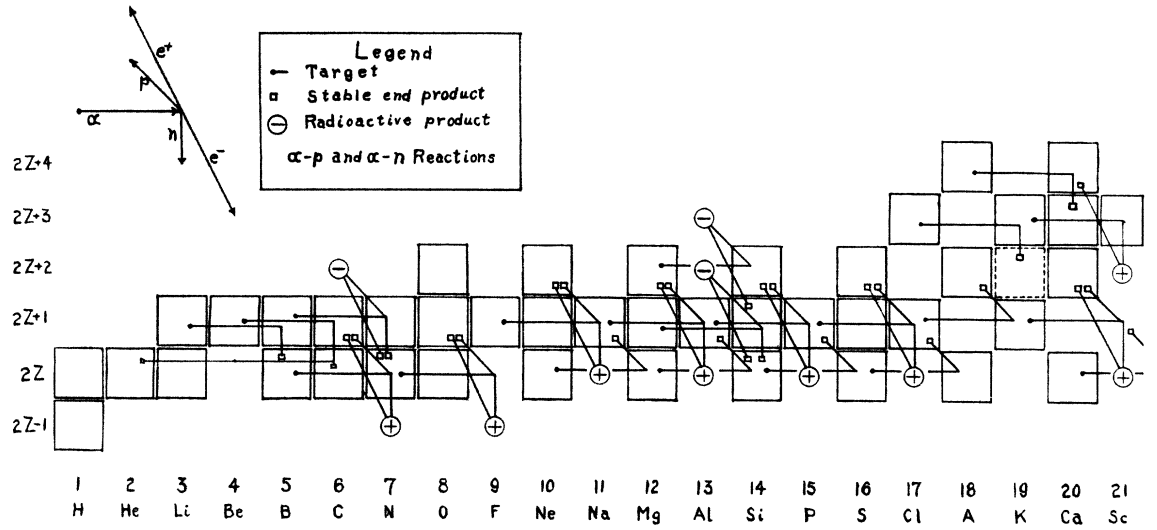

FIG. 39. Isotopic chart showing the reactions produced by α-particles in light elements. Abscissa, nuclear charge; ordinate, isotopic number. The stable isotopes are indicated by heavy squares, the reactions by two lines. The direction and length of the lines give the kind of particle emitted.

two products. These are in general alternative to a process of the ordinary type and are discussed under such reactions in the text. An example: B^{10}-d-α results in three alpha-particle products as well as in Be^8 and an alpha. It is understood, of course, that the above list of reactions may be incomplete since inconclusive evidence in many cases makes the absolute identification questionable. Only those reactions are entered in the following discussion for which, in the opinion of the authors, there is satisfactory proof.

Another valuable mechanism for correlating nuclear reactions is to plot them on an isotope diagram. For this purpose we have chosen the method used by Evans and Livingston (E11), in which the "isotopic number" $(A-2Z)$ is plotted as a function of Z. This method separates the isotopes of all elements. Reactions between elements are plotted by the use of two lines, one representing the absorbed projectile and the other the emitted particle, while the junction of the two lines denotes the compound nucleus. In Figs. 39, 40, 41, 42 the known nuclear reactions are plotted on such charts. The direction and lengths of the lines representing particle absorption or emission are indicated; emission of a neutron reduces the isotopic number by one unit, absorption of an alpha-particle (isotopic number = 0) increases Z by two units, etc. Known stable isotopes are indicated by the large squares on the diagrams. It is noted that the isotopic number, I, varies from -1 for H^1 to $+54$ for U^{238}. The target element is indicated by the small solid circle at the start of a line representing the bombarding particle; the product is a small square if stable or a large open circle if radioactive, and the radioactive process is indicated not only by the direction of the line leading from the circle but also by the + or − sign in the circle. In many instances when the same bombarding particle is used and

TABLE L. *Type reactions and number of nuclear processes.*

(1) α-p:	$Z^A+He^4 \rightarrow (Z+2)^{A+4} \rightarrow (Z+1)^{A+3}+H^1$	20	
(2) α-n:	$Z^A+He^4 \rightarrow (Z+2)^{A+4} \rightarrow (Z+2)^{A+3}+n^1$	21	
(3) p-α:	$Z^A+H^1 \rightarrow (Z+1)^{A+1} \rightarrow (Z-1)^{A-3}+He^4$	5	
(4) p-d:	$Z^A+H^1 \rightarrow (Z+1)^{A+1} \rightarrow Z^{A-1}+H^2$	1	
(5) p-γ:	$Z^A+H^1 \rightarrow (Z+1)^{A+1} \rightarrow (Z+1)^{A+1}+h\nu$	10	
(6) p-n:	$Z^A+H^1 \rightarrow (Z+1)^{A+1} \rightarrow (Z+1)^{A}+n^1$	22	
(7) d-α:	$Z^A+H^2 \rightarrow (Z+1)^{A+2} \rightarrow (Z-1)^{A-2}+He^4$	23	
(8) d-p:	$Z^A+H^2 \rightarrow (Z+1)^{A+2} \rightarrow Z^{A+1}+H^1$	50	
(9) d-p, α:	$Z^A+H^2 \rightarrow (Z+1)^{A+2} \rightarrow (Z-2)^{A-3}+H^1+He^4$	1	
(10) d-n:	$Z^A+H^2 \rightarrow (Z+1)^{A+2} \rightarrow (Z+1)^{A+1}+n^1$	26	
(11) d-n, α:	$Z^A+H^2 \rightarrow (Z+1)^{A+2} \rightarrow (Z-1)^{A-3}+n^1+He^4$	2	
(12) n-α:	$Z^A+n^1 \rightarrow Z^{A+1} \rightarrow (Z-2)^{A-3}+He^4$	23	
(13) n-p:	$Z^A+n^1 \rightarrow Z^{A+1} \rightarrow (Z-1)^{A}+H^1$	22	
(14) n-γ:	$Z^A+n^1 \rightarrow Z^{A+1} \rightarrow Z^{A+1}+h\nu$	97	
(15) n-$2n$:	$Z^A+n^1 \rightarrow Z^{A+1} \rightarrow Z^{A-1}+2n^1$	32	
(16) γ-n:	$Z^A+h\nu \rightarrow Z^A \rightarrow Z^{A-1}+n^1$	19	
	(Processes leading to more than two products)	11	
			385
(17) e^-:	$Z^A \rightarrow (Z+1)^A+e^-$	170	
(18) e^+:	$Z^A \rightarrow (Z-1)^A+e^+$	50	
			220
	Total number of nuclear reactions		605

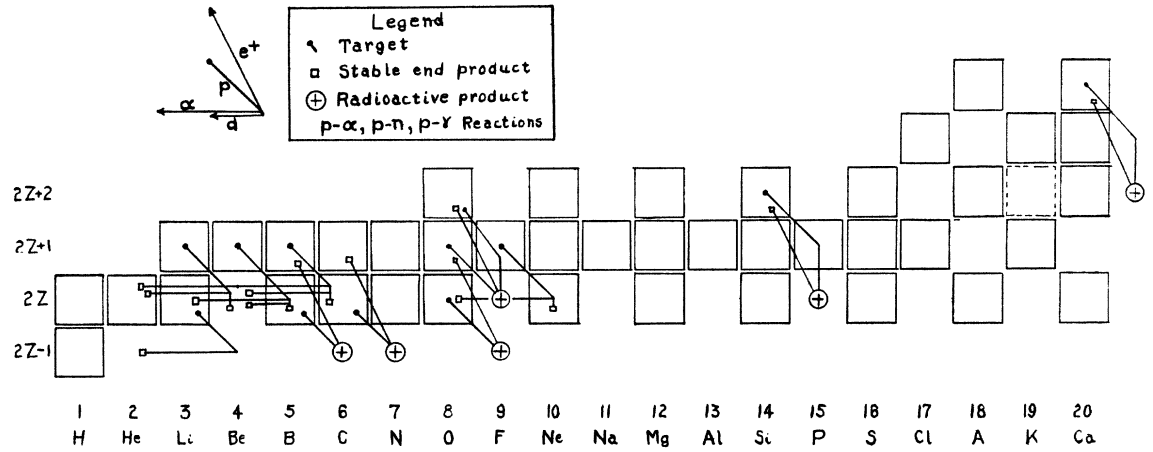

FIG. 40. Isotopic chart showing the reactions produced by protons in light nuclei.

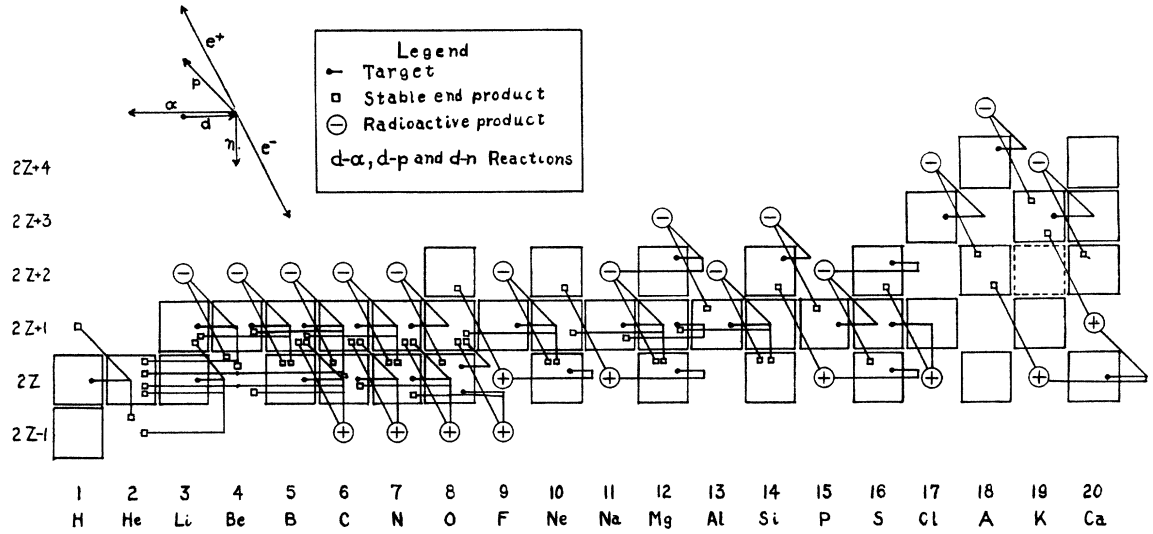

FIG. 41. Isotopic chart of reactions produced by deuterons in light elements.

different products observed this is indicated by lines branching from the common junction representing the compound nucleus. It is interesting to note that all positron emitting radioactive nuclei fall below the band of stable isotopes, while all electron emitters are above it.

Collected at the end of each type reaction are tables of the individual processes in which the more important observational data are listed. These give the observed reaction energy, the resonance levels in the compound nucleus, the excitation levels in the product nucleus and the probability of the reaction. In addition the value of the reaction energy calculated from the masses of the components of the reaction is given in each case, and also for many reactions as yet unobserved.

With this introduction we proceed to the discussion of the experimental evidence.

§99. DISINTEGRATION BY ALPHA-PARTICLES

Rutherford, in 1919, first achieved the artificial disintegration of one of the naturally stable elements. He used the highly energetic alpha-particles from Ra C′ as projectiles and observed protons ejected from a nitrogen gas target. His achievement was not only in visualizing the possible experimental method for obtaining dis-

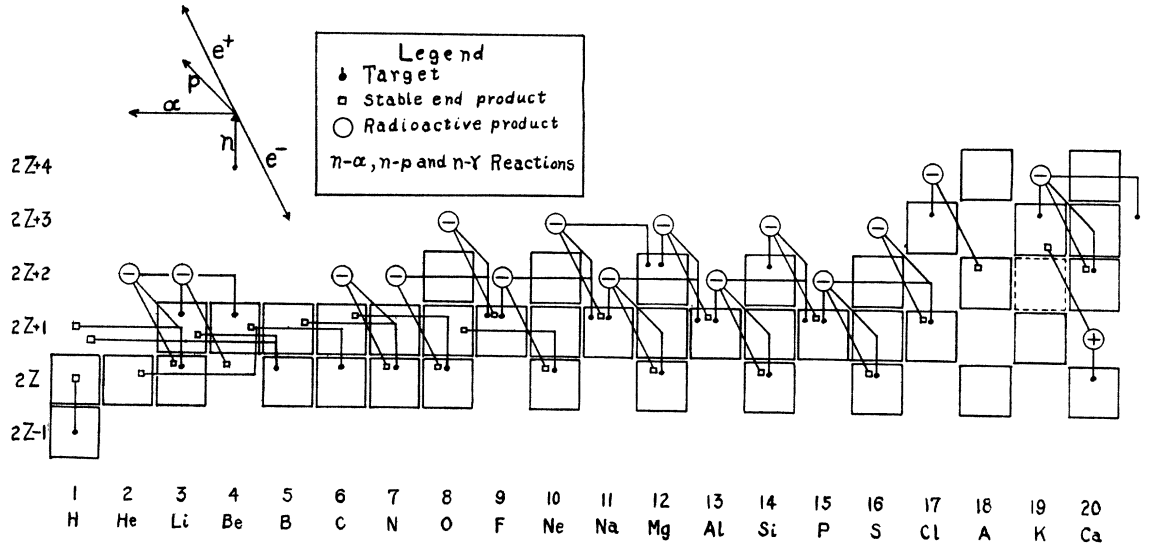

FIG. 42a. Isotopic chart of reactions produced by neutrons in light elements.

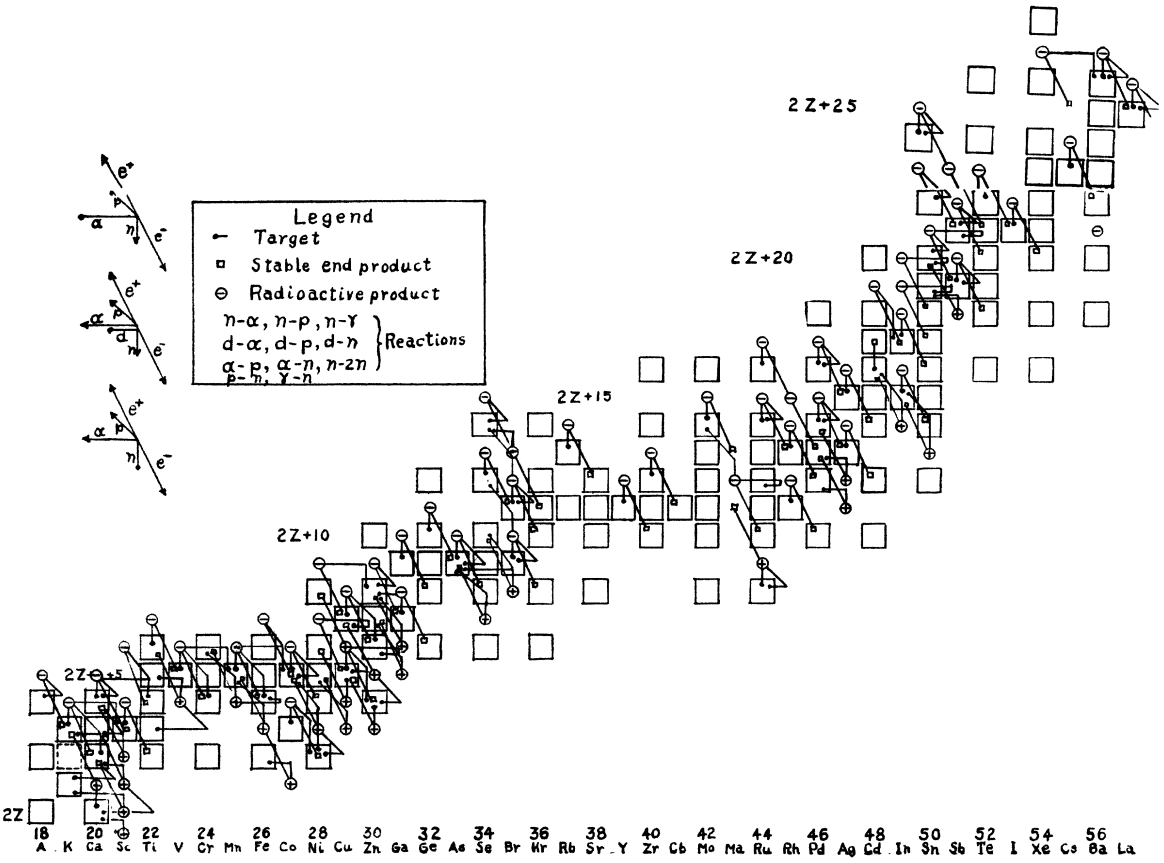

FIG. 42b. Isotopic chart of reactions produced by neutrons, protons, deuterons and gamma-rays in elements of medium atomic weight.

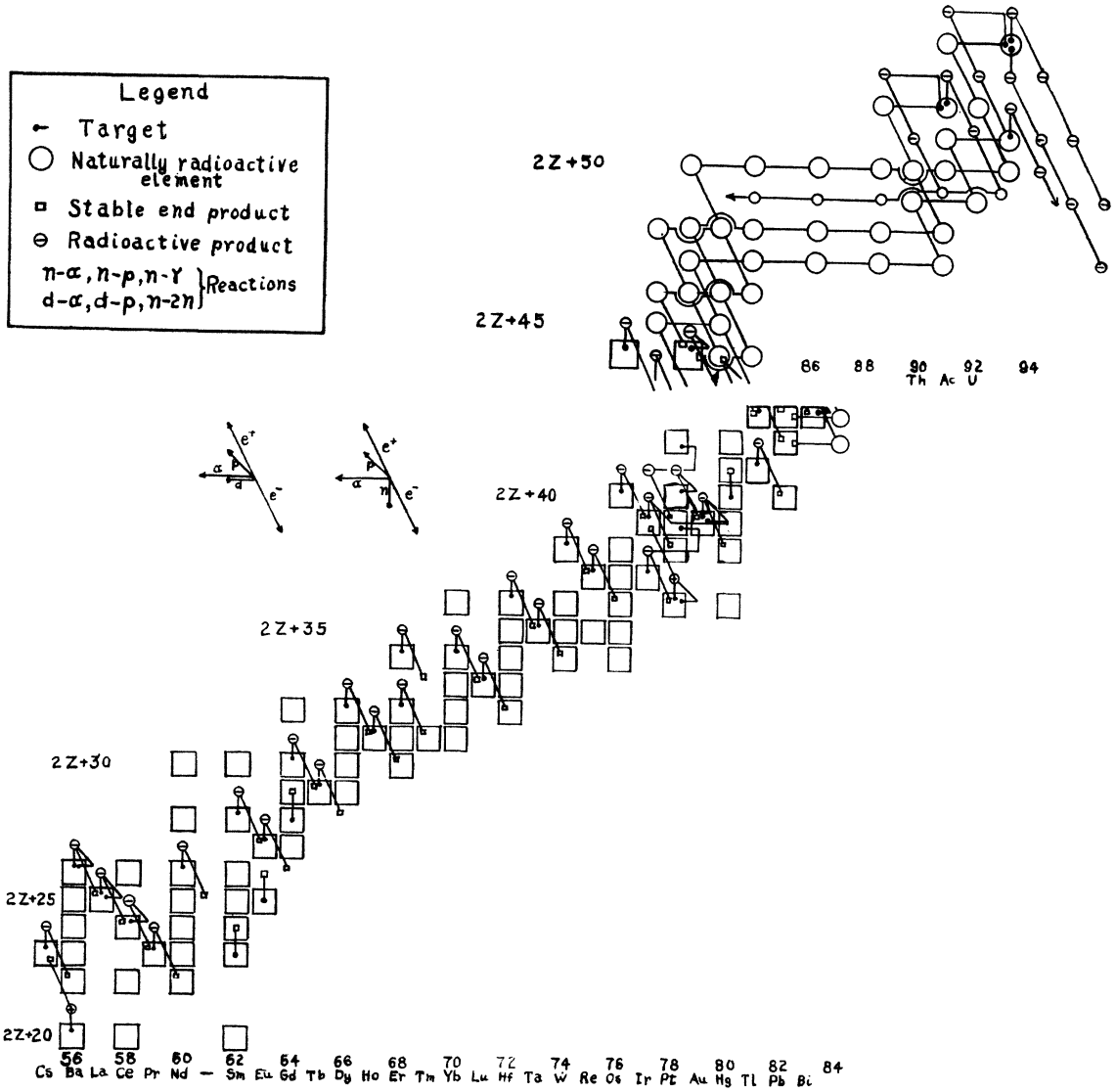

FIG. 42c. Isotopic chart of reactions produced by neutrons and deuterons in heavy elements.

integration, although the sensitivity and simplicity of the device he chose was largely responsible for his success, but also in combating all the good but pessimistic reasons for believing that the experiment could not succeed. These doubts were well grounded. In the first place there was reason to believe from scattering experiments that the lighter nuclei were of less than 10^{-12} cm in diameter, and the alpha-particle still smaller. The possibility of obtaining enough direct hits with the small number of alpha-particles available was small and this feature determined the necessity of observing the individual products of the disintegration. Secondly the energy of the alpha-particle might not have been great enough to cause a disruption of the nucleus. The Coulombian forces of repulsion between the positive charges of the nucleus and the alpha might have prevented sufficient penetration to affect the nucleus, even for a direct hit. Actually the reserve was very small; if the alphas had been moving with speeds of 0.6 their actual value the disintegrations would probably not have been observed. Even so only certain elements with

atomic number less than 19 were disintegrated. Thirdly, the products of the disintegration might have been unobservable; they might have consisted solely of neutrons and gamma-rays, or of low energy charged particles which would not have been observed with the instruments used. Again Rutherford's guess was correct, and the fluorescent screen proved to be just the thing to observe the products which appeared, the protons. Finally it could be expected that scattered alphas or recoil nuclei from them might mask the effects, which was indeed the case until better arrangements of apparatus minimized this disturbance.

It is known today that natural alpha-particles will disintegrate all of the lighter elements up to Ca ($Z=20$) and possibly one of much higher charge, Zn, with the exception of H, He, C and O. Many years of experiment and controversy and the discovery of two new nuclear radiations were required to bring the field to this state. The exceptions mentioned are very significant. Neglecting H, which is itself an elementary nucleus, they are composed of 1, 3 and 4 alpha-particle units, resulting in unusually stable nuclei. The importance of this classification fades with heavier elements, for instance Ne^{20}, Mg^{24}, Si^{28}, S^{32} and Ca^{40} have all been reported to be disintegrable.

Using the cyclotron, Lawrence and his collaborators have accelerated [He^{++}] ions to 12 MV energy with intensities thousands of times greater than those available from natural alpha-particle sources. Many induced radioactivities have been observed, of which a few reports are published (W1, W1a, S16a). The Princeton cyclotron has also been used to produce 9 MV alphas (W13a, H24a, H24b, R7b). These results indicate that the field of alpha-particle disintegrations can be expanded indefinitely with such artificial sources.

As products protons, neutrons and gamma-rays are observed, and in some cases the residual nucleus is itself unstable and decays with the emission of electrons or positrons. For general reviews of the subject the reader is referred to Chadwick and Feather's report to the 1934 International Conference on Physics (C10), Darrow's reviews (D5, D4) and the well-known book by Rutherford, Chadwick and Ellis (R21). Let us now discuss the various type reactions in more detail.

A. Type reaction α-p. (Table LI)

$$Z^A+He^4\rightarrow(Z+1)^{A+3}+H^1+Q:$$

The observation of protons emitted from nitrogen was the first evidence of artificial nuclear disintegration, and was followed by a series of experiments on other elements, chiefly by the Cavendish Laboratory group, which led to the statement in the book mentioned above (R21, p. 285): "In this way Rutherford and Chadwick found evidence of the disintegration of all elements from boron to potassium, with the two exceptions of carbon and oxygen." These processes were all determined by the observation of the ejected protons with a fluorescent screen, and carefully checked to prove that the scintillations were not due to scattered alpha-particles or recoil atoms of hydrogen existing as an impurity. The particles from several of the more intense reactions were found by deflection experiments in electric and magnetic fields to consist of protons. Not all of the disintegrations of this type have been similarly studied but it is assumed, and certainly with safety, that the particles observed on the fluorescent screen from paralleling processes are protons and can be included in the same type reaction. Most of the processes have been verified by more recent experiments,[12] but in the case of argon the only evidence is Rutherford and Chadwick's original observations.

The type reaction we have chosen to start with owes its primary position to the historical arrangement of events, although it is by no means the simplest one. The symbol Q on the right-hand side of the type equation represents the energy

[12] At this place should be mentioned the long-standing controversy between the group at the Cavendish Laboratory and that at Vienna, headed by Kirsch and Petterson. These workers have reported disintegrations of many elements, including a considerable number of heavier atomic weight than potassium, and some lighter than boron. Also they report a much greater yield of protons and deduce a larger probability of disintegration than the Cavendish group. Although the sincerity of these workers cannot be questioned many subsequent experiments have proven their results almost entirely erroneous. The best attempt to explain their anomalous results is given in a paper by Chadwick (C15), indicating that the weak scintillations due to the beta-rays of the radioactive source might be discernible under certain conditions and be confused with the alpha and proton scintillations. In the face of the existing evidence we are forced to eliminate these data from Vienna in the report to follow.

change in the reaction, and can be correlated with the resulting change in mass by means of Einstein's equation: $\Delta E=\Delta mc^2$. This quantity, referred to in certain German papers as the "Tönung," is either positive or negative according to whether the process is "exoergic" or "endoergic," that is, whether energy is emitted or absorbed in the reaction. Nearly all the known reactions of this type are of the endoergic character; the protons which are emitted having in general less energy than the alpha producing the disintegration.

With an "ideal" experimental arrangement, in which a parallel beam of alpha-particles of homogeneous energy impinges upon a thin target (in which the alpha-particle energy absorbed is negligible) the energy transferred to the proton and to the recoil nucleus can be calculated from the usual momentum and energy conservation equations (see §96). If M_1, M_2 and M_3 and E_1, E_2 and E_3 represent the masses and energies, respectively, of the alpha-particle, the proton and the residual nucleus, we find for the special case of observation at 90° to the incident beam (cf. 768, 767a):

$$Q=\left(\frac{M_1}{M_3}-1\right)E_1+\left(\frac{M_2}{M_3}+1\right)E_2. \quad (810)$$

$$E_2=\frac{M_3}{M_2+M_3}Q+\frac{M_3-M_1}{M_2+M_3}E_1, \quad (810a)$$

$$E_3=\frac{M_1}{M_3}E_1+\frac{M_2}{M_3}E_2. \quad (810b)$$

For observation in the direction of the incident beam (0°) these equations become (cf. 769):

$$Q=\left(\frac{M_1}{M_3}-1\right)E_1+\left(\frac{M_2}{M_3}+1\right)E_2 -\frac{2}{M_3}(M_1M_2E_1E_2)^{\frac{1}{2}}, \quad (811)$$

$$(E_2)^{\frac{1}{2}}=\frac{(M_1M_2)^{\frac{1}{2}}}{M_2+M_3}(E_1)^{\frac{1}{2}}+\frac{(M_3)^{\frac{1}{2}}}{M_2+M_3} \times[(M_2+M_3)Q+(M_3+M_2-M_1)E_1]^{\frac{1}{2}}, \quad (811a)$$

$$E_3=[(M_1E_1)^{\frac{1}{2}}-(M_2E_2)^{\frac{1}{2}}]^2/M_3. \quad (811b)$$

These equations show that the energy of the observed proton, E_2, is determined to a considerable extent by the alpha-particle energy. So we would expect to find proton ranges increasing with increasing energy of the alphas. Such is in fact the case for at least one group of protons in each of the disintegration processes of this type for which this phenomenon has been studied. This feature is characteristic of this "normal" type of disintegration and observation of such a variation of proton range is taken as proof of the mechanism of the disintegration.

The magnitude of the proton energy is chiefly dependent upon the value Q. It is possible to conceive of an alternative process resulting in an excited residual nucleus, in which case the Q value would be energetically smaller, and the proton ranges correspondingly less, but the same type of variation of proton range with alpha energy would be expected. The excited nucleus would then revert to the ground state with the emission of gamma-radiation.[13]

Resonance disintegration.—Experimentally we find that not all the protons observed from these processes follow this simple law. Certain groups are observed to have a definite energy which does not vary with the alpha-particle energy. Furthermore, these groups are observed only for a definite energy of the alpha, E_1. This is the phenomenon of resonance first suggested by Gurney (G24) and observed in the bombardment of aluminum by Pose (P12) in 1929. It also explains effects observed as early as 1921 by Rutherford (R24) but not interpreted in this way at that time. It has subsequently been found by these and other observers to exist also in the disintegration of Be, B, N, F, Na and Mg by alphas and in neutron and proton-produced processes.

In order to understand this effect more thoroughly we must consider the actual mechanics of the experiments. It proves to be impossible to perform experiments with the ideal and simple arrangement suggested above. In the first place the collimated beam of alpha-particles

[13] It has been the custom in the past to attempt to visualize this process as due to the entering alpha-particle falling into an excited alpha-particle level in the residual nucleus, or the ejection of a proton from a level lower than that of the most readily removable proton. These visualizations are misleading, and the excited states should be considered as existing in the residual nucleus *as a whole*, rather than for the individual particles (§51).

puts a restriction on intensity which is too severe for the experimental techniques and the quantities of radioactive materials available. The ideally thin target is also impractical since it reduces the number of disintegrations to below the observational limit. However, if a thick target is used in which the alphas are completely absorbed there will always be a lamina in the target in which the alphas do have the prescribed resonance energy, and so the protons produced at this energy are observed. The result is that with increasing alpha-energy, while the groups of normal protons are found to increase in energy correspondingly, the resonance groups will remain essentially fixed in range. See Fig. 43. (In fact, for angles of observation greater than 90°, the increased absorption of the resonance protons in coming out of the thick target results in a decreasing proton range with increasing E_1.) An equivalent technique is to use increasing thicknesses of target, in which case the energy E_1 is reduced by the absorption of the alphas in the target. Range-distribution curves of the protons will show the same "step" structure of the resonance groups, each group appearing as E_1 approaches the resonance value from above.

Despite the difficulty of working with thin targets certain observers have been successful in obtaining complementary evidence of resonance by their use. Chadwick and Constable (C4) have measured the disintegration function (number of protons emitted as a function of E_1) for thin foils of aluminum. In this case, as the energy is increased, the total number of protons observed rises to a maximum at the resonance values of E_1.

The Q value for a resonance group should be the same as that calculated for the normal or nonresonance protons. That is, the range of the resonance protons would be the same as the normal protons from alphas of the particular energy required to show the resonance effects. The distinction is in the increased probability of the reaction for that definite energy. So calculations of the Q value from resonance groups require only a knowledge of the proton energy and direction and the value of E_1 for which the probability is the greatest.

The possibility of producing an excited residual nucleus is also present in resonance disintegration, and results in two or more groups of

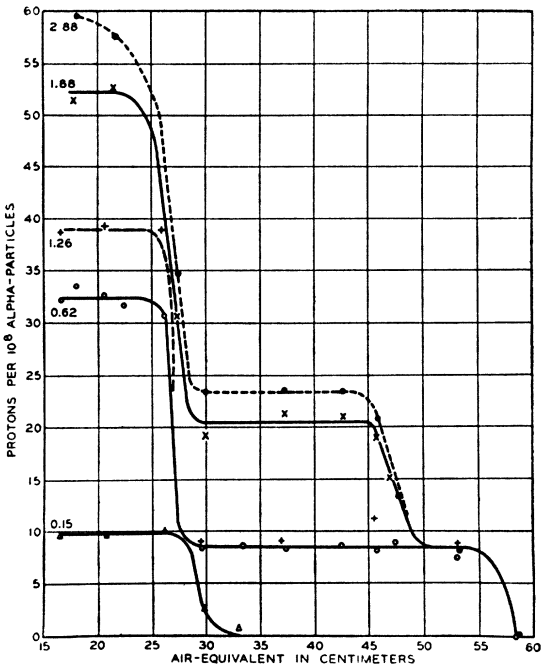

FIG. 43. Distribution-in-range curve of protons from the reaction $Al^{27}+He^4=Si^{30}+H^1$ (Pose) showing group structure dependent on alpha-energy and thus indicating resonance levels in the compound nucleus.

protons of constant range occurring simultaneously for the same energy E_1. The differences between Q values corresponding to these groups would represent the excitation states of the residual nucleus, and gamma-radiation with energies equal to these energy differences should be produced. These differences must agree for the various resonance groups and also for the "normal" groups. Gamma-radiation has been observed experimentally in many of these reactions and certain components might well be associated with such excitation levels. The data are not yet sufficiently precise to allow many accurate correlations, however, and this remains a point for further investigation.

To illustrate the features of resonance disintegration we will cite other experimental observations on aluminum. Chadwick and Constable (C4), using relatively low energy alphas, observed two groups of protons for each of four alpha-particle resonance energies, or eight groups in all. These four resonance levels were at 4.0, 4.44, 4.86 and 5.25 MV and the two proton groups in each case showed Q values of 0.0 and 2.3 MV, respectively. Using higher energy alphas

Haxel (H17) observed nonresonance protons from which the same values of Q were obtained. Duncanson and Miller (D19) have found evidence for two additional higher energy resonance levels, at 5.75 and 6.61 MV. Furthermore, they found four proton groups for each resonance level, corresponding to four Q values, given as 2.07, −0.16, −1.53 and −2.67 MV. The residual nucleus can then be left either in the ground state ($Q=2.07$ MV) or in one of three excited levels of 2.23, 3.60 or 4.74 MV above the ground state. Duncanson and Miller also found that nonresonance protons were observed for alpha-energies greater than 6.7 MV. These are interpreted as coming from alpha-particles going over the top of the potential barrier (cf. §78) an explanation which is justified by the observed increase of yield up to the limit of 7.7 MV.

The widths of the resonance levels may be stated, as in optical spectra, in terms of the width at half-maximum. Although the poor resolution of the experiments leaves some room for doubt as to the accuracy of the estimates, several methods of interpreting the data lead to a value of about 0.1 to 0.3 MV for this width (D19), for the higher energy levels. Lower energy levels would be expected to be narrower.

The results of these studies of the Al disintegration are summed up graphically in the form of an energy level diagram by Chadwick and Feather (C10) indicating the six resonance levels and the penetration through the barrier. The four Q values are represented as four arbitrarily placed alpha-particle levels in the nucleus. (See reference 13. It should be noted that there are some 22 energetically allowed proton groups from the various combinations of the 6 resonance levels and the 4 excitation levels, in addition to the protons due to normal entry.

Yield.—The values for the absolute yield of protons from a given intensity of alpha-particles on particular targets are subject to considerable error. One factor is the difficulty of estimating the thickness of the target and the solid angle subtended by the recording instrument. If the geometry of the experiment is sufficiently well defined to give such a value, the further question of the angular distribution of the ejected protons arises. An even more important point is that the probability of disintegration is a decided function of the alpha-particle energy, not only for the resonance groups but also for the normal groups. With a given thickness of target (specifying a definite range of energies), a known homogeneous alpha-particle energy and a known angular distribution, it is possible to estimate the probability of disintegration from the numbers of protons counted. This may be expressed in terms of the number of disintegrations per million alpha-particles, or equivalently, as the cross section of the process expressed in sq. cm for the individual reaction. Rutherford gives the rather rough estimate of 20 protons/10^6 alphas in N when alphas of 7 cm range are completely absorbed, and 8/10^6 for Al. Heavier targets, such as Cl, A and K yield smaller numbers of protons under similar conditions, about 1/10^6.

Protons have been observed and measured from alpha-particle bombardment of B^{10}, N^{14}, F^{19}, Ne^{20}, Na^{23}, Mg^{24}, Al^{27}, Si^{28}, P^{31}, S^{32}, Cl^{35}, K^{39} and Ca^{40}. In addition to the above-named processes determined by the observation of the protons, induced radioactivity has been found to occur in $Mg^{25, 26}$, Ca^{40}, Cr^{53} and Ni^{58} (see §105), directly attributable to this type of reaction. We will now discuss the individual reactions in more detail.

B: $B^{10}+He^4\rightarrow C^{13}+H^1$
($B^{11}+He^4\rightarrow C^{14}+H^1$)

Protons were first observed by Rutherford and Chadwick (R24), and were resolved into several groups by later observers. Miller, Duncanson and May (M16) find four groups of protons, each varying in range with the energy of the alpha and the direction of observation and giving Q values of 3.1, 0.4, −0.1 and −1.0 MV. A re-evaluation following the procedure discussed in §97 gives for these groups the values 3.3, 0.5, 0.1 and −0.8 MV. Paton (P3) checks these in principle, giving Q values of 3.1, 0.35, −0.78 and −1.86 MV. His second group (0.35) is probably a superposition of Miller and Duncanson's 0.5 and 0.1 MV groups, and the −1.86 group represents a higher excitation level. A calculation of the expected energy of disintegration into the ground state of the C^{13} residual nucleus from known masses gives a value of 4.15 MV. There is a discrepancy with the highest observed Q value of almost 1 MV, much greater than is found in any of the other α-p reactions. The mass values are good to ±0.2 MV,

and the internal consistency of the α-p reactions is also about that good. This discrepancy suggests that the group representing the transition into the ground state of C^{13} had not been observed. Brubaker and Pollard (B66) have recently searched for such a group and have found one of very weak intensity giving a Q value of 4.7 ± 0.5 MV, compatible with the expected value. If the groups discussed above are all from this process this conclusion would suggest five excitation levels; assuming the calculated 4.1 MV to represent the ground state these would be at 0.8, 3.6, 4.0, 4.9 and 6.0 MV. It may be mentioned at this point that the use of the observed 3.3 MV Q value falsified Bethe's (B11) first attempt to evaluate atomic masses from disintegration data.

One or more of the groups mentioned above and heretofore assumed to all come from the B^{10} isotope may be due to the equivalent reaction on B^{11}. The Q value obtained from masses in this case is 0.94 MV, and the large abundance of this isotope should result in an observable number of protons. It is possible that the proton group yielding the 0.5 MV Q value may be due to this reaction.

Miller, Duncanson and May (M16) also observe a broad group of protons indicating resonance for 2.9 MV alphas. The evidence is not completely satisfactory and it may be the proton group due to normal entry observed by Paton which results in the -1.86 MV Q value.

Gamma-rays, observed by Bothe and Becker (B43) to have an energy of 3 MV, are probably attributable to this reaction although the energy available in the B^{10}-α-n and B^{11}-α-n reactions is also sufficient to explain them. A group of gamma-ray lines would be expected for this reaction and the 3 MV may represent the 4.0 to 0.8 MV transition. A gamma-ray of 3.5 MV observed by Crane and Lauritsen (C43) from the C^{12}-d-p reaction resulting in a C^{13} product was at one time thought to be the gamma observed by Bothe and Becker. It is now known that there is insufficient energy available in the deuteron process to produce this excitation and another explanation of the 3.5 MV gamma-ray is required. (§101).

N^{14}: $N^{14}+He^4 \rightarrow O^{17}+H^1$.

This process is historically interesting as the first artificial disintegration ever observed. There is considerable discrepancy in the more recent literature, an indication of the difficulties involved in experiments using the low intensities of natural alpha-particle sources. The best values are obtained by Haxel (H18) who finds a Q value of -1.26 MV, which checks reasonably well with that expected from the masses, of -1.16 MV. Other evidence by Pollard (P7) and Steudel (S23) seems to confirm Haxel's value. Stegmann (S21) finds Q's of -0.41, -0.95 and -1.60 MV; two of the proton groups (longest and shortest) show characteristics indicating resonance for alphas of 3.6 and 4.1 MV. Stetter (S22) and Fischer-Colbrie (F21) report Q's of -1.4 and -2.8 MV, apparently justified by the observation of gamma-radiation of 1.3 to 1.5 MV energy observed by Savel (S6), and two resonance levels.

The lack of agreement is probably chiefly due to the poor geometry of the experiments, necessitated by the low intensities. That this is the case is also indicated by the low Q values obtained for many α-p reactions. Furthermore the calculation of Q values from groups attributed to resonance disintegration may be invalid. It is dangerous to assume resonance unless a full energy proton group is observed corresponding to the same Q value.

In the O^{16}-d-p reaction from which the O^{17} mass was obtained (used in the evaluation of the expected -1.16 MV Q value), an excitation level of 0.8 MV was observed (§101B). There seems to be no evidence for this excitation level in O^{17} from this reaction.

F^{19}: $F^{19}+He^4 \rightarrow Ne^{22}+H^1$

Six proton groups are found by Chadwick and Constable (C4), occurring in pairs and so indicating two Q values. The corrected values are 1.58 and 0.98 MV. Two resonance levels are found, at 4.1 and 3.7 MV (C10). The Q value representing the ground state transition is found to be 1.53 MV from the masses, in good agreement with the results of the observations. May and Vaidyanathan (M11) have observed at least two additional groups of protons, giving Q values of -3.2, -2.1, -0.1 and 1.4 MV, and suggesting other excitation states. Corrected values indicate excitation states at 1.4, 3.4 and 4.5 MV.

Measurements of the gamma-radiation by different observers give values of 1.2 (S5) and 2.0

MV (W4), and are probably influenced by the neutrons also emitted.

An interesting phenomenon involving the competition of nuclear processes is reported by Haxel (H18). He finds that the proton intensity increases with alpha-energy up to a certain point and then remains constant until the alpha-energy is reached at which neutrons are emitted, at which point the proton intensity decreases.

Ne^{20}: $Ne^{20}+He^4 \rightarrow Na^{23}+H^1$

Pollard and Brasefield (P9) have been the only observers to check the original report of Rutherford and Chadwick, and find a single proton group. Recalculation of their data gives a Q value of -2.54 MV. The mass values of the constituents are fairly well established, and give a Q of -1.42 MV. It is probable that they did not observe the longest range proton group, and that their data represent an excitation level at 1.1 MV.

Na^{23}: $Na^{23}+He^4 \rightarrow Mg^{26}+H^1$

The first work of importance following the preliminary reports of Rutherford and Chadwick is by König (K21). She finds 4 proton groups, whose Q values (recalculated) are 1.91, -0.2 MV and two of smaller energy. May and Vaidyanathan (M11) with higher energy alphas did not find the longest range proton group because of low intensity. For the three shorter groups their results are in sufficient agreement with those of König and if recalculated, give -0.4, -2.1, -3.1 MV. The Mg^{26} mass is determined through this reaction, using the 1.91 MV Q value. Gamma-rays occur but measurements are contradictory. The excitation states are at 2.2, 4.0 and 5.0 MV.

Mg: $Mg^{24}+He^4 \rightarrow Al^{27}+H^1$
$Mg^{25}+He^4 \rightarrow Al^{28}+H^1$
$Mg^{26}+He^4 \rightarrow Al^{29}+H^1$

The protons emitted from Mg have been found by Duncanson and Miller (D19) to have three groups, two of strong intensity and short range and one weak but of longer range. The Q values obtained from the data (recalculated) are -1.05, -1.82 and -2.87 MV for the three groups, assuming the Mg^{24} isotope responsible. More recent data by Haxel (H19) check the Q values of Duncanson and Miller.

In attempting to identify these proton groups with the Mg isotopes responsible it was found necessary to consider the Q values predicted by masses (§108). For Mg^{26} a Q of -4.5 MV is expected so that this isotope is definitely excluded. The calculated Q for the Mg^{25} target based on the reactions Al^{27}-d-α and Al^{27}-d-p is -0.6 MV which seems to agree sufficiently with the Q value observed for the low intensity proton group. (-1.05 MV.) The Q for Mg^{24} cannot be calculated with any certainty because the two nuclei involved (Mg^{24} and Al^{27}) are only connected through two mass spectrograph measurements (of Ne^{21} and Si^{28}) together with five nuclear disintegration reactions, so that the over-all error may be very large. However, an estimate of the Mg^{24} reaction energy may perhaps be obtained from analogous nuclei such as Ne^{20} ($Q=-1.4$), Si^{28} ($Q=-1.8$) and S^{32} ($Q=-2.1$). A Q value of -1.8 MV for Mg^{24} would fit well with this sequence whereas the higher Q value would not. Therefore we attribute the weak group of $Q=-1.05$ to Mg^{25} and the two other strong groups to Mg^{24}.

Duncanson and Miller also find resonance protons for alphas of 5.7 and 6.3 MV but they were unable to determine which proton groups these resonances were associated with. A knowledge of this feature would assist in assigning the groups to the respective isotopes. Nonresonance disintegration was observed to start with alphas of 6.5 MV.

Gamma-radiation expected from the excitations of the product nucleus is observed but reports of its energy vary from 0.5 MV (S5) to 5.0 MV (W4).

More positive evidence for the Mg^{25} reaction has been through the observation of an induced electron radioactivity of 2.36 min. half-life (A2, E10) and the identification of the active material as aluminum. Since the Q value of the reaction is not known to any accuracy the value of the Al^{28} disintegration energy is used for the calculation of the Al^{28} mass.

A weaker electron radioactivity of 11 minutes half-life is attributed (E10) to the Al^{29} coming from the Mg^{26} isotope ($Q=-4.5$ MV). This furnishes evidence for the existence of two radioactive isotopes both heavier than the stable isotope.

Al^{27}: $Al^{27}+He^4 \rightarrow Si^{30}+H^1$

In the introductory paragraphs the data of Chadwick and Constable (C4), Haxel (H17), Duncanson and Miller (D19), etc., have been discussed. These lead to the Q values (recalculated) of 2.26, −0.02, −1.32 and −2.49 MV and show excitation levels in the Si^{30} nucleus at 2.3, 3.6 and 4.8 MV. Savel (S4) shows that the gamma-radiation is composed of at least two components and gives a value for one of them of about 2.0 MV. The highest Q value (2.26 MV) is used to obtain the Si^{30} mass. Aluminum has six resonance levels, as discussed earlier, for 4.0, 4.44, 4.86, 5.25, 5.75 and 6.61 MV alphas.

Si^{28}: $Si^{28}+He^4 \rightarrow P^{31}+H^1$

Proton groups having ranges of 20, 28 and 37 cm at 90° from 7.68 MV alphas observed by Haxel (H17) indicate Q values (recalculated) of −2.23, −3.28 and −3.92 MV. The large abundance of the Si^{28} isotope and the fact that P^{31} is a stable product determine that this isotope is the only one involved. This reaction allows a direct comparison with the masses of Si^{28} and P^{31} determined by Aston, and from which a Q of −1.4 MV is obtained. The adopted mass values (§108) are chosen to split this discrepancy so that the Q obtained is −1.8 MV. This agreement is fairly satisfactory but is at the same time another indication that the low intensities and poor geometry of the α-p reactions lead to low Q values. However, it is possible that the observed group should be attributed to a transition to an excited state rather than to the ground state.

P^{31}: $P^{31}+He^4 \rightarrow S^{34}+H^1$

From the data of Paton (P1), May and Vaidyanathan (M11), and Pollard and Brasefield (P8) a set of average Q values are obtained which are 0.31, −1.0, −2.5, and −4.5. No resonance was found. By analogy with other reactions on this type of nucleus, in which ground state Q values of about 2 MV are common we judge that the longest range proton group was not observed. The Q obtained from masses is 1.8 MV.

S^{32}: $S^{32}+He^4 \rightarrow Cl^{35}+H^1$

Brasefield and Pollard (B50) and Haxel (H19) find three groups of protons. An average of the recalculated Q values gives the values −2.10, −2.7 and −3.6 MV. The −2.1 MV value is used for the determination of the Cl^{35} mass. There is no evidence for resonance.

$Cl^{35, 37}$: $Cl^{35, 37}+He^4 \rightarrow A^{38, 40}+H^1$

Three well-defined proton groups reported by Pollard and Brasefield (P8) show Q values of 0.1, −2.5 and −4.2 MV and have no resonance characteristics. Mass values give Q values of 2.0 and −1.2 MV for the Cl^{35} and Cl^{37} isotopes, suggesting that the long range protons are from Cl^{35}.

A: (not observed)

Rutherford and Chadwick, in their early experiments, reported protons from argon. Recently Pollard and Brasefield (P9) made an extended study of the supposed process and found no evidence for disintegration. This is the only instance in which the early work of Rutherford and Chadwick has not been checked by subsequent experimenters. The protons observed were probably due to nitrogen or neon contamination.

K^{39}: $K^{39}+He^4 \rightarrow Ca^{42}+H^1$

Three proton groups measured by Pollard and Brasefield (P9) result in corrected Q values of −0.89, −2.3 and −3.5 MV. From comparisons with the Q values in analogous nuclei it seems probable that this −0.89 MV does not represent the ground state transition, but the first or second excitation level.

Ca^{40}: $Ca^{40}+He^4 \rightarrow Sc^{43}+H^1$

Frisch (F32) found a radioactivity in Ca chemically separable as Sc which has only one unit higher charge than Ca and so determines the reaction. Walke (W1) has checked this observation with the 11 MV He^{++} ions from the cyclotron and finds a period of 4.0 hr.

Following Frisch's report Pollard and Brasefield (P9) have observed a single proton group from which we calculate a Q of −4.3 MV.

$Ti^{46, 47}$: $Ti^{46, 47}+He^4 \rightarrow V^{49, 50}+H^1$

An activity identifiable as V has been observed by Walke (W1a) to come from Ti on bombardment with artificially accelerated He^{++} ions of 11 MV. This has a period of 35 min. Other activities, of 2.7 hr., 5.5 hr. and 85 days are not yet identified.

TABLE LI. *Summary of α-p type reaction.*

TARGET Z	TARGET El	PRODUCT El	Q(MV) (CALC.)	Q(MV) (OBS.)	REFERENCE	RESONANCE LEVELS (MV)	EXCIT. LEVELS (MV)	YIELD p/α @ (MV)
2	He^4	Li^7	−17.25					
3	Li^6	Be^9	−2.25					
	Li^7	Be^{10}	−2.58					
4	Be^9	B^{12}	< −7.2					
5	B^{10}	C^{13}	4.15	4.7?	B66	2.9?	0.8 3.6? 4.0	$2/10^6$ @ 2.9
	B^{11}	C^{14}	0.94	Obs. ?	M16		4.9 6.0	
6	C^{12}	N^{15}	−4.79					
	C^{13}	N^{16}	−7.4					
7	N^{14}	O^{17}	−1.16	−1.26	H18	3.6? 4.1?	?	$2/10^5$ @ 7.8
	N^{15}	O^{18}	−2.83					
8	O^{16}	F^{19}	−8.14					
9	F^{19}	Ne^{22}	1.53	1.58	C4	3.7 4.1	0.6 1.4 3.4 4.5	$2/10^6$ @ 7.8
10	Ne^{20}	Na^{23}	−1.42	(−2.54)	P9		1.1	$1.2/10^5$ @ 7.8
	Ne^{21}	Na^{24}	−1.8					
11	Na^{23}	Mg^{26}	1.9*	1.91	K21		2.2 4.0 5.0	$2.5/10^6$ @ 4.4
12	Mg^{24}	Al^{27}	−1.6*	−1.82	D19	5.7 6.3	1.0	$1/10^6$ @ 7.8
	Mg^{25}	Al^{28}	−0.6	−1.05	E10			$1/10^7$ @ 7.8
	Mg^{26}	Al^{29}	−4.5	Obs.	E10			$1/10^8$ @ 7.8
13	Al^{27}	Si^{30}	2.26*	2.26	D19	4.0 4.44 4.86 5.25 5.75 6.61	2.3 3.6 4.8	8/10⁶ @ 7.8
14	Si^{28}	P^{31}	−1.8*	−2.23	H19		1.05 1.7	$1/10^6$ @ 7.8
	Si^{29}	P^{32}	−1.6					
15	P^{31}	S^{34}	1.9	(0.31)	P8		x(1.5) x+1.3 x+2.8 x+4.8	$1/10^6$ @ 8.3
16	S^{32}	Cl^{35}	−2.1*	−2.10	H19		0.6 1.5	$1/10^6$ @ 7.8
	S^{34}	Cl^{37}	−4.0					
17	Cl^{35}	A^{38}	2.0	(0.16)	P8		x(1.9) x+2.6 x+4.3	$1/10^6$ @ 8.3
	Cl^{37}	A^{40}	−1.2					
19	K^{39}	Ca^{42}	—	−0.89	P8		x x+1.4 x+2.6	$1/10^6$ @ 7.8
20	Ca^{40}	Sc^{43}	—	−4.3	P9			$5/10^6$ @ 8.3
22	Ti	V	—	Obs.	W1a			
24	Cr^{53}	Mn^{56}	—	Obs.	H24b			
28	Ni^{58}	Cu^{61}	—	Obs.	R7b			

* Q (Observed) used to calculate mass values.

Cr^{53}: $Cr^{53}+He^4 \rightarrow Mn^{56}+H^1$

Henderson and Ridenour (H24b) report a 160-min. electron activity produced in Cr by 8 MV alphas. Mn^{56} is known to have such a period from Mn-n-γ, Co-n-α, and Fe-n-p reactions (A7).

Ni^{58}: $Ni^{58}+He^4 \rightarrow Cu^{61}+H^1$

A 3.4-hr. positron activity, chemically identified as Cu, has been found by Ridenour and Henderson (R7b, R7c) after bombardment of nickel by 7 MV alphas. Such an activity had been found previously to be produced in the

Ni-*d*-*n* (T10a) and perhaps Ni-*p*-*n* (B4a) reactions.

Correlations in excited states of similar nuclei.— Before leaving the discussion of the α-*p* type of disintegration we must mention the apparent correlations in the magnitudes and spacings of the excitation states from similar nuclei. By similar we mean those of the same nuclear type, having mass numbers $4n+2$, $4n+3$, etc. The excitation states exist in the product nuclei so the type designation will be applied to the product nucleus in each case. These correlations have been pointed out and discussed by Haxel (H19), Pollard and Brasefield (P8), May and Vaidyanathan (M11), etc., and have been used as arguments for the alpha-particle sub-unit in the nucleus. In order to study such correlations the corrected Q values and their differences, which represent the spacings between excitation levels, have been tabulated. See Table LII. We see that the similarity in the excitation level spacings is not quantitative, but is still apparent. Furthermore the values of the reaction energies themselves are roughly equivalent, or at least vary consistently. The main point is that the spacings of low excitation levels in *odd* product nuclei are smaller than the spacings of levels in *even* product nuclei, a result which would be expected theoretically (see Feenberg and Wigner (F10)). These similarities add weight to the arguments for the existence of closed proton-neutron shells in the nucleus. They do not give much evidence for periodicities with the period 4 (alpha-particle sub-units), however.

TABLE LII. *Correlations in excitation states of similar nuclei in α-p reactions.*

Product nuclei type $4n+2$						Excitation level Spacings:		
Target	Product	Q_0	Q_1	Q_2	Q_3	(1)	(2)	(3)
Na^{23}	Mg^{26}	1.9	−0.3	−2.1	−3.1	2.2	1.8	1.0
Al^{27}	Si^{30}	2.3	0.0	−1.3	−2.5	2.3	1.3	1.2
P^{31}	S^{34}	?	0.3	−1.0	−2.5	?	1.3	1.5
K^{39}	Ca^{42}	?	−0.9	−2.3	−3.5	?	1.4	1.2
Product nuclei type $4n+3$								
Mg^{24}	Al^{27}	−1.8	−2.9			1.1		
Si^{28}	P^{31}	−2.2	−3.3	−3.9		1.1	0.6	
S^{32}	Cl^{35}	−2.1	−2.7	−3.6		0.6	0.9	

B. Type reaction α-*n*. (Table LIII)

$$Z^A + He^4 \rightarrow (Z+2)^{A+3} + n^1 + Q:$$

Certain anomalous properties and effects of the supposed gamma-radiation from Be under alpha-particle bombardment had been under investigation by several experimenters when Chadwick (C6) concluded that these properties were due, not to gamma-radiation, but to a new elementary particle of unit mass and zero charge, the neutron. Other workers immediately started searching for these disintegration products from other targets, and they have been found as well in the alpha-bombardment of Li, B, F, Na, Mg and Al. The Be reaction yields the greatest intensities and also the highest energy neutrons, and constitutes at present the source used by many investigators for studies of the properties of and disintegrations produced by neutrons.

In some reactions the neutrons are observed and measured through the recoil protons they produce in hydrogen. Such protons have been studied with ionization chambers behind paraffin absorbers (D21) and with hydrogen or methane filled cloud chambers (B40). Other reactions of this type have been determined through the observation of positron radioactivity, utilizing chemical analysis and comparison of half-life values. This has resulted in establishing the process for several elements in addition to those from which neutrons have been recognized.

As in the α-*p* type reaction a few processes have been found to have characteristics suggesting resonance entry of the alpha-particle, of which Be^9 and B^{10} are most certain.

H^2: $H^2 + He^4 \rightarrow H^1 + n^1 + He^4$ (noncapture)

Schultz (S8a) reports that neutrons are produced when deuterium is bombarded by Th C alphas (8.78 MV). This is interpreted as due to a noncapture disintegration of the deuteron for which the energy required is 2.20 MV.

Li^7: $Li^7 + He^4 \rightarrow B^{10} + n^1$

Large intensities of neutrons were observed from Li both before (B43) and after (C56) Chadwick gave the new particle a name. The neutron energies have not been measured, but calculations from masses indicate that the Q value is -2.99 MV and that the neutron energies should extend up to a maximum of 1.0 MV for Po alphas.

Gamma-rays of about 0.4–0.6 MV (W4, B47) have been the subject of controversy. Curie and Joliot (C59), Schnetzler (S7) and Savel (S6) have found that gammas were observed for alphas of more than about 3 MV, while they did not detect neutrons until alphas of about 5 MV were used. This seemed to indicate two processes and since Li was not known to yield protons of any intensity a *noncapture* excitation of the Li was sugtested (C10) to explain the gamma-rays.

$$Li^7+He^4\rightarrow{}^*Li^7+He^4;\quad {}^*Li^7\rightarrow Li^7+h\nu.$$

This conclusion was forced by the impossibility of balancing the mass-energy equation of the α-n type process under discussion if the gamma-ray was the result of an excited B^{10} nucleus. The Q value calculated from the present mass values is -2.99 MV. Since only the relative kinetic energy of the alpha-particle is available for excitation or disintegration, alpha-particles of $11/7\times 2.99$ MV $=4.7$ MV are required to produce neutrons, in accord with the experimental results of Savel, etc. An even higher energy would be required to leave the B^{10} nucleus in an excited state. Other possible reactions caused by alpha-particles on Li would have similar Q values (e.g., Li^6-α-n, $Q<-4.2$ MV; Li^6-α-p, $Q=-2.3$ MV; Li^7-α-p, $Q=-2.6$ MV), and can therefore not be produced by 3 MV alphas, especially if the residual nucleus is to be left in an excited state. There remain therefore only two processes, namely the "noncapture" excitation of Li^7 and the radiative capture of the alpha-particle forming B^{11} (B53a). According to our present knowledge, the probability of emission of particles from a light compound nucleus is always much larger (by a factor of 10^4 or more) than the probability of emission of gamma-rays (§81), unless the particle emission is forbidden by a rigorous selection rule which is not the case here. Therefore the noncapture excitation seems to be the more probable process, which is also confirmed by the energy of the gamma-rays (B47) which should be 9 MV for the radiative capture process but is actually less than 1 MV.

From the Li^6-d-p reaction (R19) it is known that Li^7 possesses an excited state with 0.44 MV excitation energy (§101B). The γ-ray measurements of Bothe (B47) indicate γ-rays of approximately this energy. Bothe analyzes his curve as showing two γ-rays of 0.4 and 0.6 MV[14] and possibly a third of 0.2 MV. It is hard to understand how such a spectrum could originate from the Li^7 nucleus because theoretically this nucleus should have only two low levels ($^2P_{\frac{3}{2}}$, $_{\frac{1}{2}}$) including the ground state, and the next higher level should have an excitation energy of at least 2 MV.

We expect, therefore, that only one gamma-ray (of 0.44 MV) will be produced by alpha-particles of energies from 0.7 MV up to about 5.6 MV. Above 5.6 MV the B^{10} product nucleus of the α-n reaction might be left in the excited state at 0.6 MV known from the Be^9-d-n reaction.

Be^9: (a) $Be^9+He^4\rightarrow C^{12}+n^1$
(b) $Be^9+He^4\rightarrow 3He^4+n^1$

Because of its intensity and prominence as a source of neutrons for studies of induced radioactivity and other processes, this reaction has received considerable attention. The first good distribution in range curve of projected protons was published by Dunning (D21), using a paraffin layer in front of a shallow ionization chamber actuating a linear amplifier. With a radon alpha-source in which there are three groups of alphas, of 5.44, 5.97 and 7.68 MV from Rn, Ra A and Ra C′, respectively, he observed many groups: 13.7, 12.0, 7.6, 6.2, 4.6 MV and large intensities in unresolved groups between 0.5 and 1.5 MV. See Fig. 44. The proton groups expected from the first two alpha-groups are probably unresolved, so two groups should be expected for each Q value of the process. Although the intensity of the longest range proton group is extremely small (from 7.68 MV alphas), it can be used to obtain a Q value (recalculated) of 6.3 MV. The value obtained from the masses is 5.56 MV. A better experimental value is given by Bernardini (B7a) who finds neutrons of 11 MV using Po alphas and obtains a Q of 5.8 MV.

The group structure of the neutrons has been most carefully studied by Bernardini and

[14] Crane and Lauritsen (C43) have observed a gamma-ray of essentially the same energy (0.7 MV) from deuterons on Be, supposedly from a B^{10} isotope. Evidence from neutron groups in the same reaction (B35) also shows a 0.6 MV excited level in the B^{10} nucleus. This was originally correlated (C43) with the Li-α gamma-ray and said to be due to B^{10}. Since this is now shown to be energetically impossible the coincidence in values must be regarded as fortuitous.

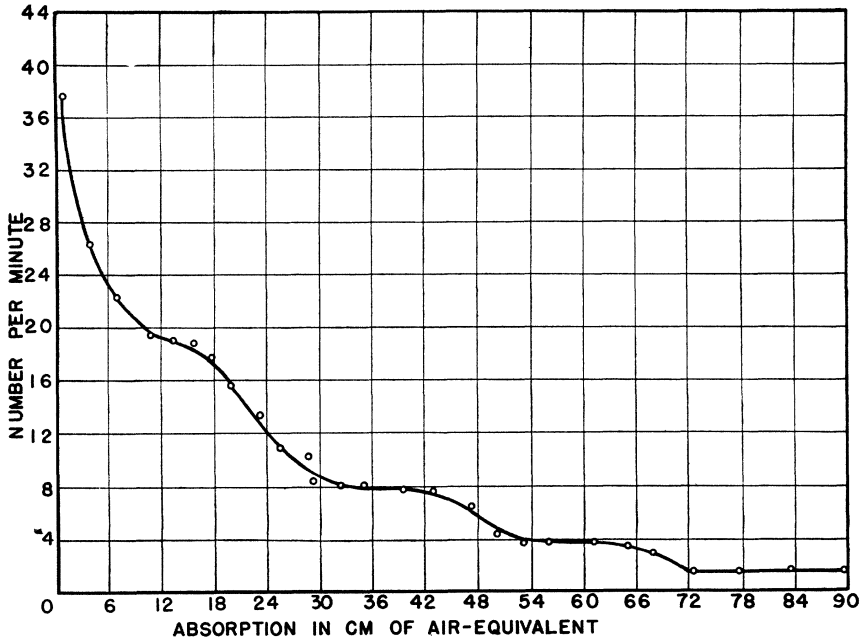

FIG. 44. Distribution-in-range curve of the recoil protons projected by the neutrons from the Be^9-α-n reaction, according to Dunning. The curve shows various energy groups indicating excitation levels in the final nucleus C^{12}, and a very great number of slow neutrons which probably originate from the four-particle disintegration $Be^9+He^4=3He^4+n^1$.

Bocciarelli (B7b). Using Po alphas, which have the advantage of having only one alpha-group (5.3 MV), they find neutron groups representing Q values of 2.8, 1.4 and -0.6 MV. Using Bernardini's value for the highest energy group (5.8 MV Q) this indicates excitation levels in C^{12} at 3.0, 4.4 and 6.4 MV. Blau (B64), using the photographic emulsion technique, reports a total of 10 neutron groups of which three are strong enough to be considered (28, 47 and >100 cm). These lead to Q values of -0.7, 1.1 and >4.1 MV. Bonner and Mott-Smith (B35), using the pressure cloud chamber and the same source, observe a large number of groups (22 in all) very few of which are justified statistically. They were not able to observe the longest range recoils representing the highest Q value.

From the measurements of Bothe (B47) the gamma-radiation from this process is found to have three components, at 6.7, 4.2 and 2.7 MV. Gammas of essentially the same energy (6.7, 4.2 and 2.4 MV) have been found by Crane, Delsasso, Fowler and Lauritsen (C44) in the bombardment of B by deuterons (in addition lines at 5.6 and >10 MV were observed). The first three mentioned may well be interpreted as coming from $*C^{12}$ in the B^{11}-d-n reaction and be identical with those of Bothe. They also agree fairly well with the excitation states of the C^{12} nucleus as determined from neutron groups. From groups in the B^{11}-d-n reaction yielding the same product nucleus (§102) an excitation level is found at 4.4 MV, and another at 9.5 MV. Rasetti (R2) observes that the excitation curves for the production of neutrons and gamma-rays are identical, indicating that they come from the same process.

In all observations there are found large numbers of slow neutrons, usually not resolved into groups. From the "evaporation model" of nuclear disintegrations (§54) not many neutrons of energies below 2 MV would be expected. It was suggested by Bohr that the slower neutrons are due to a different process, namely:

$$Be^9+He^4\rightarrow *C^{13}\rightarrow *Be^9+He^4;\quad *Be^9\rightarrow Be^8+n^1.$$

The final products would be 3 alpha-particles and a neutron; the same set of products have been observed in other processes where the $*C^{13}$ compound nucleus is formed, e.g., $C^{12}+n^1$ and $B^{11}+H^2$. The calculated Q value for the complete reaction is -1.59 MV.

Bernardini (B7) has observed definite evidence

for a resonance level for 3.3 MV alphas. Chadwick (C7) reports two levels, at 1.5 and 2.6 MV, but with much less satisfactory data.

The complete evidence indicates four neutron groups, for Q's of 5.8, 2.8, 1.4 and -0.6 MV and one resonance level at 3.3 MV, besides the slow neutrons attributed to an alternate reaction.

B^{10}: $B^{10}+He^4 \rightarrow N^{13}+n^1$

Of the large intensities of neutrons observed from B about 1/10 are thought to come from the B^{10} isotope and lead to the radioactive N^{13} isotope (B35). Although this number may be observable as groups superimposed on those originating in the B^{11} disintegration, discussed in the following reaction, no information is at hand to identify them. The calculated Q value of this reaction is 1.11 MV.

The Curie-Joliots found an induced radioactivity with positron emission and half-life of about 14 min. in their first reports of this phenomenon. Ellis and Henderson (E5), with more careful measurements, have shown the period to be 11.0 min. (see §105). The most accurate values of positron energy are obtained from N^{13} produced by the C^{12}-*d*-*n* reaction (§102) and show a maximum of 1.25 MV.

The alternative reaction yielding protons is known to result in the same ultimate product, C^{13}. The calculated Q is 4.1 MV, the measured value was 3.3 MV. By combining these twe primary reactions with the energy release of tho radioactive process a value may be obtained for the neutron mass. This method was proposed by Curie and Joliot (C55) before the more accurate methods now employed were known. The assumption made by Curie and Joliot was that all neutrons originated from B^{10} and that their experimentally determined energy could be used in calculating masses. Since only about 1/10 of the neutrons seem to so originate the cycle is invalidated unless the particular group of neutrons can be identified.

B^{11}: $B^{11}+He^4 \rightarrow N^{14}+n^1$

The greater number of neutrons from B are from the B^{11} isotope, yielding a stable N^{14} nucleus (B35). Chadwick (C5) first identified this radiation as neutrons and in following work by the Curie-Joliots (C59) and Chadwick (C7) the maximum neutron energy was found to be 3.3 MV for Po alphas. Bonner and Mott-Smith (B35) have made a cloud chamber study of the neutron energy distribution using Po alphas and find many groups, of which the most energetic is 4.1 MV. The statistical error involved in plotting curves through such a small amount of data makes most of these groups uncertain. Assuming the most energetic group to come from B^{11} with alphas of maximum energy and without excitation of the residual nucleus, $Q=-0.7$ MV. The calculated value is $+0.32$ MV.

Gamma-rays from B have been measured by Bothe and Becker (B43) and others to be about 3.0 MV but are attributed to the excited C^{13} product of the α-p reaction. Chadwick (C7) reports a resonance level for alphas of >2.6 MV.

N^{14}: $N^{14}+He^4 \rightarrow F^{17}+n^1$

Danysz and Zyw (D3) and Wertenstein (W12) have found a 1.2 min. positron activity in nitrogen due to the F^{17} resulting from this process. Other observers (E5) have found it as a spurious period on other targets bombarded in air. The same activity has more recently been found by Newson (N6) in deuteron bombardment of O^{16} with a half-life of 1.16 min. The positron energy spectrum has been measured by Kurie, Richardson and Paxton (K33) to have a 2.1 MV maximum.

In studies of the α-p reaction on nitrogen Haxel (H18) found a positron radioactivity of 1.2 min. period for alphas of greater than 7 MV energy. The fraction of this energy available for the reaction is 5.45 MV, so this suggests a Q value of -5.45 MV for the primary process. The Q calculated from masses is -4.8 MV.

F^{19}: $F^{19}+He^4 \rightarrow Na^{22}+n^1$

The neutrons from F were first observed and studied by Chadwick and the Curie-Joliots. Bonner and Mott-Smith (B35) find 5 groups, the most energetic being 2.12 and 2.54 MV, and resulting in Q values (re-evaluated) of -2.3 and -2.6 MV. Some of the groups can be explained by considering the two resonance levels found in the α-p reaction at 3.7 and 4.1 MV. From the mass of Na^{22} obtained by using the radioactive energy evolution we judge the primary reaction to have a Q value of about -0.7, so the highest energy neutrons were not observed.

Meitner (M14) and Frisch (F32) have found a

long lived positron activity ($T \sim 6$ months) in F attributed to this process. Meitner reported a positron energy maximum of 0.4 MV which is of questionable accuracy and probably low, while Frisch estimated the period and performed chemical separation tests to identify the product as Na.

Na^{23}: $Na^{23}+He^4 \rightarrow Al^{26}+n^1$

Although neutrons have been observed (C59), (S5), no energy measurements are available. The positron radioactivity of 7 sec. half-life has been studied by Frisch (F31) to identify the reaction.

Mg^{24}: $Mg^{24}+He^4 \rightarrow Si^{27}+n^1$

Savel (S5) reports neutrons from Mg, corroborating the reaction discovered by the Curie-Joliots (C54) leading to positron radioactivity. Mass values give a Q of -5.3 MV. The half-life is 6.7 min. (F1) and the maximum positron energy is given as 2.0 MV (A2a). Ellis and Henderson (E10) and Fahlenbrach (F1) suggest resonance levels for alphas of 5.4 and 6.1 MV; these check the resonance levels found in the α-p process at 5.7 and 6.3 MV, and indicate excitation levels in the compound nucleus Si^{28}.

Al^{27}: $Al^{27}+He^4 \rightarrow P^{30}+n^1$

Curie and Joliot (C54) reported radioactivity from Al as one of their three original reactions. The half-life is 2.5 min. (R7a) and the radioactive energy 3.6 MV (A1). The neutrons from the primary reaction have been observed by Savel (S4) and others. Waring and Chang (W3) have studied the resonance levels for neutron production and finds 6 or 7 levels agreeing closely with those found for proton emission. A Q of -3.3 MV is expected.

P^{31}: $P^{31}+He^4 \rightarrow Cl^{34}+n^1$

Frisch (F31) observed a positron activity of 40 min. half-life from P activated by alphas and estimated the positron energy to be 1.8 MV. His comparison with the energy of positrons from Al, however, suggests a much higher value. Although neutrons are not observed, due to the low intensities, chemical tests prove the validity of the reaction. The calculated Q value is -1.6 MV.

Cl^{35}: $Cl^{35}+He^4 \rightarrow K^{38}+n^1$

A 7.7 min. positron activity resulting from the α-particle bombardment of Cl (H24a, H39a) can only be due to K^{38}, since other likely reactions produce stable isotopes.

Pollard, Schultz and Brubaker (P10) report the observation of neutrons from chlorine under alpha-particle bombardment for alpha energies of more than 6.6 MV. The observers assign the neutrons to a Cl^{37}-α-n reaction. It is possible that both occur.

A^{40}: $A^{40}+He^4 \rightarrow Ca^{43}+n^1$

Neutrons have been observed by Pollard, Schultz and Brubaker (P10) for alphas of more than 6.8 MV.

$K^{39, 41}$: $K^{39}+He^4 \rightarrow Sc^{42}+n^1$;
$K^{41}+He^4 \rightarrow Sc^{44}+n^1$

Zyw (Z3) first observed a positron activity, of 3 hr. period, in K after alpha-bombardment. Walke (W1), using 11 MV He^{++} ions from the cyclotron, finds periods of 4.1 hr. and 52 hr. The 52 hr. period is also found in the Ca-d-n reaction and so must be Sc^{44}; the 4.1 hr. period is then Sc^{42}.

Cr^{50}: $Cr^{50}+He^4 \rightarrow Fe^{53}+n^1$

The 8.9 min. positron activity chemically identified with Fe by Henderson and Ridenour (H24b) is assigned to Fe^{53} because a 91 min. period found by the Rochester group (B4a) to result from a Mn-p-n reaction must be due to Fe^{55}.

Co^{59}: $Co^{59}+He^4 \rightarrow Cu^{62}+n^1$

Ridenour and Henderson (R7b, H24b) find the 10 min. positron activity characteristic of Cu^{62} (see Tables LXVI and LXVIa) to result from the bombardment of Co by alphas.

Ni^{60}: $Ni^{60}+He^4 \rightarrow Zn^{63}+n^1$

Only the greater abundance of Ni^{60} over Ni^{62} favors this assignment for the 37 min. activity found by Ridenour and Henderson (R7c) and already known from Zn-n-$2n$ and Zn-γ-n reactions (§102, 103).

$Cu^{63, 65}$: $Cu^{63}+He^4 \rightarrow Ga^{66}+n^1$
$Cu^{65}+He^4 \rightarrow Ga^{68}+n^1$

Henderson and Ridenour (H24b) find that two positron activities (9.4 hr. and 68 min.), identified chemically with Ga, are produced from Cu under alpha-bombardment. The 68 min. period is probably the same as the 60 min. period found in a Ga-γ-n reaction (§103) and is there-

TABLE LIII. *Summary of α-n type reaction.*

TARGET Z	TARGET El	PRODUCT El	Q(MV) (CALC.)	Q(MV) (OBS.)	REFERENCE	RESONANCE LEVELS (MV)	EXCIT. LEVELS (MV)	YIELD n/α(Rn α's)
2	H^2	He^4+H^1	−2.20	obs.	S8a			
3	Li^7	B^{10}	−2.99	−5?	C59			
4	Be^9	C^{12}	5.56	5.8	B7a	3.3	3.0 4.4 6.4	$2.5/10^4$
	Be^9	$3He^4$	−1.59	obs.?				
5	B^{10}	N^{13}	1.11	obs.	C54			$1/10^5$
	B^{11}	N^{14}	0.32	−0.7?	B35	3?	many	$1/10^4$
6	C^{12}	O^{15}	−8.3					
	C^{13}	O^{16}	2.3					
7	N^{14}	F^{17}	−4.8	−5.5?	H18			
	N^{15}	F^{18}	−5.4					
8	O^{18}	Ne^{21}	−0.99					
9	F^{19}	Na^{22}	−0.7	−2.3?	B35		1.6 1.9	$3/10^5$
10	Ne^{21}	Mg^{24}	2.3					
	Ne^{22}	Mg^{25}	0.0					
11	Na^{23}	Al^{26}	−1.8	obs.	C59			$5/10^6$
12	Mg^{24}	Si^{27}	−5.3	obs.	C54	5.4 6.1		
	Mg^{25}	Si^{28}	2.0					
	Mg^{26}	Si^{29}	−1.7					
13	Al^{27}	P^{30}	−3.3	obs.	W3	4.0 4.5 5.0 5.25 (5.55) 6.0 6.7		$1/10^5$
14	Si^{29}	S^{32}	−0.7					
15	P^{31}	Cl^{34}	−1.6	obs.	F31			$2/10^6$
17	Cl^{35}	K^{38}	—	obs.	H24a, P10			$2/10^6$
18	A^{40}	Ca^{43}	—	obs.	P10			
19	K^{39}	Sc^{42}	—	obs.	Z3			
	K^{41}	Sc^{44}	—	obs.	W1			
24	Cr^{50}	Fe^{53}	—	obs.	H24b			
27	Co^{59}	Cu^{62}	—	obs.	R7b			
28	Ni^{60}	Zn^{63}	—	obs.	R7c			
29	Cu^{63}	Ga^{66}	—	obs.	H24b			
	Cu^{65}	Ga^{68}	—	obs.	H24b			
33	As^{75}	B^{78}	—	obs.	S16a			

fore assigned to Ga^{68}. This leaves Ga^{66} to account for the 9.4-hr. half-life.

As^{75}: $As^{75}+He^4 \rightarrow Br^{78}+n^1$

In a report by Snell (S16a) a positron active period of 6.3 min. from As bombarded by artificially accelerated He^{++} ions is found to be chemically Br, so specifying this type reaction.

§100. DISINTEGRATION BY PROTONS

A. Type reaction *p*-α. (Table LIV)

$Z^A+H^1 \rightarrow (Z-1)^{A-3}+He^4+Q$:

It was early in 1932 that Cockcroft and Walton (C21) were first successful in producing the disintegration of lithium by protons. The apparatus used was a condenser-rectifier voltage multiplier to produce the high voltage, applied to a discharge tube through which hydrogen ions were accelerated (§92). These experimenters, as were many others, were striving for a really high voltage source, but upon the introduction of the quantum-mechanical penetration idea, development was halted long enough to allow search for disintegrations. The observations were made on that time-honored instrument, the scintillation screen. An exhaustive series of experiments, using elements throughout the periodic table, showed that only in Li, B and F were any definite results then obtainable (C19). Many elements were found to give alpha-particles, but as was suggested at that time, they were later identified as due to impurities (of boron). With improvements in experimental techniques other

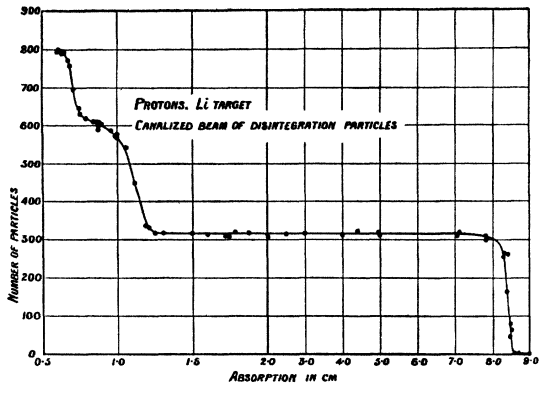

FIG. 45. Distribution in range of the α-particles produced by proton bombardment of lithium, showing the 8 cm alphas from $Li^7+H^1=2He^4$ and the short range particles He^3 (1.2 cm) and He^4 (0.8 cm) from $Li^6+H^1=He^4+He^3$. (Oliphant, Kinsey and Rutherford.)

reactions have been added to the list. It will be well to take up these elements individually.

Li^7: $Li^7+H^1\rightarrow He^4+He^4$

In the case of Li^7 the residual nucleus is itself an alpha-particle, so the energy evolved is divided equally between the two. These alphas were found to have a range of slightly over 8 cm, and are commonly referred to as the "8 cm group from Li." See Fig. 45. As we shall see later, this range depends to some extent on the bombarding proton energy. Oliphant, Kempton and Rutherford (O8) report that the normal process results in alpha-particles of 8.31 cm mean range (our corrected value, obtained from the 8.40 cm extrapolated range given by the observers) for protons of 0.19 MV if observed at 90° to the proton beam. The momentum-energy considerations for this case (§92) show that $Q=2E_2-\frac{3}{4}E_1$ or twice the energy of the alpha measured at 90° less $\frac{3}{4}$ the bombarding proton energy. Using the range-energy relation of §95 we find $Q=2(8.63)-\frac{3}{4}(.19)=17.13$ MV. This is in good agreement with the value of 17.25 MV obtained from the masses and justifies the masses and range-energy relations used. When higher energy protons are used alphas of longer range are observed, as for instance the 9.1 cm alphas (extrapolated range) observed at 90° by Livingston, Henderson and Lawrence (L28) for 1.4 MV protons. This extrapolated range[15] is equivalent to about 9.0 cm mean range or 9.1 MV and so $Q=17.1$ MV with somewhat less accuracy.

The assumed mechanism of the reaction is justified by the cloud chamber photographs of Dee and Walton (D6) using protons of less than 0.2 MV, in which the two oppositely directed alpha-particles are observed to originate from the same point on the thin target. The alphas will be co-linear only for very low energy protons. The momentum relations show that if one alpha is emitted at 90° the other alpha will make an angle to the direction of the proton beam of 79° for 1.4 MV protons, or 86° for 0.2 MV.

The alpha-particles from Li^7 have been reported for proton energies ranging from 8 kv (Burhop (B68)) for which one-half milliampere of ions was required, to 1.4 MV (L28) at which energy a microampere gave large yields. The excitation function (intensity *vs.* proton energy) has been a subject of considerable investigation, because of its theoretical importance (O15). Studies in the extreme low voltage range are reported by Doolittle (D16) and Burhop (B68). For somewhat higher voltages (up to 0.40 MV) accurate data have been taken for both thick and thin targets by Herb, Parkinson and Kerst (H27). In this voltage range both the thick and thin target curves show the approximately exponential rise with voltage expected from a penetration function. Hafstad and Tuve (H4), with thin targets, find the curve tending toward a maximum at a point above 1.0 MV. Ostrofsky, Breit and Johnson (O15) have calculated the depth and radius of the potential hole required to explain the data of Herb, Parkinson and Kerst.

Li^6: $Li^6+H^1\rightarrow He^4+He^3$

A search for shorter range particles from lithium led Oliphant, Kinsey and Rutherford (O3) to the discovery of two groups of doubly-charged ions of about 0.65 and 1.15 cm range. (See Fig. 45.) They suggested that the Li^6 isotope was responsible and was yielding an alpha-particle and a He^3 nucleus. This reaction was verified by later work of Oliphant, Shire and Crowther (O1) using separated isotopes of lithium. A more accurate determination by Neuert (N4) in a cloud chamber gives values of 0.82 and 1.19 cm mean range

[15] It should be noted that the mean range, not the extrapolated range usually measured, represents the average energy of the alpha. This correction is discussed and a curve given in §97.

for the two particles, when produced by 0.12 MV protons.

The qualitative agreement of the two range groups with that expected from He^4 and He^3 particles justifies the suggested interpretation. The He^3, being the lighter product, will get 4/7 of the reaction energy, while the He^4 has 3/7. The energy of the He^3 can be obtained from the alpha-particle range-energy relations in a region in which they are fairly satisfactory. This energy is found to be 2.12 MV, from which a reaction energy of 3.72 MV is obtained. The quantitative check of this value with that obtainable from masses (3.76 MV) justifies the use of the shorter He^4 range to determine the range-energy relation for this region (§95).

Be^9: $Be^9+H^1\rightarrow Li^6+He^4$

Several early reports of low intensities of alpha-particles of about 3 cm range have been ascribed to impurities of B or Li. Dee first observed particles of about 8 mm range and judged them to be singly-charged ions, probably deuterons. Döpel (D17) and also Kirchner and Neuert (K16) observed these particles and called them alpha-particles, Kirchner and Neuert being the first to suggest the now accepted reaction resulting in Li^6, and measuring a range of 7.4 mm for the alphas. Oliphant, Kempton and Rutherford (O9) then performed a series of experiments in which they found two groups of particles, one of alphas and one of deuterons (§100B) of almost identically the same range of 7.4 mm at 90°. They based their conclusion on the different specific ionizations observed in the ionization chamber, and found the e/m values to be the same in deflection experiments in electric and magnetic fields. Near the end of their range H^2 and He^4 particles have very nearly the same specific ionization, which explains why the two particles were at first confused. The alphas, of 7.4 mm mean range, have energies of about 1.4 MV. We find that $Q=2.33$ MV, while the calculated value is 2.25 MV. Allen (A4) reports results in agreement with those above and measures the probability cross section to be 5×10^{-29} cm^2 at 0.1 MV. This reaction is important as supporting evidence for the mass of Be^9 and also in checking the validity of the alpha-particle range-energy relation in this low energy region.

B^{11}: (a) $B^{11}+H^1\rightarrow He^4+He^4+He^4$
(b) $B^{11}+H^1\rightarrow Be^8+He^4$

Boron yields large intensities of alpha-particles, of diverse ranges. The first observation, by Cockcroft and Walton (C19), indicated an ill-defined range of about 3.5 cm. Further experiments (C23) showed a distribution of energies with a few alphas of nearly 5 cm range, and they suggested reaction (a), considering a mechanism involving simultaneous emission of the three alphas. Oliphant and Rutherford (O2) measured the maximum range to be 4.7 cm but found that the observed distribution-in-range curve could not be explained by the simplest assumption, that the angular distribution was symmetrical and centered about a most probable value of angle of 120° between the particles. Using this picture the Q value calculated from the masses was not in accord with that calculated from the maximum range.

Dee and Gilbert (D9) have resolved these difficulties in a report of cloud chamber investigations in which the supposed simultaneity and angular distribution of tracks were carefully studied. They find no evidence for simultaneity, or of a preferred 120° angle, but rather, that one alpha is always emitted with a range of approximately 2.4 cm. They conclude that in the process this alpha is first emitted, leaving an excited Be^8 nucleus which subsequently disintegrates into two other alphas. The Be^8 is in a 2.8 MV excited state with a width of 0.77 MV (see §85A). This large width is due to its short life time, and explains the variation in range of the initial 2.4 cm alphas. The life-time of this particle disintegration can be calculated from the width and is found to be 8.5×10^{-22} sec. On this assumption the calculated distribution-in-energy and the angular distribution of tracks in the individual reactions are found to agree with the experimental observations (Fig. 25 in §85). They calculate the reaction energy from pairs of associated tracks, of which many are observed, and obtain 8.7 ± 0.2 MV. There are two other less accurate methods of using the observations to obtain the reaction energy. From the cut-off of the continuous distribution, using the interpretation above, we obtain the value 8.62 MV. From the average energy of all alphas emitted Oliphant and Ruther-

TABLE LIV. *Summary of p-α type reaction.*

TARGET Z	TARGET E1	PRODUCT E1	Q(MV) (CALC.)	Q(MV) (OBS.)	REFERENCE	RESONANCE LEVELS (MV)	EXCIT. LEVELS (MV)	YIELD α/p @ (MV)
3	Li^{6}	He^{3}	3.76	3.72	N4			$1/10^{7}$ @ 0.4
	Li^{7}	He^{4}	17.25	17.13	O8			$1/10^{7}$ @ 0.4
4	Be^{9}	Li^{6}	2.25	2.28	K16			$2/10^{9}$ @ 0.1
5	B^{11}	Be^{8}	8.60*	8.60	O9	0.18		$1/10^{14}$ @ 0.15
	B^{11}	$2He^{4}$	8.72	8.7	D9		2.9 (Be^{8})	$1/10^{12}$ @ 0.15
6	C^{13}	B^{10}	−4.15					
7	N^{14}	C^{11}	−3.3					
	N^{15}	C^{12}	4.79					
8	O^{16}	N^{13}	−5.40					
	O^{17}	N^{14}	1.3					
	O^{18}	N^{15}	2.82					
9	F^{19}	O^{16}	8.14	8.15	H22			$1/10^{7}$ @ 1.8
10	Ne^{20}	F^{17}	−4.2					
	Ne^{22}	F^{19}	−1.52					
11	Na^{23}	Ne^{20}	1.42					
12	Mg^{25}	Na^{22}	−2.0					
	Mg^{26}	Na^{23}	−1.9					
13	Al^{27}	Mg^{24}	1.6					
14	Si^{29}	Al^{26}	−1.9					
	Si^{30}	Al^{27}	−2.26					
15	P^{31}	Si^{28}	1.8					
16	S^{34}	P^{31}	−1.9					
17	Cl^{35}	S^{32}	2.2					
18	A^{38}	Cl^{35}	−2.0					

* Q (observed) used to calculate mass values.

ford (O2) get a value of 8.60 MV. These methods are subject to interpretational and experimental errors, so we use the value of 8.7 MV obtained from the data of Dee and Gilbert to compare with that calculated from masses of 8.72 MV.

The existence of an alternate mode of disintegration in which only two products are formed (reaction *b*) is suggested by the observations of Kirchner and Neuert (K15) and Oliphant, Kempton and Rutherford (O9) of a homogeneous group of alphas of 4.4 cm mean range. This is interpreted as due to the formation of a Be^{8} nucleus in the ground state rather than the excited state assumed for the three particle process. The *Q* value obtained from this evidence is 8.60 MV, only slightly lower than that for the alternative reaction; it is used to determine the mass of Be^{8}, which proves to be unstable (heavier than two He^{4} atoms) by 0.13 MV.

The excitation curve for the production of alphas from B exhibits a somewhat different character than that for Li, in that it is lower for energies of less than 100 kv and rises more steeply in the 200–400 kv region (N4). It can be fitted to a Gamow probability function with reasonable assumptions. Williams, *et al.* (W21a) studied the excitation function of the homogeneous alpha group from reaction (b) and found good evidence for a resonance level at 180 kv with a half-width of slightly less than 10 kv. This represents a level in the excited C^{12} compound nucleus at 16.1 MV. Gentner (G26) has observed the same resonance state in the production of gamma-radiation. A higher resonance level at about 0.4 MV proton energy is also indicated.

Neuert (N4a) has studied the angular distribution of the alpha-particles of discrete range from this reaction and finds it nonisotropic, with a strong minimum for an angle of 90° to the proton beam.

F^{19}: $F^{19}+H^{1}\rightarrow O^{16}+He^{4}$

The observation of alpha-particles from fluorine was first indicated by Cockcroft and Walton (C19) and somewhat better measurements were made later by Oliphant and Rutherford (O2). At such low proton energies (O. and R. used 0.20 MV) the yields are small and range measurements are not precise. Henderson, Livingston and Lawrence (H22) have made the most complete survey of this reaction for higher energies, showing alphas of 6.95 cm extrapolated range for 1.69 MV protons. Indications of a shorter range of

about 3 cm are ascribed to boron impurities. In this case the particles showed a definite group structure, indicating only two resulting particles, and the assumed reaction is that given above. For this reaction $Q=5/4E_2-15/16E_1$ (§99), from which we find a value of 8.15 MV by taking an average of the results obtained at several bombarding energies (H22). This is in excellent agreement with the value of 8.14 MV obtained from the mass values.

The excitation curve of fluorine is found to be lower for low proton energies than that for B or Li, but once again there is no indication of a sharp threshold. In the curves given for protons of high energy and rather low intensity (H22) there is no observable emission below 0.5 MV, but Oliphant has observed alphas at 0.2 MV with considerably larger proton currents. Observational data (H22) show some deviations from a correct Gamow curve (see §78), which are best interpreted as due to changes in the internal disintegration probability.

B. Type reaction p-d: $Z^A+H^1\rightarrow Z^{(A-1)}+H^2+Q$

This type reaction has been observed for only one element, Be^9, and is based chiefly on the data and conclusions of a single paper by Oliphant, Kempton and Rutherford (O9). An earlier report by Oliphant (O6) of investigations on a 7 mm group of particles from Be observed by Dee concluded that they were singly charged, i.e., hydrogen ions. With scant evidence at that time he suggested the reaction:

$$Be^9+H^1\rightarrow Be^8+H^2.$$

Döpel (D17), Kirchner and Neuert (K16) also observed these particles, but identified them as alpha-particles, having a double charge. In the paper mentioned above (O9) Oliphant, Kempton and Rutherford reported experiments from which they concluded that both H^2 and He^4 particles were present in about equal numbers, thus establishing the reaction above. In magnetic and electrostatic deflection experiments they found the particles to have the same e/m ratio, and obtained estimates of the energy assuming the character of the ions. Furthermore, both groups disappeared at almost exactly the same thickness of absorber: 7.4 mm. (Further experiments with different bombarding energies might assist in separating the two groups.) When the particles traversed a shallow ionization chamber, however, and the pulses were amplified linearly by a vacuum tube amplifier, they were found to be of two sizes, one corresponding to alpha-particles and the other to singly charged ions. The reactions are highly probable, and both groups occur with about the same intensity at 100 kv. The Q value obtained from the reaction is 0.46 MV, while that obtained from the masses is 0.48 MV. The excitation curve (O6) is of the type expected for an element of such low atomic number.

C. Type reaction p-γ. (Table LV)

$$Z^A+H^1\rightarrow(Z+1)^{(A+1)}+h\nu:$$

This type of simple capture reaction has been the subject of much controversy. It involves the emission of gamma-radiation, which must come from the residual nucleus. It is now apparent that the reaction occurs usually only for protons of discrete energies—the phenomenon of resonance. This resonance characteristic plays an important role in the general scheme of the theories of Breit and Wigner (B51) and of Bohr (B32). (Chapter IX, and §81.)

Following the announcement by the Curie-Joliots of the α-n type reactions yielding neutrons and radioactive elements such as N^{13} and Si^{27}, and their suggestion that the same radioactive products might be expected from deuteron and proton bombardment of other elements, several laboratories started to search for this effect. The C^{12}-d-n process was readily observed to give the N^{13} activity (see §101C). When proton bombardment of carbon was found (in three laboratories (H21, C24, C39) to give the same activity, so strong was the analogy that the process: $C^{13}+H^1\rightarrow N^{13}+n^1$ was at first suggested. It is now known to be energetically impossible, as indeed are all such p-n reactions, except for very high energy protons.

Hafstad and Tuve (H2), however, failed to observe radioactivity with protons. Deuteron contamination of the proton beam was suggested and eliminated as an explanation of the other observations. With improved mass values it was possible for Cockcroft (C26) to conclude that the reaction was simple capture in the C^{12} isotope, but still without any suggestion of resonance. This feature was discovered experimentally by

Hafstad and Tuve (H3, H4), who found that the excitation curve of the production of N^{13} was not the monotonic increase observed in other nuclear processes and explained by the Gamow penetration theory, but consisted of several sharp maxima. Since their first data were taken with thin (gas cell) targets in which the proton energies were higher than those of the resonance maxima, their original negative results are explained and their data are found to be compatible with those from other laboratories in which thick targets were used.

With this knowledge other processes in which resonance features have been observed have been entered under this type reaction.

Li^7: $Li^7+H^1 \rightarrow Be^8+h\nu$

The gamma-rays observed from Li under proton bombardment have been the subject of much speculation and research, and their complete interpretation is still uncertain. A summary of their history will serve to illustrate the changes and progress in the techniques of gamma-ray measurements.

They were first observed by Traubenberg, Eckardt and Gebauer (T13), and later, independently, by Lauritsen and Crane (L6). The first absorption measurements in Pb indicated a quantum energy of about 1.6 MV, which was changed to 6.3 MV (C42) with the application of the theory of pair production to absorption measurements (§93E). Crane and Lauritsen (C42) then introduced the cloud chamber method of measurement of gamma-energies and showed that there were at least two groups, of 4 and 12 MV. With improvements in technique and more data Crane, Delsasso, Fowler and Lauritsen (C51) found what seemed to be evidence for as many as 11 gamma-ray lines, ranging from 2.9 MV to 16 MV. Statistical factors make many of these uncertain but later evidence indicates that at least a few of the higher energy lines were valid. Development of the method of measuring gamma-rays from the sum of the energies of electron and positron pairs suggested for a time that the radiation was almost entirely a single gamma-ray of 17.5 MV energy (D12, G2). A recent report by Gaertner and Crane (G3) gives evidence for gamma-ray lines at 17.5, 14.5, 11.0 and 8.5 MV from the Compton secondary electrons, but only the 17.5 MV line from the pairs. On the other hand Delsasso, Fowler and Lauritsen (D13) find evidence from studies of pairs and of recoil electrons for a line at 17.1 MV, possibly one or more between 10 and 17 MV, but none of lower energy. They show that the gammas of 2 to 6 MV are due to absorption of the 17.1 MV line, and found no lines of energies between 2 and 10 MV. When a gamma-ray of less then 17.5 MV is emitted the residual $*Be^8$ breaks up into two alpha-particles of energy 1.5 MV or higher (Lauritsen, private communication) similar to the Be^8 nucleus formed in the β-decay of Li^8 (§101B).

In studying the yield of gammas from Li Crane, Delsasso, Fowler and Lauritsen (C51) found a decided resonance maximum in the excitation curve. This has been more carefully studied by Hafstad and Tuve (H4) who find two very sharp resonances, at 440 and 850 kv. Analysis of the shape of the resonance peaks using very thin targets and calibrating the energy spread of the proton beam shows that the peak at 440 kv has a natural width of not more than 11 kv (H5) (see §81). Herb, Kerst and McKibben (H28a) check the first peak but observe the second to be at 1.0 MV and much broader than Hafstad and Tuve's findings indicated. Bothe and Gentner (B47g) report a resonance level at 0.20 MV. The resonance character of these gamma-rays suggests that they are due to this simple capture type process, arising from an excited Be^8 nucleus. From the alternative process resulting in two alphas and having a Q value of 17.25 MV, the mass difference between Be^8 and two He^4 atoms (0.13 MV) and the fraction of the proton energy absorbed by the Be^8 nucleus ($\frac{7}{8}$ of 0.44 MV or 0.38 MV) we can calculate the resonance level in Be^8 to be at: $17.25-0.13+0.38$, or 17.50 MV, a sufficiently good check of the observed gamma-ray energy. The normal Be^8 nucleus is then thought to break up into two low energy alphas. The only assumption required for this explanation is that the excited nucleus cannot break up into the usual 8 cm alpha-particles According to the selection rules (§81) the protons responsible for the resonance gammas have even orbital momentum while those yielding alphas have odd. The two reactions are therefore quite independent and this resonance process cannot be detected in the excitation curve of the 8 cm

alphas. The observed yield at resonance is about 1 gamma per 2 alpha pairs.

Be^9: $Be^9+H^1\rightarrow B^{10}+h\nu$

The gamma-rays observed from Be on proton bombardment have a maximum energy of about 6 MV (C45, C47). This is too large to be due to the p-α type process, for which the particle energies are measured, and no other processes are known which would explain it. The conclusion is that it must be due to this simple capture reaction resulting in stable B^{10}. The energy available for the gamma-ray, calculated from the masses involved, is 6.39 MV plus the resonance energy of the proton, a satisfactory check of the proposed explanation. Herb, Kerst and McKibben (H28a) find a single broad resonance for protons of 0.99 MV. Other lower energy gamma-ray groups have been reported, but may be largely due to statistical fluctuations of the data.

B^{10}: $B^{10}+H^1\rightarrow C^{11}+h\nu$

When boron was bombarded by protons a positron activity with the half-life characteristic of C^{11} was observed by Crane and Lauritsen (C39). Since the proton energies used were insufficient to cause the B^{11}-p-n type process in the heavier isotope ($Q=-3$ MV), the conclusion must be that the activity is due to simple capture. The assignment is justified by the observation of a resonance level at 0.18 MV by Shepherd, Haxby and Williams (S11a). The energy evolution in the gamma-ray, calculated from masses, should be 8.55+ MV, and there is some slight evidence for a gamma-ray of approximately this energy from cloud chamber studies of Crane, Delsasso, Fowler and Lauritsen (C50).

B^{11}: $B^{11}+H^1\rightarrow C^{12}+h\nu$

The evidence for this reaction on the heavier boron isotope is entirely from gamma-ray measurements, since the product C^{12} is stable. Crane, Delsasso, Fowler and Lauritsen (C50) have observed and measured the gamma-rays produced by proton bombardment and find a maximum energy of 14.5 MV. No other reaction yields sufficient energy to account for this gamma-ray, but assuming simple capture the Q value calculated from the masses is 15.89 MV. Herb, Kerst and McKibben (H28a) observe a weak resonance effect for protons of 0.82 MV. This may indicate an excitation level in the C^{12} nucleus, or in C^{11} if the B^{10} isotope is responsible for the γ-rays observed.

C^{12}: $C^{12}+H^1\rightarrow N^{13}+h\nu$

As discussed in the introductory paragraphs, the observation of the N^{13} radioactivity suggested this process, which has been confirmed by Hafstad and Tuve (H4) in the observation of resonance maxima in the excitation function at 0.40 and 0.48 MV, with an experimental width of the levels of about 10 kv. The Q value obtained from masses is 1.93 MV, so the gamma-ray energy will be 2.30 or 2.37 MV for the two resonances. No direct measurements are available, but absorption estimates by the above authors indicate a value of about 2 MV. The properties of the N^{13} radioactivity are best determined from the more probable deuteron reaction, and are discussed in §101. The N^{13} radioactivity appears as a contamination when targets are bombarded by fast protons (§100C).

O^{16}: $O^{16}+H^1\rightarrow F^{17}+h\nu$
($O^{17}+H^1\rightarrow F^{18}+h\nu$)

Radioactivities having the known periods of F^{17} and F^{18} were observed when O was bombarded by fast protons by DuBridge, Barnes and Buck (D28). The F^{18} activity may be produced through this reaction or through the O^{18}-p-n process (§100D). These activities are prominent as a contamination when other targets are bombarded in air, eliminated by activation in an atmosphere of hydrogen.

F^{19}: $F^{19}+H^1\rightarrow Ne^{20}+h\nu$

The gamma-rays from fluorine were originally detected by McMillan (Mc4) who found a Pb absorption indicating 2 MV which was raised to 5.4 MV by using different absorbers and considering pair production. Assuming this radiative capture process the energy available, as shown by the mass values, is 12.89 MV.

Hafstad and Tuve (H5) found resonance maxima in the excitation curve for gamma-ray production at 0.328, 0.892 and 0.942 MV. (See Fig. 46.) The width of the first resonance level at 0.328 MV proves to be exceedingly narrow, only 4 kv actually observed, which is just the known

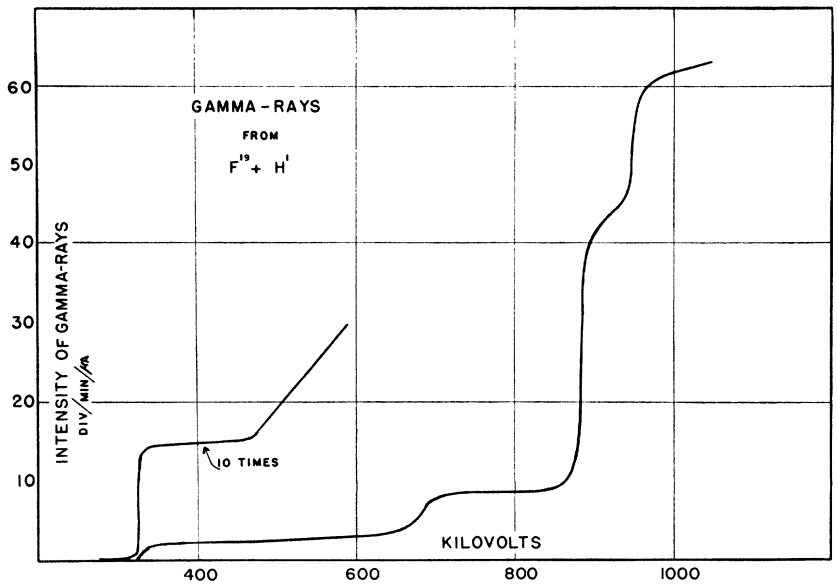

FIG. 46. Excitation curve of the γ-radiation from the radiative capture of protons by F^{19} showing three pronounced resonance levels. (Hafstad, Heydenburg and Tuve.)

inhomogeneity of the proton beam so that the width of the level must be considerably less than 4 kv. Herb, Kerst and McKibben (H28a) have extended these data to higher energies and find a broad resonance at 0.6–0.7 MV, a sharp one at 1.40 MV and indications of one at 1.76 MV.

Delsasso, Fowler and Lauritsen (D14) find a single line at 6.0 MV by analysis of pairs observed in a cloud chamber. They were using protons of 0.75 MV, so only the 0.328 MV resonance level was effective. No evidence for high energy gammas was obtained.

Although there is sufficient energy available in the p-α reaction to give the gamma-ray, the resonance features and especially the narrow resonance maxima favor the interpretation as a simple capture reaction.

Na^{23}: $Na^{23}+H^1 \rightarrow Mg^{24}+h\nu$

In studies of the gamma-radiation from proton bombardment, Herb, Kerst and McKibben (H28a) found a broad resonance for protons of 1.15 to 1.32 MV. This requires a capture reaction for its explanation and indicates a level in the Mg^{24} nucleus.

Al^{27}: $Al^{27}+H^1 \rightarrow Si^{28}+h\nu$

Herb, Kerst and McKibben (H28a) find that the γ-ray intensity from Al has resonance maxima for protons of 0.75, 0.99, 1.16, 1.37 (strong), 1.62 and 1.85 MV. The resonance feature specifies this capture reaction.

D. Type reaction p-n. (Table LVa)

$$Z^A+H^1 \rightarrow (Z+1)^A+n^1+Q:$$

Exploratory work with high energy protons (3.8 MV) carried out at the University of Rochester (B4a, B67, D28) has resulted in the discovery of a great number of radioactivities some of which can be identified with known radioactive substances while the greater part represent new radioactive nuclei. It seems likely that with sufficiently fast protons and sufficiently heavy nuclei the type reaction giving neutrons will be the most probable. This hypothesis is confirmed by chemical analysis and a consideration of the possible radioactive isotopes which may be formed. The p-n reactions will all be endoergic. If the radioactive substance formed emits positrons and thus returns to the target substance, the energy required is equal to the difference between n^1 and H^1 mass (0.8 MV) plus the mass of two electrons (1.0 MV) plus the upper limit of the positron energy spectrum from the radioactive substance produced. The excitation functions should therefore show a definite threshold of 2 MV or more which should be directly correlated with the positron energy. The type

TABLE LV. *Summary of p-γ type reaction.*

TARGET Z	TARGET El	PRODUCT El	Q(MV) (CALC.)	Q(MV) (OBS.)	REFERENCE	RESONANCE LEVELS (MV)	EXCIT. LEVELS (MV)	YIELD γ/p @ (MV)
1	H^2	He^3	5.39					
3	Li^7	Be^8	17.12	17.1	G3	0.20 0.44 0.85	3–7?	$7/10^{10}$ @ 0.44
4	Be^9	B^{10}	6.39	6	C47	0.99?		
5	B^{10}	C^{11}	8.55	obs.	C50	0.18	?	
	B^{11}	C^{12}	15.89	14.5	C50	0.82?	?	
6	C^{12}	N^{13}	1.93	2	H4	0.40 0.48		$1/10^{10}$ @ 0.52
	C^{13}	N^{14}	7.7					
7	N^{14}	O^{15}	7.3					
	N^{15}	O^{16}	12.12					
8	O^{16}	F^{17}	0.5	obs.	D28			
	O^{17}	F^{18}	6.5	obs.?	D28			
	O^{18}	F^{19}	6.8					
9	F^{19}	Ne^{20}	12.89	obs.	H5 H28a	0.328 0.6–0.7 0.892 0.942 1.40 1.76	7.2	$1.2/10^9$ @ 1.0
10	Ne^{21}	Na^{22}	7.1					
	Ne^{22}	Na^{23}	9.9					
11	Na^{23}	Mg^{24}	11.0	obs.	H28a	1.2		
12	Mg^{25}	Al^{26}	8.3					
	Mg^{26}	Al^{27}	7.5					
13	Al^{27}	Si^{28}	10.6	obs.	H28a	0.75 0.99 1.16 1.37 1.62 1.85		
14	Si^{29}	P^{30}	6.1					
	Si^{30}	P^{31}	6.6					
15	P^{31}	S^{32}	9.4					
16	S^{34}	Cl^{35}	5.4					
17	Cl^{37}	A^{38}	11.3					

reaction should then be particularly suitable for a study of the relation between energy evolution, K-U limit and observational limit in beta-transformations. If the product nucleus is electron active the threshold may be lower (by 1.0 MV). In this case the measurement of the threshold and the electron energy gives a direct comparison of the masses of three isobaric nuclei.

In a few instances among the lighter elements the identification of the activity indicates simple capture of the proton (§100C). This *p*-γ type reaction will have very small probability if it has to compete with the *p*-*n* reaction and can therefore only be observed if the *p*-*n* reaction is energetically impossible. It is to be expected that in some instances a *p*-α reaction might also occur, and might sometimes lead to a radioactive product.

Although at the time of writing this report the Rochester experiments are in a preliminary stage the list as given in Table LVa will give an indecation of the results obtained to date:

§101. DISINTEGRATION BY DEUTERONS

The isotope of hydrogen of mass 2, now called deuterium, was discovered by Urey, Brickwedde and Murphy (U1) following the prediction of its existence by Birge and Menzel (B20) from considerations of the discrepancies between the physical and chemical atomic weights. It was first produced in quantity by Lewis and Macdonald (L20). A thorough discussion of the history and properties of deuterium is contained in the book by Farkas and Farkas (F2) and in the review paper of Urey and Teal (U2). The atomic ion, the "deuteron," [16] was first used for dis-

[16] Other names which have been used for this projectile are: (a) "deuton," introduced by Lawrence, Livingston

TABLE LVa. *Evidence for p-n reactions.*†

TARGET					
Z	El	PERIODS*	THRESHOLD EN. (MV)	ASSUMED PRODUCT	EVIDENCE
8	O	107 min.	2.6	F^{18}	Ne^{20}-d-α, F^{19}-n-$2n$ (108 min.)
14	Si	1.9 min.	>2	P^{30}	Al^{27}-α-n, S^{32}-d-α (2.5 min.)
20	Ca	40 hr.	>2	Sc^{44}	Ca-d-n, K-α-n, Sc-n-$2n$ (52 hr.)
24	Cr	40 min.	>2	Mn^{53}	Cr-d-n (46 min.)
25	Mn	91 min.	>2	Fe^{55}	
27	Co	2.4 hr.	>2	Ni^{59}	Ni-n-γ, Ni-d-p (3 hrs.)
28	Ni	4.1 hr. 20 hr.	>2	Cu^{61} Cu^{64}	Ni-α-p, Ni-d-n (3.4 hr.) Cu-n-γ, Cu-d-p, Zn-n-p, Zn-d-α (12.8 hr.)
30	Zn	26 min. 40 hr.	>2	Ga^{70} Ga	Ga-n-γ, Ga-γ-n (20 min.)
33	As	1.3 min. 113 min.	>2	Se(?)	(Only As^{75} known)
34	Se	19.5 min. 7 hr. 14 hr.	2.9	Br^{80} Br^{82}	Br-n-γ, Br-d-p, Br-γ-n (18 min., 4.2 hr.) Br-n-γ, Br-d-p (36 hr.)
42	Mo	0.5 min. 31 min.	>2	Ma	
48	Cd	1.2 min. 6 min. 37 min. 128 min.	>2	In^{112} In	In-γ-n (1.1 min.) In-n-γ (13 sec., 54 min., 3 hr.)
49	In	14 min.	>2	Sn(?)	

* An activity of 11–12 min. was found in Si, Mn, Co, Ni, Zn, and As. It is very probable that this is to be ascribed to N^{13} formed from carbon contamination through the p-γ reaction.
† Preliminary data (private communication), also (B4a, B67, D28).

integration experiments by Lawrence, Livingston and Lewis, using the large magnetic resonance accelerator at the University of California as the accelerating device. In a rapid series of survey experiments (L21, L12, L22) they observed the production of alpha-particles and protons by these new projectiles from many targets, and later observed neutrons and induced radioactivity. The first valuable summary papers were Oliphant's and Cockcroft's reports to the 1934 International Conference on Physics, (O6) (C26) while others of more recent date are by Kirchner (K14), Fea (F4), and Flügge and Krebs (F26, F26a).

A. Type Reaction d-α. (Table LVI)

$$Z^A + H^2 \rightarrow (Z-1)^{A-2} + He^4 + Q:$$

When deuterons were first used to bombard elements, large numbers of protons were observed from many elements. In addition, however, in certain of the lighter elements, alpha-particles were found, of ranges distinctly different than those known to occur with proton bombardment. In most instances the alphas showed the decided group structure indicating two resultant particles and defining the type reaction given above. With the increasing availability of deuterium more and more laboratories have utilized it for nuclear studies. It has been particularly valuable in the hands of the Cavendish Laboratory group who, with their accurately calibrated low voltage apparatus, have been able to secure more detailed and accurate data on these processes.

With the low deuteron energies available in those laboratories which have specialized in accurate measurement of disintegration reactions the processes observed have been limited to those which are exoergic, and in the lighter elements. This is most readily understood by considering that the ejected alpha must penetrate a potential barrier twice as high as the entering deuterons. The group at the University of California, on the other hand, with deuterons of up to 6 MV (C33), have been able to identify processes yielding alphas from the heavier nuclei, chiefly through the identification of induced radioactivities.

Li^6: $Li^6 + H^2 \rightarrow He^4 + He^4$

One of the first experiments performed by Lewis, Livingston and Lawrence (L21) with

and Lewis and used by American physicists for a time, but now replaced by the more widely accepted term "deuteron"; (b) "diplon," suggested by Lord Rutherford and used until recently by English physicists. These terms apply only to the H^2 nucleus or the high speed ionic projectile, paralleling the usage of "proton" and "alpha-particle" in this sense.

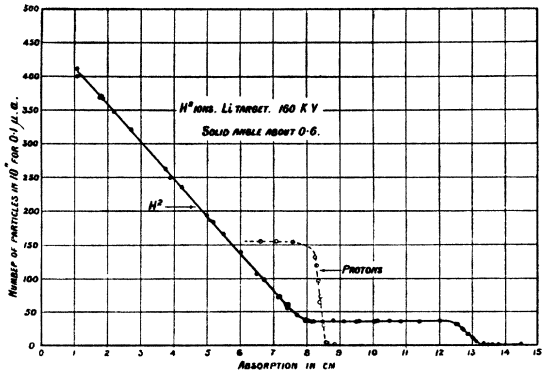

FIG. 47. Distribution-in-range of the α-particles from deuteron bombardment of lithium showing the 13 cm alphas from $Li^6+H^2=2He^4$ (homogeneous group) and the continuous distribution from the three-product reaction $Li^7+H^2=2He^4+n^1$. (Oliphant, Kinsey and Rutherford.)

deuteron projectiles was on Li. A group of alphas were observed of 14.5 cm extrapolated range, or 12.0 MV, the highest energy alphas observed up to that time. The incident deuteron energy was about 1.33 MV and the alphas were observed at 90°. The existence of such a group of alpha-particles of definite range indicated only two products. Furthermore, these particles were present in numbers about 1 : 10 of the 8 cm alphas from an equivalent current of protons (the approximate ratio of abundance of Li^6 and Li^7) so the above reaction was suggested with Li^6 as the disintegrated isotope. Using these data, the energy evolved is: $Q=2(12.0)-\frac{3}{4}(1.3)=23.0$ MV, which is the largest reaction energy measured for any nuclear process.

Oliphant, Kinsey and Rutherford (O3), using deuterons of 0.16 MV, observed these long range alphas to have a mean range of 13.0 cm, while in an accompanying paper by Dee and Walton (D6) the assumed mechanism was justified by cloud chamber photographs of the two oppositely directed alphas of equal range. Using a separated sample of the Li^6 isotope, Oliphant, Shire and Crowther (O1) were able to prove conclusively that this isotope was responsible for the long range alphas (of 13.2 cm). The most careful measurement of their range has been made by Oliphant, Kempton and Rutherford (O8) using a gas cell in which pressure could be varied to give accurate range values. On the basis of this determination of 12.70 cm mean range measured at 90° to the direction of the deuterons of 0.19 MV, they calculate a Q value of 22.06 MV, which is corrected to 22.07 MV by the more recent considerations discussed in §97. This is considered more accurate than mass-spectrograph measurements and is used to determine the mass of Li^6, in conjunction with the Li^6-d-p results. The adopted masses give the value 22.17 MV for this reaction.

An excitation curve of the process at low voltages (O3) shows a much more rapid increase with deuteron energy in the 100–200 kv region than the paralleling process of Li^7-p-α, but can also be fitted by a Gamow probability function with suitable constants. The total probability of disintegration is the product of two factors, the probability of penetration of the barrier and the internal probability of disintegration after the particle has entered the nucleus. The first involves the mass of the projectile, being given by $e^{-(m)^{\frac{1}{2}}}\cdots$. This means that the heavier deuteron has a higher momentum and so a smaller wavelength, resulting in a smaller probability for low energies where this is the determining factor. The second factor, the internal probability, depends on the effect of nuclear spins, (§83). Goldhaber's (G15) analysis indicates that the Li^6 reaction is allowed and the Li^7 reaction forbidden. Indeed the experiments show a higher probability for the Li^6 case at high deuteron energies where the internal probability predominates. From the experimental observations, Goldhaber predicted the spin of Li^6 to be 1, later confirmed experimentally by Fox and Rabi (F29), while the spin of Li^7 is $\frac{3}{2}$.

Li^7: (a) $Li^7+H^2\rightarrow He^4+He^4+n^1$
(b) $Li^7+H^2\rightarrow He^5+He^4$

The first reaction may also be classified under the d-n type process, since neutrons are also products. The classification really depends upon the mechanism of the reaction; if it belongs to the d-α type the mechanism would have to be:

$$Li^7+H^2\rightarrow {}^*Be^9\rightarrow {}^*He^5+He^4\rightarrow He^4+n^1+He^4;$$

if it belongs to the d-n type the mechanism would be:

$$Li^7+H^2\rightarrow {}^*Be^9\rightarrow {}^*Be^8+n^1\rightarrow He^4+He^4+n^1.$$

From studies of the experimental data it seems possible that both mechanisms are involved. The discovery of the process occurred through ob-

servations of the alphas and many features of the reaction have been studied through their properties. These features will be discussed at this time and those having to do more specifically with the neutron properties are entered under the *d-n* process.

Using a pure deuteron beam (magnetically separated from proton contamination) Oliphant, Kinsey and Rutherford (O3) first observed this process as a group of alphas having a continuous distribution of ranges from 1 cm up to 7.8 cm, superimposed on the 13 cm alphas from the Li^6 isotope. (See Fig. 47.) Such a distribution indicated a three-particle process and they suggested reaction (**a**) above. They observed the excitation function to be a rapidly rising curve with deuteron energy, of a type similar to that in the Li^6 process previously mentioned. The subsequent work with separated isotope targets (O1) confirmed their suggestion, naming 8 cm as the end of the range for 0.16 MV deuterons. In the more exact range measurements of Oliphant, Kempton and Rutherford (O8) this value is given as 7.6 to 7.8 cm (8.2 to 8.3 MV). The neutron should have the most energy when the two alphas have paralleling paths (a Be^8 nucleus), while one alpha has the greatest energy when the other alpha and the neutron take the same direction. In this case the alpha observed will have maximum energy when it has 5/9 Q, corresponding to the other alpha and the neutron having the same velocity (a temporary He^5 nucleus). This can be shown by considering the motion of the center of gravity of the (He^4+n^1) system and the relative motion of the He^4 and n^1 separately, in which case the maximum energy of the observed alpha corresponds to zero relative motion of the other components. From the momentum considerations and the experimental data the Q value (recalculated) is estimated to be 14.9 MV with considerable allowance for error, and is in sufficient agreement with the mass value of 15.04 MV.

An equally important aspect of this reaction is the neutron produced, discovered independently by Crane, Lauritsen and Soltan (C38), and discussed in detail in the section on *d-n* processes. Evidence from neutron studies by Bonner and Brubaker (B37) shows a continuous distribution of neutron energies and so justifies the assumed three particle process. The excitation curve for neutron production observed by Crane, Lauritsen and Soltan (C41) is for a higher energy range than that observed by Oliphant for alpha-particles, which makes direct comparison difficult, but apparently fits the Gamow probability function. It has been suggested (K2) that the true process involves a two-stage disintegration, going through a phase in which an excited Be^8 nucleus supplies the energy for the recoil nucleus, later breaking up to give the alphas. The expected neutron groups due to the discrete energy levels expected in this $*Be^8$ nucleus are not observed, however, so this suggestion does not seem valid in principle, and the possibility of an excited He^5 must be considered.

Williams, Shepherd and Haxby (W21c) have recently found evidence for a homogeneous group of α-particles having a most probable range of 7.10 cm. These are attributed to the reaction (**b**) above. Applying the corrections of §97 to the observed range, we find a Q value of 14.3 MV. From this the mass of He^5 is found to be 5.0137, indicating that this isotope is unstable against neutron emission by 0.78 MV. This fits in with the fact that the observed alpha group is not strictly homogeneous but has a natural width. No group representing the He^5 particles was observed.

Although gamma-rays are observed from Li targets by McMillan (Mc4) and others, Lauritsen and Crane (L8) are satisfied from intensity considerations that they arise only from hydrogen impurity of the deuteron beam, indicating that the particle ranges observed correspond to the full energy evolution.

Be^9: $Be^9+H^2 \rightarrow Li^7+He^4$

Lewis, Livingston and Lawrence (L21) first observed alphas from Be, of about 3 cm range and in numbers 100 times those from proton bombardment. In Oliphant's report to the International Conference (O6) he reports experiments in which two groups of particles were observed, of 1 and 3 cm, respectively, in nearly equal numbers, indicating that they are the two products of a single reaction. The mass values available at that time gave a Q value which would predict ranges much larger than those observed and Oliphant was forced to suggest the reaction resulting in Li^6 and He^5. With the development of a

consistent set of mass values it was found unnecessary to assume the production of the unknown nucleus He^5, and it became possible to make the much more natural assumption that Li^7 and He^4 were the products. Oliphant, Kempton and Rutherford (O9) have measured the particle ranges and with the corrections discussed in §97 the Q value of the process is found to be 7.19 MV, which is used together with the B^{11}-d-α results to determine the mass of Be^9. The adopted masses predict a Q of 7.17 MV.

B^{10}: (a) $B^{10}+H^2 \rightarrow He^4+He^4+He^4$
(b) $B^{10}+H^2 \rightarrow Be^8+He^4$

It might be expected that this process would result in three alpha-particles in a manner similar to the $B^{11}+H^1$ reaction, and so result in a continuous distribution of ranges. Such was observed by Cockcroft and Walton (C25, C27) who measured the maximum range to be 14.3 cm or 12.0 MV with deuterons of 0.5 MV. As in the proton reaction the end of this distribution is obscured by the homogeneous group due to reaction (b), and exact range measurements cannot be made. Cockcroft and Lewis (C28), although they are not able to separate this continuous group from the homogeneous one, have analyzed the energy distribution and find the average energy compatible with that calculated from the assumed three-alpha reaction. The Q value calculated from masses is 18.03 MV. The distribution shows two maxima. It is probable that the reaction passes through an excited Be^8 stage, and is similar to that suggested by Dee and Gilbert (D9) for the proton disintegration. Probably more than one excited level of Be^8 takes part in the process. Wheeler (private communication) has analyzed the alpha-particle distribution function and has found it compatible with the assumption of two excitation levels, namely the 3 MV level known from the B^{11}-p-α process and another level at about 6 MV. Evidence for the latter has also been obtained from the scattering of alphas by alphas (§74) and the existence of such a level seems to be in agreement with theoretical expectations (F10).

The homogeneous group observed by Cockcroft and Lewis (C28) having an extrapolated range of 14.75 cm at 90° to the deuteron beam of 0.55 MV is believed to follow reaction (b), resulting in a Be^8 product. In this case an exact value of the reaction energy can be obtained, given as 17.5 MV, corrected to 17.76 MV. The calculated value is 17.90 MV.

Gamma-rays from B by deuteron bombardment have been observed by Crane, Delsasso, Fowler and Lauritsen (C44). They were not successful in measuring the energy of the line of highest energy (given as >10 MV). It may arise from the reaction under discussion, from that yielding neutrons from B^{11}, or from a simple capture of the deuteron, all of which yield sufficient energy to produce it.

B^{11}: (a) $B^{11}+H^2 \rightarrow Be^9+He^4$
(b) $B^{11}+H^2 \rightarrow 3He^4+n^1$

In their experiments on the deuteron disintegration of B Cockcroft and Lewis (C28) observed a group of alphas of 4.60 cm range which best fit reaction (**a**) above, and a continuous distribution of less than 4.5 cm thought to be due to reaction (**b**). These are similar to the groups attributed to the B^{10} isotope except for their range. The Q value for the two particle disintegration is found to be 8.13 MV; it is used (together with Be^9-d-α) to determine the Be^9 mass from which the calculated value of 8.11 MV is obtained. Although the continuous distribution cannot be analyzed to give an experimental value of Q, the results are compatible with the assumption of the (b) reaction, from which, with the use of the known masses, the reaction energy of 6.53 MV and the maximum energy of 4.5 MV expected for the alphas can be computed. These are the same products found in the C^{12}-n-α and the Be^9-α-n (b) reactions; the mechanism may involve $*Be^9$ or Be^8 and $*He^5$.

C^{13}: $C^{13}+H^2 \rightarrow B^{11}+He^4$

Although the Q value for the C^{12}-d-α reaction is negative (-1.39 MV) and the process has not been observed, Cockcroft and Lewis (C29) have found an alpha-group of 2.7 cm range from carbon targets bombarded with 0.55 MV deuterons which fits the expected value for the C^{13} reaction. The recalculated Q value is 5.24 MV while mass values predict 5.14 MV.

N^{14}: $N^{14}+H^2 \rightarrow C^{12}+He^4$
$N^{14}+H^2 \rightarrow 4He^4$

Lewis, Livingston and Lawrence (L21) in pre-

liminary experiments observed alpha-particles from a nitrogen compound bombarded by deuterons of 1.2 MV, which had ranges of about 6.8 cm. Later work by Lawrence, McMillan and Henderson (L16) with the N in air as a target showed two valid groups of alphas, the most energetic of which gives a Q value of 13.4 MV if corrected for forward direction of the alphas. The best measurements are those of Cockcroft and Lewis (C29), using 0.575 MV deuterons, in which two groups of alphas were found, and attributed to this reaction, at 6.20 and 11.37 cm, from which corrected Q values of 9.08 and 13.40 MV are obtained. The calculated Q value is 13.37 MV. The two alpha-groups indicate an excitation state of the C^{12} nucleus at 4.32 MV.

Cockcroft and Lewis also observed a continuous distribution of alphas extending up to 4.0 MV. This suggests a multiple product reaction, probably leading to four alphas through the steps: $N^{14}+H^2\rightarrow{}^*O^{16}\rightarrow{}^*C^{12}+He^4\rightarrow Be^8+2He^4\rightarrow 4He^4$. The initial O^{16} compound nucleus would have an excitation energy of 20.7 MV at zero bombarding energy; the secondary C^{12} compound nucleus would have an excitation energy of more than 8 MV. Such a level which is unstable against alpha-emission is known from the B^{11}-d-α reaction and has an excitation energy of 9.5 to 14.5 MV. The over-all energy evolution in this multiple disintegration is 6.2 MV as calculated from the known mass values.

Gamma-radiation, observed and measured by Crane, Delsasso, Fowler and Lauritsen (C49), shows indications of several lines, the most energetic of which is of nearly 7.0 MV energy. Other evidence for the C^{12} excitation states comes from Bothe's (B47) measurements of the gamma-radiation from the Be^9-α-n reaction. He finds a gamma of 6.7 MV which corresponds to that of Crane, etc. and one of 4.2 MV which fits with the 4.3 MV excitation state from the alpha groups of Cockcroft and Lewis in this reaction, and also with the 4.4 MV level found by Bonner and Brubaker (B40) in the neutron groups from B^{11}-d-n. The same two excitation levels are indicated in the neutron groups from the Be^9-α-n process (§99B).

O^{16}: $O^{16}+H^2\rightarrow N^{14}+He^4$

Cockcroft's original observation of this reaction (C26) was made definite by further experiments with Lewis (C29) in which alphas of 1.59 cm range were observed. This gives a Q value of 3.13 MV when corrected for geometrical factors. The value obtained from masses is 3.11 MV.

F^{19}(?): $F^{19}+H^2\rightarrow O^{17}+He^4$

Alphas have been observed of about 3.8 cm range with 1.33 MV deuterons by Lewis, Livingston and Lawrence (L21). If these are not due to an impurity the Q value indicated is 2.1 MV while that obtained from masses is 10.10 MV. Certainly the maximum range group was not observed.

Ne^{20}: $Ne^{20}+H^2\rightarrow F^{18}+He^4$

A positron activity of 112 min. half-life was found by Snell (S16) from deuteron bombardment of Ne gas. It was identified as F and so is probably F^{18} following this reaction. This is supported by the observations of the same period in O-p-γ and O-p-n processes. The alphas have not been observed.

Na^{23}: $Na^{23}+H^2\rightarrow Ne^{21}+He^4$

In the course of a series of experiments investigating all the processes produced in Na on deuteron bombardment, Lawrence (L15) found a 6.5 cm alpha-group with 2.15 MV deuterons. A recalculation of the reaction energy gives 6.85 MV, and it is used for the determination of the Na^{23} mass from the mass-spectroscopic value of Ne^{21}. A discrepancy in the mass values obtained from disintegration data as compared to mass spectrographic data in this region is divided among the several reactions used (see §108). This results in a mass of Na^{23} from which a Q value of 6.76 MV is obtained for this reaction.

The probability of the reaction was found to be considerably smaller than for reactions yielding protons or neutrons; since the alpha is energetic enough to escape over the top of the potential barrier this must be due to a small internal disintegration probability.

Mg: $Mg^{24}+H^2\rightarrow Na^{22}+He^4$
$Mg^{25}+H^2\rightarrow Na^{23}+He^4$
$Mg^{26}+H^2\rightarrow Na^{24}+He^4$

The only observation of alphas from Mg is by Lewis, Livingston and Lawrence (L21). These

alphas were of about 6 cm range. The values of Q calculated from masses are 2.8, 7.9 and 3.0 MV for the Mg^{24}, Mg^{25} and Mg^{26} isotopes respectively. The Mg^{25} isotope is the only one yielding sufficient energy to result in the observed alphas; interpreted in this way the data show a Q of about 7.2 MV.

The process on the Mg^{24} isotope has been verified through the long period ($T \sim 9$ months) positron activity observed by Laslett (L2), no doubt correctly interpreted as being due to radioactive Na^{22} which is also known to result from the F-α-n reaction.

Another induced radioactivity, of more measurable intensity, has been found by Henderson (H24) to yield electrons and to have the characteristic 15 hr. half-life of the Na^{24} isotope. This identifies the reaction as due to the third isotope, Mg^{26}. The calculated Q value is 3.0 MV, so the alphas should have a range of 3.5 cm in Henderson's experiments; this is too low in energy to be the group observed and which has been ascribed to the Mg^{25} reaction. The excitation function for the production of radioactivity is found by Henderson to be much steeper than that for the production of protons in the d-p process. This seems to be connected with an increase in the number of possible excited states of the product nucleus with increasing deuteron energy (cf. §79).

Al^{27}: $Al^{27} + H^2 \rightarrow Mg^{25} + He^4$

Again the preliminary experiments of Lewis, Livingston and Lawrence (L21) showed alpha-particles of about 6 cm range resulting from 1.2 MV deuterons on Al. An improved measurement is given by McMillan and Lawrence (Mc5) showing two groups of 5.7 and 6.5 cm at 90° with 2.2 MV deuterons, corresponding to reaction energies of 5.8 and 6.46 MV (corrected). The higher of these is used for obtaining the mass of Mg^{25}. The yield is about 6 per 10^9 deuterons for each group and the groups indicate an excitation level of 0.7 MV in the resultant Mg^{25} nucleus. Experimental difficulties in observing these alphas in the presence of longer range protons of about 100 times the intensity make these range measurements somewhat uncertain.

A possible variation of this type reaction is indicated by the report of Pool and Cork (P11) who find a 12.8 hr. positron activity from Al under deuteron bombardment which is separable as Mg. If this is Mg^{23} as is suggested it represents the emission of a He^6 particle in place of the more usual alpha. He^6 has been found as a product of the Be^9-n-α reaction and is itself radioactive with a 1 sec. period. Unless the 12.8 hr. activity is due to some spurious effect it may represent the production of two radioactive products in the same reaction, the only known instance.

$S^{32, 34}$: $S^{32} + H^2 \rightarrow P^{30} + He^4$
$S^{34} + H^2 \rightarrow P^{32} + He^4$

Sagane (S1), using the high energy deuterons from the Berkeley cyclotron, has observed a positron activity with the 3 min. half-life characteristic of P^{30} and previously observed in the Al-α-n reaction, and also an electron activity of 14 days period known from several other processes to be P^{32}. Chemical separations which show that both activities are phosphorus verify the assignment.

Ca^{40}: $Ca^{40} + H^2 \rightarrow K^{38} + He^4$

Hurst and Walke (H39a) found an activity of 7.6 min. period in the K fraction of a chemical separation of the products of deuteron bombardment of Ca. It is attributed to K^{38}, a positron emitter also produced by a Cl-α-n reaction.

Fe: $Fe^{54, 56} + H^2 \rightarrow Mn^{52, 54} + He^4$

Deuteron bombardment of chemically pure Fe has been found to result in an activity of 21 min. period separable as Mn by Darling, Curtis and Cork (D3a). The experiment was repeated by Livingood, Seaborg and Fairbrother (L27a), who detected in addition, a 5 day positron activity and an electron activity of several months' period. Since only two Fe isotopes can be transformed into radioactive Mn isotopes by means of (d-α) reactions, one of the three periods is not accounted for. It may be due to neutrons known to be released from the Fe target.

Cu^{65}?: $Cu^{65} + H^2 \rightarrow Ni^{63} + He^4$

An electron activity of 130 days half-life found by Livingood (L26) in copper is tentatively ascribed to an alpha-emission process. It cannot be due to the known d-p reaction giving Cu^{64} (12.8

hr.) or Cu^{66} (5 min.). Chemical analysis of the active products was inconclusive.

Zn^{66}: $Zn^{66}+H^2 \rightarrow Cu^{64}+He^4$

Livingood (L26) reports an electron activity of 12 hr. half-life produced in Zn by high energy deuterons and chemically separable as copper. The same period is found in the Cu-*n*-γ, Cu-*d*-*p*, Zn-*n*-*p* and, perhaps, Ni-*p*-*n* reactions.

Sn:

Livingood (private communication) refutes the activities ascribed to In in a previous report (L27). The In fraction is found to be inactive.

Sb^{123}: $Sb^{123}+H^2 \rightarrow Sn^{121}+He^4$

An activity of 24 hr. half-life found by Livingood (L26) seems to be the same as a 28 hr. period in the Sn-*d*-*p* reaction so suggesting this type reaction. The only Sb isotope available to give a radioactive Sn by a (*d*-α) process is Sb^{123}, which yields Sn^{121}.

B. Type reaction *d*-*p*. (Tables LVII and LVIII)

$Z^A+H^2 \rightarrow Z^{A+1}+H^1+Q$:

The first reports of the use of deuterons as nuclear projectiles (L12, L22) included the observation of large numbers of protons from all targets investigated.[17] Of these protons there were found, in general, one or more groups characteristic of each target element. The reaction follows the usual laws, in some instances resulting in excitation states of the residual nucleus and gamma-radiation. The protons are in all instances in homogeneous groups, indicating only two particle products, and measurements of the range lead to accurate Q values, since the proton range is much more extended than that of alphas of the same energy and so can be more exactly determined.

The binding energy of the deuteron (2.20 MV) is in general much smaller than the average energy of binding of neutrons in nuclei. That is, the energy released by a nucleus in absorbing a neutron is larger than the energy required to separate the proton and neutron of the deuteron. This means that the reaction energy will in general be positive. The potential barrier of a nucleus for a proton is relatively small (half that for alphas). These factors suggest that the reaction should be quite probable and should be observed for most of the light elements, while with the high energy particles from the magnetic accelerator type of apparatus this would be extended to quite heavy elements.

Studies of the excitation curves of processes of this type by Lawrence, McMillan and Thornton (L17) revealed a less rapid increase of yield with increasing deuteron energy than for processes resulting in alpha-emission, and they did not fit a Gamow curve calculated on the usual assumption that the finite extension of nuclear forces could be neglected. Oppenheimer (O10) suggested a mechanism to explain the results and Oppenheimer and Phillips (O11) have calculated probabilities on the basis of the new concept. This suggestion is that the deuteron is essentially "polarized" and split in the nuclear field and that the neutron only is absorbed by the nucleus while the proton is repelled by the field. With this assumption the shapes of the curves could be explained (H24), (L17).

As is indicated in §80 the Oppenheimer-Phillips penetration function can not be used to explain these experimental results in most cases. Since the energies of the bombarding deuterons used are not small compared to the potential barriers of the elements chosen, the simplified Gamow formula (see §78) is not sufficient. When the more exact formula (§80) is used, the experimental excitation curves are found to fit the Gamow probability function sufficiently. The steeper curves obtained from alpha-particle emission processes are readily explained because of the necessary factor involving the probability of penetration of the potential barrier by the outgoing alpha.

The O-P theory can be used, however, for very heavy nuclei ($A>100$). As indicated in §80 an entry of the deuteron as a whole into the nucleus will in general be followed by emission of a neutron, whereas the *d*-*p* process usually follows the O-P mechanism. The probabilities of the two processes are comparable.

[17] A group of protons common to all targets, of 18 cm range with 1.3 MV deuterons, was at first incorrectly interpreted as being due to disintegration of the deuterons without capture. These are now identified with the $H^2+H^2 \rightarrow H^3+H^1$ reaction and are found in all disintegration experiments with deuterons due to the deposition of deuterium on the target by the beam. Neutrons from the accompanying process $H^2+H^2 \rightarrow He^3+n^1$ are also observed from all targets.

TABLE LVI. *Summary of d-α type reaction.*

TARGET Z	TARGET El	PRODUCT El	Q(MV) (CALC.)	Q(MV) (OBS.)	REFERENCE	RESONANCE LEVELS (MV)	EXCIT. LEVELS (MV)	YIELD α/d @ (MV)
3	Li^6	He^4	22.17*	22.07	O8			$3/10^{11}$ @ 0.16
	Li^7	He^5	14.3*	14.3	W21c			$2/10^{12}$ @ 0.16
	Li^7	He^4+n^1	15.04	14.9	O8			$2/10^{10}$ @ 0.16
4	Be^9	Li^7	7.17*	7.19	O9		?	
5	B^{10}	Be^8	17.90	17.76	C28			$1/10^9$ @ 0.57
	B^{10}	$2He^4$	18.03	obs.	C28		2.9(Be^8)	$2/10^8$ @ 0.57
	B^{11}	Be^9	8.11*	8.13	C28			$2/10^9$ @ 0.57
	B^{11}	$2He^4+n^1$	6.53	obs.	C28			$1/10^9$ @ 0.57
6	C^{12}	B^{10}	−1.39					
	C^{13}	B^{11}	5.14	5.24	C29			
7	N^{14}	C^{12}	13.37	13.40	C29		4.32	$5/10^{10}$ @ 0.57
	N^{15}	C^{13}	7.56					
8	O^{16}	N^{14}	3.11	3.13	C29			$3/10^{10}$ @ 0.57
	O^{17}	N^{15}	10.5					
	O^{18}	N^{16}	3.0					
9	F^{19}	O^{17}	10.10	2.1?	L21			
10	Ne^{20}	F^{18}	3.8	obs.	S16			
	Ne^{21}	F^{19}	5.59					
	Ne^{22}	F^{20}	<4.9					
11	Na^{23}	Ne^{21}	6.76*	6.85	L15			$6/10^8$ @ 2.15
12	Mg^{24}	Na^{22}	2.8	obs.	L2			
	Mg^{25}	Na^{23}	7.9	7.2	L21			
	Mg^{26}	Na^{24}	3.0	obs.	H24			
13	Al^{27}	Mg^{25}	6.46*	6.46	Mc5		0.7	$1/10^8$ @ 2.2
14	Si^{28}	Al^{26}	4.2					
	Si^{29}	Al^{27}	7.3					
	Si^{30}	Al^{28}	3.5					
15	P^{31}	Si^{29}	7.0					
16	S^{32}	P^{30}	4.6	obs.	S1			
	S^{34}	P^{32}	4.3	obs.	S1			
	etc.							

* Q (observed) used to calculate mass values.

H^2: $H^2+H^2 \rightarrow H^3+H^1$

Oliphant, Harteck and Rutherford (O7) first recognized a group of 14.3 cm protons as coming from this reaction and also observed the H^3 particles to have 1.6 cm range. Dee (D7) took cloud chamber photographs and found two tracks of these ranges to be co-linear in each case. The best values are reported by Oliphant, Kempton and Rutherford (O8), who find 14.7 cm extrapolated range for the proton when measured at 90° to the beam of 0.20 MV deuterons. With the application of small corrections for the effect on the straggling of the thick target and of the finite angular resolution of the recording instruments the Q value is found to be 3.98 ± 0.02 MV. This is the most accurately measured of any nuclear disintegration. The accurate knowledge of the H^3 mass, determined through this reaction, is of great theoretical value for the calculation of nuclear forces.

The calculated energy of the H^3 particle may be used to check the range energy relation for protons in the low energy region, and the observed range of 1.6 cm checks well with the 1.55 cm obtained from the range energy relation of §95.

The reaction is extremely probable, even for low energies, due to the low potential barrier for the deuterons, and has been observed for energies as low as 8 kv (B68). About 1 disintegration/10^6 deuterons is observed at 0.1 MV (O6). Kempton, Browne and Maasdorp (K3) have studied the angular distribution of protons and find it not spherically symmetrical. Neuert (N4a) has studied the asymmetry and finds a minimum near 90°.

Whenever deuterons are used the deposition of deuterium on the targets may produce this group of protons as a contaminant of other reactions.

Li^6: $Li^6+H^2 \rightarrow Li^7+H^1$

Protons of about 40 cm range were first detected by Lawrence, Livingston and Lewis (L12) with deuterons of 1.3 MV. The reaction was iden-

tified by Oliphant, Shire and Crowther (O4) by the observation of 30 cm protons from bombardment of a separated Li^6 target with 0.16 MV deuterons. A better value seems to be that of Cockcroft and Walton (C25) of 30.5 cm at 90° to a beam of 0.5 MV deuterons. A recent measurement by Delsasso, Fowler and Lauritsen (D11) gives an extrapolated range of 31.7 cm with 0.7 MV ions. Using this data we obtain a Q value (recalculated) of 5.02 MV. The other values are all reasonably consistent if the different bombarding energies are considered. The Q value predicted by the masses is 4.92 MV.

This reaction is of most value in checking the accuracy of the mass values and reaction energy determinations in the light element region. This can be done most readily by considering the cycle: $(Li^6\text{-}d\text{-}p)+(Li^7\text{-}p\text{-}\alpha)-(Li^6\text{-}d\text{-}\alpha)=5.02+17.13-22.07=0.08$ MV. This cycle should give exactly zero; the difference is well within the limits of error of the measurements.

Studies of the reactions produced by deuterons on separated isotopes of Li^6 and Li^7 by Rumbaugh and Hafstad (R19) show two proton groups from Li^6, at 27.2 and 31.4 cm extrapolated range for 0.54 MV deuterons. The longer range group is that observed by Cockcroft and Walton, while the shorter range group indicates an excitation level in Li^7 of 0.44 MV and predicts a gamma-ray of this energy. The value given by Rumbaugh and Hafstad is 0.40 MV but becomes 0.44 when the recoil of the Li^7 and the new range-energy relations are considered. Williams, Shepherd and Haxby (W21b) have studied the relative yields of the two proton groups as a function of deuteron energy and find distinct differences. They also obtain evidence for the expected 0.44 MV gamma-ray (S11a). A small asymmetry in the angular distribution of the protons has been observed by Neuert (N4a) but not identified as to behavior of the separate groups.

Li^7: $Li^7+H^2\rightarrow Li^8+H^1$

This reaction has been identified by the observation of Crane, Delsasso, Fowler and Lauritsen (C48) of an electron radioactivity of 0.5 sec. period from a Li target. The period was more accurately measured by Lewis, Burcham and Chang (L24) to be 0.88 sec. As would be expected from such a short period activity, the electrons were found to have an exceedingly high maximum energy. The visually extrapolated limit was originally reported to be about 10.0 MV while a K-U extrapolation gave 11.2 MV (F28). A recent report by Bayley and Crane (B5a) gives a visual limit of 12.0 MV (Cf. below).

A proton group of 26 cm extrapolated range with 0.7 MV deuterons was attributed by Delsasso, Fowler and Lauritsen (D11) to this process, and used to calculate the Q value. It was later shown to be due to the Li^6 isotope (see above). Rumbaugh, Roberts and Hafstad (R19, R19a) found no proton groups of range greater than 1.7 cm from the Li^7 isotope using deuterons of 0.86 MV, which gives an upper limit to the reaction energy of 0.28 MV corresponding to a Li^8 mass of >8.0245.

An upper limit for the mass of Li^8 may be obtained from the fact that deuterons of 0.36 MV give an appreciable yield of Li^8 (B5a, R19a). Therefore $Q>-0.3$ MV and the upper limit to the mass is <8.0251. It is quite possible that this value represents the actual mass. The disintegration function shows an abrupt rise above 0.36 MV which cannot be explained satisfactorily by the penetrability of the deuteron but suggests a definite threshold, i.e., an endoergic reaction. Both of the above masses are higher than that calculated from the radioactive beta-energy of 12 MV which is 8.0208. This suggests that the beta-decay results in an excited Be^8 product which transforms to the ground state with the emission of gamma-radiation (3.5−4.0 MV). In fact, Lewis, Burcham and Chang (L24) have shown that the residual Be^8 does break up into alpha-particles. Their distribution curve (private communication) shows a broad group with maximum intensity at an alpha-energy of 2.4 MV and a width at half-maximum of about 0.7 MV indicating that Be^8 is left in a level of 4.7 MV excitation energy and 1.4 MV width. In addition to this group there is a small number of alphas (about 2–3 percent of the total) having energies extending up to 6 MV, corresponding to a Be^8 excitation of 12 MV. The beta-particles of maximum energy should correspond to the lower limit of the main level (about 4 MV). This would agree with a $Q=\pm 0.3$ MV in the primary reaction together with a limit of 12.0 MV for the

beta-spectrum. The spectrum is expected to be a superposition of simple beta-spectra with their upper limits varying between 10 and 12 MV.

Fowler and Lauritsen (F28a) have also obtained a distribution curve for the alphas. All its features agree with the above except that the maximum occurs at 1.3 MV. Rumbaugh, Roberts and Hafstad (R19a) find no maximum at all, down to energies as low as 1 MV. This means that the Be^8 level in question may lie much lower than 4.7 MV. There is a possibility that it is identical with the level at 2.9 MV with a width of 0.8 MV which is observed in the B^{11}-p-α reaction. Wigner and Breit (W16) have shown that selection rules forbid beta-disintegration from the ground state of Li^8 to the ground state of Be^8 but would allow transitions to an excited state of angular momentum 2, assuming that the theoretical determinations of the angular momenta of the states involved is correct.

Be^9: $Be^9+H^2 \rightarrow Be^{10}+H^1$

Oliphant (O6) reported the observation of three or more groups of protons from Be, the most prominent of which were at 8, 14 and 26 cm. He attributed the 8 cm group to oxygen present as a contaminant and the 14 cm group to deuterium in the target, but offered no explanation for the 26 cm ones. Later Oliphant, Kempton and Rutherford (O9) measured the range to be 25.6 cm and suggested this process. Assuming the bombarding energy to be 0.20 MV (not stated) the Q value of this reaction is found to be 4.59 MV, and is used to obtain the mass of Be^{10}. From this value the expected electron energy is calculated to be 0.37 MV. The electron radioactivity has been observed by McMillan (Mc7) to have a half-life of more than 10 years and a very low electron energy (estimated to be 0.3 MV).

In the same paper Oliphant, Kempton and Rutherford found again a broad group of singly charged ions (8 to 10 cm), but rather than referring it to oxygen they prefer to consider it a H^3 particle coming from a new reaction: $Be^9+H^2 \rightarrow Be^8+H^3$. Whether this can be justified must be determined by e/m measurements. The calculated reaction energy is 4.47 MV and the H^3 particle would have 3.25 MV and a range of 7.8 cm. An alternative interpretation is that it is a proton corresponding to an excitation state of the Be^{10} nucleus, in which case the energy difference would be 1.4 MV.

B^{10}: $B^{10}+H^2 \rightarrow B^{11}+H^1$

Cockcroft and Walton (C25) found three groups of protons from boron under deuteron bombardment which have been more accurately studied and reported in a later paper by Cockcroft and Lewis (C28). The extrapolated ranges are found to be 90.7, 58.5 and 30.7 cm, and the Q values obtained for the three groups are 9.14 7.00, and 4.71 MV, suggesting excitation states of the B^{11} nucleus at 2.14 and 4.43 MV. No protons of ranges of greater than 91 cm have been found so this must represent the disintegration into the ground state for which the calculated Q value is 9.30 MV. We have for comparison the measurements of the gamma-ray lines by Crane, Delsasso, Fowler and Lauritsen (C44). They report five lines, all well resolved although not allowing very accurate measurements. Two of these at 2.4 and 4.2 MV suggest a correspondence with the proton group differences, although they have an alternative interpretation in the B^{11}-d-n reaction. A 6.7 MV line is also attributed to the B^{11}-d-n reaction, while one of >10 MV may be from B^{10}-d-α. The fifth line, of 5.5 MV, is not yet identified.

B^{11}: $B^{11}+H^2 \rightarrow B^{12}+H^1$

Lawrence and Thornton first found evidence of high energy radioactive electrons from B, and suggested the B^{11} isotope as responsible. Following this suggestion Crane, Delsasso, Fowler and Lauritsen (C46) arranged a cloud chamber to photograph the electron tracks and found them to have a distributed energy spectrum with a practical maximum limit at 11 MV. The K-U extrapolation has been reported by Fowler, Delsasso and Lauritsen (F28) to be 13 MV. A recent report by Bayley and Crane (B5a) gives an observational limit of 12 MV. By using an automatic timing device to turn off the ion beam a short time before the cloud chamber expansion and counting the number of tracks formed after different time intervals it was possible to estimate the half-life as 0.02 sec. This activity has the highest energy electrons and the shortest half-life yet reported.

If the mass of the B^{12} obtained from the radio-

active process into C^{12} with the emission of electrons of 12 MV energy is used to calculate the primary reaction energy we obtain the value of 2.46 MV, predicting protons of over 2.28 MV (9 cm range). (The electrons were found to have 20 times the abundance of the 91 cm proton group from B^{10}.) Cockcroft and Lewis (C28) searched for such a group and found none with ranges greater than 2.7 cm with 0.55 MV deuterons. This indicates a reaction energy of less than 0.90 MV and a mass of the B^{12} formed in the primary reaction of >12.0186, or >1.7 MV higher than that from the radioactive beta-energy. This result is similar to that obtained for the Li^7-*d*-*p* reaction, and may be interpreted as due to a β-ray of less energy than the maximum available and the formation of an excited C^{12} product, and predicts an accompanying gamma-ray of >1.7 MV.

This activity was observed with deuterons of <0.3 MV (B5a) so that certainly Q is >-0.25 MV. This gives an upper limit to the B^{12} mass of 12.0198 and an upper limit to the gamma-ray energy of 2.7 MV.

There is some slight evidence (§99B) for a C^{12} excitation level at 3.0 MV which may represent the level at <2.7 MV discussed above. However, it seems desirable to repeat the search for proton groups with separated B isotopes.

C^{12}: $C^{12}+H^2\rightarrow C^{13}+H^1$

The protons from this reaction were first recognized by Cockcroft and Walton (C25) who measured an extrapolated range of 14.0 cm with 0.5 MV deuterons. The more recent results of Cockcroft and Lewis (C29) show this range to be 13.9 cm from which we get a Q value of 2.71 MV. The calculated value is 2.76 MV.

A gamma-ray from carbon targets bombarded by deuterons played a large part in the early discussions of the disintegration mass scale. This was measured by Lauritsen and Crane (L7), McMillan (Mc4) and others to be of about 3.7 MV, using absorption techniques. With cloud chamber methods Tuve and Hafstad (T15) found it to consist of a strong line of 2.7 MV and a much weaker one extending to 4 MV or higher. It was thought to have the proper intensity to be associated with the protons of this reaction and in the first analyses was added to the proton energy to determine the reaction energy. In calculating masses from disintegration data Bethe (B11) found that a consistent set of values would be obtained only if this gamma-ray were not included in the reaction energy. The recent mass spectroscopic measurements by Bainbridge and Jordan (B2) of C^{12} and C^{13} show definitely that the observed proton group corresponds to the formation of C^{13} in the ground state. Moreover, there is not sufficient energy to produce the more energetic gamma-ray in this reaction and it has been tentatively ascribed to C^{13}-*d*-*n*. The 4 MV gamma-ray is of sufficiently low intensity to be due to the less abundant isotope. Whether the 2.7 MV radiation belongs to the C^{12}-*d*-*p* reaction and is associated with a very slow proton is still an open question. A gamma-ray of similar energy was observed from B^{10}-α-*p*, and there is also some evidence for a level of C^{13} near 3 MV from the proton groups of that reaction.

Carbon is a common contaminant of targets, especially in apparatus using oil diffusion pumps, and this group of protons share with those from imbedded H^2 in producing a contamination group observed in many other experiments.

C^{13}?: $C^{13}+H^2\rightarrow C^{14}+H^1$

McMillan (Mc7) suggests this reaction to explain a 3 months electron activity found on many samples of Mo and brass after H^2 bombardment and supposedly due to some common contaminant. The electrons were estimated to have energies of about 0.3 MV. From the mass of C^{14} obtained from other disintegration data the Q for the primary reaction is found to be 6.08 MV and the energy available for the radioactive decay process is 0.16 MV.

N^{14}: $N^{14}+H^2\rightarrow N^{15}+H^1$

Preliminary investigations at Berkeley showed protons from N, followed by the report of Lawrence, McMillan and Henderson (L16) of two groups, of 24 and 85 cm range. Cockcroft and Lewis (C29) measure these ranges to be 18.3 and 85.1 cm with 0.5 MV deuterons. The corrected Q values corresponding to these groups are 8.55 and 3.11 MV, while that obtained from masses is 8.57 MV. The two experimental Q values must represent an excitation state of N^{15} of 5.4 MV. One of the gamma-ray lines observed

by Crane, Delsasso, Fowler and Lauritsen (C49) is reported to have an energy of 5.3 MV and may be tentatively attributed to this excitation.

N^{15}(?): $N^{15}+H^2 \rightarrow N^{16}+H^1$

Some slight evidence for this reaction is in the observation by Fowler, Delsasso and Lauritsen (F28) of a group of radioactive electrons from a sodium nitrite target with an energy maximum of 6 MV. These were of low intensity but separable from the Na^{24} electrons and O^{15} positrons also observed. N^{16} is also produced in the F^{19}-n-α reaction and its half-life measured. The predicted Q value is 0.2 MV.

O^{16}: $O^{16}+H^2 \rightarrow O^{17}+H^1$

Cockcroft and Walton (C25) observed protons from a target of oxidized tungsten. In the more recent work of Cockcroft and Lewis (C29) two groups are found which can be associated with this process, at 9.22 and 4.65 cm. The corrected values for the Q's of these two groups give 1.95 and 1.12 MV, specifying an excitation level in the O^{17} nucleus at 0.83 MV. The higher value is assumed to lead to a normal nucleus and is used to calculate the mass of O^{17}. This mass value is of theoretical interest in determining the shell structure of nuclei, and shows the high mass expected from the assumption of a completed shell in O^{16}. See §33.

F^{19}: $F^{19}+H^2 \rightarrow F^{20}+H^1$

A target of CaF was found by Henderson, Livingston and Lawrence (H21) to yield an electron activity of short half-life, supposedly from this reaction. Crane, Delsasso, Fowler and Lauritsen (C47) found a half-life of 12 sec., and later measured the energy of the radioactive electrons to be 5.0 MV. The production of the same activity by slow neutrons on F and by fast neutrons on Na makes this assignment definite.

Protons of 10.0 cm range are reported by Fowler, Delsasso and Lauritsen (F28) in the bombardment of F by 0.9 MV deuterons. The reaction energy obtained from this datum is 1.75 MV. If this proton group represents the full energy evolution the mass of the F^{20} formed is 20.0092. On the other hand the mass calculated from the radioactive energy and Ne^{20} is 20.0042. This again indicates that the Ne^{20} product of the radioactive process is left in an excited state and a gamma-ray is expected, of 4.6 MV, in this case.

Na^{23}: $Na^{23}+H^2 \rightarrow Na^{24}+H^1$

Lawrence (L10, L15) observed an electron radioactivity from Na having a half-life of 15.5 hr., chemically identifiable as Na^{24}. A better value of the half-life, obtained by Van Voorhis (V6) is 14.8 hr. The same period activity had previously been produced by neutrons in three different ways, and also identified as this Na^{24} isotope. The protons were found to have ranges of 49 and 17 cm for deuteron energies of 2.15 MV. The assumed stopping power of the Al foils used for range measurements is 12 percent low so a correction to the reported ranges is required. This gives a recalculated Q value for the primary reaction of 4.92 MV. The Q for the shorter range group is 1.72 MV, indicating an excited level in Na^{24} of 3.20 MV. The 4.92 MV Q value is used to obtain the Na^{24} mass.

The excitation curve of the intensity of the observed radioactivity (supposedly the same as that for proton emission) was found not to fit the usual Gamow probability function (L17) and the Oppenheimer-Phillips theory was introduced as an explanation. As explained in the introductory paragraphs to this type reaction, these observations are adequately interpreted by a correct Gamow function.

The electron radiation from Na^{24} has been found by Kurie, Richardson and Paxton (K33) to have an energy distribution with maximum energy at 1.7 MV. Gamma-radiation of high intensity accompanies the electrons (the same half-life) and Lawrence (L15) first measured it by its absorption coefficients in several absorbers to be 5.5 MV. Using the cloud chamber method of magnetic deflection of secondary electrons Richardson and Kurie (R7) observed gamma-ray lines at 0.95, 1.93 and 3.08 MV. Later measurements of Richardson and Emo (R6a) based on the photo-disintegration of deuterium by the gamma-ray give the maximum energy the value 2.8 MV. It is plausible to assume that Mg^{24} is left in an excited state of about 2.9 MV and goes over to the ground state with the emission of a quantum of this energy or of two of lesser energy. The total energy evolution in the secondary process would be 4.6 MV, and represents a

TABLE LVII: *Evidence for d-p type reaction in heavy elements.*

TARGET						
Z	El	Raa PRODUCT	T	CHEM. IDENTIF.	ALSO PRODUCED BY	REF.
14	Si^{30}	Si^{31}	160 min.	Yes	P-*n*-*p*, Si-*n*-γ	N5, N7b
15	P^{31}	P^{32}	14.5 da.	Yes	P-*n*-γ, S-*n*-*p*, Cl-*n*-α, S-*d*-α	N5, N7b
17	$Cl^{35, 37}$	$Cl^{36, 38}$	37 min.		Cl-*n*-γ	V6
18	A^{40}	A^{41}	110 min.	Yes	K-*n*-*p*, A-*n*-γ	S15
19	K^{41}	K^{42}	12.2 hr.		K-*n*-γ, Sc-*n*-α	K33
20	Ca^{44}	Ca^{45}	2.4 hr.	Yes	Ca-*n*-γ, Ti-*n*-α	W1
22	Ti^{50}	Ti^{51}	2.8 min.	Yes	Ti-*n*-γ	W1a
25	Mn^{55}?	Mn^{56}	2.5 hr.	Yes	Fe-*n*-*p*, Co-*n*-α, Mn-*n*-γ, Cr-α-*p*	D3a
26	Fe^{58}	Fe^{59}	40 da.	Yes	Co-*n*-*p*	L27a
27	Co^{59}	Co^{60}	$\sim$ yr.		(Co-*n*-γ)(?)	T10
28	Ni^{58}	Ni^{59}	3.5 hr.		Ni-*n*-γ, Co-*p*-*n*(?)	T10
29	Cu^{63}	Cu^{64}	12.8 hr.	Yes	Cu-*n*-γ, Zn-*d*-α, Zn-*n*-*p*, Ni-*p*-*n*	V7
30	$Zn^{64, 68}$	$Zn^{65, 69}$	1 hr. 97 hr.			L26
33	As^{75}	As^{76}	27 hr.		As-*n*-γ	T10
34	Se^{82}	Se^{83}	10–20 min.	Yes	Se-*n*-γ?	S16a
35	Br^{79}	Br^{80}	18 min.	Yes	Br-*n*-γ, Br-γ-*n*	S16a
	Br^{79}	Br^{80}	4.2 hr.	Yes	Br-*n*-γ, Br-γ-*n*	S16a
	Br^{81}	Br^{82}	35 hr.	Yes	Br-*n*-γ	S16a
44	$Ru^{96, 102}$	$Ru^{97, 103}$	39 hr. 11 da.			L26
46	Pd	Pd^{+1}	10 hr.	Yes	Pd-*n*-γ	K25
48	Cd^{114}	Cd^{115}	4.3 hr.	Yes	Cd-*n*-γ	C36a
	Cd^{116}	Cd^{117}	58 hr.	Yes		C36a
50	Sn^{120}	Sn^{121}	28 hr.	Yes	(Sb-*d*-α)	L27
51	$Sb^{121, 123}$	$Sb^{122, 124}$	2.5 da. 60 da.		Sb-*n*-γ	L26, L27b
56	Ba^{138}	Ba^{139}	85.6 min.	Yes	Ba-*n*-γ	P11a
57	La^{139}	La^{140}	31 hr.	Yes	La-*n*-γ	P11a
58	Ce	Ce(?)	2.4 hr.			P11a
78	$Pt^{192, 196}$	$Pt^{193, 197}$	49 min. 14.5 hr.	Yes	Pt-*n*-γ	C35
79	Au^{197}	Au^{198}	(2.7 da.)	Yes	Au-*n*-γ	C36
82	Pb	Pb^{+1}	8.6 da.	Yes		T11
83	Bi^{209}	Bi^{210}	5 da.		Ra*E*	L26

case in which the full energy beta-emission is a forbidden transition. This value is used to obtain the Mg^{24} mass from Na^{24}.

Mg^{26}: $Mg^{26}+H^2 \rightarrow Mg^{27}+H^1$

Preliminary experiments (H21) showing an induced radioactivity in Mg have been followed up in other experiments by Henderson (H24) in which he finds two radioactive periods. One of these (15.8 hr.) is identifiable as Na^{24}, while the second, having a half-life of 10.2 min. is doubtless the Mg^{27} isotope observed by Fermi under neutron bombardment of Mg and Al. The radiations were found to be negative electrons. Absorption curves of these electrons in Al give the somewhat inconclusive maximum energy value of 2.05 MV. Cloud chamber determinations of the energy spectrum have not been reported. Gamma-rays are also emitted from the radioactive process and rough determinations of their energy with Pb absorbers indicate about 1.3 MV. The protons from the primary process have not been observed but the calculated Q value is 4.2 MV.

Al^{27}: $Al^{27}+H^2 \rightarrow Al^{28}+H^1$

Al was first found to emit protons under deuteron bombardment by Lawrence and Livingston (L13). These protons have been found by McMillan and Lawrence (Mc5), with 2.2 MV deuterons, to consist of several groups, two strong ones at 10 and 21 cm, two weaker ones at 30 and 53 cm and another extending up to 62 cm range. Assuming this last group to be due to the normal disintegration a reaction energy of 5.79 MV is indicated, corrected for geometry and the stopping power of the Al foils used to measure the range. The successively smaller Q values of 5.11, 3.10, 2.12 and 0.64 MV for the shorter range groups suggest excitation levels of the Al^{28} nucleus. Gamma-radiation has been observed by

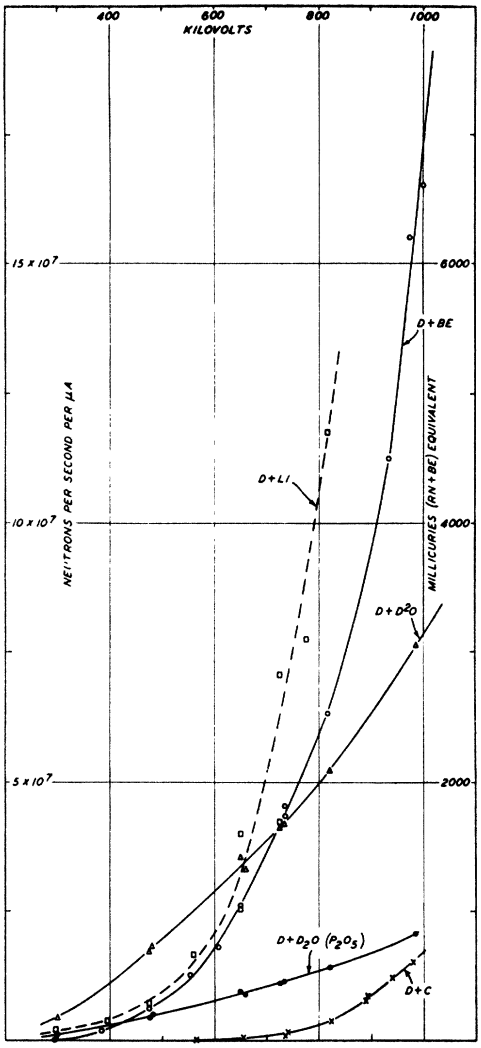

FIG. 48. Neutron yields from various targets bombarded by deuterons. Abscissa: deuteron energy in kilovolts. Ordinate: Neutron yield. Left-hand scale: Number of neutrons per microampere of deuterons. Right-hand scale: Strength of radon-beryllium source in millicuries equivalent to one microampere of deuterons. (Amaldi, Hafstad and Tuve (A11a).)

McMillan (Mc4) but its line structure has not been analyzed. The highest Q value is used to determine the Al^{27} mass.

The radioactive half-life of Al^{28} is found to be 2.6 min. and the maximum of the energy distribution is shown by Cork, Richardson and Kurie (C34) to be 3.3 MV. This is used to connect the mass of Al^{28} with that of Si^{28}. Gamma-radiation of 2.3 MV is also observed in the radioactive process. In this case the gammas are probably alternative to and not consecutive to the beta-emission. The excitation function for the production of the radioactivity (assumed to be the same for the primary reaction) has been found by Lawrence, McMillan and Thornton (L17) and follows a correct Gamow relation.

Targets of higher atomic number.—Using the large magnetic accelerator a group of investigators chiefly at the University of California have studied the radioactivities produced through this type of reaction in many heavy elements. Chemical identification of the radioactive products in many reactions have shown these products to be isotopes of the target element, so specifying this type reaction. In other cases the observation of a half-life period also observed in neutron produced reactions has been sufficient to determine the reaction. The processes in the heavier elements may follow the O-P mechanism (§80). Table LVII indicates the nature and extent of these observations:

A point of interest in the reactions in Table LVII is the observation of positrons. Van Voorhis (V7) has observed positrons and electrons in approximately equal numbers from activated copper. They have similar energy distributions and exactly identical half-life periods, and are interpreted as coming from a branching process in the radioactive C^{64} isotope leading alternately to Ni^{64} and Zn^{64}. A few positrons were observed by Paxton (P4) from irradiated phosphorus, and may possibly have a similar explanation. Furthermore, Cork and Lawrence (C35) have observed positrons from activated platinum, and have identified them as coming from the 49 min. period activity.

C. Type reaction *d-n*. (Table LIX)

$$Z^A + H^2 \rightarrow (Z+1)^{A+1} + n^1 + Q:$$

The production of neutrons by deuteron bombardment was discovered by Crane and Lauritsen (C37, C38) in Li and Be targets. The neutrons were found to be emitted in large intensities, increasing with bombarding energy. Before that time neutrons had been produced only by alpha-particle bombardment of certain targets such as Be, and intensities were dependent upon the relatively weak natural sources of such alpha-particles. This new method of production is hundreds of times more intense than the earlier alpha-particle sources, and is limited only by the

TABLE LVIII. *Summary of d-p type reaction.*

TARGET Z	TARGET El	PRODUCT El	Q(MV) (CALC.)	Q(MV) (OBS.)	REFERENCE	RESONANCE LEVELS (MV)	EXCIT. LEVELS (MV)	YIELD p/d @ (MV)
1	H^2	H^3	3.98*	3.98	O8			$1/10^6$ @ 0.1
2	He^4	He^5	−3.0					
3	Li^6	Li^7	4.92*	5.02	D11		0.44	1/2(Li^6-d-α @ 0.5)
	Li^7	Li^8	−0.3*	−0.3?	B5a			
4	Be^9	Be^{10}	4.59*	4.59	O9		2.4?	
5	B^{10}	B^{11}	9.30	9.14	C28		2.14 4.43	$6/10^9$ @ 0.57
	B^{11}	B^{12}	<0.9	obs.	C46			
6	C^{12}	C^{13}	2.76	2.71	C29			$3/10^9$ @ 0.57
	C^{13}	C^{14}	6.08	obs.	Mc7			
7	N^{14}	N^{15}	8.57	8.55	C29		5.42	$2/10^{10}$ @ 0.57
	N^{15}	N^{16}	0.2	obs.	F28			
8	O^{16}	O^{17}	1.95*	1.95	C29		0.82	$1/10^9$ @ 0.57
9	F^{19}	F^{20}	>1.8*	1.75	F28			
10	Ne^{20}	Ne^{21}	5.33					
	Ne^{21}	Ne^{22}	7.11					
11	Na^{23}	Na^{24}	4.94*	4.92	L15		3.20	$6/10^7$ @ 1.7
12	Mg^{24}	Mg^{25}	4.7					
	Mg^{25}	Mg^{26}	9.9					
	Mg^{26}	Mg^{27}	4.2	obs.	H24			$5/10^7$ @ 3.0
13	Al^{27}	Al^{28}	5.79*	5.79	Mc5		0.68 2.69 3.67 5.15	$3/10^7$ @ 1.9
14	Si^{28}	Si^{29}	6.1					
	Si^{29}	Si^{30}	9.3					
	Si^{30}	Si^{31}	3.3	obs.	N5			
15	P^{31}	P^{32}	6.3	obs.	N5			
17	Cl^{37}	Cl^{38}	—	obs.	V6			
18	A^{40}	A^{41}	—	obs.	S15			

* Q (observed) used to calculate mass values.

intensity and voltage of the accelerating apparatus. Using Be targets and the 5 to 6 MV deuterons available in the magnetic accelerator Lawrence estimates that as many as 10^{10} neutrons per second are produced with about 10 microamperes of deuterons. These intensities make this a superior source for studying the properties of and disintegrations produced by neutrons.

The deuteron must itself be absorbed in this process, while the neutron, having no potential barrier to penetrate, would be readily emitted. The probability of disintegration should, therefore, be proportional to the probability of the deuteron penetrating the nuclear barrier, following the simple Gamow theory.

H^2: $H^2+H^2 \rightarrow He^3+n^1$

These neutrons were first recognized by Oliphant, Harteck and Rutherford (O5, O7) in addition to the protons and H^3 particles also emitted from deuterium. The necessary balance of mass and charge in the reaction require He^3 as the residual nucleus. The neutrons were found to be essentially monokinetic, as would be expected from the simple two particle reaction, and should have energies of 2.38 MV plus $\frac{1}{4}$ the deuteron energy for 90° observation. Dee and Gilbert (D8) have observed the He^3 residual nucleus to have a range of 4.3 mm if extrapolated to zero bombarding energy. Bonner and Brubaker (B38) observe a 2.53 MV maximum for the neutron energy at 90° to the incident 0.5 MV deuterons. This indicates a Q of 3.18 MV when corrected and seems more accurate than the previous results. Using the masses of H^2 and H^1 we can calculate the mass of He^3.

The probability of disintegration is quite large for low voltages. The most complete information about absolute neutron yields from various targets was obtained by Amaldi, Hafstad and Tuve (A11a) using the Amaldi and Fermi (A11) method for measuring neutron intensities. The results are given in Fig. 48.[18] At 300 kv the

[18] We are indebted to the Director of the Department of Terrestial Magnetism of the Carnegie Institution for permission to publish these results.

number of neutrons per 10^6 deuterons is about 0.7 from a "heavy" ice target. The increase with voltage is not very rapid, so that above 0.7 MV the neutron yield from Li or Be targets becomes larger than from the ice target. The excitation curve above 0.5 MV is nearly linear with the range of the deuterons, but at low voltages exhibits the Gamow exponential-type increase. At 60 kv Zinn and Seeley (Z2) report a neutron intensity equivalent to 125 millicuries of Rn-Be per milliampere of ion current containing both molecular and atomic ions. They find the neutron yield to double for each 20 kv voltage increase in this voltage range.

The low voltages for which this reaction occurs make it possible to apply standard low voltage techniques to the artificial production of neutrons. Most attempts to date have been handicapped by the lack of a suitable heavy hydrogen target. Heavy water ice has been used, but requires liquid-air cooling and limits the allowable ion beam. Moreover, only a small fraction of the beam as usually used consists of atomic ions, while the molecular ions have only half the equivalent energy and so are very inefficient compared to their heating effect on the target.

A particular advantage of the neutrons from this reaction is their monokinetic character, in which property they are unique. This feature makes them invaluable in studies of neutron scattering and disintegrations by fast neutrons.

Li^6(?): $Li^6+H^2\rightarrow He^4+He^3+n^1$

In their experiments on separated isotopes of Li Rumbaugh and Hafstad (R19) observed neutrons from the Li^6 target in sufficient intensities to preclude the possibility of contamination of Li^7, H^2, O, C, etc. The excitation function shows significant differences from that of the most reasonable impurity (C), and leads to a value for the yield of $6/10^8$ deuterons at 0.75 MV. A reasonable guess as to the reaction is the formation of He^4 and He^3 in a manner similar to the Li^7 reaction below. The calculated Q value for this reaction is 1.56 MV, of which a maximum of $\frac{7}{8}$ would be available to the neutron. The observations show more energetic neutrons than from C, partially justifying the assumption. An alternative would be the formation of Be^7, in which case the Q value can be estimated as 3.1 MV if the Be^7 mass is chosen 1 MV greater than that of Li^7.

Li^7: (a) $Li^7+H^2\rightarrow He^4+He^4+n^1$
(b) $Li^7+H^2\rightarrow Be^8+n^1$

The alpha-particle products of reaction (a) have been discussed under the d-α type reaction. The accompanying neutrons were first observed by Crane, Lauritsen and Soltan (C38), in intensities nearly as great as from Be, and they independently suggested this reaction as responsible. The excitation function and yield relative to other processes is shown in Fig. 48.

In cloud chamber measurements of the proton recoils from the neutrons in this process, Bonner and Brubaker (B37) observed a continuous distribution in energy compatible with the three particle products, with a maximum of about 13.6 MV from which a Q value of 14.6 MV can be estimated. In addition to the neutrons of continuous energy a monokinetic group was found at 13.5 MV, which indicates the alternative formation of a Be^8 nucleus with a Q of 14.5 MV. The calculated values for the two modes of disintegration are 15.05 and 14.91 MV.

Be^9: $Be^9+H^2\rightarrow B^{10}+n^1$

Be was the first element in which Crane, Lauritsen and Soltan (C37) observed the production of neutrons by deuteron bombardment, and is the source from which Lawrence and his colleagues obtain their extremely high neutron intensities. The reaction is widely used as a source of neutrons in high voltage apparatus.

Only recently have neutron energy measurements been made which are free from criticism on the grounds of scattering and statistical errors. These are obtained by Bonner and Brubaker (B40) using the cloud chamber technique and measuring only those proton recoils in the forward direction. The highest energy group shows a Q value of 4.20 MV while the Q calculated from masses is 4.18 MV. Other neutron groups having Q values of 3.7, 2.2, and 0.9 MV suggest excitation states of 0.5, 2.0 and 3.3 MV in the B^{10} product nucleus. Gamma-radiation from this (and the other $Be+H^2$ reactions) was first noted by McMillan (Mc4). From cloud chamber studies Crane, Delsasso, Fowler and Lauritsen (C45) and later Kruger and Green (K26b) each report as many as six gamma-ray lines. In both cases

there is some evidence for lines which may represent the same excitation states as the neutron groups. Only a small fraction of the neutrons have the maximum energy. The excitation curve relative to other targets is given in Fig. 48.

B^{10}: $B^{10}+H^2 \rightarrow C^{11}+n^1$

Crane and Lauritsen (C40) observed a positron radioactivity of 20 minute half-life from B and also observed neutrons (L5) although these are probably chiefly from the B^{11} isotope. After some confusing reports the half-life has been found to be 20.5 minutes (Y1) and the radioactive isotope chemically identified as *C*. The positron energy spectrum has a maximum of 1.15 MV (F28). Yields are small, about 1 positron being observed for 10^8 deuterons of 0.57 MV at equilibrium.

One group of neutrons from B observed by Bonner and Brubaker (B40) have been identified with this process and have a *Q* value (recalculated) of 6.08 MV. This compares favorably with the mass value of 6.34 MV. The observed group may be superposed on one from the B^{11} isotope leading to the 7.0 MV excited level of C^{12}, so that the reaction energy deduced from it may not be very accurate. Another group attributed by Bonner and Brubaker to this reaction would give a *Q* value of 4.0 MV, indicating an excitation state of 2.2 MV in C^{11}. Since this second group is even stronger than the highest energy one it is possible that it belongs rather to the B^{11}-*d*-*n* process.

B^{11}: (a) $B^{11}+H^2 \rightarrow C^{12}+n^1$
(b) $B^{11}+H^2 \rightarrow 3He^4+n^1$

The neutrons observed when boron is bombarded by deuterons are largely due to the two reactions above. Bonner and Brubaker (B40) have obtained cloud chamber data of recoil protons and He atoms which they analyze into the various processes. The most probable reaction is (b), giving rise to a continuous group of neutrons with energies below 3 MV. This is in accord with the alpha-particle observations of Cockcroft and Lewis (C11) (§101A) who find a similar continuous distribution of alphas. The shape of the curve cannot be analyzed to give an experimental *Q* value, but using mass values this is found to be 6.53 MV.

Reaction (a) is thought responsible for the group of highest energy neutrons, from which a corrected *Q* value of 13.4 MV is obtained; the calculated value is 13.68 MV. Another group gives a *Q* of 9.0 MV; it can only be ascribed to this reaction since no other has sufficient energy. This predicts an excitation level at 4.4 MV in the C^{12}, for which there is also other evidence (see below). Two additional neutron groups with *Q* values of 6.0 and 3.9 MV can on energetic grounds be attributed either to B^{10} or B^{11}. If attributed to B^{11} they would indicate two further excitation levels of C^{12} at 7.4 and 9.5 MV. For the first-named level there is again evidence from other reactions and from gamma-rays so that the observed neutron group is probably a superposition of groups from B^{10} and B^{11}. The second group is of very high intensity which may indicate that its source is the more abundant B^{11} isotope.

The gamma-radiation has been studied by Crane, Delsasso, Fowler and Lauritsen (C44), and is found to have components at 2.4, 4.2, 5.6 and 6.7 MV. What may be the same gamma-rays from C^{12} are also found (C49) in the N^{14}-*d*-α process, with energies of 4.0, 5.3, 7.0 MV and two of lower energy. Bothe (B47) has observed gamma-radiation of 2.7, 4.2 and 6.7 MV from the C^{12} product of the Be^9-α-*n* reaction. Neutron groups in this reaction also fit the two excitation levels at 4.4 and 6.7 MV (§99B).

The complete evidence for possible excitation states in the C^{12} nucleus shows the following levels:

(1) 3.0 MV(?): Be^9-α-*n* group.

(2) *4.3* MV: N^{14}-*d*-α group, B^{11}-*d*-*n* group, Be^9-α-*n* gamma, B^{11}-*d*-*n* gamma, N^{14}-*d*-gamma (compatible with Be^9-α-*n* groups). *7.0−4.3=2.7* MV: Be^9-α-*n* gamma, B^{11}-*d*-*n* gamma.

(3) *7.0* MV: Be^9-α-*n* group, Be^9-α-*n* gamma, B^{11}-*d*-*n* (group may be present), B^{11}-*d*-*n* gamma, N^{14}-*d*-α gamma.

7.0−4.3=2.7 MV: Be^9-α-*n* gamma, B^{11}-*d*-α gamma.

(4) *9.5* MV: B^{11}-*d*-*n* group (may be from B^{10}-*d*-*n*, however), relative intensity of group to positrons from C^{11} makes it seem likely that this group is due to C^{12}.

9.5−4.3=5.2: B^{11}-*d*-*n* gamma, N^{14}-*d*-α gamma (may be a N^{15} level as indicated by N^{14}-*d*-*p* group).

(5) *14.5* MV: B^{11}-*p*-γ gamma (no other resonable interpretation).

(6) *16.16* MV: B^{11}-*p*-α resonance level.

(7) Another level between *9.5* and *14.5* MV is indicated for the alpha-emission process: $C^{12} \rightarrow Be^{8} + He^{4}$. Observed in B^{11}-*d*-α as a discrete alpha-group in the continuous distribution, also as groups in B^{11}-*d*-*n* and N^{14}-*d*-α.

C^{12}: $C^{12} + H^{2} \rightarrow N^{13} + n^{1}$

A positron radioactivity chemically separable as nitrogen was observed by Henderson, Livingston and Lawrence (H21) and by Crane and Lauritsen (C40) when C was bombarded by deuterons. The best determination of the half-life of the N^{13} produced is the value of 11.0 minutes observed by Ellis and Henderson (E5) in the B^{10}-α-*n* reaction. The excitation function for the production of this activity shows the exponential-type rise represented by the Gamow function (Fig. 46). Newson (N7a) has obtained an excitation curve up to 5 MV and it exhibits a flat maximum at about *3.3* MV. Since the potential barrier for deuterons is of the order of 2.2 MV the further increase beyond this value indicates the variation of the internal probability of disintegration.

The neutrons were found by Tuve and Hafstad (T15) to have very low energies. Bonner and Brubaker (B40) obtain a measurement of recoil proton range which gives a Q value of -0.37 MV, a reasonable check with the statement by Cockcroft and Lewis (C29) that neutron emission begins sharply at 0.32 MV deuteron. The latter value is assumed to be the most accurate since it must be the lower limit. Thus $Q = -0.28$ MV (the relative energy), and it is used to obtain the N^{13} mass.

Using the mass values of N^{13} and C^{13} we are able to predict the energy expected in the positron radioactive process (considering the mass of two electrons) and find it to be 1.24 ± 0.07 MV. The limit of the positron spectrum has been measured by Fowler, Delsasso and Lauritsen (F28) to be 1.25 MV, and the K-U extrapolated limit of 1.45 MV was also obtained. In this case it seems quite certain that the visual limit is closer to the correct value than the K-U limit, a conclusion that is borne out with somewhat less certainty by several other such cycles. Alichanian, Alichanow and Dzelepow (A1) find an even higher "visual limit" of 1.45 MV, using a magnetic beta-ray spectrograph. This is hard to reconcile with the evidence given above but is even stronger proof that the K-U limit cannot be valid.

C^{13}: $C^{13} + H^{2} \rightarrow N^{14} + n^{1}$

Bonner and Brubaker (B40) find a neutron group representing about 1 percent of the total number of neutrons from *C* from which a Q value of 5.2 MV is obtained. The calculated value is 5.47 MV. They suggest this reaction as the source of the 4 MV gamma-rays which have been a disturbing factor in the carbon disintegrations (§101B). This would predict a second neutron group at 1 MV which could not be observed in the experiments.

N^{14}: $N^{14} + H^{2} \rightarrow O^{15} + n^{1}$

A positron activity of 2.1 minutes half-life was found by Livingston and McMillan (L30, Mc6) to be produced in N, and chemically identified as an oxygen isotope. Any target bombarded in air or N_2 gas was found to have this radioactive element deposited on its face by recoil. An excitation curve by Newson (N7) shows the Gamow exponential rise and a break at *3.2* MV followed by a slow decrease. The positron energy has been measured by Fowler, Delsasso and Lauritsen (F28) to have a maximum at 1.7 MV. The neutrons have been observed only qualitatively. From the mass of O^{15} determined through the radioactive energy evolution the Q value can be estimated as 5.1 MV, which would give neutrons of 4.8 MV energy for zero energy deuterons.

O^{16}: $O^{16} + H^{2} \rightarrow F^{17} + n^{1}$

Newson (N6) has observed a positron radioactivity identifiable as F, of 1.16 minutes half-life, from an oxygen target. It is found to occur only for deuterons of more than 1.8 MV, indicating a -1.7 MV value of Q which is used to determine the F^{17} mass. Using this mass to calculate the expected positron energy we find nearly sufficient energy (2.0 MV) to explain the observed limit of 2.1 MV (K33). This result suggests again that the K-U limit (2.4 MV) is untenable.

The neutrons from the reaction were not detected above the general contamination back-

ground, but a study of the angles of recoil of the F^{17} gave results compatible with neutron emission and a Q of -1.7 MV. With increased energies the excitation curve is found to have a break at 3.7 MV followed by a slower increase (N7a).

F^{19}: $F^{19}+H^2\rightarrow Ne^{20}+n^1$

Although the neutrons observed from CaF_2 by Lawrence and Livingston (L13) might have been partially due to deuterium in the target, a later check of this reaction by Tuve and Hafstad (T14) reports neutrons from only two targets, Be and CaF_2, indicating that F is undergoing this reaction. Strong gamma-rays from F observed by Hafstad, Tuve and Brown (H1) may come from excited levels in the Ne^{20} nucleus, or from the alternative F^{20} nucleus from the d-p reaction. The calculated Q value is 10.68 MV.

Na^{23}: $Na^{23}+H^2\rightarrow Mg^{24}+n^1$

Neutrons have been observed by Lawrence (L15) in numbers about equal to the protons occurring in the alternate process, that is, 1 per 10^6 deuterons of 1.7 MV. From the known masses this process should have a Q of 8.8 MV, and yield neutrons of 8.5 MV maximum energy with zero energy deuterons.

Al^{27}: $Al^{27}+H^2\rightarrow Si^{28}+n^1$

McMillan and Lawrence (Mc5) have observed neutrons with yields of 1 per 5×10^8 deuterons of 1.7 MV energy. The calculated Q is 8.4 MV, predicting high energy neutrons.

S^{33}: $S^{33}+H^2\rightarrow Cl^{34}+n^1$

Positron activity of 33 min. half-life was found by Sagane (S1) to result from deuteron bombardment of sulphur. Chemical separations showed this activity to be Cl. It is probably Cl^{34} which was found by Frisch (F31) in the P-α-n reaction to have a period of 40 min.

$Ca^{40,\ 42,\ 43}$: $Ca^{40}+H^2\rightarrow Sc^{41}+n^1$
$Ca^{42}+H^2\rightarrow Sc^{43}+n^1$
$Ca^{43}+H^2\rightarrow Sc^{44}+n^1$

Walke (W1) reports three radioactive periods from Ca under deuteron bombardment which are chemically separable as Sc and yield positrons. A 4.0 hr. period is no doubt the 4.4 hr. period found by Frisch in the Ca-α-p reaction, and so is identified as Sc^{43}. The other two periods, of 53 min. and 52 hr. half-life represent Sc^{41} and Sc^{44} respectively; this assignment follows from the observation of the 52 hr. period from K-α-n and Sc-n-$2n$.

Ti: $Ti^{48,\ 49}+H^2\rightarrow V^{49,\ 50}+n^1$
Ti $+H^2\rightarrow$ V $+n^1$

Walke (W1a) has reported periods of 33 min. and 16 days from Ti under deuteron bombardment which he ascribes to this type of reaction. The 33 min. period is also observed in the Ti-α-p reaction suggesting either V^{49} or V^{50} as the active body. If due to V^{49} positrons would be expected, while V^{50} might yield either positrons or electrons. The 16 day period, which is positron active, may be $V^{47,\ 48\ or\ 49}$.

Fe^{54}: $Fe^{54}+H^2\rightarrow Co^{55}+n^1$

Darling, Curtis and Cork (D3a) find an 18.2 hr. positron period from Fe under deuteron bombardment which is chemically separable as Co. The only Fe isotope which could result in radioactive Co other than the known active and stable isotopes is Fe^{54}. This Co^{55} should decay into Fe^{55} (radioactive, T = 91 min.). Besides confirming the above findings, Livingood, Seaborg and Fairbrother (L27a) report other Co activities (100–200 da.; e^+, e^-) as yet unidentified.

Cr^{52}: $Cr^{52}+H^2\rightarrow Mn^{53}+n^1$

The 46 min. positron period reported by Livingood, Seaborg and Fairbrother (L27a) as due to Mn produced from Cr by deuterons has previously been found to result from a Cr-p-n reaction. This makes the assignment definite, since Mn^{54} is occupied by one of the Fe-d-α activities.

Ni^{60}: $Ni^{60}+H^2\rightarrow Cu^{61}+n^1$

Thornton (T10a) has observed a positron activity of 3.4 hr. half-life, chemically separable as copper, in the deuteron bombardment of Ni. This activity has also been observed in Ni-α-p and Ni-p-n reactions.

Se^{82}: $Se^{82}+H^2\rightarrow Br^{83}+n^1$
($Se^{82}+H^2\rightarrow Br^{82}+2n^1$?)

Snell (S16a) reports an activity from Se separable as Br with a period of 2.5 hrs. It is attributed to Br^{83}. Confirmation of this assignment

comes through the observation of a 10–20 min. Se period also produced by deuterons, which decays into the same active Br isotope found in this d-n reaction. The only Br isotope that could result from these two reactions is Br^{83}. Snell also reports the observation of the 35 hr. Br activity (known to be Br^{82}) from Se; this does not follow the usual type reactions from any of the known Se isotopes; it may be an instance of a d-$2n$ reaction.

$Pd^{104, 105}$: $Pd^{104}+H^2 \rightarrow Ag^{105}+n^1$
$Pd^{105}+H^2 \rightarrow Ag^{106}+n^1$

Two activities chemically separable as Ag were found by Kraus and Cork (K25) to result from deuteron bombardment of Pd. The periods of 32 min. and 7.5 days (reported earlier as 2 hr. and 150 hr.) are probably Ag^{106} and Ag^{105}, respectively. The shorter period is probably the 24 min. period known from the Ag-n-$2n$ and Ag-γ-n reactions. Positrons would be expected.

Sn^{119}: $Sn^{119}+H^2 \rightarrow Sb^{120}+n^1$
$Sn \ +H^2 \rightarrow Sb^{+1}+n^1$

Livingood and Seaborg (L27b) find radioactive Sb isotopes from a Sn target. A 16 min. positron activity is also observed in the Sb-n-$2n$ and Sb-γ-n reactions but not in Sb-n-γ (slow neutrons) so it is certainly Sb^{120}. Livingood (private communication) indicates that the 13 hr. period reported earlier (L27) is due to a Cu contamination, but that other activities are present, with half-lives of 3–5 hr., 1–4 da., (60–80 da.) and (>100 da.).

No d-n process has been observed for elements heavier than Sn. This is probably due to an instability of the nucleus produced in the d-n reaction against alpha-decay, leading generally to a d-n,α reaction (cf. §101D, below).

D. Type reaction d-n,α.

$$Z^A+H^2 \rightarrow (Z-1)^{A-3}+n^1+He^4+Q:$$

For heavy nuclei the particle most frequently emitted in the primary nuclear process is a neutron. According to the Bohr evaporation model (§54) the neutron will in general have low energy ($\sim$1 MV) and the residual nucleus will thus be left in a highly excited state. It will then be capable of emitting an alpha-particle. See §79 for a more complete discussion.

Pt: $Pt^{195}+H^2 \rightarrow Ir^{192}+n^1+He^4$
$Pt^{198}+H^2 \rightarrow Ir^{195}+n^1+He^4$

The bombardment of Pt by 4 to 5 MV deuterons by Cork and Lawrence (C35) has been found to result in both positron and electron activities. Two of the electron activities, with half-lives of 28 min. and 8.5 hr. are chemically separable as Ir, necessitating an alpha-emission process. The mechanism consists probably in an emission of a neutron of about 1 MV followed by an alpha-particle (§79). From the known stable isotopes of Pt (192, 194, 195, 196, 198) the Ir isotopes 189, 191, 192, 193, 195 can be formed. Of these 191 and 193 are stable and 189 would emit positrons. Thus the two activities should be attributed to Ir^{192} and Ir^{195}. At least two periods are found with slow neutrons (A7, S20) on Ir, one of which seems to be identifiable with the deuteron activities (50 min$\backsimeq$28 min.), and so should be Ir^{192}. This means that the 8.5 hr. period is probably Ir^{195}.

The excitation function shows several broad maxima in the region between 3.5 and 5.0 MV which are interpreted as due to a resonance effect. Present theories (see §§53, 60) indicate that resonance levels in such a heavy nucleus as Pt should be very closely spaced, so it is most satisfactory to interpret the broad maxima as due to fluctuations in the density of such resonance levels. The probability was high for such a heavy element disintegration, having an activation cross section of about 10^{-27} cm^2. This favors the large nuclear radius proposed by Bethe (B14) which would predict correspondingly lower and narrower potential barriers.

E. Type reaction d-p,α.

$$Z^A+H^2 \rightarrow (Z-2)^{A-3}+H^1+He^4+Q:$$

As in the d-n type reaction, the residual nucleus formed in a d-p reaction may also be left with sufficient excitation energy to be unstable against alpha-emission (§80), giving rise to a d-p, α reaction.

Au^{197}: $Au^{197}+H^2 \rightarrow Ir^{194}+H^1+He^4$

Cork and Thornton (C36) have observed an activity (half-life not reported) separable as Ir from deuteron bombardment of Au. The chemical identification of Ir necessitates the emission

TABLE LIX. *Summary of d-n type reaction.*

TARGET		PRODUCT	Q(MV)	Q(MV)	REFERENCE	RESONANCE	EXCIT. LEVELS	YIELD
Z	El	El	(CALC.)	(OBS.)		LEVELS (MV)	(MV)	n/d @ (MV)
1	H^2	He^3	3.18*	3.18	B38			$1/10^7$ @ 0.1 $8/10^6$ @ 0.5
3	Li^6	He^4+He^3	1.56	obs.	R19			$1.7/10^5$ @ 0.8
	Li^7	$2He^4$	15.05	14.6	B37			
	Li^7	Be^8	14.91	14.55	B37			$1/10^6$ @ 0.8
4	Be^9	B^{10}	4.18	4.20	B40		0.5 2.0 3.3	$2.7/10^5$ @ 1.0
5	B^{10}	C^{11}	6.34	6.08	B40			$1/10^8$ @ 0.57
	B^{11}	C^{12}	13.68	13.4	B40		4.4 7.4 9.5	
	B^{11}	$3He^4$	6.53	obs.	B40			
6	C^{12}	N^{13}	−0.28*	−0.28	C29			$3/10^6$ @ 1.0
	C^{13}	N^{14}	5.47	5.2	B40		4.0(γ)	
7	N^{14}	O^{15}	5.1	obs.	Mc6			$2/10^{10}$ @ 0.57
	N^{15}	O^{16}	9.92					
8	O^{16}	F^{17}	−1.7*	−1.7	N6			$1/10^6$ @ 2.5
	O^{18}	F^{19}	4.59					
9	F^{19}	Ne^{20}	10.68	obs.	T14		?(γ)	
10	Ne^{21}	Na^{22}	4.9					
	Ne^{22}	Na^{23}	7.73					
11	Na^{23}	Mg^{24}	8.8	obs.	L15			$3/10^7$ @ 2.15
12	Mg^{25}	Al^{26}	6.2					
	Mg^{26}	Al^{27}	5.3					
13	Al^{27}	Si^{28}	8.4	obs.	Mc5			$2/10^7$ @ 2.15
14	Si^{29}	P^{30}	3.9					
	Si^{30}	P^{31}	4.3					
15	P^{31}	S^{32}	7.2					
16	S^{34}	Cl^{35}	3.2					
17	Cl^{37}	A^{38}	9.1					
etc.								

* Q (observed) used to calculate mass values.

of three units of nuclear charge (if the deuteron is absorbed), and thus suggests the type reaction. The high energy of the deuterons used (6 to 7 MV) probably explains the emission of alpha-particles in a secondary process. (Cork and Lawrence used only 4 to 5 MV deuterons in their experiments on Pt in which this type reaction was not observed.) Since Au has only one known stable isotope the product must be Ir^{194}, known to have a half-life of 3 days from neutron capture experiments.

§102. DISINTEGRATIONS BY NEUTRONS

Disintegrations produced by neutrons are of four types, three yielding particle products (alphas, neutrons and protons), and another resulting in simple capture with gamma-ray emission. The first neutron disintegration reported ($N^{14}+n^1 \rightarrow B^{11}+He^4$) was by Feather (F5) and followed immediately upon Chadwick's report of the identification of this new particle. The cloud chambers used to measure neutron recoils served to show the forks characteristic of fast neutron disintegration processes. The forks showed alpha-particle tracks of considerable length originating from the same point as the more dense, short-ranged track of the residual nucleus. Other experimenters followed and discovered similar reactions in other elements. This method proved to be tedious, as it required thousands of photographs to detect a few of the rare forks. Its peculiar advantage, however, is that a single track is sufficient to identify the reaction under suitably controlled conditions. The chief difficulty is in the momentum determinations. Since the neutron produces no track its direction must be assumed and its momentum must be determined from the momenta of the two observed branches of the fork. Conclusions based on forks caused by scattered neutrons may lead to serious errors of interpretation.

The discovery of radioactivity induced by

alpha-particles was the clue which led Fermi (F14) to search for a similar effect with neutrons and disclose this simple and most satisfying method of studying neutron processes. The neutron, having no charge, experiences no potential barrier, and so the probabilities of penetration and of disintegration are large. Furthermore, the detection and observation of such induced radioactivities, which can be carried on in the absence of the source, has proven to be unique and simple. Chemical identification of the active materials showed that three of the processes named above occur. Rapid development of the field has led to a knowledge of scores of neutron reactions and has materially broadened the field of nuclear physics. Theoretical analysis has kept step with the development and it is safe to say that there is a better knowledge of disintegrations produced by neutrons than of any other type (cf. Chap. X).

The simple capture reactions yield the most direct evidence on nuclear structure because the results are not influenced by potential barriers. Recent discoveries have led to some knowledge of the resonance levels of nuclear systems. The new nuclear model proposed by Bohr (B32) is based on these experiments.

In addition to the three main types of disintegrations produced by neutrons (n-α, n-p and n-γ) there is some evidence for another type involving the emission of two neutrons. This means, in effect, that the incident neutron ejects another neutron from the nucleus and is itself not absorbed. Another prominent process is the inelastic scattering of neutrons by which no actual transmutation of the scattering nucleus is obtained but only an excitation which is followed by emission of gamma-radiation. Both of these are most readily visualized as leading to a compound nucleus which then releases a neutron of low energy; the excitation energy goes to liberate a second neutron in the first instance and a gamma-ray in the inelastic scattering process.

A. Type reaction n-α. (Tables LX and LXI)

$$Z^A + n^1 \rightarrow (Z-2)^{A-3} + \mathrm{He}^4 + Q:$$

The first type of neutron disintegration to be recognized, that yielding alphas, has been observed in three ways. For those elements available in the gaseous form (C, N, O, F, Ne) the cloud chamber is readily adaptable. Fast neutrons penetrate the chamber walls easily and produce reactions in the gas which are observable as forked tracks. Up to the present the sources have usually been limited to the intensities available in naturally radioactive materials (radon +Be). Photographs are sometimes confused by the many tracks of atoms recoiling from the neutrons. The neutron is assumed to come from the source (preferably small to subtend a small angle at the cloud chamber). If the two observed prongs of the fork are co-planar with the line from the source this assumption is partially justified. Some tracks are discarded by the observers because this condition is obviously not fulfilled, indicating a scattered neutron coming from a direction other than the source. Even for co-planar tracks there is still the possibility of scattering in that plane. Such tracks are useless since the information obtained from the observed tracks is not sufficient to determine both neutron energy and direction uniquely.

In order to analyze forks which are deemed satisfactory the neutron energy is determined from the momenta of the two particles. It is first necessary to assume a reaction mechanism, so naming the masses of the charged particles. From the measured components of alpha-particle momentum and the angle of the heavy track the energies of the neutron and residual nucleus can be estimated. Since the heavy particle carries most of the momentum and the angle of its short track with the assumed neutron direction cannot be measured with any accuracy, the errors in this method have been considerable.

In a large share of tracks measured the sum of observed particle energies is less than the neutron energy calculated from the momenta. It is extremely doubtful how much of the evidence in this respect can be trusted. Often extremely large energies of incident neutrons are concluded, certainly much larger than the energies available determined through other, more recent, evidence on masses. Examples: Kurie (K28), 17 MV instead of 10.7 MV from Be^9+He^4(Po); Harkins (H12), 15.8 MV instead of 10.7 MV from Be^9+He^4(Po). However, in the remaining evidence there is still enough to indicate energy losses.

Attempts to explain this energy loss have taken several forms. Feather (F5) and for a time Har-

kins, Gans and Newson (H12), favored a noncapture reaction, in which varying amounts of energy are absorbed from the neutron. Later Harkins and Gans (H13) disproved the noncapture reaction directly by statistical analysis of neutron directions. There is at present no good evidence for noncapture disintegration but it remains a possibility which should not be discarded. Kurie (K31) hypothecated an intermediate stage in the N^{14} reaction passing through a radioactive N^{15} with subsequent emission of the alpha-particle. This has no justification either theoretically or experimentally, and has subsequently been discarded. All workers have considered the possibility of excitation levels in the residual nucleus as responsible, but the data failed to show the unique values of Q that this would predict. One paper by Jaeckel (J1) on the disintegration of Ne, however, indicates a grouping of the amounts of the energy loss in the individual forks about two distinct values. This suggests that the process is actually producing excited residual nuclei, that the observed deviations from these values are unavoidable experimental errors inherent in the method, and that the processes follow the same rules as apply to the other types of disintegration. In the discussion to follow we consider the processes as conserving mass-energy and resulting in excited states and gamma-radiation.

The second method of observation of neutron disintegrations yielding heavy particles is through the use of electrical recording devices such as ionization chambers to observe the alphas. These have been successful only in those processes produced by slow neutrons. By definition this means exoergic reactions, and the energy of the resulting alpha is limited by the reaction energy. Therefore these reactions occur with appreciable probability only for light elements, whose low potential barriers allow the comparatively slow alphas to escape. Several such processes have extremely large cross sections (Li^6, B^{10}), and have the great advantage of having no neutron momentum to influence the accuracy of the results. Lacking the impediment of indeterminate neutron energies these processes have resulted in accurate observations of reaction energy in spite of difficulties in the technique. Such slow neutron processes have also been observed in cloud chambers and in photographic emulsions, in which case a single straight track is observed, of a length equal to the sum of the ranges of the ejected particle and the recoil nucleus.

The observation of induced radioactivity has been useful as a third method of establishing this type reaction. Either chemical identification of the radioactive element (of Z two less than the target) or the observation of a half-life period characteristic of a known element has been considered sufficient evidence to justify the existence of the process. Where a target is known to have only one isotope the observation of three half-life periods is good evidence for the existence of the three type reactions n-α, n-p, and simple capture. For example Al^{27} is known to result in three distinctive radioactive decay periods, characteristic of Na^{24}, Mg^{27} and Al^{28}.

The potential barrier for the escaping alphas from such processes would lead us to expect a relatively low probability for elements of high atomic number, as discussed by Bethe (B12). The observations show a limit at present at $Z=31$ (Ga). Only for the heaviest of heavy elements (U and Th) is this process again observed, due in these cases to the small binding energy for alphas in this region of the atomic table, as indicated by the natural alpha-radioactivity observed. The probability should be large for slow neutrons if the reaction energy Q is positive (the $1/v$ law) and should increase again for neutrons of several MV energy, for which the increased energy of the alphas would make penetration of the potential barrier more probable. We would expect, therefore, that the observations would be separated rather definitely into those produced by slow and by very fast neutrons.

Li^6: Li^6+n^1 (slow)$\rightarrow H^3+He^4$

In their early experiments with slow neutrons Amaldi, D'Agostino, Fermi, Pontecorvo, Rasetti and Segrè (A7) found a large absorption of slow neutrons in Li, but no radioactivity or gamma-radiation, which led to the suggestion of a process of this type. Chadwick and Goldhaber (C12) searched for heavy particle products with an ionization chamber and linear amplifier and found singly charged ions of about 5.5 cm range and doubly charged ions of less than 1.5 cm. Taylor and Dabholkar (T3) have observed single

straight tracks in a photographic emulsion from this reaction and measure a total range (in air-cm equivalent) of 6.64 cm. Rotblat (R16) reports a H^3 range of 5.36 cm and a Q value of 4.5 MV. The best measurement is that of Livingston and Hoffman (L32) using the shallow ionization chamber technique and giving a range of 5.73 cm for the H^3 particles. By comparison of the range of the H^3 with that of a proton of the same velocity, the particle energy is obtained, from which they obtain a Q value for the reaction of 4.67 MV. The calculated value of Q is 4.56 MV.

This process should follow the simple theory of neutron capture (B12) discussed in §64, and should have a probability inversely proportional to the velocity of the neutron. Thermal energy neutrons will be most effective. The most interesting feature of this reaction is its large cross section, measured by Mitchell (M21) to be 70×10^{-24} cm^2 for the mixed isotopes which means 900×10^{-24} cm^2 for the reaction on Li^6. This is larger than the geometrical cross section of the Li^6 nucleus by a factor of nearly 1000 and can only be understood in terms of the long associated wave-lengths of the slow neutrons and their corresponding uncertainty of position. The reaction is valuable as a detecting mechanism for slow neutrons; ionization chambers lined with Li are used (D24) to measure their numbers and relative velocities (§93D).

The process also occurs with fast neutrons, but with a much smaller probability. This results in a fast neutron "background" which is present even with Cd shielding and which must be subtracted to obtain the slow neutron effects.

Be^9: $Be^9+n^1\rightarrow He^6+He^4$

An electron radioactivity of about 1 sec. half-life which had the properties of an inert gas was reported by Bjerge (B23) to result from fast neutron bombardment of Be. Nahmias and Walen (N1) have also observed the activity, finding a period of 0.7 sec. Further work by Bjerge and Broström (B24) gives a value for the maximum of the beta-spectrum of 3.7 MV, from which a mass of He^6 is obtained relative to Li^6. The Q value for the primary reaction is then found to be -0.63 MV, requiring fast neutrons, as observed.

B^{10}: (a) $B^{10}+n^1$ (slow)$\rightarrow Li^7+He^4$
(b) $B^{10}+n^1\rightarrow H^3+He^4+He^4$

Amaldi, D'Agostino, Fermi, Pontecorvo, Rasetti and Segrè (A7) found a strong absorption of slow neutrons in B, but no gamma-radiation, indicating a heavy particle disintegration. The heavy disintegration products were observed by Chadwick and Goldhaber (C12, C16), who found doubly charged ions of up to 0.5 cm range (alphas) and also singly charged ions of longer range, and suggested the three particle reaction given above. Amaldi (A8) suggested the alternative two particle reaction to explain his observations of alphas of 5 to 10 mm range with slow neutrons. Taylor's (T2) photographic emulsion technique has shown that both processes occur, that is both straight tracks and three prong forks are observed. He calculated a small negative Q for the three particle process, indicating that slow neutrons would not produce it, and checking with the observation that the total momentum of the three prongs of the forks was not equal to zero. The present mass values show a Q of 0.41 MV, so low that in order to explain the observed lengths of the tracks it is necessary to assume neutrons of several million volts energy.

The straight tracks observed by Taylor and Dabholkar (T3) were found to have a range in air of 1.14 cm, representing the combined Li^7 and He^4 ranges from reaction (a). Assuming a range-velocity relation for the Li^7 atoms they find a reaction energy of 2.25 MV. Rotblat (R16) measures an alpha-range of 0.82 cm and a Li^7 range of 0.36 cm and calculates a Q of 2.24 MV which becomes 2.43 MV with the range energy relations of §95. These results have been checked by Fünfer (F33a) who finds an alpha-range of 0.86 cm and a reaction energy of 2.52 MV. Haxel (H19a) has studied this reaction using low intensity neutron sources and finds some evidence for two groups of alphas (of 0.94 and 0.64 cm range). He calculates Q values of 2.6 and 1.7 MV, which become 2.8 and 1.8 MV with the new range energy relations, and indicates an excitation state of Li^7 at 0.9 MV. The low intensity and consequent poor collimation possible in the experiment makes his method of extrapolation questionable; a single group of alphas of 8.5 cm range ($Q=2.55$ MV) would be a reasonable alternate interpretation.

The experimental evidence points to a reaction energy of about 2.5 MV; that calculated from mass values, however, is 2.99 MV. This is too large a discrepancy (0.5 MV) to be due to experimental errors. A possible explanation is that the transition to the ground state of Li^7 is forbidden and that the reaction leads to an excitation state in the Li^7 nucleus, with different angular momentum, for which the transition is allowed. Two pieces of experimental evidence support this interpretation. Firstly, the noncapture excitation of Li by alphas (§99A) results in gamma-radiation of about 0.4–0.6 MV, indicating such a level; the excitation energy of the compound B^{11} nucleus formed in each case is equivalent. Secondly, from proton groups in the Li^6-d-p reaction (§101B) an excitation level in Li^7 at 0.44 MV is indicated. It is probable that these values represent a single level, since only one low lying level would be expected in such a light nucleus.

Kikuchi, Aoki and Husimi (K8) have observed gamma-radiation under slow neutron bombardment with a cross section of 1/20 the total boron absorption cross section. This may represent the excitation state or may indicate a simple capture reaction.

This slow neutron reaction is even more probable than the Li^6 process, having a cross section of 3000×10^{-24} cm^2 (A11), measured by the absorption of slow neutrons in B. It is of correspondingly greater value as a slow neutron detector and has had its most successful application in the form of a large ionization chamber filled with boron trifluoride gas (C30) in which the alpha-particles are detected and counted with a linear amplifier and counter. It is also useful as a neutron absorber, following the $1/v$ dependence of cross section on neutron velocity, and in this respect differs from Cd which absorbs chiefly thermal energy neutrons and has a constant cross section with neutron velocity in that region of energies. This feature has been utilized in the methods in use for the determination of the selective energy regions responsible for induced radioactivity by neutron capture in many elements (see §60).

C^{12}: $C^{12}+n^1\rightarrow Be^9+He^4$
$C^{12}+n^1\rightarrow 3He^4+n^1$

Evidence for the fast neutron disintegration of C is based upon photographs of forks produced in cloud chambers filled with CO_2 gas. Feather (F8) has reported three such forks, and Harkins, Gans and Newson (H14) have added one more. The two product reaction is the reverse of the well-known Be^9-α-n process and is endoergic by 5.57 MV, which explains the infrequency of the process.

Another mode of disintegration is indicated by the observation of a "trident" track (three heavy particle tracks originating from the same point) by Chadwick, Feather and Davies (C8). This is interpreted as a break-up of the compound nucleus, $*C^{13}$, into three alphas and a neutron, a process well known from the $B^{11}+H^2$ reaction and also found in the Be^9-α-n process (§101A). It may be written out in detail:

$$C^{12}+n^1\rightarrow *C^{13}\rightarrow *Be^9+He^4$$
$$\rightarrow *Be^8+n^1+He^4\rightarrow 3He^4+n^1.$$

Since a neutron is a product as well as a projectile it has been referred to as a noncapture disintegration. However, in the light of the present interpretation involving compound nuclei it is better to view this as a normal alternative of the two particle reaction, yielding multiple products. The Q value is found from masses to be -7.16 MV.

N^{14}: $N^{14}+n^1\rightarrow B^{11}+He^4$

Feather (F5) first reported disintegration forks in an air filled cloud chamber and suggested the reaction. Harkins, Gans and Newson (H12), Kurie (K31) and others have also studied the reaction, which is quite probable, and have observed enough forks upon which to base statistical calculations. The measurements of energy and momentum of the tracks shows a widely varying Q value, reported as a "loss in energy" in the disintegration.

Mass values indicate a Q of -0.32 MV and excitation levels in the B^{11} nucleus have been suggested from proton groups in the B^{10}-d-p reaction at about 2 and 4 MV above the ground state. These would allow alternate Q's of -2.3 and -4.3 MV. Bonner and Brubaker (B41) have recently studied and tabulated the results from cloud chamber forks, and find that with low energy neutrons no loss in energy is indicated and an average Q of -0.3 MV is obtained. They also find several cases of excitation in which an

TABLE LX. *Evidence for n-α reactions in heavy elements.*

TARGET Z	TARGET ELEMENT	Raa El	T	CHEM. IDENTIF.	ALSO PRODUCED BY	REF.
11	Na^{23}	F^{20}	12 sec.		F-*d*-*p*, F-*n*-γ	N1
12	Mg^{26}	Ne^{23}	33 sec.	Yes	Na-*n*-*p*	A7,B24a
13	Al^{27}	Na^{24}	14.8 hr.	Yes	Na-*n*-γ, Mg-*n*-*p* Na-*d*-*p*, Mg-*d*-α	A7, K17
15	P^{31}	Al^{28}	2.36 min.		Al-*n*-γ, Si-*n*-*p* Al-*d*-*p*, Mg-α-*p*	A7
17	Cl^{35}	P^{32}	15 days	Yes	P-*n*-γ, S-*n*-*p* P-*d*-*p*, S-*d*-α	A7
19	$K^{39, 41}$	$Cl^{36, 38}$	37.5 min.	Yes	Cl-*n*-γ, Cl-*d*-*p*	H39a
21	Sc^{45}	K^{42}	12.2 hr.	Yes	K-*n*-γ, K-*d*-*p*	A7, W1
22	Ti^{48}	Ca^{45}	2.3 hr.		Ca-*n*-γ, Ca-*d*-*p*	W1
25	Mn^{55}	V^{52}	3.7 min.	Yes	V-*n*-γ, Cr-*n*-*p*	A7
27	Co^{59}	Mn^{56}	2.5 hr.	Yes	Mn-*n*-γ, Fe-*n*-*p* Mn-*d*-*p*, Cr-α-*p*	A7
30	Zn^{68}	Ni^{65}	100 min.	Yes	Ni-*n*-γ(?), Cu-*n*-*p*	M1
31	Ga^{69}	Cu^{66}	5 min.		Cu-*n*-γ, Zn-*n*-*p*	C16a
56	Ba	Xe ?	3 min.			A7
90	Th^{232}	Ra^{229}	1 min.	Yes		C60
92	U^{238}	Th^{235}	4 min.	Yes		M15

"energy loss" of about 6 MV is observed.

Chadwick and Goldhaber (C16) and Bonner and Brubaker (B36) reported particles from N on slow neutron bombardment which they at first considered to be alphas. However, energies calculated from the data on this assumption led to a serious discrepancy in the mass-energy balance, and Bonner and Brubaker (B39) have since shown that the particles are protons and so do not belong to this reaction.

O^{16}: $O^{16}+n^1 \rightarrow C^{13}+He^4$

Meitner and Phillipp (M12) observed the first disintegration of oxygen by neutrons and later reported several more forks (M13). Feather (F6) has observed and measured a total of 8 disintegrations in the cloud chamber. These have alpha-tracks of the order of 1 cm range and recoil C^{13} tracks of about 2 to 3 mm, depending on the angles and the neutron energy. From the best mass values the process is found to have a Q of -2.36 MV.

F^{19}: $F^{19}+n^1 \rightarrow N^{16}+He^4$

Harkins, Gans and Newson (H14) reported on 13 or more disintegration forks observed in a cloud chamber filled with a F gas, and suggested the reaction above, predicting a possible instability of the N^{16} product. The tracks show the characteristic loss in kinetic energy of similar reactions and can not be critically analyzed.

An estimate of the average "energy loss" in Harkins' data is 2 MV. If we choose $Q=-2$ MV to represent the ground state reaction energy we get a mass of N^{16} of 16.0113 MV. This is 4.5 MV heavier than that calculated from the beta-energy and so the full energy beta disintegration must be a forbidden transition; a gamma-ray of about 4.5 MV would be expected.

Fermi, Pontecorvo and Rasetti (F13) first observed a radioactivity of 9 sec. half-life in F by neutron bombardment and ascribed it, rather arbitrarily at that time, to this process. A second activity of 40 sec. period was found by Bjerge and Westcott (B22) with 5 percent of the intensity of the 9 sec. period. A lack of evidence of the "water effect" (increase of intensity with slowing down of the neutrons) made it difficult to determine whether either of these periods was of the *n*-γ type, or whether they belonged to the *n*-α type resulting in N^{16} and the *n*-*p* type yielding O^{19}. The F^{20} product of the *n*-γ reaction is also obtained from the F^{19}-*d*-*p* process, with a half-life of 12 sec. (C48). Nahmias and Walen (N1) found two periods, of 8.4 and 31 sec. half-life, and observed that the intensity of the short period was slightly increased with interposition of paraffin (slow neutrons) and at the same time the period increased to 8.9 sec. This is interpreted as due to two nearly equal periods, one of which is water sensitive and has a slightly longer half-life ($F^{19}+n^1 \rightarrow F^{20}$; $T \backsimeq 12$ sec.). The remaining activity comprising most of the intensity is not water sensitive and has a shorter half-life ($T \backsimeq 8.4$ sec.). From the cloud chamber evidence which indicates that the *n*-α reaction is more probable than the *n*-*p* process we can ascribe this short period to N^{16}. This leaves the weak 31 sec. period (also measured as 40 sec.) to the otherwise unobserved *n*-*p* reaction resulting in O^{19}. Further confirmation of this explanation comes from Chang, Goldhaber and Sagane (C16a) who observed the 8 sec. N^{16} period in an O-*n*-*p* reaction (producible only by very fast neutrons).

Ne^{20}: $Ne^{20}+n^1 \rightarrow O^{17}+He^4$

Cloud chamber studies by Harkins, Gans and Newson (H14) show eleven forks indicating this reaction. An "energy loss" was observed in all instances, roughly correlated with the neutron energy. Jaeckel (J1) has made a careful study of this process with some exceedingly valuable results. Although he observes an energy loss in each

case, the losses group closely around two distinct values, −0.7 and −5.3 MV. This is to be expected from the general principles involved in other type reactions, and indicates an excitation level in the O^{17} nucleus at 4.6 MV. It suggests that the other disintegrations of this type in which non-constant energy losses were observed will show similar groupings with sufficient experimental resolution. The value for the disintegration into the ground state is found from masses to be −0.58 MV, in sufficient agreement with the observed value.

Other targets.—The other reactions of this type are all inferred from electron radioactivity produced by neutrons. Fermi's laboratory is chiefly responsible for the list given in Table LX:

B. Type reaction *n-p*. (Tables LXII and LXIII)

$$Z^A+n^1\rightarrow(Z-1)^A+H^1+Q:$$

In this type of reaction the product formed is an isobar of the target and will transform back into the target element with electron radioactivity. The neutron absorbed in the primary process is 0.78 MV heavier than the combined masses of the ejected proton and the radioactive electron, so slow neutrons can cause this reaction only when the mass of the radioactive product is less than 0.78 MV heavier than the target element, in which case the induced radioactivity would be of long life and low energy. With fast neutrons the energy of the escaping proton and that of the radioactive process must be supplied (less 0.78 MV) by the kinetic energy of the neutron. In heavier elements the escaping proton must have an energy comparable with the height of the potential barrier for the reaction to have any observable probability. Thus we can expect it to occur in general only for very fast neutrons and only in the lighter elements (see Chap. X). If the neutron and proton energies could be accurately determined and good measurements made on the radioactive energy, this would be an ideal reaction for checking the beta-ray theory, since the *p-n* mass difference is well known.

The identification has been accomplished chiefly through the induced radioactivities, with the assistance of chemical analysis or correlating activities from other processes.

TABLE LXI. *Summary of n-α type reaction.*

TARGET		PRODUCT	Q(MV)	Q(MV)	REFERENCE	RESONANCE	EXCIT. LEVELS	CROSS SECTION IN
Z	El	El	(CALC.)	(OBS.)		LEVELS (MV)	(MV)	10^{-24} CM²
3	Li^6	H^3	4.56	4.67	L32			900
4	Be^9	He^6	−0.63	obs.	B24			
5	B^{10}	Li^7	2.99	2.43	R16		0.5	3000
	B^{10}	He^4+He^3	0.41	obs.	T2			
	B^{11}	Li^8	−6.6					
6	C^{12}	Be^9	−5.57	obs.	F8			
	C^{12}	$2He^4+n^1$	−7.16	obs.	C8			
	C^{13}	Be^{10}	−3.75					
7	N^{14}	B^{11}	−0.32	−0.3	B41		~6	
	N^{15}	B^{12}	<−8.0					
8	O^{16}	C^{13}	−2.36	obs.	F6			
9	F^{19}	N^{16}	−2*	−2	H14			2.5
10	Ne^{20}	O^{17}	−0.58	−0.7	J1		4.6	
	Ne^{21}	O^{18}	1.0					
11	Na^{23}	F^{20}	<−2.8	obs.	N1			
12	Mg^{24}	Ne^{21}	−2.3					
	Mg^{25}	Ne^{22}	0.2					
	Mg^{26}	Ne^{23}	—	obs.	A7			
13	Al^{27}	Na^{24}	−2.3	obs.	A7			
14	Si^{28}	Mg^{25}	−2.0					
	Si^{29}	Mg^{26}	1.7					
	Si^{30}	Mg^{27}	−3.6					
15	P^{31}	Al^{28}	−0.8	obs.	A7			
16	S^{32}	Si^{29}	0.7					
17	Cl^{35}	P^{32}	1.3	obs.	A7			
etc.								

* Q (observed) used to calculate mass values.

Li^6?: $Li^6+n^1 \rightarrow He^6+H^1$

Knol and Veldkamp (K20, V8) have reported the observation of an electron radioactivity in Li under n bombardment. Using a rotating wheel method they measure the half-life to be 0.8 sec. In their report they assumed the activity to come from the reaction: $Li^7+n^1 \rightarrow Li^8+\gamma$, since Li^8 was known at that time to be produced in the Li^7-d-p reaction with a period of about 0.5 sec. If the reaction is produced by slow neutrons the reaction is doubtless the one they suggest; however, they apparently did not search for a fast neutron effect. Subsequently Bjerge and Bronström (B24) and Nahmias and Walen (N1) have identified a radioactive He^6 as a product of the Be^9-n-α reaction and find a half-life of 0.7 sec. This suggests that the activity observed by Knol and Veldkamp may be due to He^6, produced from Li^6 following this type reaction. The simple capture process is less probable than the n-p process for such a light element (see §57). This feature, plus the coincidence in half-life periods, makes it seem more satisfactory to attribute the activity to this process. Using the mass of He^6 obtained from the radioactive energy of the Be^9-n-α reaction we can predict a reaction energy in this case of -2.9 MV.

N^{14}: $N^{14}+n^1 \rightarrow C^{14}+H^1$

This reaction was first observed by Kurie (K30), in an air-filled cloud chamber bombarded by fast neutrons. He found forked tracks in which one prong was long range and of the low density characteristic of protons.

Using slow neutrons Chadwick and Goldhaber (C16) measured the energy of the disintegration particles by an ionization method, and at first called them alphas. Bonner and Brubaker (B36) observed the ranges of the particles in a cloud chamber (1.06 cm) also using slow neutrons, and found that the energy indicated by the range measurement did not check with Chadwick and Goldhaber's ionization value. This led them to re-study the photographs and assign the tracks to protons (B39), in which case the Q value is found to be 0.58 MV. A recalculated value of 0.62 MV is used to obtain the mass of C^{14}. Burcham and Goldhaber (B63) have verified the mechanism by use of the photographic emulsion technique.

McMillan (Mc7) has observed the radioactivity of C^{14} produced through the C^{13}-d-p reaction, and finds the long half-life (*ca.* 3 months) and low energy electrons (*ca.* 0.3 MV) expected, as discussed in the introductory paragraphs.

The reaction probability is quite large, as would be expected for a slow neutron process, and in air filled ionization chambers used to record other slow neutron disintegration processes it results in a large "background" effect, removable by substituting a nondisintegrable gas.

Other targets.—Other processes which have been identified through their radioactivities are listed in Table LXII:

TABLE LXII. *Evidence for n-p reactions.*

Z	Target	Raa El	T	Chem. Identif.	Also produced by	Ref.
8	O^{16}	N^{16}	8 sec.		F-n-α, N-d-p	C16a
9	F^{19}	O^{19}	31 sec.			N1
11	Na^{23}	Ne^{23}	33 sec.	Yes	Mg-n-α	A7, N 1
12	Mg^{24}	Na^{24}	14.8 hr.	Yes	Al-n-α, Na-n-γ; Na-d-p, Mg-d-α	A7
13	Al^{27}	Mg^{27}	10.2 min.		Mg-n-γ, Mg-d-p	A7
14	Si^{28}	Al^{28}	2.36 min.	Yes	P-n-α, Al-n-γ; Al-d-p, Mg-α-p	A7
15	P^{31}	Si^{31}	2.4 hr.	Yes	Si-n-γ, Si-d-p	A7
16	S^{32}	P^{32}	15.0 da.	Yes	Cl-n-α, P-n-γ; P-d-p, S-d-α	A7
17	Cl^{35}	S^{35}	80 da.			A14
19	K^{39}	A^{39}?	4 min.			P11d
	K^{41}	A^{41}	110 min.		A-n-γ, A-d-p	H39a
20	Ca^{42}	K^{42}	12.5 hr.	Yes	K-n-γ, K-d-p, Sc-n-α	H39a
22	Ti	Sc	1.7 hr.; 28 hr.			W1a, P11d
24	Cr^{52}	V^{52}	3.75 min.	Yes	Mn-n-α, V-n-γ	A7
26	Fe^{56}	Mn^{56}	2.5 hr.	Yes	Co-n-α, Mn-n-γ; Mn-d-p, Cr-α-p	A7
27	Co^{59}	Fe^{59}	40 da.	Yes	Fe-d-p	L27a
28	Ni^{58}	Co^{58}	20 min.		Co-n-γ	R15
29	Cu^{65}	Ni^{65}	160 min.	Yes	Ni-n-γ, Zn-n-α	O½
30	Zn^{64}	Cu^{64}	12.8 hr.	Yes	Cu-n-γ, Cu-d-p; Zn-d-α, Ni-p-n	A7
	Zn^{66}	Cu^{66}	5 min.	Yes	Cu-n-γ	B21, A7, F16

C. Type reaction n-γ. (Tables LXIV and LXV)

$$Z^A+n^1 \rightarrow Z^{A+1}+h\nu:$$

This type reaction, known as "simple capture" of the neutron, was discovered by Fermi, *et al.* (F13) through the radioactivity induced in many substances, and the identification of the radioactive element as an isotope of the target. If the product nucleus of the primary reaction exists the reaction must be exoergic by an amount approximately equal to the binding energy of the neutron (5 to 10 MV), which energy is given off in the form of gamma-radiation. Since there is no emission of charged particles it can occur for heavy elements with even higher probability than for light ones, since heavy nuclei possess many closely spaced resonance levels (see Chap. X).

The product nucleus may be either radioactive

TABLE LXIII. *Summary of n-p type reaction.*

TARGET		PRODUCT	Q(MV)	Q(MV)	REFERENCE	RESONANCE	EXCIT. LEVELS	CROSS SECTION IN
Z	El	El	(CALC.)	(OBS.)		LEVELS (MV)	(MV)	10^{-24} CM²
3	Li^{6}	He^{6}	−2.9	obs.?	K20			
5	B^{10}	Be^{10}	0.41					
6	C^{12}	B^{12}	<−12.8					
7	N^{14}	C^{14}	0.62*	0.62	B39			11.3
8	O^{16}	N^{16}	−9.7					
9	F^{19}	O^{19}	—	obs.	N1			
10	Ne^{20}	F^{20}	<−4.2					
11	Na^{23}	Ne^{23}	—	obs.	N1			
12	Mg^{24}	Na^{24}	−3.9	obs.	A7			
13	Al^{27}	Mg^{27}	−1.4	obs.	A7			
14	Si^{28}	Al^{28}	−2.7	obs.	A7			
15	P^{31}	Si^{31}	−1.0	obs.	A7			
16	S^{32}	P^{32}	−0.9	obs.	A7			
17	Cl^{35}	S^{35}	—	obs.	A14			
etc.								

* *Q* (observed) used to calculate mass values.

or stable. In the first case the radioactivity is used as an indicator of the process, in the second the occurrence of the reaction may be inferred from an observed absorption of neutrons (as in Cd). With fast neutrons the probability is small, but observable (§65). When the neutrons are slowed down by the interposition of paraffin or other light materials the intensity of the observed activity is increased. This increase was found by Fermi to be as much as 40 times in some substances. The activities observed with fast neutrons (no water or paraffin) are probably in some part due to the slow neutrons at all times present in the beam, produced by scattering in the target and adjacent materials. Since the reactions with slow neutrons yielding particle products are in general not probable in heavy elements the observation of a "water sensitive" activity is taken to be strong evidence for this type of reaction.

The reaction energy of the primary process is equal to the binding energy of the neutron in the product nucleus, and must appear in the form of gamma-radiation. This may be emitted in a single gamma-ray, or more probably, as several successive rays determined by the arrangement of energy levels in the product nucleus (§90). Certain of these processes have been found by Rasetti (R3), Kikuchi (K6 *et seq.*) and Fleischmann (F25) to result in gamma-radiation, and measurements on the average energy made. This capture radiation may be confused with that due to a noncapture excitation of the nucleus, discussed in a later section of this paper. Where actual observations of the gammas are available, it is so indicated in the table to follow.

The increased activity due to paraffin indicated that the neutrons most effective in this process were of thermal energies. Experiments with absorbers mounted on a rotating wheel (R4) and with neutrons slowed down in scatterers at liquid-air temperatures proved that this was the case. Cd was found to absorb these thermal neutrons although it was not rendered radioactive in the process; it was found to have an absorption coefficient essentially constant throughout the thermal energy region.

The discovery of the selective absorption of neutrons of different energies in various targets by Moon and Tillman (M26) initiated a new field of research and has led to a most promising theoretical interpretation. These experiments were followed by others by Szillard (S29) and by Amaldi and Fermi (A11) who separated the neutron groups of different energies responsible for the residual activity (Cd filtered) in several elements. To give an example of this effect: the activity in Ag (22 sec.) caused by slow neutrons is reduced to about $\frac{1}{3}$ by interposing a Cd absorber; this residual activity may be largely suppressed by Ag absorbers, but to a much smaller degree by other elements such as Rh and Hg; using a Rh target the opposite is true, Rh absorbs the neutrons strongly while Ag and Hg do not, etc. This is interpreted as indicating regions of neutron energy, somewhat above the thermal region, selectively responsible for the activities.

TABLE LXIV. *Evidence for n-γ reactions.*

Target Z	Target El	Raa El	T	Water Sensit.	Res. Levels Chap. X	Chem. Identif.	Also produced by	COMMENTS	REF.
3	Li^{7}	Li^{8}?	0.88 sec.	>1			Li-*d*-*p*		K20
9	F^{19}	F^{20}	12 sec.	>1			Na-*n*-α, F-*d*-*p*	gammas	B21, A7, N1
11	Na^{23}	Na^{24}	14.8 hr.	>1			Al-*n*-α, Mg-*n*-*p* Na-*d*-*p*, Mg-*d*-α	gammas	A7, B21
12	Mg^{26}	Mg^{27}	10.2 min.	>1			Mg-*d*-*p*, Al-*n*-*p*	gammas	A7
13	Al^{27}	Al^{28}	2.36 min.	>1			P-*n*-α, Si-*n*-*p* Al-*d*-*p*, Mg-α-*p*	$\gamma=5.8$ MV	A7, F25
14	Si^{30}	Si^{31}	2.4 hr.	>1			Si-*d*-*p*, P-*n*-*p*	gammas	A7
15	P^{31}	P^{32}	15 da.				Cl-*n*-α, S-*n*-*p* P-*d*-*p*, S-*d*-α		P15
17	Cl^{37}	Cl^{38}	37 min.	>1			Cl-*d*-*p*, K-*n*-α	$\gamma=6.6$ MV	A3, A7, R3
18	A^{40}	A^{41}	110 min.				A-*d*-*p*, K-*n*-*p*		S15
19	K^{41}	K^{42}	12.2 hr.	>1			Sc-*n*-α, K-*d*-*p*	gammas	A7, W1
20	Ca^{44}	Ca^{45}	2.4 hr.	>1			Ca-*d*-*p*, Ti-*n*-α		H29, W1
21	Sc^{45}	Sc^{46}	(long)						H32
22	Ti^{50}	Ti^{51}	3 min.				Ti-*d*-*p*	gammas	A7
23	V^{51}	V^{52}	3.75 min.	40			Mn-*n*-α, Cr-*n*-*p*	gammas	A7
25	Mn^{55}	Mn^{56}	2.5 hr.	23	*	Yes	Co-*n*-α, Fe-*n*-*p* Cr-α-*p*, Mn-*d*-*p*	gammas	A7
27	Co^{57}	Co^{58}	11 min.	>1			Ni-*n*-*p*	$\gamma=5.0$ MV	R15, A7, R3
	Co^{59}	Co^{60}	~ 1 year	>1		Yes	Co-*d*-*p*		R9a, L27a
28	Ni^{58}	Ni^{59}	3 hr.	>1				gammas	R15, N3
29	Cu^{65}	Cu^{66}	5 min.	15	*		Zn-*n*-*p*, Ga-*n*-α	$\gamma=7.4$ MV	A7, L29, F25
	Cu^{63}	Cu^{64}	12.8 hr.	>1			Cu-*d*-*p*, Zn-*n*-*p* Zn-*d*-α, Ni-*p*-*n*	$\gamma=7.4$ MV	A7, B21
31	Ga^{69}	Ga^{70}	20 min.	3			Zn-*p*-*n*, Ga-γ-*n*	gammas	A7
	Ga^{71}	Ga^{72}	23 hr.	>1			Zn-*d*-γ(?)	gammas	A7
32	$Ge^{(70),\ 7}$	$Ge^{(71),\ 75}$	30 min.						A7, S25
33	As^{75}	As^{76}	26 hr.	6	*	Yes	As-*d*-*p*	gammas	A7
34	Se	Se^{+1}	22 min.	4			Se-*d*-*p*	$\gamma=5.8$ MV	A7, F25, H33b
35	Br^{79}	Br^{80}	18 min.	10	*	Yes	Br-*d*-*p*, Se-*p*-*n*, Br-γ-*n*	gammas	A7, J2
	Br^{79}	Br^{80}	4.2 hr.	>1		Yes	Br-*d*-*p*, Se-*p*-*n*, Br-γ-*n*	gammas	K34
	Br^{81}	Br^{82}	36 hr.?			Yes	Br-*d*-*p*, Se-*p*-*n*, Se-*d*-2*n*(?)	gammas	
37	$Rb^{85,\ 87}$	$Rb^{86,\ 88}$	20 min.				γ-*n*-α		F13
39	Y^{89}	Y^{90}	70 hr.	$\gg$1				Strong abs'n. $\gamma=4$ MV	A7, R3, H31
40	Zr^{92}	Zr^{93}	40 hr.	>1					H29
42	Mo	Mo^{+1}	25 min. 36 hr.	>1 >1					A7, Mc1, H33b
44	Ru	Ru^{+1}	40 sec. 100 sec. 11 hr. 75 hr.				Ru-*d*-*p* (39 hr., 11 da.)		K35
45	Rh	Rh^{+1}	44 sec. 3.9 min.	15 >1	** *				A7
46	Pd	Pd^{+1}	15 min. 3 min. 12 hr. 60 hr.	>1			Pd-*d*-*p* (10 hr.)		A7, Mc1, K36
47	Ag^{107}	Ag^{108}	2.3 min.	15	*		Ag-γ-*n*	$\gamma=3.7$ MV	A7, F25
	Ag^{109}	Ag^{110}	22 sec.	30	**				
48	Cd	Cd^{+1}	—— 5 hr. 52 hr.	$\gg$1 >1 >1	**		Cd-*d*-*p*	strong abs'n. $\gamma=4.1$ MV	A7, F25 M20a
49	In^{113} In^{115}	In^{114} In^{116}	13 sec. 54 min. 3 hr.	15 >1	** **		Cd-*p*-*n*, Sn-*n*-*p*		A7, S28
50	Sn	Sn^{+1}	8 min.				Sn-*d*-*p*		N3
	Sn^{112}	Sn^{113}	18 min.				Sn-*d*-*p*, In-*p*-*n*		N3
51	$Sb^{121,\ 123}$	$Sb^{122,\ 124}$	2.5 da. 60 da.	>1			Sb-*d*-*p*	gammas	A7, L27b
52	Te	Te^{+1}	45 min.	>1			Te-*n*-2*n*, Te-γ-*n*		A7
53	I^{127}	I^{128}	25 min.	5	**	Yes		gammas	A7
55	Cs^{133}	Cs^{134}	1.5 hr.	>1					A7, L3

* Resonance energy determined.
** Energy and width of resonance level determined.

TABLE LXIV.—*Continued.*

Target Z	Target El	Raa El	T	Water Sensit.	Res. Levels Chap. X	Chem. Identif.	Also produced by	COMMENTS	REF.
56	Ba	Ba^{+1}	80 min.	8			Ba-*d*-*p*		A7, A8
57	La^{139}	La^{140}	1.9 da.	12			La-*d*-*p*		M7, H31
59	Pr^{141}	Pr^{142}	19 hr.				Nd-*n*-*p*		A7, H30
60	Nd	Nd^{+1}	1 hr.						A7, H30
62	Sm	Sm^{+1}	40 min. 2 da.					Very strong abs'n. $\gamma = 3.3$ MV	A7, H30, F25 H31a
63	Eu	Eu^{+1}	9.2 hr.	40				Very strong abs'n. $\gamma = 4.0$ MV	S25, M7, H31
64	Gd	Gd^{+1}	8 hr.	>1				*Very strong* abs'n.	A7, H30, F25
65	Tb^{159}	Tb^{160}	3.9 hr.						H30, M7, S25
66	Dy^{164}	Dy^{165}	2.5 hr.	20					H30, M7
67	Ho^{165}	Ho^{166}	35 hr.	15					H31a, M7, Mc3
68	Er	Er^{+1}	5.8 min. 12 hr.						Mc3, S25, H31a
69	Tm^{169}	Tm^{170}	8 mo.						C61
70	Yb	Yb^{+1}	3.5 hr.						H30, M7, S25
71	Lu^{175}	Lu^{176}	3.6 hr. 6 da.						H31, M7, Mc3
72	Hf^{180}	Hf^{181}	*ca.* mo.						H29
73	Ta^{181}	Ta^{182}	(200 da.)						F27
74	W	W^{+1}	23 hr.	15				gammas	A7, Mc1
75	Re	Re^{+1}	20 hr. 85 hr.	>1	*				A7, K36
76	Os	Os^{+1}	40 hr.						K36
77	Ir	Ir^{+1}	19 hr. 2 mo. 50 min. 3 da.	>1	**	Yes	Pt-*d*-α, Pt-*n*-*p* Au-*d*-α, *p*	$\gamma = 3.3$–4.4MV	A7, 3R, S20, F27
78	Pt	Pt^{+1}	50 min.	>1			Pt-*d*-*p*		A7, Mc1
79	Au^{197}	Au^{198}	2.7 da.	>1	**	Yes	Au-*d*-*p*	gammas	A7
80	Hg	Hg^{+1}	40 hr.	>1				absorption $\gamma = 4.5$ MV	A7, R3, A13, F25
81	Tl	Tl^{+1}	1.3 hr. 4 min.						P15, Mc2
90	Th	Th^{+1}	25 min.	>1		Yes		New Raa Series	C60
92	U^{238}	U^{239}	——	>1		Yes		New Raa elements with $Z > 92$	A7, M15

The true significance of these selective effects has been realized in the theory of Breit and Wigner (B51) in which they are interpreted as "resonance" effects. Bohr (B32) has formulated a nuclear model which extends the interpretation to other type reactions. On this picture the compound nucleus formed from the original nucleus and the entering neutron may exist in a variety of quasi-discrete excitation states, becoming more closely spaced for heavy nuclei. The states above the dissociation energy will correspond to definite neutron energies, so these neutrons are selectively absorbed. The probability of re-emission of a slow neutron from this excited nucleus (scattering) is extremely small compared with the probability of radiation of energy to form a normal nucleus (capture). This would predict resonance capture of neutrons of certain definite energies in a particular nucleus; these resonance levels would be in general closer spaced and therefore closer to zero energy in heavier nuclei. Bethe and Placzek (B15) have calculated the probability of neutron capture due to these levels and have shown how the widths and spacings of these levels may be determined from experiment.

A method for the measurement of the neutron energies responsible for these selective effects was suggested by Frisch and Placzek (F33), and independently by Weekes, Livingston and Bethe

(W5). In this method the $1/v$ dependence of capture probability in the B^{10}-n-α process was used to determine the neutron velocities responsible, compared to the known velocities of thermal neutrons. Goldsmith and Rasetti (G17) have measured such resonance levels for many elements, and find values ranging from fractions of a volt to 100 volts. These values probably represent the resonance level nearest zero or some average of the low levels (cf. §60). Other methods for measuring resonance energies have been presented, such as Fermi's technique of determining the "age" of the slow neutron through the thickness of water required to give the highest intensity of this residual activity (§59D). The results of all these measurements are presented in Table XXII of §60, with corrections for scattering.

H^1: $H^1+n^1\rightarrow H^2+\gamma$

Lea (L19) has observed gamma-radiation from many elements under neutron bombardment, explaining it as due to inelastic scattering, i.e., noncapture excitation of the nucleus by fast neutrons. See §65. In paraffin Lea observed such gamma-radiation, from the hydrogen. The elementary nature of the proton makes noncapture excitation seem impossible and it is assumed that the radiation comes from the synthesis of H^2. This is the reverse of the photoelectric disintegration of the deuteron which is known to require 2.20 MV (see §103), so this process should be exoergic by this amount. The gammas have been tentatively measured by Lea as 2 to 4 MV, by Fleischmann (F25) to be 2.26 MV and by Kikuchi, Aoki and Husimi (K6) to be 2.2 MV. The probability of the process has been calculated (§17) and has been shown to be very small for fast neutrons and fairly large for slow ones. With slow neutrons it is the only known method of ultimate absorption in hydrogen, and it can be assumed that only slow neutrons are effective.

Other targets.—In Table LXIV are listed the processes of the n-γ type which have been identified through the radioactivity induced by or the strong absorption for slow neutrons.

In Table LXIV are certain features of particular interest. The observed activities are spread uniformly throughout the atomic table with the exception of the lighter elements. They are found for as many as 64 of the known elements, suggesting that the lack of evidence for the other elements is probably due to experimental difficulties such as extremely long or short periods or low intensities. In many instances two or more activities of different half-lives have been observed, indicating processes from two or more isotopes. In practically all these cases the stable isotopes are known to be spaced two mass units apart. In addition to the activities the list contains 6 elements, Y, Cd, Sm, Eu, Gd and Hg, for which the absorption of slow neutrons is so great that although they show no strong radioactivities the reaction must be assumed to occur leading to stable isotopes. The expected gamma-radiation is observed in most of these cases.

Several reactions are marked with a question, indicating incomplete evidence. In Li^7 the evidence is insufficient to determine whether the activity is due to this type reaction or the n-p reaction (see §101B), for which the half-life value is essentially the same. Other questionable cases are due to insufficient chemical evidence or observations of the water sensitivity. The complex activities found in U and Th will be more fully discussed in §105.

D. Type reaction n-$2n$: $Z^A+n^1\rightarrow Z^{A-1}+2n^1$ (Table LXVI)

This reaction has been assumed in several instances to explain the observation of more discrete half-life periods due to isotopes of the target element than the known number of stable isotopes. The earliest positive proof was the observation by Heyn (H33, H33a) of positron activity chemically analyzed as the target element in Cu and Zn after neutron bombardment indicating a light isotope. It has also been suggested by Rusinow (R20) to explain an increase in the total number of neutrons (as indicated by total intensity of radioactivity produced) when a neutron source is surrounded by Be. Such reactions require fast neutrons and should not be invoked, as has been done in some instances (J2), to explain an excessive number of slow neutron activities; these require another explanation, in terms of isomeric nuclei (see §105).

This reaction amounts in effect to a noncapture disintegration of the target element, but its mechanism is no doubt analogous to the usual reactions (§85). The n-$2n$ reaction leads to an

TABLE LXV. *Summary of n-γ type reaction.*

TARGET		PRODUCT	Q(MV)	Q(MV)	REFERENCE	RESONANCE	EXCIT. LEVELS	CROSS SECTION IN
Z	El	El	(CALC.)	(OBS.)		LEVELS (MV)	(MV)	10^{-24} CM²
1	H^1	H^2	2.20	2.26	F25			
	H^2	H^3	6.19					
3	Li^6	Li^7	7.12					
	Li^7	Li^8	>2.0	obs.?	K20			
4	Be^9	Be^{10}	6.80					
5	B^{10}	B^{11}	11.51					
	B^{11}	B^{12}	>1.9					
6	C^{12}	C^{13}	5.0					
	C^{13}	C^{14}	8.3					
7	N^{14}	N^{15}	10.78					
	N^{15}	N^{16}	2.4					
8	O^{16}	O^{17}	4.15					
9	F^{19}	F^{20}	>4.0	obs.	N1			
10	Ne^{20}	Ne^{21}	7.54					
	Ne^{21}	Ne^{22}	9.32					
11	Na^{23}	Na^{24}	7.2	obs.	A7			4.2
12	Mg^{24}	Mg^{25}	7.0					
	Mg^{25}	Mg^{26}	11.9					
	Mg^{26}	Mg^{27}	6.2	obs.	A7			3.5
13	Al^{27}	Al^{28}	8.0	obs.	A7			1.5
14	Si^{28}	Si^{29}	8.4					
	Si^{29}	Si^{30}	11.5					
	Si^{30}	Si^{31}	5.6	obs.	A7			2.5
15	P^{31}	P^{32}	8.5	obs.	P15			14.7
17	Cl^{37}	Cl^{38}	5.6	obs.	A7			39.
18	A^{40}	A^{41}	—	obs.	S15			
19	K^{41}	K^{42}	—	obs.	A7			8.2
etc.								

isotope of the target element of lower mass number and so results in the same product as the γ-n reaction. Observation of the same period produced by gamma-rays and by fast neutrons (but not by slow neutrons) indicates this type reaction.

Pool, Cork and Thornton (P11d) have studied the radioactivity produced in some 60 targets by the high energy neutrons from the Li-d-n reaction, using the 6.3 MV deuterons from the cyclotron. They observe some 113 radioactive periods and make many assignments to the isotopes responsible. Four of the activities (Al, Cl, Mn and Co targets) can be definitely ascribed to n-α reactions, through chemical analysis and recognition of known half-life periods, and are entered in §102A. Twelve or thirteen are n-p reactions (§102B). Of the remainder, many are found to have periods identical with known slow neutron (n-γ) periods, in some instances from targets known to have only one isotope (i.e., V^{52}, Mn^{56}, Y^{90}, I^{128} etc.). This suggests that the n-γ reaction is responsible for a large share of the unidentified activities isotopic with the target element especially since slow neutrons are always present in the bombardment. There are many other activities, however, which can only be ascribed to the n-$2n$ reaction, through recognition of a known period, the observation of a new period isotopic with the target and not found with slow neutrons, etc. In some instances the period is also observed in a γ-n reaction. Most of these are positron active. In Table LXVI are listed those for which the evidence seems sufficient to justify designation of this type reaction. (Activities reported by other observers are included in the table.) Those activities for which there is not sufficient evidence to include in this table are not listed under a primary reaction but only as activities (usually under the target element) in the tabulation of induced radioactivities (Table LXIX).

The most conclusive evidence for the n-$2n$ type reaction is through the technique used by Heyn (H33a) and others of using neutrons of different maximum energy from several reactions (H^2-d-n, Be-d-n, Li-d-n, etc.). An observation of a new period with very fast neutrons (Li-d-n) but not with slower neutrons (H^2-d-n),

TABLE LXVI. *Evidence for n–2n reactions.*

Target Z	Target El	Raa El	T	Raa	Comments	Refs.
4	Be^{9}	Be^{8}	—	—	Increase in number of n's	R20
6	C^{12}	C^{11}	20 min.	e^+	Known T	P11d
7	N^{14}	N^{13}	10.5 min.	e^+	Known T	P11d
8	O^{16}	O^{15}	2.1 min.	e^+	Known T	P11d
9	F^{19}	F^{17}	1.2 min.	e^+	Known T, (F^{19}-n-$3n$)	P11c
	F^{19}	F^{18}	108 min.	e^+	Known T, chem.	P11d
14	Si^{28}	Si^{27}	6 min.	e^+	Known T	P11d
15	P^{31}	P^{30}	3 min.	e^+	Known T	P11d
16	S^{32}	S^{31}	26 min.	e^+	New T, best assignment	P11d
17	Cl^{35}	Cl^{34}	33 min.	e^+	Known T, chem.	P11c
19	K^{39}	K^{38}	7.5 min.	e^+	Known T	P11d
20	Ca^{40}	Ca^{39}	4.5 min.	e^+	New T, best assignment	P11d
21	Sc^{45}	Sc^{43}	4 hr.	e^+	Known T, (Sc^{45}-n-$3n$)	P11c, P11d
	Sc^{45}	Sc^{44}	52 hr.	e^+	Known T	P11c, P11d
28	Ni^{58}	Ni^{57}?	2 hr.		Fast n's only	H33a, P11d
29	Cu^{63}	Cu^{61}	3.5 hr.	e^+	Known T, (Cu^{63}-n-$3n$)	P11c
	Cu^{63}	Cu^{62}	10.5 min.	e^+?	Known T (Cu-γ-n), fast n's	C16a, H33a, R16a
30	Zn^{64}	Zn^{63}	40 min.	e^+	Known T (Zn-γ-n), chem.	P11d, H33a, R16a
31	Ga^{69}	Ga^{68}	55 min.	e^+	Known T (Ga-γ-n?), chem.	C16a, P11d
33	As^{75}	As^{74}?	13 da.		New T, best assignment	P11d
34	Se^{80}	Se^{79}?	56 min.	e^-	Fast n's only, chem.	H33b, P11d
35	Br^{79}	Br^{78}	5 min.	e^+	Known T (Br-γ-n)	C16a, P11d, H33b
37	Rb^{85}	Rb^{84}?	22 hr.	e^-	New T, best assignment	P11d
38	Sr^{86}	Sr^{85}?	3 hr.	e^+	New T, chem.	P11d
42	Mo^{92}	Mo^{91}?	17 min.	e^-	Known T (Mo-γ-n)	H33b, P11d
47	Ag^{107}	Ag^{106}	25.5 min.	e^+	Known T (Ag-γ-n)	R16a, P11d; C16a, H33b
48	Cd^{110}	Cd^{109}?	33 min.	e^+	Fast n's only	H33b, P11d
49	In^{113}	In^{112}	1.1 min.	e^-	Known T (In-γ-n)	C16a, P11d
51	Sb^{121}	Sb^{120}	15.4 min.	e^+	Known T (Sb-γ-n, Sn-d-n)	C16a, P11d; H33b, L27b
52	Te^{128}	Te^{127}?	1.1 hr.	e^-	Known T (Te-γ-n)	H33b, P11d
57	La^{139}	La^{138}?	2.2 hr.		New T, best assignment	P11d
59	Pr^{141}	Pr^{140}?	3 min.	e^+	New T, best assignment	P11d, H31a
79	Au^{197}	Au^{196}	17 min.		New T, best assignment	P11d
80	Hg^{198}	Hg^{197}	45 min.	e^-	New T, fast n's only	H33b, P11d
92	U^{238}	U^{237}?	40 sec.?	e^-	Too many U activities	M15

and chemical analysis of the radioactive isotope, make the assignment definite.

In line with the theoretical suggestions of Bohr that "cascade" disintegrations are probable with sufficiently high excitation energy, Pool, Cork and Thornton (P11c) have found evidence for a reaction of the type n-$3n$ in Sc, in which the known Sc^{43} period was found to be produced by neutrons of >8 MV bombarding the Sc^{45} target. They suggest the same explanation for the F^{17} and Cu^{61} activities. These are also listed in Table LXVI.

E. Excitation without capture

Experiments by Ehrenberg (E1), Fermi (F17), Lukirsky and Careva (L37) and others on the slowing down of fast neutrons in heavy elements such as Pb indicate an energy absorption in excess of that expected from elastic scattering (§65). Furthermore, gamma-radiation has been observed by Lea (L19), Kikuchi, Aoki and Husimi (K11), and others to come from all elements under fast neutron bombardment, and with intensities much greater than that associated with the observed activities representing capture. Part of the radiation is no doubt due to the simple capture processes, but the larger share must be interpreted as due to noncapture excitation, or inelastic scattering. Bohr's theory is more definite than experiments on this point and predicts more inelastic than elastic collisions for neutrons with heavy nuclei. Many excitation states and a complexity of the radiation are to be expected. Further evidence for the production of excitation radiation is in the observation by Kikuchi, Aoki and Husimi (K12) of high energy electrons from all substances when bombarded by neutrons. These are most readily interpreted as

secondary electrons from this radiation, and not from the break-up of the neutron into proton and electron in nuclear fields as was suggested by Kikuchi, *et al.*

§103. Photoelectric Disintegration

Type reaction γ-n: $Z^A+h\nu\rightarrow Z^{A-1}+n^1$ (Tables LXVIa and LXVII)

With two of the light elements (*viz.* H^2 and Be^4) this type of disintegration can be produced by the natural gamma-rays from Th C″. All other nuclei, as far as is known, require more energetic gamma-rays and in all cases except the two mentioned, the gamma-rays of 17.5 MV from the capture of protons by Li^7 have been used. It should occur with gamma-energies equal to or greater than the binding energy of the neutron in the nucleus (see Table XLVII).

Gamma-rays may also produce other type reactions, particularly in heavy nuclei. With comparatively low energy gamma-rays (6–8 MV) there may result the splitting off of an alpha-particle, while with very energetic gamma-rays a cascade disintegration may take place in which a neutron and an alpha-particle or two neutrons may be emitted in succession (§101D).

The cross section for most photoelectric disintegrations seems to be of the order of 10^{-27} cm^2 (B47c) in agreement with theoretical expectations (§91).

H^2: $H^2+\gamma\rightarrow H^1+n^1$

Chadwick and Goldhaber (C14) discovered the effect experimentally using Th C″ gamma-rays of 2.62 MV energy, by measuring the ionization produced by the protons released. If the proton energy is doubled (to include the equal neutron energy) and subtracted from 2.62 MV, the value obtained for the Q of the reaction and hence the binding energy of the neutron in H^2 is -2.16 MV. In a report before the British Association, Feather (F9) gives what seems to be a better value of proton range, and obtains a Q of -2.26 MV. When this is corrected for the range energy relations used it becomes -2.23 MV.

Chadwick and Goldhaber and also Banks, Chalmers and Hopwood (B3) observed neutrons using radium gammas on H^2. More careful work by Mitchell, Rasetti, Fink and Pegram (M22) with radium sources shows a neutron intensity so low that it can only be separated from neutrons produced in the glass containers with some difficulty. The neutrons show the very low energy expected. The highest energy gamma-rays from Rn are from Ra C, of 2.198 MV energy (E8), which is lower by 0.03 MV than the Q value obtained from the Th C″ gammas. Although this is only slightly outside the errors of Feather's experiment it is significant in that this binding energy value determines the relative masses of H^1 and n^1. Either the experimental evidence with radium gammas is spurious or Feather's results are incorrect by this amount. We feel it necessary to compromise with these experiments by choosing the value -2.20 MV for the binding energy.

Knowledge of the binding energy of the deuteron is of great theoretical importance. It is used to calculate the neutron mass from the mass spectroscopic values of H^2 and H^1, and the n^1-H^1 mass difference so obtained (0.78 MV) will be of vital importance in theories of the elementary particles. The binding energy is also invaluable in the determination of n-p forces in nuclei and in interpreting the results of scattering experiments. Bethe and Peierls (B10), Hall (H11) and others have calculated the probability cross section of the reaction and find results in accord with the experiments. Breit and Condon (B52) have shown that from studies of the cross section at higher energies the nature of the forces between proton and neutron (exchange *vs.* ordinary) and the range of such forces can be easily inferred.

Richardson and Emo (R6a) have reported on the photoelectric disintegration of H^2 with the radioactive gamma-rays from Na^{24}. They use the observed proton energies (0.30 MV) to determine the gamma-ray energy, which proves to be 2.8 MV. The cross section at this energy is found to be 1×10^{-27} cm^2. This result suggests the use of this method as a method for measurement of gamma-ray energies.

Be^9: $Be^9+\gamma\rightarrow Be^8+n^1$

This process was discovered by Szilard and Chalmers (S26) and studied more thoroughly by Chadwick and Goldhaber (C14). They determined the energy of gamma-ray required to produce the disintegration by measuring the maximum energy of He recoils from the neutrons in a

cloud chamber. From these observations they find a Q of -1.6 MV. The value calculated from masses is -1.72 MV.

Radium gamma-rays produce neutrons through this process, both the 1.761 and 2.198 MV radiations being effective. The neutrons have lower energy than those from Th C″ gammas, as shown by Mitchell, Rasetti, Fink and Pegram (M22) and others. Studies of the reaction probability with different gamma-energies have been made by Fleischmann and Gentner (F24), etc.

The reaction has also been observed with x-rays of energy less than 2 MV (B48) through the neutron induced radioactivity.

Goloborodko and Rosenkewitsch (G18b) study the angular distribution and find it to be isotropic.

Table LXVIa contains the results obtained with the gamma-rays from the Li-p-α reaction. Most of these data have been obtained by Bothe and Gentner (B47b, B47c, B47d). Some of the activities observed have been confirmed in the Cavendish Laboratory by Chang, Goldhaber and Sagane (C16a) and additional activities found. In some instances the activity is the same as that produced by neutrons, which is valuable in that it allows identification of the active isotope in certain instances (cf. §105).

§104. Disintegrations by Other Particles and Radiations

Disintegrations by Li ions

If Li ions bombard a hydrogen-containing substance the same disintegration should be observed as for protons bombarding Li, with a probability determined by the relative velocity of the two ions: $H^1+Li^7 \rightarrow He^4+He^4$. Zeleney, Brasefield, Bock and Pollard (Z1) first observed this expected result with Li ions of 240 kv energy. This is equivalent to proton bombardment by 34 kv protons, which is known to be observable. Kinsey (K13) used Li ions of 1 MV (143 kv protons) and found large intensities of the expected 8 cm alphas, from all targets, due to the hydrogen impurities present, but found no indication of any other type of disintegration using Li and Be targets.

Whitmer and Pool (W14) reported alphas and neutrons from bombardment of Li by Li ions of 120 kv energy. As indicated by the results of Kinsey these observations are spurious.

Coates (C17) reports studies of the effects of bombardment of various targets with 2.8 MV Hg^{++} ions obtained with the "linear accelerator" of Sloan and Coates (S13). He finds characteristic x-rays in low intensities but no evidence for disintegration, as expected.

A search for radioactivity produced by high speed electrons is reported by Livingood and Snell (L25) to give negative results. Thomson and Saxton (T9) find no radioactivity to be produced by positrons.

Disintegrations by cosmic rays

The production of "showers" by certain components of the cosmic radiation has been studied by many investigators using cloud chambers, coincidences between three or more counters, etc. Certain arguments indicating that these showers may be due to nuclear disintegrations have been advanced, but the most probable explanation is that they are due to a multiplication of the complementary processes of pair production and radiative energy loss of the electrons and positrons formed (C1). In addition to showers, however, Anderson and Neddermeyer (A12) have observed many heavy particles, usually ejected from Pb by nonionizing radiation. These may well be interpreted as due to disintegration processes. It is known that high energy gamma-radiation does produce particle disintegration of certain of the lighter elements, and since in the secondary or tertiary products of the degradation of cosmic radiation there are large intensities of high energy gamma-rays, it is to be expected that similar disintegrations will be produced. Neutrons may also accompany cosmic radiation, possibly themselves produced through disintegration processes. It is to be expected that such heavy-particle tracks will be directly attributable to neutron recoils and to disintegrations.

§105. Induced Radioactivity

The phenomenon of induced radioactivity is among the most striking of recent developments in nuclear physics and has done much to clarify concepts regarding the constitution and stability of nuclei. At the time of its discovery in January of 1934 by Curie and Joliot (C54) the field of

TABLE LXVIa. *Evidence of γ-n reactions in heavy elements.*

TARGET		PROD. EL	T	Raa PARTICLE	REF.	OTHER EVIDENCE
Z	El					
1	H^2	H^1	—		F9	
4	Be^9	Be^8	—		C14	
8	O^{16}	O^{15}	2.1 min.	e^+	C16a	$T(O^{15})=126$ sec.
15	P^{31}	P^{30}	2–3 min.		B47b	$T(P^{30})=2.5$ min.
29	Cu^{63}	Cu^{62}	10.5 min.	e^+	B47b, C16a	Chem., Cu-n-2n, Co-α-n ($T=10.5$ min.)
30	Zn^{64}	Zn^{63}	38 min.	e^+	B47d, C16a	Zn-n-2n, Ni-α-n ($T=40$ min.)
31	Ga^{69}	Ga^{68}	60 min.	e^+	B47d	Ga-n-2n, Ga-n-γ ($T=20$ min., 23 hr.)
	Ga^{71}	Ga^{70}	20 min.	e^-	C16a	
35	Br^{79}	Br^{78}	5 min.		B47c	Chem. Br-n-γ ($T=18$ min., 4.2 hr., 36 hr.); Br-n-2n ($T=5$ min.)
	Br^{81}	Br^{80}	18 min., 4.2 hr.	e^-	C16a, B47e	
42	Mo^{92}	Mo^{91}	17 min.		B47d	Mo-n-2n ($T=21$ min.)
47	Ag^{107}	Ag^{106}	24 min.		B47c, B47c, C16a	Ag-n-γ ($T=22$ sec., 2.3 min.); Ag-n-2n ($T=25.5$ min.)
	Ag^{109}	Ag^{108}	2.3 min.	e^-		
49	In^{113}	In^{112}	1 min.		B47d, C16a	In-n-2n ($T=1$ min.)
51	Sb^{121}	Sb^{120}	13 min.	e^+	B47c, C16a	Sn-d-n, Sb-n-2n ($T=13$ min.)
52	$Te^{128, 130}$	$Te^{127, 129}$	60 min.		B47d	Te-n-γ ($T=45$ min.)
73	Ta^{181}	Ta^{180}	15 min.		B47d	Only one stable Ta isotope

TABLE LXVII. *Summary of γ-n type reaction.*

TARGET		PRODUCT EL	Q(MV) (CALC.)	Q(MV) (OBS.)	REFERENCE	RESONANCE LEVELS (MV)	EXCIT. LEVELS (MV)	CROSS SECTION IN 10^{-24} CM^2
Z	El							
1	H^2	H^1	− 2.20*	−2.20	F9			6.6×10^{-4}@2.62
2	He^4	He^3	−20.61					
3	Li^7	Li^6	− 7.12					
4	Be^9	Be^8	− 1.72	−1.6	C14			$>1\times10^{-4}$@2.62
	Be^9	$2He^4$	− 1.59					
5	B^{11}	B^{10}	−11.51					
6	C^{12}	C^{11}	−18.85					
7	N^{14}	N^{13}	−10.71					
8	O^{16}	O^{15}	−15.61					
9	F^{19}	F^{18}	− 4.0	Obs.	C16a			
10	Ne^{21}	Ne^{20}	− 7.54					
	Ne^{22}	Ne^{21}	− 9.32					
11	Na^{23}	Na^{22}	−12.2					
12	Mg^{25}	Mg^{24}	− 7.0					
	Mg^{26}	Mg^{25}	−11.9					
13	Al^{27}	Al^{26}	−11.1					
14	Si^{28}	Si^{27}	−14.4					
	Si^{29}	Si^{28}	− 8.4					
	Si^{30}	Si^{29}	−11.5					
15	P^{31}	P^{30}	−12.0	Obs.	B47b			

* Q (observed) used to calculate mass values.

nuclear physics was so well developed that many laboratories were immediately able to repeat and extend their observations. Sources to produce it and instruments capable of detecting it had been in existence for many years. One of the most amazing features was that such an easily observable phenomenon had remained undiscovered for so long.

Soon after the discovery of the positive electron the Curie-Joliots (C57) reported the observation of these new particles from targets bombarded by alphas. They suggested that in part they might be due to the "materialization" of gamma-radiation produced in the disintegration process, that is, the formation of electron pairs by the rays, which no doubt occurs. They also suggested

at first that the positrons might result from the alternative formation of a neutron and positive electron instead of the usual proton, and as such would be a product of the disintegration itself. For a time it was thought that this represented a reaction yielding three particle products, and was reported as such (D4). Subsequent experiments showed, however, that the positrons resulted from a delayed disintegration of the product nucleus in each case, a phenomenon known as "artificial" or "induced" radioactivity.

The Curie-Joliots (C54, C58), in their first papers, reported the observation of such delayed positron emission from B, Mg and Al. The initial intensity of the radioactivity was found to decay in the exponential manner common for the naturally radioactive elements and could be accurately expressed by the same equation: $I=I_0e^{-\lambda t}$, where λ is the decay constant and related to the half-life T by the usual relation: $T=\log 2/\lambda=0.693/\lambda$. Chemical tests determining the radioactive element were performed in each case by the separation of the target element from the product element and the observation of the radioactivity only in the latter. For example, after boron nitride (BN) had been irradiated by alphas for some minutes it was heated with caustic soda, liberating all the nitrogen as gaseous ammonia whereupon the ammonia was found to have all the radioactivity. The half-life was the same as that found in other B targets, and was not found in nitrogen targets. This constitutes chemical proof of the "artificial" transformation of one element to another by disintegration and was the first such definite chemical evidence, although earlier physical evidence was so conclusive that the validity of such processes was unquestioned. The usefulness of having such chemical means of determining the products of nuclear reactions is evident, and they supply the most definite proof of the validity of reactions in doubtful cases. The nature of the ejected particles was determined by their ionization and by deflection in a magnetic field. With this evidence it was possible to write the disintegration equations with confidence.

The announcement of the discovery of this type of induced radioactivity was accompanied by the suggestion that the same radioactive elements might be produced in other ways; e.g., the activity produced in B: $B^{10}+He^4\rightarrow N^{13}+n^1$; $N^{13}\rightarrow C^{13}+e^+$ might also be produced by deuteron or proton bombardment following the reactions: $C^{12}+H^2\rightarrow N^{13}+n^1$ or $C^{13}+H^1\rightarrow N^{13}+n^1$. Three laboratories (H21, C24, C40) equipped for using deuteron projectiles looked for the effect and found the expected radioactivity in C, of the same half-life,[19] almost simultaneously.

A study of a wider range of targets under alpha-bombardment by other observers revealed certain new features. Activities were found in many elements, of the positron type, and supposedly from the same α-n type reaction. The radioactivity has been found to be easier to observe than the neutrons accompanying the reaction, and in many of the processes is the only evidence of their validity. A variation was the observation that Mg emits electrons as well as positrons (A2), identified as coming from a radioactive Al instead of the radioactive Si which yields the positrons. A simple consideration of the mass and charge values of the elements involved showed that this was due to a different primary reaction yielding protons (see §99A). involving a Mg^{25} target and yielding Al^{28}. A weaker electron activity from Mg (A2, E6) of different half-life is interpreted as coming from Mg^{26} and yielding radioactive Al^{29}.

Although the second alternative suggested by the Curie-Joliots for the production of N^{13} activity is now known to be energetically impossible, another method was found to be through the capture of protons in C^{12} without particle emission. It was first observed by Henderson, Livingston and Lawrence (H21) as an activity in C under proton bombardment with an identical half-life as the deuteron produced activity. Many similar reactions are now known to occur.

A new chapter to induced radioactivity was added by Fermi (F13), in the observation of radioactivity from neutron bombardment of many elements. For the three most important processes which are known to cause this effect (n-α, n-p and n-γ type reactions) the radioactivity was found to consist of electrons in all cases investigated. The active isotope was always heavier

[19] An early discrepancy in the half-life values of the N^{13} produced by alpha and by deuteron bombardment led Gamow (G4) to suggest the existence of "isomeric" nuclei and the "negative" proton. This discrepancy has been removed by the work of Ellis and Henderson (E5).

than the stable isotopes of the element, and in a few cases the same activity was produced by each of the three processes. Chemical analysis was used to prove the nature of the active product in many cases, but in others the identification of the half-life itself was sufficient. For example the observation of the same period activity in each of three consecutive elements was proof of the simple capture, proton emission and alpha-emission type reactions, in order, for the three elements.

The climax came with the discovery by the group at Rome (F15) of the "water effect," the increased activity of the simple capture process when the neutrons were slowed down to thermal energies by the interposition of hydrogenous materials. This was found to increase the yields in some cases by as much as 40 times, and to make definitely observable many reactions on the heavy elements. Nearly a hundred activities are found to be produced by this simple capture reaction with slow neutrons.

With the development of the magnetic accelerator to produce deuterons of as much as 5 to 6 MV, Lawrence and his collaborators observed radioactivity yielding electrons and in some instances positrons for elements as heavy as Bi and Pt. The high energies reduce the problem of penetration of the potential barrier. The large yields from the *d-p* type process have resulted in intensities of radioactivities comparable with the naturally radioactive sources, and suggest a possible utilization as chemical indicators and in biological and medical research.

Classifying the reactions resulting in induced radioactivity we find eleven type reactions producing electron activity and nine giving positrons. Those producing electrons are

$$\left.\begin{array}{ll}
\alpha\text{-}p: & (Z-1)^{A-3}+\mathrm{He}^4 \rightarrow Z^A+\mathrm{H}^1 \\
p\text{-}n: & (Z-1)^A+\mathrm{H}^1 \rightarrow Z^A+n^1 \\
d\text{-}\alpha: & (Z+1)^{A+2}+\mathrm{H}^2 \rightarrow Z^A+\mathrm{He}^4 \\
d\text{-}p: & Z^{A-1}+\mathrm{H}^2 \rightarrow Z^A+\mathrm{H}^1 \\
d\text{-}p,\alpha: & (Z+2)^{A+3}+\mathrm{H}^2 \rightarrow Z^A+\mathrm{H}^1+\mathrm{He}^4 \\
d\text{-}n,\alpha: & (Z+1)^{A+3}+\mathrm{H}^2 \rightarrow Z^A+n^1+\mathrm{He}^4 \\
n\text{-}\alpha: & (Z+2)^{A+3}+n^1 \rightarrow Z^A+\mathrm{He}^4 \\
n\text{-}p: & (Z+1)^A+n^1 \rightarrow Z^A+\mathrm{H}^1 \\
n\text{-}\gamma: & Z^{A-1}+n^1 \rightarrow Z^A+h\nu \\
n\text{-}2n: & Z^{A+1}+n^1 \rightarrow Z^A+2n^1 \\
\gamma\text{-}n: & Z^{A+1}+h\nu \rightarrow Z^A+n^1
\end{array}\right\} Z^A \rightarrow (Z-1)^A+e^-.$$

Those producing positrons are[20]

$$\left.\begin{array}{ll}
\alpha\text{-}p: & (Z-1)^{A-3}+\mathrm{He}^4 \rightarrow Z^A+\mathrm{H}^1 \\
\alpha\text{-}n: & (Z-2)^{A-3}+\mathrm{He}^4 \rightarrow Z^A+n^1 \\
p\text{-}\gamma: & (Z-1)^{A-1}+\mathrm{H}^1 \rightarrow Z^A+h\nu \\
p\text{-}n: & (Z-1)^A+\mathrm{H}^1 \rightarrow Z^A+n^1 \\
d\text{-}\alpha: & (Z+1)^{A+2}+\mathrm{H}^2 \rightarrow Z^A+\mathrm{He}^4 \\
d\text{-}p: & (Z)^{A-1}+\mathrm{H}^2 \rightarrow Z^A+\mathrm{H}^1 \\
d\text{-}n: & (Z-1)^{A-1}+\mathrm{H}^2 \rightarrow Z^A+n^1 \\
n\text{-}2n: & Z^{A+1}+n^1 \rightarrow Z^A+2n^1 \\
\gamma\text{-}n: & Z^{A+1}+h\nu \rightarrow Z^A+n^1
\end{array}\right\} Z^A \rightarrow (Z-1)^A+e^+.$$

The same radioactive isotope may be produced by several different disintegration processes, but in all such cases the properties of the activity such as the disintegration energy, the half-life and the mass of the isotope are identical within the limits of experimental error. Na^{24}, Al^{28} and Cu^{64}, for instance, are each produced by five of the reactions listed above.

The *α-n* type radioactivity (positrons) occurs more often than the *α-p* kind (electrons in general). This is understandable through a consideration of the types and relative abundance of the stable isotopes in the light element region. C^{13} and $O^{17\text{ and }18}$ are rare and so the possible N^{16} and $F^{20\text{ and }21}$ radioactive nuclei from the *α-p* reactions are not observed. Transformations of the same type from the more common isotopes of B^{10}, C^{12}, N^{14} and O^{16}, etc. would result in stable nuclei; N^{15} would give a stable O^{18}, while the C^{14} that results from B^{11} has a very long life and so is hard to observe. For heavier elements the higher potential barriers, both for the entering alpha and the escaping proton would be prohibitive. Mg is the only such element for which there is good proof of the reaction.

The number of excess neutrons (the isotopic number) in the stable nuclei increases more or less regularly with increasing charge, observable in the isotopic charts of Figs. 39 to 42. The unstable, radioactive nuclei, above or below this region of stability, will tend to return to the stable region with the emission of those particles which best accomplish this result. Isotopes heavier than the known stable ones are electron active, resulting in a product nucleus of the same mass but higher charge. Isotopes too light to be stable will emit positrons, thus lowering their charge. This results in either case in the produc-

[20] The type reaction *p-α* should also, in some instances, give e^+ radioactive products, but no instance has yet been observed.

tion of a nucleus having a more stable ratio of charge to mass. In most cases observed the unstable isotope is found to have a mass number differing by one unit from the extremes of the stable isotopes of that element. N^{14} and N^{15}, for example, are flanked by positron-active N^{13} and electron-active N^{16}. In a few instances the known unstable isotope differs by two or more mass units ($F^{17, 18}$, $Al^{28, 29}$, $Sc^{41, 42, 43, 44}$ etc.). In many instances, a radioactive isotope fills the gap between two known stable ones. Ag, for instance, has two stable isotopes of mass numbers 107 and 109; the two water sensitive periods observed with neutrons (22 sec. and 2.3 min.) can occur only through the n-γ reaction and so represent radioactive Ag^{108} and Ag^{110}.

Electron emission is common for activities produced by the n-γ, n-p n-α, d-p and d-α processes, since these lead generally to an isotope heavier than those in the stable band of isotopes. In a few cases, however, positrons are observed; they come from lighter isotopes which have isobars of lower atomic number (cf. Pt^{193}). In several instances branching processes occur, yielding both electrons and positrons from the same radioactive isotope. These are found in all cases to have stable isobars of both lower and higher Z.

In several instances, the products of radioactive decay of the initial isotope are also radioactive, leading to subsequent decay processes, continuing until a stable product is reached. This involves alpha-radioactivity in the Bi, Th and U processes.

The measurement of the half-life periods of the decaying substances has proven to be relatively simple in most cases, and can be observed with an accuracy dependent on the intensity of the radiation and the sensitivity of the instruments. With thin walled Geiger counters the decreasing number of counts with time is directly observable. Ionization chambers equipped with sensitive electrometers or electroscopes are equally adaptable and somewhat more reliable for measuring long periods. Each radioactive element was found to have a characteristic half-life, and values range from 0.02 sec. (B^{12}) to more than 10 years (Be^{10}). These limits have both been obtained from deuteron induced processes, in which case the high voltages and high intensities have made these extreme cases just observable. The shortest lived element named was observed by counting the number of electron tracks in a cloud chamber arranged to be automatically expanded at short intervals following the instant when the deuteron beam was cut off. The longest lived one was found by studying the activity in a Be target which had been bombarded by deuterons for a period of 6 months as a neutron source. It is to be expected that with suitable arrangements of apparatus still longer and shorter half-lives will be found.

Certain discrepancies have appeared in measurements of the period, in particular that of N^{13} which was said to be 14 minutes by observers using alphas to produce it and to be 10.5 minutes by those using deuterons. These have been shown to be identical by Ellis and Henderson (E5), with a value of 11.0 ± 0.1 minutes. Such errors are in part experimental, as pointed out by Van Voorhis (V6), and the apparatus and potentials for collecting the ionization must be arranged to eliminate effects of ionization space charge. The methods of analysis of decay data taken in various ways are known, and Peierls (P5) gives methods for determining the most accurate values of the half-life.

In cases where contamination is suspected the measurement of the half-life provides an ideal method of distinguishing activities. In cases where an activity of known half-life is being searched for through a different reaction the observation of the expected period is considered satisfactory proof.

It can be seen that the production of radioactivity in elements provides a very sensitive method for the detection of a disintegration of those elements, even though the heavy particle produced in the reaction cannot be observed. Instruments for the detection of this activity can be made compact and extremely sensitive and can be isolated from the source of the particles used for producing the original disintegration. Observation of such an activity is just as complete proof of the validity of the primary reaction as the observation of the heavy particles, and sometimes more definite in interpretation, especially if supplemented by chemical separations.

The electron and positron radiations were

found by absorption and deflection techniques to have maximum energies varying from below 0.3 MV to 13 MV. They have been found, in all cases studied, to have the same general shape of energy distribution curve as the beta-particles from naturally radioactive elements except for the obvious influence of the different nuclear charge. This type of curve has puzzled physicists for years and has resulted in the neutrino hypothesis (see §39). One consequence is that the maximum energy must be used to balance the mass-energy equations.

The chief difficulty with the original Fermi (F12) theory of beta-decay (see Chap. VI), in which the existence of the neutrino was postulated[21] in order to conserve energy and angular momentum, is that it leads to an energy distribution curve essentially symmetrical about the half-energy value and distinctly different from the observed distributions, which show in all cases an optimum beta-energy of much less than this half-value and tailing off to high energies. The Konopinski and Uhlenbeck (K22) modification of this theory usually seems to give a much better fit to the observed distribution curves. The neutrino mass is put equal to zero in the theoretical formulae. Kurie, Richardson and Paxton (K32) have indicated how the K-U theory can be used to obtain a value for the theoretical energy maximum from experimental data, and such a value has been obtained from many of the observed distributions. On the other hand, in those few cases in which it is possible to predict the energy of the beta-decay from data on heavy particle reactions (*viz.* C^{12}-*d*-*n*, O^{16}-*d*-*n*, Al^{27}-*d*-*p*), the visually extrapolated limit has been found to fit the data better than the K-U value. The fact that the shape of the distribution curves is checked by the theory over wide ranges suggests, however, that the K-U limit has some significance, and it is recorded in the tabulations to follow wherever observed. For calculation of atomic masses we have decided to use the visually extrapolated limit. This procedure gives satisfactory results only if the experimental data are based on the observation of a sufficiently large number of electrons. Otherwise, the visual limit is apt to be considerably too low.

TABLE LXVIII. *Forbidden beta-ray transitions.*

Raa El	Product	Beta En. (MV)	Excit. En. (MV)	Total En. (MV)	Evidence
Li^8	Be^8	12.0	3.5–4.0	15.5–16.0	Li^7-*d*-*p* $Li^8 \rightarrow e^-$ (L24)
B^{12}	C^{12}	12.0	1.7–2.7	13.7–14.7	B^{11}-*d*-*p*
N^{16}	O^{16}	6.0	~5	~11	F^{19}-*n*-α
F^{20}	Ne^{20}	5.0	4.6	9.6	F^{19}-*d*-*p*
Na^{24}	Mg^{24}	1.7	2.9	4.6	Na^{23}-*d*-*p*
Al^{28}	Si^{28}	3.3	(γ=2.3)	3.3	Al^{27}-*d*-*p*
P^{32}	S^{32}	1.69	—	1.69	Raa. En.
K^{40}	Ca^{40}	0.7	—	0.7	Nat. Raa.

In several of the radioactive processes gamma-rays are also observed to be emitted with the betas. These are much too strong in intensity to be due to conversion of the betas themselves, and appear to be in general monoenergetic. They must be considered as coincident with the beta-emission and as representing a transition of the residual nucleus from an excited state in which it is left after the beta-emission. In some cases (Li^8, B^{12}, N^{16}, F^{20} and Na^{24}) the beta-emission leads practically always to an excited state of the residual nucleus (Be^8, etc.) (see Table LXVIII) so that the gamma-energy is additive to the beta-maximum. This will result when the beta-transition to the ground state is highly forbidden. This is indicated experimentally by a simple beta-ray distribution and measurements indicating that the number of gamma-quanta equals the number of radioactive electrons. In other cases (Cl^{38}, A^{41}, K^{42}, Mn^{56}, and As^{76}) the beta-decay leads sometimes to the ground state and sometimes to an excited state. This gives rise to a complex beta-spectrum (K33, B62) consisting of several "groups," analogous to the heavy particle groups in ordinary nuclear reactions. The absolute maximum of the beta-spectrum corresponds then to the total energy evolution while the gamma-ray energy should be correlated with the difference between the maximum energies of the beta-ray groups. The observed shape of beta-ray distribution curves does not lend itself to analysis into groups, and in this

[21] It should be mentioned at this point that the neutrino suggested by Pauli and used by Fermi and by Konopinski and Uhlenbeck in their theories has not been observed. The properties attributed to it by the theories are essentially zero mass, zero charge, spin $\frac{1}{2}$ and zero or very small magnetic moment. The only observable property is its momentum. It may be hoped that studies of the recoil of light nuclei in beta disintegrations will give more direct evidence about the neutrino.

instance the use of the Konopinski-Uhlenbeck theory makes it possible to separate them even though it may not predict the correct maximum energies.

Of considerable interest because of their theoretical importance are the data on the energies involved in the beta-ray transitions from nuclei of the "$4n$ type." In many of these processes the beta-ray does not represent the full energy, due probably to forbidden transitions. Estimates of the total energy available can be made from analysis of the primary reactions; the difference is then entered as excitation energy. In a few instances this gamma-radiation is observed and measured and found to decay with the half-life of the beta-decay. In other instances it is inferred from other evidence.

The total energy is found to decrease regularly from the light to the heavy nuclei. For Al^{28} and the two heavier elements it seems probable that the gamma-radiation is alternative rather than consecutive to the beta-ray, and is so indicated. The similarity in nuclei of this type and the general trend of the total energy evolution are to be expected theoretically (see Part A, §30). A thorough discussion of the theory is given by Wigner (W18).

A few generalizations can be drawn concerning the methods useful in the analysis of the evidence from the various type reactions to give specific information about the radioactivities involved. These are more readily followed by referring to the stable isotopes and their abundance (Table LXXVII) and to the isotopic charts (Figs. 39 to 42).

Activities showing the "water effect" with neutrons (slow neutrons) give generally isotopes of the target element of one unit higher mass, and are usually electron active. Deuteron bombardment resulting in the same chemical element as the target (the d-p reaction) will in general duplicate the slow neutron activities. Whenever positron activities are obtained by either of these two reactions it indicates reactions in light isotopes of the elements. d-n reactions lead to an element of one unit higher charge and in general are positron activities; d-α reactions give elements of lower charge; n-p and n-α reactions result in elements of one and two units lower Z, respectively. So observation of identical periods produced in these various ways from adjacent chemical elements will usually result in the positive identification of the isotope responsible for the activity. The results of proton and gamma-ray activation are of even greater value. If a target element has only two stable isotopes and two periods are observed with slow neutrons and two periods with gamma-rays, one of which is common, this common activity will belong to the isotope between the two stable isotopes. The other neutron period is one unit heavier than the heavy stable isotope and the other gamma-period one unit lighter than the lighter stable isotope. In this way the 2.3 min. period of Ag is identified as Ag^{108}, the 18 min. period of Br is Br^{80}, and the 20 min. period of Ga is Ga^{70}. In other cases the observation of a period different from any observed neutron period specifies an isotope other than those which can be produced by neutron capture (e.g., In).

In Table LXIX are collected the best data on the half-lives, disintegration energies and other features of all the radioactive elements produced in nuclear disintegrations for which these quantities have been measured. The natural radioactivities are not included. In many cases the evidence is sufficient to lead to a unique interpretation; in others the particular isotope responsible cannot be determined. In order to indicate the certainty each reaction is marked with a letter in the column headed "class" according to the following code:

A—Isotope certain
B—Isotope probable
C—One of few isotopes
D—Element certain
E—Element probable
F—Insufficient evidence

For a large share of the radioactive elements the evidence given in the table (chiefly through the indicated primary reactions) is sufficient to justify classification, and such cases are not discussed in detail. In other instances the interpretation is based upon more varied and uncertain evidence and these cases are discussed individually in the following pages.

The assignments in Table LXIX requiring a more involved justification are discussed individually below.

TABLE LXIX. *Induced radioactivities.*

Raa ELEMENT					Raa ENERGY				
Z	A	CLASS	Raa PARTICLE	HALF-LIFE T	Obs. (MV)	K−U (MV)	Raa γ's (MV)	PRODUCED BY	OBSERVERS
2	He^{6}	A	e^-	0.7 sec.	3.7			Be-*n*-α, (Li-*n*-*p*)	B24, N1, K20
3	Li^{8}	A	e^-	0.88 sec.	12			Li-*d*-*p*, (Li-*n*-γ)	B5a, L24, C48
4	Be^{10}	A	e^-	≥10 yr.	<0.3(?)			Be-*d*-*p*	Mc7
5	B^{9}	F	e^+	——	0.3(?)			Li-α-*n*	M14
	B^{12}	A	e^-	0.02 sec.	12	13.0		B-*d*-*p*	C46, F28, B5a
6	C^{11}	A	e^+	20.5 min.	1.15	1.3		B-*d*-*n*, B-*p*-γ, C-*n*-2*n*	C39, F28, P11d
	C^{14}	F	e^-	~3 mo.	0.3(?)			{(N-*n*-*p*) (C-*d*-*p*)(B-α-*p*)}	Mc7, M16, B39
7	N^{13}	A	e^+	11.0 min.	1.25	1.45		{B-α-*n*, N-*n*-2*n* C-*d*-*n*, C-*p*-γ}	E5, H4, F28, P11d
	N^{16}	A	e^-	8.4 sec.	6.0	6.5		N-*d*-*p*, F-*n*-α, O-*n*-*p*	F28, N1, C16a
8	O^{15}	A	e^+	126 sec.	1.7	2.0		N-*d*-*n*, O-γ-*n*, O-*n*-2*n*	Mc6, F28, P11d
	O^{19}	A	e^-	31 sec.				F-*n*-*p*	N1
9	F^{17}	A	e^+	70 sec.	2.1	2.4		O-*d*-*n*, N-α-*n*, O-*p*-γ, F-*n*-3*n*	{N6, W12, K33, D28, P11c}
	F^{18}	A	e^+	112 min.				Ne-*d*-α, (O-*p*-γ), O-*p*-*n*, F-*n*-2*n*	S16, D28, P11d
	F^{20}	A	e^-	12 sec.	5.0	5.9		{Na-*n*-α F-*d*-*p*, F-*n*-γ}	C48, N1, F28
10	Ne^{23}	A	e^-	33 sec.				Mg-*n*-α, Na-*n*-*p*	A7, N1
11	Na^{22}	A	e^+	~6 mo.	0.4(?)			Mg-*d*-α, F-α-*n*	L2, F32
	Na^{24}	A	e^-	14.8 hr.	1.7	1.95	{0.95 1.93 3.08}	{Na-*d*-*p*, Na-*n*-γ Al-*n*-α, Mg-*n*-*p*, Mg-*d*-α}	{A7, H24, V6 K33, R7, L15}
12	Mg^{27}	A	e^-	10.2 min.	2.05(?)		1.3	{Mg-*d*-*p* Al-*n*-*p*, Mg-*n*-γ}	A7, H24
13	Al^{26}	A	e^+	7.0 sec.	1.8(?)			Na-α-*n*	F31
	Al^{28}	A	e^-	2.36 min.	3.3		2.3	{Si-*n*-*p*, Al-*d*-*p*, Al-*n*-γ Mg-α-*p*, P-*n*-α}	E10, A7, C34
	Al^{29}	B	e^-	11.0 min.	>3.3(?)			Mg-α-*p*	E10
14	Si^{27}	A	e^+	6.7 min.	2.0			Mg-α-*n*, Si-*n*-2*n*	E10, F1, P11d
	Si^{31}	A	e^-	170 min.	1.8	2.05		Si-*d*-*p*, P-*n*-*p*, Si-*n*-γ	{A7, N5, K33 N7b, P11d}
	Si	F	e^+	11 min.				(Si-*n*-3*n*)	P11d
15	P^{30}	A	e^+	2.5 min.	3.6			{Al-α-*n*, S-*d*-α, P-*n*-2*n* Si-*p*-*n*, P-γ-*n*}	{C54, A1, R7a B4a, P11d}
	P^{32}	A	e^-	14.5 da.	1.69	2.15(?)		{P-*d*-*p*, S-*d*-α P-*n*-γ, S-*n*-*p*, Cl-*n*-α}	{N5, K33, P11d A7, S12, L36, N7b}
16	S^{31}	F	e^+	26 min.				S-*n*-2*n*	P11d
	S^{35}	A	e^-	80 da.				Cl-*n*-*p*	A14
17	Cl^{34}	A	e^+	33 min.	1.8(?)			P-α-*n*, S-*d*-*n*, Cl-*n*-2*n*	F31, S1, P11d
	Cl^{38}	B	e^-	37.0 min.	4.8	1.5, 6.1	2.0, 2.5	Cl-*d*-*p*, Cl-*n*-γ, K-*n*-α	A3, R6, K33, H39a
18	A^{39}	F	e^-	4 min.				(K-*n*-*p*)	P11d
	A^{41}	A	e^-	110 min.	2.7	1.5, ~5	1.37	A-*d*-*p*, K-*n*-*p*, A-*n*-γ	S15, R7, K33, H39a
19	K^{38}	A	e^+	7.7 min.				Cl-α-*n*, Ca-*d*-α, K-*n*-2*n*	H24a, H39a, P11d
	K^{42}	A	e^-	12.2 hr.	3.5	1.4, 4.4		{K-*n*-γ, Ca-*n*-*p* K-*d*-*p*, Sc-*n*-α}	W1, A7, K33, H39a
20	Ca^{39}	B	e^+	4.5 min.				Ca-*n*-2*n*	P11d
	Ca^{45}	A	e^-	2.4 hr.	1.9(?)		<0.5	{Ca-*n*-γ, Ca-*d*-*p* Ti-*n*-α}	H29, W1
21	Sc^{41}	A	e^+	53 min.				Ca-*d*-*n*	W1
	Sc^{42}	A	e^+	4.1 hr.	1.5(?)			K-α-*n*	A7, Z3, W1
	Sc^{43}	A	e^+	4.0 hr.	0.4(?)			Ca-α-*p*, Ca-*d*-*n*, Sc-*n*-3*n*	F32, W1, P11c
	Sc^{44}	A	e^+	52 hr.				Ca-*d*-*n*, K-α-*n*, Ca-*p*-*n*, Sc-*n*-2*n*	W1, B4a, P11d
	Sc^{46}	F	e^-(?)	—long—	low			Sc-*n*-γ	H32
	Sc	F	e^-	{1.7 hr. 28 hr.}				Ti-*n*-*p*, (V-*n*-α)	W1a, P11d
22	Ti^{51}	A	e^-	2.8 min.				Ti-*n*-γ, Ti-*d*-*p*	A7, W1a
23	$V^{49, 50}$	C	?	35 min.				Ti-α-*p*, Ti-*d*-*n*	W1a
	V^{52}	A	e^-	3.75 min.				Mn-*n*-α, V-*n*-γ, Cr-*n*-*p*	A7, P11d
	V	F	e^+	16 da.				Ti-*d*-*n*	W1a
	V	F		1.8 da.				V-*n*-?	P11d
24	Cr	F	e^-	1.7 hr.				Cr-*n*-?	P11d
25	Mn^{52}	B	e^+	5 da.				Fe-*d*-α	L27a
	Mn^{53}	A	e^+	40 min.				Cr-*p*-*n*, Cr-*d*-*n*	B4a, L27a
	Mn^{54}	b	e^-, e^+(?)	21 min.			1.65	Fe-*d*-α	D3a, M20b
	Mn^{56}	A	e^-	2.5 hr.	2.8	(1.2, 2.9)		{Fe-*n*-*p*, (Mn-*d*-*p*?) Co-*n*-α, Mn-*n*-γ, Cr-α-*p*}	{A7, G1, B62, H24b, P11d}
	Mn	F	e^-	*ca.* mo.				(Fe-*d*-α)	L27a
26	Fe^{53}	B	e^+	8.9 min.				Cr-α-*n*	H24b
	Fe^{55}	D	e^+(?)	91 min.				Mn-*p*-*n*	B4a
	Fe^{59}	A	e^-	40 da.				Co-*n*-*p*, Fe-*d*-*p*	A15, L27a
27	Co^{55}	A	e^+	18.2 hr.				Fe-*d*-*n*	D3a
	Co^{58}	B	e^-	11 min.				Ni-*n*-*p*, Co-*n*-γ	R15
	Co^{60}	B	e^-	~ yr.	0.15?		2.0	Co-*n*-γ, Co-*d*-*p*	S2, T10
	Co	D	e^+, e^-(?)	100–200 da.				Fe-*d*-*n*	L27a
28	Ni^{57}	D		2 hr.				Ni-*n*-2*n*(?)	P11d
	Ni^{59}	B	e^+	3 hr.				Ni-*n*-γ	N3
	Ni^{63}	F	e^-	130 da.				Cu-*d*-α	L26
	Ni^{65}	b	e^-	160 min.				Zn-*n*-α, Cu-*n*-*p*	M1, O½
	Ni	F		6 da.				Ni-*n*-?	P11d
29	Cu^{61}	B	e^+	3.4 hr.	0.9			Ni-*p*-*n*, Ni-α-*p*, Ni-*d*-*n*, Cu-*n*-3*n*	B4a, T10a, R7b, P11c
	Cu^{62}	B	e^+	10.5 min.				Cu-*n*-2*n*, Cu-γ-*n*, Co-α-*n*	H33, B47b, R7b
	Cu^{64}	A	e^-, e^+	12.8 hr.	0.7	{e^-=0.83 e^+=0.79}	No	{Zn-*n*-*p*, Ni-*p*-*n* Cu-*d*-*p*, Zn-*d*-α, Cu-*n*-γ}	V7, L26, B21, B4a
	Cu^{66}	A	e^-	5 min.				Zn-*n*-*p*, Cu-*n*-γ, Ga-*n*-α	A7, F16, C16a

TABLE LXIX.—*Continued.*

Raa Element Z	Raa Element A	Class	Raa Particle	Half-life T	Raa Energy Obs. (MV)	Raa Energy K−U (MV)	Raa γ's (MV)	Produced by	Observers
30	Zn^{63}	*B*	e^+	37 min.				Zn-*n*-2*n*, Ni-α-*n*, Zn-γ-*n*	H33, R7c, P11d, B47d
	Zn^{65}	*B*	e^+(?)	1 hr.				Zn-*d*-*p*	L26
	Zn^{69}	*B*	e^-	100 hr.				Zn-*d*-*p*	L26
31	Ga^{66}	*A*	e^+	9.4 hr.				Cu-α-*n*	H24b
	Ga^{68}	*A*	e^+	60 min.				Ga-γ-*n*, Cu-α-*n*, Ga-*n*-2*n*	B47d, H24b, P11d
	Ga^{70}	*B*	e^-	20 min.				Ga-*n*-γ, Ga-γ-*n*, Zn-*p*-*n*	A7, B47d, B4a
	Ga^{72}	*B*	e^-	23 hr.				Ga-*n*-γ, (Zn-*d*-γ), Zn-*p*-*n*, Ge-*n*-*p*	A7, L26, B4a, P11d
	Ga	*F*	e^+	1.7 hr.				Ga-*n*-?	P11d
32	Ge^{75}	*D*	e^-	30 min.				Ge-*n*-γ	A7, S25
	Ge	*F*	e^-	1.3 hr.				Ge-*n*-?	P11d
33	As^{74}	*E*		13 da.				As-*n*-2*n*	P11d
	As^{76}	*A*	e^-	26 hr.	1.5(?)	1.1, 3.4	Yes	As-*n*-γ, As-*d*-*p*	A7, T10; B62
34	Se	*F*	e^+(?)	1.3 min., 113 min.				As-*p*-*n*	B4a
	Se^{79}	*D*	e^-	56 min.				Se-*n*-2*n*	H33b
	Se^{83}	*B*	e^-	10–20 min.				Se-*d*-*p*, Se-*n*-γ	S16a, A7
35	Br^{78}	*A*	e^+	6.3 min.				As-α-*n*, Br-γ-*n*, Br-*n*-2*n*	S16a, B47c, C16a, P11d
	Br^{80}	*A*	e^-	18 min.	2.00			Br-*n*-γ, Se-*p*-*n*; Br-*d*-*p*, Br-γ-*n*	A7, A1, B4a, B47b
	Br^{80}	*A*	e^-	4.2 hr.	2.05			Br-*n*-γ, Se-*p*-*n*; Br-*d*-*p*, Br-γ-*n*	A7, A1, B4a, B47e
	Br^{82}	*A*	e^-	36 hr.	0.85		Yes	Br-*n*-γ, Se-*p*-*n*; Br-*d*-*p*, (Se-*d*-2*n*)	K34, A1, J2; B4a, S16a
	Br^{83}	*B*	e^-?	2.5 hr.				Se-*d*-*n*	S16a
37	Rb^{84}	*E*	e^-	22 hr.				Rb-*n*-2*n*	P11d
	Rb^{86}	*B*	e^-	11 min.				Rb-*n*-γ, γ-*n*-α	F13, P11d
38	Sr^{85}	*B*	e^+	3 hr.				(Sr-*n*-2*n*)	P11d
	Sr	*F*	e^-	18 min.				Sr-*n*-?	P11d
39	Y^{90}	*A*	e^-	70 hr.				Y-*n*-γ	H31, P11d
	Y	*F*	e^-	1.2 hr.; 6.5 hr.				Y-*n*-?	P11d
40	$Zr^{93, 95}$	*D*	e^-	40 hr.				Zr-*n*-γ	H29
	Zr	*F*		10 min.; 5 hr.				Zr-*n*-?	P11d
41	Cb	*F*		7.3 min.; 3.8 da.				Cb-*n*-?	P11d
42	Mo^{91}	*D*	e^-	17 min.				Mo-γ-*n*, Mo-*n*-2*n*	B47d, H33b
	Mo^{93}	*B*	e^+	25 min.				Mo-*n*-γ	A7
	$Mo^{99, +}$	*D*	e^-(?)	36 hr.				Mo-*n*-γ	A7, Mc1
	Mo	*F*	e^-	5 da				Mo-*n*-?	P11d
43	Ma	*F*	e^-	4 hr.; 46 da.				Ru-*d*-α	L26
	Ma	*F*	e^+(?)	0.5 min.; 31 min.				Mo-*p*-*n*	B4a
44	$Ru^{97, 103}$	*F*	e^-(?)	11 hr. (39 hr.); 75 hr. (11 da.)				Ru-*n*-γ, Ru-*d*-*p*	K35, L26
	Ru^{105}	*F*	e^-	40 sec.→100 sec.				Ru-*n*-γ	K35
	Ru	*F*		24 min.; 3.6 hr.				Ru-*n*-?	P11d
45	Rh^{102}	*B*	e^-	3.9 min.				Rh-*n*-γ	A7, S3
	Rh^{104}	*B*	e^-	44 sec.	2.5	2.8		Rh-*n*-γ	A7, A1, G1
	Rh^{105}	*F*	e^-	100 sec.				Ru-*n*-γ-β	K35
	Rh	*F*	e^-	1.1 hr.				Rh-*n*-?	P11d
46	Pd	*D*	e^-(?)	3 min.; 15 min.; 12 hr.; 60 hr.				Pd-*n*-γ, Pd-*d*-*p*	A7, K36, K25
47	Ag^{106}	*B*	e^-	7.5 da.				Pd-*d*-*n*, Ag-*n*-2*n*	K25, P11d
	Ag^{105}	*A*	e^+	25.5 min.				Pd-*d*-*n*, Ag-γ-*n*, Ag-*n*-2*n*	K25, B47c, P11d
	Ag^{108}	*A*	e^-	2.3 min.	2.8?			Ag-*n*-γ, Ag-γ-*n*	A7, G1, B47c
	Ag^{110}	*A*	e^-	22 sec.	2 6	2.8		Ag-*n*-γ	A7, G1, N2
48	Cd^{109}	*E*	e^+	33 min.				Cd-*n*-2*n*	P11d, H33b
	Cd^{115}	*B*	e^-	4.3 hr.				Cd-*d*-*p*, Cd-*n*-γ	C36a, M20a
	Cd^{117}	*B*	e^-	58 hr.				Cd-*d*-*p*, Cd-*n*-γ	C36a, M20a
49	In^{111}	*D*	e^-	2 mo.				(In-*n*-3*n*)	P11d
	In^{112}	*B*		1 min.				In-γ-*n*, In-*n*-2*n*, Cd-*p*-*n*	B47d, P11d
	In^{114} / In^{116}	*C*	e^-	13 sec.	3.0	3.2		In-*n*-γ, (Cd-*p*-*n*)	A7, G1, B4a
		C	e^-	54 min.	1.1	1.3	1.39	In-*n*-γ, (Cd-*p*-*n*), Sn-*n*-*p*	A7, G1, B4a, M20b; P11b, P11d
		C	e^-	3.5 hr.				(In-*n*-γ)	S28
	In^{117}	*A*	e^-	2.3 hr.	1.0			Cd-*d*-*p*, Cd-e^-, (Cd-*p*-*n*)	C36a
	In	*D*	e^-	3 hr.				In-*n*-γ	B47f
50	Sn^{113}	*B*	e^+(?)	14 min.				In-*p*-*n*, Sn-*n*-γ, Sn-*d*-*p*	B4a, N3
	Sn^{121}	*A*	e^-	28 hr.				Sn-*d*-*p*, Sb-*d*-α	L27, L26
	Sn^{123}	*D*	e^-	~ mo.				Sn-*d*-*p*	L27
	Sn^{125}	*D*	e^-	8 min.→18 min.?				Sn-*n*-γ, Sn-*d*-*p*	N3, L27
51	Sb^{120}	*A*	e^+	13 min.				Sn-*d*-*n*, Sb-γ-*n*, Sb-*n*-2*n*	L27, B47c, P11d
	Sb^{122}	*C*	e^-	2.5 da.				Sb-*n*-γ, Sb-*d*-*p*	A7, L26
	Sb^{124}	*C*	e^-	60 da.				Sb-*d*-*p*, Sb-*n*-γ	L26, P11d
	Sb	*D*	e^-	112 da.				Sn-*d*-*n*	L27
52	$Te^{127, 129}$	*C*	e^-	60 min.				Te-*n*-γ, Te-γ-*n*, Te-*n*-2*n*	A7, B47d, P11d, H33b
	Te	*F*		30 da.				Te-*n*-?	P11d
53	I^{128}	*A*	e^-	25 min.	2.10			I-*n*-γ	A7, A11, A1, P11d
54	Xe	*F*	e^-?	3 min.				Ba-*n*-α	A7
55	Cs^{124}	*A*	e^-	1.5 hr.				Cs-*n*-γ	A7, L3

TABLE LXIX.—*Continued.*

Raa Element					Raa Energy				
Z	A	Class	Raa Particle	Half-life T	Obs. (MV)	K−U (MV)	Raa γ's (MV)	Produced by	Observers
56	Ba^{139}	*A*	e^-	85.6 min.				Ba-*n*-γ, Ba-*d*-*p*	A7, A8, P11a, d
57	La^{138}	*E*		2.2 hr.				La-*n*-2*n*	P11d
	La^{140}	*A*	e^-	31 hr.				La-*n*-γ, La-*d*-*p*	M7, H31, P11a
58	Ce	*F*	e^-?	2.4 hr.				Ce-*d*-*p*, Nd-*n*-α	P11a, P11d
	Ce	*F*	e^-	40 min.				Ce-*n*-?	P11d
59	Pr^{140}	*E*	e^+	3 min.				Pr-*n*-2*n*	P11d
	Pr^{142}	*D*	e^-	19 hr.				Pr-*n*-γ, Nd-*n*-*p*	A7, P11d
60	Nd	*D*	e^-	1 hr.				Nd-*n*-γ	A7, H30
62	Sm	*D*	e^-	40 min. 2 da.				Sm-*n*-γ	A7, H30, H31a
63	Eu	*D*	e^-	9.2 hr.	2.6(?)			Eu-*n*-γ	S25, M7, N2
64	Gd	*D*	e^-	8 hr.				Gd-*n*-γ	A7, H30
	Gd	*F*	e^-	19 hr.				Nd-*n*-?	P11d
65	Tb^{160}	*A*	e^-	3.9 hr.				Tb-*n*-γ	H30, M7
66	Dy^{165}	*A*	e^-	2.5 hr.	1.2	1.4		Dy-*n*-γ	H30, M7, G1
67	Ho^{166}	*A*	e^-	35 hr.				Ho-*n*-γ	M7, H31, H31a
68	Er	*D*	e^-	5.8 min. 12 hr.				Er-*n*-γ	Mc3, H31a, S25
69	Tm^{170}	*A*	e^-	8 mo.				Tm-*n*-γ	C61
70	Yb	*D*	e^-	3.5 hr.				Yb-*n*-γ	H30, M7
71	Lu^{176}	*D*	e^-	3.6 hr. 6 da.				Lu-*n*-γ	M7, Mc3, H31
72	Hf^{181}	*A*	e^-	~ mo.				Hf-*n*-γ	H29
73	Ta^{180}	*A*	e^+(?)	15 min.				Ta-γ-*n*	B47d
	Ta^{182}	*A*	e^-	200 da.				Ta-*n*-γ	F27
	Ta	*F*		9.1 hr.				Ta-*n*-?	P11d
74	$W^{185,\ 187}$	*D*	e^-	23 hr.				W-*n*-γ	A7, Mc1
75	$Re^{186,\ 188}$	*D*	e^-	20 hr. 85 hr.				Re-*n*-γ	A7, K36
76	$Os^{191,\ 193}$	*D*	e^-	40 hr.				Os-*n*-γ	K36
77	Ir	*C*	e^-	28 min.	1.1		0.4	Ir-*n*-γ; Pt-*d*-*n*, α	S20, C35
	Ir	*C*	e^-	3 da. 19 hr.? 2 mo.	2.20?			Ir-*n*-γ; Au-*d*-*p*, α Pt-*n*-*p*	S20, C36, A1, F27 P11d
	Ir	*C*	e^-	8.5 hr.				Pt-*d*-*n*, α	C35
78	Pt^{193}	*B*	e^+	49 min.				Pt-*d*-*p*, Pt-*n*-γ	A7, C35
	Pt^{197}	*B*	e^-	14.5 hr.				Pt-*d*-*p*	C35
	Pt	*F*	e^-	1.8 hr.				Pt-*n*-?	P11d
79	Au^{196}	*E*		17 min.				Au-*n*-2*n*	P11d
	Au^{198}	*A*	e^-	2.7 da.	1.15			Au-*n*-γ, Au-*d*-*p*	A7, A1, C36
80	Hg^{197}	*E*	e^-	45 min.				Hg-*n*-2*n*	H33b
	Hg^{205}	*C*	e^-	40 hr.				Hg-*n*-γ	A13
81	$Tl^{204,\ 206}$	*C*	e^-	4 min. 1.3 hr.				Tl-*n*-γ	P15
82	Pb^{209}	*D*	e^-	8.6 da.				Pb-*d*-*p*	T11
	Pb	*F*	e^-	5 min. 1.5 hr.				Pb-*n*-?	P11d
83	Bi^{210}	*A*	$e^- \rightarrow \alpha$	5 da.				Bi-*d*-*p*	L26
88	Ra^{229}	*D*	e^-	1 min.				Th-*n*-α	C60
89	Ac^{229}	*D*	e^-	15 min. 3.5 hr.				Ra^{229}-β	C60
90	Th^{233}	*D*	e^-	25 min.				Th-*n*-γ	C60
	Th^{235}	*E*	e^-	4 min.				U-*n*-α	M15
	Th	*F*	e^-	5 min. 1.4 hr.				Th-*n*-?	P11d
91	Pa^{235}	*E*	e^-	very short				Th^{235}-β	M15
	Pa^{233}	*D*	e^-	2 min.				Th^{233}-β(?)	C60
92	U^{239}	*E*	e^-	15 sec.				U-*n*-γ	M15, A7
	U^{237}	*E*	e^-	40 sec.				U-*n*-2*n*	M15
	U^{236}	*D*	e^-	24 min.				U-*n*-γ	M15
	U	*F*	e^-	4 hr. 13 hr.				U-*n*-?	P11d
93	$93^{237,\ 239}$	*D*	e^-	2.2 min. 16 min.				U-β	M15
94	$94^{237,\ 239}$	*E*	e^-	59 min. 6–12 hr.				93-β	M15
95 96		*F*	e^-	3 da. 3 hr.				94-β	M15

N^{16}; O^{19}; F^{20}

A discussion of the evidence whereby the activities of these three isotopes were identified was given in §102*A* under the F^{19}-*n*-α reaction, in order to justify the primary process. The evidence is largely in a report by Nahmias and Walen (N1) who found a water-sensitive period (F^{20}) with a half-life only slightly greater than a nonsensitive period (8.4 sec.) which is identified with N^{16} by considerations of relative probabilities of the *n*-α and *n*-*p* processes in F. The remaining weak activity with a longer period (31 sec. must then be due to O^{19}. The interpretation is verified by the *d*-*p* reactions on N and F which give activities of nearly equal half-lives (F28).

(Si)

Pool, Cork and Thornton (P11d) report that fast neutrons produce a 11 min. positron activity in Si besides the 6 min. period characteristic of Si^{27}. A 11 min. electron activity could be understood as due to a Si-n-p reaction producing Al^{29} or a Si-n-α process giving Mg^{27}, but the reported positron period cannot be ascribed to a definite element at present. It may be Si^{26} from an n-$3n$ process.

Cl^{38}

It seems probable that the Cl^{38} rather than the Cl^{36} isotope should be responsible for the observed activity which has a rather short period and high energy because Cl^{36} should have a very low energy and long period if it is similar to the analogous nuclei P^{32} and K^{40}.

Ca^{45}

The 2.4 hr. period found by Walke (W1) with deuterons on Ca and neutrons on Ti is probably the same as the 4 hr. period reported by Hevesy and Levy (H29) from slow neutron bombardment of Ca. Walke found this period in the Ca fraction of the chemical separation, specifying Ca-d-p and Ti-n-α reactions. The radioactive particles were electrons, thus determining Ca^{45} as the isotope responsible, since the only alternative, Ca^{41}, would be positron active.

$Sc^{41, 42, 43, 44, 46, 48}$

Walke (W1) has observed three periods chemically separable as Sc from Ca after deuteron bombardment. The periods were 53 min., 4.0 hr. and 52 hr. From the known isotopes of Ca and Sc these must be Sc^{41}, Sc^{43} and Sc^{44} if the reaction is Ca-d-n. The radioactive particles were found to be positrons in all cases. The 4.0 hr. period is certainly the positron activity of 4.4 hr. period obtained by Frisch (F32) from the Ca-α-p reaction and Sc^{43} is the only possibility for this common period. In a note added in proof Walke reports the production of the 52 hr. period from alpha-particle bombardment of K, defining it as due to Ca^{44}. The 53 min. period must then be Sc^{41}. Sc^{44} and Sc^{43} are also produced (P11c) by very fast neutrons on Sc. Zyw (Z3) first found a 3 hr. positron activity from K-α-n; Walke, using He^{++} ions accelerated to 11 MV in the Berkeley cyclotron, has repeated the experiment, naming 4.1 hr. for the period. Since Sc^{44} is excluded by the results discussed above this must be due to Sc^{42}. A slow neutron produced activity in Sc reported by Hevesy (H32) to have a long period and low energy can only be Sc^{46} unless due to a contamination. Finally a fast neutron period of 16–28 hr. in Ti (W1a, P11d) may be either a n-α or n-p reaction but seems most probably a n-p reaction leading to Sc^{48}.

V, Cr

It is as yet impossible to assign to definite elements a 1.8 day activity found in V and a 1.7 hour electron period found in Cr (P11d) with very fast neutrons.

$Co^{58, 60}$

The evidence given by Rotblat (R15) for a 20 min. period (later corrected to 11 min. (L27a)) from Ni under neutron bombardment which was not water sensitive (Ni-n-p), and the same period from Co which was water sensitive (Co-n-γ), is sufficient to identify this period with a radioactive Co even though chemical tests were not made. The intensity was too low to account for the large neutron absorption coefficient. This feature was cleared up by Sampson, Ridenour and Bleakney (S2) who found mass-spectroscopic evidence for a stable Co^{57} isotope (0.2 percent abundance) and a second neutron produced activity of some years period. The long period has a much greater total intensity than the short one and so is ascribed to Co^{60}, while the 11 min. period is due to the rare isotope and is Co^{58}. The long period should also be produced by the Cu^{63}-n-α reaction if this interpretation is correct.

$Ni^{59, 63}$

Rotblat (R15) first reported a water sensitive neutron induced activity in Ni, measured by Naidu (N3) to have a 3 hr. half-life. Thornton (T10a) finds an activity with a similar period (3.4 hr.) produced by deuterons on Ni, but chemical separations identify it as Cu (Cu^{61}). The same period (3.6 hr.) is found by Thornton from Co under deuteron bombardment. Unless due to a Ni impurity which is unlikely, or a coincidence of half-life values, it would require an unusual reaction to explain it, possibly; $Co^{59}+H^{2}\rightarrow Ni^{59}+2n^{1}$.

A period of 130 days observed by Livingood (L26) from Cu with deuterons is probably Ni^{63} from a Cu-*d*-α reaction. Madsen (M1) finds a 100 min. period from Zn-*n*-α, probably Ni^{65}. Two fast neutron induced periods (2 hr. and 6 da.) found in Ni (P11d) cannot at present be assigned to definite elements.

(Cu)[61, 62, 64, 66]

A 12.8 hr. period identified as Cu from the Cu-*d*-*p* reaction has been shown to consist of both electrons and positrons, by Van Voorhis (V7). This isotope should have stable isobars of both Ni and Zn, and so is certainly Cu^{64}. It is also observed in the Zn-*d*-α reaction (L26) and the Zn-*n*-*p* and Cu-*n*-γ reactions (6 hr.) (B21), the Cu-*n*-2*n* process (P11d) and also probably in a Ni-*p*-*n* reaction (B4a). An electron activity of 5 min. period observed with slow neutrons on Cu and fast neutrons on Zn (F16) is chemically copper, and so must be Cu^{66}. Heyn (H33) finds an activity which yields positrons from Cu under only fast neutron bombardment which has a period of 10.5 min. but separates chemically as Cu. As discussed in §102D this is interpreted as due to a *n*-2*n* reaction, and so is Cu^{62}. It is also produced by the Cu-γ-*n* reaction which confirms the interpretation (B47b). Cu^{61} probably has the 3.4 hr. positron period found in Ni-*d*-*n*, Ni-α-*p* and Ni-*p*-*n* reactions.

Zn[63, 65, 69]

In the deuteron bombardment of Zn Livingood (L26) found a variety of radioactive periods. Certain of these can be shown by coincidence of half-life values to be isotopes of Cu, others may be Ga. The *d*-*p* reaction would be expected to result in Zn^{65}, Zn^{69} and possibly Zn^{71} although the target isotope is in this last case extremely rare. Of the two periods which cannot readily be explained as due to other elements the 100 hr. period yields electrons and so is probably Zn^{69} while the 1 hr. period may be positron active and so be Zn^{65}. A 37 min. positron activity observed in the Ni-α-*n* (R7c), Zn-γ-*n* (B47d) and Zn-*n*-2*n* (P11d) reactions is most probably Zn^{63}.

Ga[68, 70, 72]

Amaldi, *et al.* (A7) observed two slow neutron activities of 20 min. and 23 hr. periods yielding electrons, from the known two stable isotopes of Ga. Bothe and Gentner (B47d) find periods of 20 min. and 60 min. with gamma-rays on Ga. This identifies the 20 min. period as Ga^{70}, the 60 min. as Ga^{68} and the 23 hr. as Ga^{72}. An activity of 25 hr. period found by Livingood (L26) in the deuteron bombardment of Zn is probably identical with Ga^{72} from neutrons. If so it represents a *d*-γ reaction, otherwise unknown. A 1.7 hr. positron activity produced in Ga by fast neutrons (P11d) cannot as yet be given a definite assignment.

Ge, As

A 1.3 hr. electron activity in Ge and a 13 day activity in As produced by fast neutrons (P11d) cannot be assigned to any definite element at present.

Br[78, 80, 82, 83]

In addition to the two slow neutron produced periods in Br originally observed by Amaldi, *et al.* (A7), Kurtschatov, etc. (K34) have found a third, also produced by slow neutrons. The periods and beta energy distributions have been studied by Alichanian, Alichanow and Dzelepow (Al). They find the 18 min. period to have an energy maximum of 2.00 MV, the 4.2 hr. period 2.05 MV and the 36 hr. (also measured as 24 hr. (J2)) period 0.85 MV, accompanied by gamma-radiation. Only two stable isotopes of Br are known and a search for another has been unsuccessful (B28). The measurements and chemical identification cannot be questioned so some unusual interpretation is required. The *n*-2*n* process has been suggested (K34), but is quite impossible for slow neutrons. The best interpretation seems to be the formation of an isomeric pair in one instance (either Br^{80} or Br^{82}) which decay with different periods into the same product nucleus (see §87). When Br is bombarded by high energy gamma-rays (B47b, B47c, B47d) three periods are observed (18 min., 4.2 hr. and 3.5 min.) two of which are identical with slow neutron periods. The isomeric nuclei must then be Br^{80}; the 3.5 min. period is Br^{78}. This leaves the 35 hr. period for Br^{82}. A still heavier isotope, Br^{83}, is formed in the Se-*d*-*n* reaction with a period of 2.5 hr. (S16a).

Rb, Y, Zr, Cb, Mo

Activities produced in these elements by fast neutrons (P11d) and which have not so far been attributed to definite radioactive elements have the half-lives: 22 hr. (e^-) in Rb, 1.2 hr. and 6.5 hr. (e^-) in Y, 10 min. and 5 hr. in Zr, 7.3 min. and 3.8 days in Cb, and 5 days (e^-) in Mo.

$Ru^{97, 103, 105}$

Kurtschatow, Nemenow, and Selinow (K35) found four activities in Ru produced by slow neutrons; 40 sec., 100 sec., 11 hr., 76 hr. There are only three vacancies in the known stable isotopes of Ru, at 97, 103 and 105. Intensities of the two short periods are identical and the two-step transition is suggested:

$$Ru^{104}+n^1\rightarrow Ru^{105}\ (T=40\text{ sec.})$$
$$\rightarrow Rh^{105}\ (T=100\text{ sec.})\rightarrow Pd^{105}.$$

The first period must be the shorter lived one if the second is to be observable. It should be possible to check this feature by analysis of the half-life curves with short activation times. The two longer periods are then Ru^{97} and Ru^{103}. The 97 isotope would probably be positron active, and so would supply a means of identification, but this feature has not been reported. Livingood (L26) observes periods of 4 hr. 39 hr., 11 da. and 46 da. from Ru on deuteron bombardment. It is probable that the 11 hr. (inaccurately measured) and 75 hr. periods of Kurtschatow are identical with the 39 hr. and 11 da. (very weak intensity) periods of Livingood; such errors in measurement are easily possible under the circumstances. The short periods were not observed by Livingood. This leaves the 4 hr. and 46 da. periods to be assigned to other elements. $Rh^{101, 103}$ are stable, $Rh^{102, 104}$ are known from Rh-*n* reactions and Rh^{105} is excluded by the two-step reaction of Kurtschatow. This makes it improbable that Rh is the source of these activities and they are ascribed to Ma through *d*-α reactions and for which there are many possibilities.

$Rh^{102, 104, 105}$

Two water sensitive neutron produced activities in Rh (A7) suggested a second isotope, which was found by Sampson and Bleakney (S3). The strong period (44 sec.) is ascribed to the more abundant isotope and so is Rh^{104}; the weaker period (3.9 min.) is from the new isotope and is Rh^{102}. The observation of a 100 sec. activity in Ru by neutrons has required the assumption of another radioactive isotope, Rh^{105} (see preceding paragraph). An electron activity of 1.1 hr. half-life, induced in Rh by fast neutrons (P11d), cannot as yet be assigned to a particular element.

$Pd^{107, 109, 111}$

Four radioactive periods are found in Pd on slow neutron bombardment (A7, K36) which are 3 min., 15 min., 12 hr. and 60 hr. There are four available spaces for radioactive isotopes, at 103, 107, 109 and 111, although the first is from an isotope of very low abundance. The 12 hr. period has also been observed in bombardments by deuterons (K25).

$Ag^{105, 106, 108, 110}$

The two usual Ag periods of 22 sec. and 2.3 min. ($Ag^{108, 110}$) are produced by slow neutrons on Ag (A7). The observation of a 24 min. and a 2.3 min. period from gamma-bombardment (B47b, B47c) and fast neutron bombardment (H33b) through what must be Ag-γ-*n* and Ag-*n*-2*n* reactions indicates that the 2.3 min. period, which is common, is Ag^{108}. The 24 min. must then be Ag^{106} and the 22 sec. Ag^{110}. Kraus and Cork (K25) have observed two periods of 32 min. and 7.5 days from the Pd-*d*-*n* reaction. The 32 min. period is probably identical with the 24 min. half-life found in the Ag-γ-*n* and Ag-*n*-2*n* reactions (Ag^{106}). The 7.5 day period has also been produced in Ag by *fast neutrons* (P11d) (the original report of 13 days has been corrected to 7.9 days in a private communication) and was found to emit *electrons*. A tentative explanation might be that Ag^{106} is isomeric, emitting positrons with a period of 24 min. and electrons with the longer half-life.

$In^{112, 114, 116}$

Two periods are observed with slow neutrons (13 sec., 54 min.) and three with fast neutrons (3.5 hr., 1 min., 2 mo.) (A7, S28, C16a, P11d). Gaerttner, Turin and Crane (G1) have measured the beta-spectra of the two slow neutron periods and find 3.0 and 1.1 MV for the limits. A gamma-ray of about 1 MV from the 54 min. period

suggests an excitation state of the product nucleus in this case.

The 1 min. period is observed in the In-γ-n (B47d), the In-n-$2n$ (C16a) and the Cd-p-n reactions and seems certainly to be In^{112}. The 2 mo. activity may be In^{111} through an n-$3n$ process. This still leaves three periods for In^{114} and In^{116} and suggests the existence of an isomeric pair.

$Sn^{121, 123, 125}$

Slow neutron periods of 8 min. and 18 min. are reported by Naidu (N3). Livingood (L27) finds periods of 28 hr. and several months from deuterons on Sn, chemically separable as Sn. The vacancies in the isotopic table for n-γ and d-p reaction products are 113, 121, 123, 125; Sn^{113} would be positron active and such has not been observed. The strong 28 hr. period is also observed in a Sb-d-α reaction and so is Sn^{121}. This leaves the 8 min., 18 min. and several months activities to the two isotopes Sn^{123} and Sn^{125}. It may be that the 8 min. and 18 min. periods are a consecutive process (as in Ru):

$$Sn^{124}+n^1\rightarrow Sn^{125}(T=8m)\rightarrow Sb^{125}(T=18m)\rightarrow Te^{125},$$

which is possible from the arrangement of stable isotopes, and if so the period of some months is Sn^{123}. Livingood also finds short periods of 12 min. and 45 min. on short bombardment without chemical analysis; these are probably the same as Naidu observed, the latter one possibly intermixed with the 54 min. period of In, which might be produced through a d-α reaction.

$Sb^{120, 122, 124, 125}$

Periods of 2.5 da. and 60 da. are observed with slow neutrons (A7, L27b). These are checked by Livingood (L26) with Sb-d-p who measures them as 68 hr. and 50 days. These then represent Sb^{122} and Sb^{124}, coming from the known stable isotopes. A 25 hr. period also observed, but not chemically separated, may well be the 28 hr. period of Sn^{121}, produced in this case by Sb^{123}-d-α. A 16 min. period in Sn bombarded with deuterons (L27b) and separable as Sb must be from a Sn-d-n reaction. The same period is observed with γ-rays and fast neutrons and must be Sb^{120}.

Te, La, Ce, Gd, Ta

Fast neutrons produce in Te a 30 day period, in La a 2.2 hr. period, in Ce a 40 min. period (e^-), in Gd a 19 hr. (e^-) period and in Ta a 9.1 hr. period of which none can be definitely assigned to particular elements at present (P11d).

$Ir^{192, 194, 195}$

A 19 hr. water sensitive period in Ir on neutron bombardment (A7) has not been checked by Sosnowski (S20), who finds two periods of 50 min. and 3 da. Fomin and Houtermans (F27) report still another slow neutron activity of about 2 months half-life. Pool, Cork and Thornton (P11d) find that a 15 hr. electron activity is induced in Ir and a 3 day activity in Pt by fast neutrons. In the disintegration of Pt by deuterons Cork and Lawrence (C35) find electron activities of 28 min. and 8.5 hr., shown by chemical separations to be Ir. These are thought to follow the d-n, α reaction (§102D). The short period is the one for which certain resonance effects are observed in the energy-activation curves. A radioactive Ir isotope is also reported by Cork and Thornton (C36) from Au following the Au-d-p,α reaction discussed in §102E. Since Au has only one isotope this must be Ir^{194}. No assignments are possible with the present complexity of data.

$Pt^{193, 197}$

Platinum shows a 50 min. water sensitive activation with neutrons (A7). Cork and Lawrence (C35) find a 49 min. positron activity from Pt-d-p (supposedly the same activity), and also a 14.5 hr. electron activity, both proven chemically. The 49 min. period would then be Pt^{193} and the long period probably Pt^{197}. A 1.8 hr. electron activity induced in Pt by fast neutrons (P11d) can not be assigned to an element.

Bi^{210}

Livingood (L26) gives satisfactory evidence for the synthesis of Ra E (Bi^{210}) from Bi under deuteron bombardment. It shows the characteristic 5 day electron period and produces an alpha active product identical with Po. A report by Sosnowski (S19) of a 1 hr. period from Bi with neutrons is not confirmed by other observers (A13).

Th

The activity produced in Th is complex, yielding at least 4 distinct periods of beta decay and also alpha-particles. Curie, von Halban and Preiswerk (C60) have made a complete separation and identification of all the activities and find them to consist of a radioactive family of mass type $4n+1$, where n is integral. This is a new type of radioactive family, and adds to the U, Th and Ac series to make a complete paralleling set. It can be described as follows:

$$90^{233} \xrightarrow[25\text{ m}]{\beta} 91^{233} \xrightarrow[2.5\text{ m}]{\beta} 92^{233} \xrightarrow{\alpha}$$

$$90^{229} \xrightarrow{\alpha} 88^{225} \xrightarrow{\alpha} 86^{221} \xrightarrow{\alpha} \text{etc.}$$

Slow neutrons are found to lead to a member of this family though the reaction: $Th^{232}+n^1 \rightarrow Th^{233}$; the resultant beta-activity has a period of 25 min., followed by the subsequent activities of the chain. Fast neutrons are found to emit alphas through the reaction: $Th^{232}+n^1 \rightarrow 88^{229}+He^4$; this isotope has a beta-activity of 1 min. half-life, and is isotopic with radium. A subsequent beta disintegration of period either 15 min. or 3.5 hr. leads to 90^{229}, a member of the above chain:

$$Th^{232}+n^1 \longrightarrow He^4+88^{229}$$

$$\xrightarrow[1\text{ m}]{\beta} 89^{229} \xrightarrow[\begin{cases}15\text{ m}\\3.5\text{ hr}\end{cases}]{\beta} 90^{229} \longrightarrow \text{etc.}$$

More extensive analysis will be necessary before periods of 5 min. and 1.4 hr. induced in Th by fast neutrons (P11d) can be placed.

U

A total of 10 radioactive periods have been reported by Fermi and his associates (A7) and by Meitner and Hahn (M15, M15a). At the most three of these can be listed as direct products of neutron disintegrations, the others being radioactive decay products. The experiments are difficult; they must be performed in the presence of the natural UX_1 and UX_2 beta-active decay products of U, and require some of the most difficult radioactive chemistry. Some of the new activities can be chemically identified with Ac, Pa, or U (90, 91 and 92), but others are not separable with any of the known heavy elements and are certainly due to elements of atomic number 93, 94, 95, etc. Meitner and Hahn have attempted to analyze the results into the radioactive series which must result. Several improbable assumptions are required, but in the present stage it seems the best that can be done with the data. They suggest:

$$U^{238}+n\begin{pmatrix}\text{slow}\\\text{fast}\end{pmatrix} \longrightarrow U^{239} \xrightarrow[10\text{ s}]{\beta} 93^{239} \xrightarrow[2.2\text{ m}]{\beta}$$

$$94^{239} \xrightarrow[59\text{ m}]{\beta} 95^{239} \xrightarrow[66\text{ hr}]{\beta} 96^{239} \xrightarrow[2.5\text{ hr}]{\beta} ?$$

$$U^{238}+n(\text{fast}) \longrightarrow 2n^1+U^{237} \xrightarrow[40\text{ s}]{\beta}$$

$$93^{237} \xrightarrow[16\text{ m}]{\beta} 94^{237} \xrightarrow[6\text{ hr}]{\beta} 95^{237} \longrightarrow ?$$

$$U^{238}+n(\text{slow}) \longrightarrow He^4+90^{235} \xrightarrow[4\text{ m}]{\beta}$$

$$91^{235} \xrightarrow[\text{very short}]{\beta} 92^{235} \longrightarrow ?$$

It is also possible that U^{235} (AcU), which is present to about 5 percent, may be involved to give some of the activities:

$$U^{235}+n(\text{slow}) \longrightarrow U^{236} \xrightarrow[23\text{ m}]{\beta} 93^{236} \longrightarrow ?$$

XVIII. Nuclear Masses

§106. The Mass Spectrograph

The term "mass spectrograph" is applied to instruments designed to study the mass and the relative abundance of atomic species. By the use of electric and magnetic fields these instruments separate ions of different e/m values; ions having a common e/m but differing in direction and energy within certain limits are brought to a common focus. Masses are determined by comparison of the deflections obtained to that of O^{16} ions or suitable sub-standards.

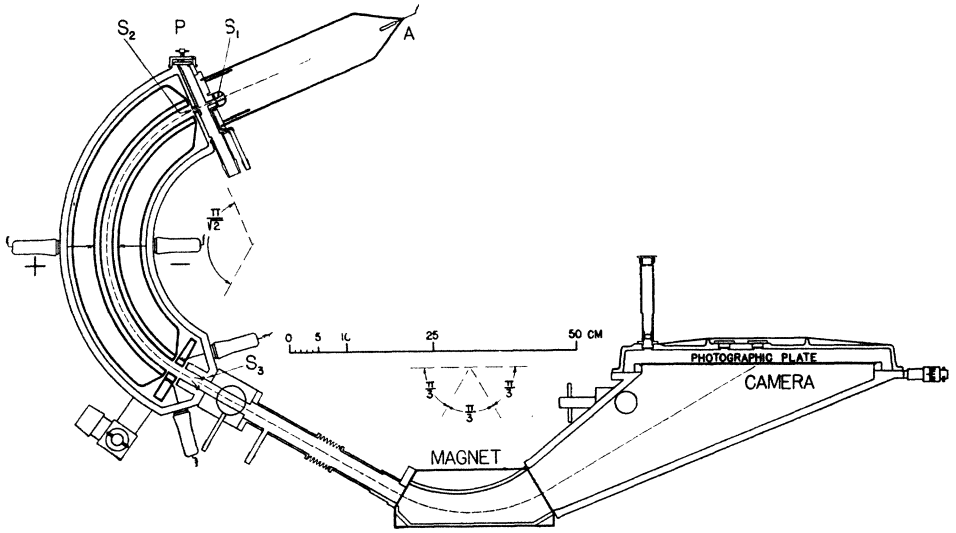

FIG. 49. Scale diagram of mass spectrograph. (Bainbridge and Jordan.)

A variety of focusing schemes have been utilized, some resulting in velocity focusing, some in direction focusing (of noncollimated ion beams), some aimed more directly at achieving a linear mass scale. The instrument was originally developed by Aston (A18), using consecutive electrostatic and magnetic focusing of a well collimated ion beam. If θ is the average angle of deflection of the electric field and ϕ that of the magnetic field the focusing condition requires that $d\theta/\theta = 2d\phi/\phi$. This results in a focus of the different ions along a flat photographic plate; the mass scale is not linear and must be determined from calculations of the geometry of the focusing conditions. The resolution is determined by the accuracy of collimation of the slits defining the beam of ions from the source.

A method perfected by Dempster (D27) uses the focusing of ions of different primary directions by a 180° magnetic field. The ions must have homogeneous energy, which limits the resolution in this case. The e/m values of ions traversing the fixed slit systems are inversely proportional to the square of the magnetic field required to bring the ions to the exit slit.

Many subsequent improvements and modifications, involving several different types of focusing, have resulted in instruments adaptable to a variety of purposes. Excellent reviews of the subject and discussions of the focusing principles are contained in the publications of Brüche and Scherzer (B65) and of Mattauch (M10a).

The instrument which has been most successful in obtaining accurate values of atomic masses is that developed by Bainbridge and Jordan (B2a). The focusing principle involves the radial electric field velocity analyzer of Hughes and Rojansky and the magnetic focusing of ions which differ in velocity. A radial electrostatic field of $\pi/(2)^{\frac{1}{2}}$ radians extent and a magnetic field of $\pi/3$ radians are used. The fields are so placed that the dispersion of ions of different velocities produced by the electric field is just compensated by the dispersion of the magnetic field. A scale drawing of the instrument is given in Fig. 49. Ions entering the radial electric field having a spread in velocities of 3 percent are brought to focus on a flat photographic plate. Furthermore the method allows the use of ion beams diverging in direction by a considerably greater amount than possible in other types of apparatus, thus resulting in higher intensities.

The ions are produced in a low pressure discharge tube of standard design. Ions of gaseous elements are obtained by introducing the gas directly into the discharge tube. Metallic elements are used as cathodes or introduced into other cathodes to provide ions of other elements; neon gas is used to stabilize the discharge in such cases. The ions have energies of 15,000 to 20,000 volts, and are deflected through the electrostatic analyzer (radius 25 cm) by fields

of the order of 1200 volts/cm. The magnet provides a suitable field across a 0.32 cm. gap, and the edges of the poles are machined to correct for the effect of stray fields. This focusing principle results in a linear mass scale along the photographic plate; over a region 14 cm long the divergences from linearity are of the order of 1 part in 5000. The resolving power of the instrument can be calculated from the geometry and shows a maximum of $M/\Delta M = 5000$. This instrument has the special advantages of a linear mass scale, a high resolving power and a simultaneous focusing of velocity and direction of the ions.

In the analysis of the results of mass-spectrographic observations the direct comparison of the photographic traces of the ions with e/m values differing from that of O^{16} is handicapped by any nonlinearity of the mass scale and by the many sources of experimental error. This has resulted in the past in mass values now known to be in error by amounts greatly exceeding those computed from the internal consistency of the data. The method of bracketing ion "doublets" of essentially the same e/m values has eliminated most of these difficulties. This involves the simultaneous analysis of ions differing in nature but having the same integral values of e/m. In this way two closely-spaced photographic traces can be obtained whose spacing represents the mass difference of the two ions, and is relatively free from errors in the absolute calibration of the mass scale. For instance $(O^{16})^+$ and $(S^{32})^{++}$ may be compared directly since they have the same e/m values (the electronic masses must be added to obtain the atomic masses usually quoted).

The method of using ion doublets has been most satisfactorily employed by Bainbridge and Jordan (B2 etc.). They use doublets matched in intensity so that the spacings can be measured accurately. A variety of molecular ion doublets have been studied, such as: $(O^{16}H^1)^+$ and $(N^{14}H^1_3)^+$, $(O^{16})^+$ and $(C^{12}H^1_4)^+$, $(N^{14})^+$ and $(C^{12}H^1_2)^+$, etc. Triplets such as $(C^{12})^{++}$, $(He^4H^2)^+$ and $(H^2_3)^+$ are also obtained. By grouping and comparing mass differences from such doublets accurate values of the atomic masses of many of the light atoms have been obtained. The errors involved are in general smaller than those of mass values calculated from disintegration data.

An interesting application of this method is in the possibility of obtaining the mass difference representing the reaction energy of a nuclear reaction, enabling a direct comparison with disintegration data. For example, Bainbridge and Jordan (B1) have obtained the Q value of the C^{12}-d-p reaction from the two doublets $(C^{12}H^1)^+ - (C^{13})^+$ and $(H^2)^+ - (H^1_2)^+$ and find it to be 0.00297 mass units, or 2.76 MV, while that obtained by an evaluation of the disintegration data of Cockcroft and Lewis (C29) is 2.71 MV.

§107. Masses from Mass Spectrograph

The most extensive and accurate mass determinations are those made during the last year by Bainbridge and Jordan (B1, B2, J5, J6, and private communication[22]) using the doublet method. Care was always taken that each "line" was symmetrical and that the lines of a doublet were of equal intensity. The region of "linear dispersion" of the mass spectrograph was used. Many internal cross checks are provided by comparing connected doublets, such as $C^{12}H_4 - O^{16}$, $C^{12}H_2 - N^{14}$, $N^{14}H_2 - O^{16}$ and $N_2 - C^{12}O^{16}$, and all of them check within the given "experimental error." The agreement with the best disintegration data (§108) is also gratifying, including the few cases (e.g., $C^{12}H_4 - O^{16}$) in which Bainbridge and Jordan's data do not agree with Aston's. With very few exceptions (see below), we have used Bainbridge and Jordan's measurements as a basis of our mass table (Table LXX).

Aston's measurements (A17, A18, A19, A20, A21) agree, in general, with those of Bainbridge and Jordan within the experimental errors given. The most notable exceptions are the doublets $C^{12}H_4 - O^{16}$ and $C^{12}H_2 - N^{14}$. Our decision in favor of Bainbridge and Jordan's values (cf. also Mattauch, M10b) was made on the basis of the cross checks mentioned above which confirm Bainbridge and Jordan's values. In some other cases, the combined evidence of all mass spectrograph and disintegration data agrees slightly better with Aston's determination than with Bainbridge and Jordan's. This is true of the doublet $B^{10} - \frac{1}{2}Ne^{20}$ (Table LXXI) for which the

[22] We are very much indebted to Professor Bainbridge for communicating his most recent (March 24, 1937) results to us which made it possible to bring this section up to date.

value derived from the "adopted masses" (Table LXXIII) differs by 0.16 units from Bainbridge-Jordan, but only 0.07 units from Aston. Also Aston's value of the He^4 mass seems to give better agreement with the numerous disintegration data from α-particle reactions (§108) therefore we have used the average between his determination and that of Bainbridge-Jordan for the mass of He^4.

Aston's measurements extend to higher atomic weights, including F^{19} Si^{28} Si^{29} P^{31} S^{32} Cl^{35} Cl^{37}. These data were used in Table LXX, due corrections being made for the atomic weights of the "standards": E.g., Si^{28} was measured against $C^{12}O^{16}$; the value for the doublet separation CO-Si was taken from Aston's data but the mass of C^{12} inserted from Bainbridge's determination.

Mattauch (M10) measured the masses of the rare isotopes N^{15} and O^{18} against $N^{14}H$ and $O^{16}H_2$, respectively. The former was also measured by Bainbridge and Jordan, the agreement being sufficient.

The key measurements for the determination of all the masses lighter than oxygen are the three doublets measured by Bainbridge and Jordan (rechecked values, private communication):

$$H_2-D=\ 1.53\pm0.04, \qquad (a)$$

$$D_3-\tfrac{1}{2}C^{12}=42.19\pm0.05, \qquad (b)$$

$$C^{12}H_4-O^{16}=36.49\pm0.08. \qquad (c)$$

All values here, and in Table LXXI, are given in thousandths of a mass unit. The errors are those given by Bainbridge and Jordan in cases (a) and (b) while we have given a smaller error for CH_4-O. This doublet is based on 24 independent measurements, from 4 different plates, none of the measurements deviating more than 0.3 unit, so that 0.08 is more than twice the mean square error. The value given in (c) agrees, within the error given, with the sum of the two doublets

$$C^{12}H_2-N^{14}=12.74\pm0.11, \qquad (d)$$

$$N^{14}H_2-O^{16}=23.69\pm0.15, \qquad (e)$$

viz. 36.43 ± 0.19. These doublets have also been measured many times. Another check was provided by

$$N_2-CO=11.17\pm0.2, \qquad (f)$$

based on not quite so many measurements. The values derived are

$$2(d)+(f)=36.65\pm0.3,$$
$$2(e)-(f)=36.21\pm0.4.$$

The larger deviation from the direct determination (c) does not seem serious, in view of the fact that the mean error in $2(d)+(f)$ and $2(e)-(f)$ is enhanced by the necessity of multiplying the result for one of the doublets by two, and by the smaller intrinsic accuracy of (f).

From the doublets (a) (b) (c) we find

$$H=\tfrac{1}{16}O^{16}+\tfrac{3}{8}(a)+\tfrac{1}{8}(b)+\tfrac{1}{16}(c),$$
$$D=\tfrac{1}{8}O^{16}-\tfrac{1}{4}(a)+\tfrac{1}{4}(b)+\tfrac{1}{8}(c),$$
$$C^{12}=\tfrac{3}{4}O^{16}-\tfrac{3}{2}(a)-\tfrac{1}{2}(b)+\tfrac{3}{4}(c),$$

i.e., for the atomic weights

$$H=\ 1.008\ 13\pm0.000\ 017,$$
$$D=\ 2.014\ 73\pm0.000\ 019,$$
$$C^{12}=12.003\ 98\pm0.000\ 09.$$

From these "secondary standards," the determination of other masses is straightforward. N^{14} is found by averaging the results obtained from d, e, and f. (The result differs by 0.04 unit from that obtained by B. and J. from d and e only.) Li^7 is connected to N^{14} by the doublet $Li^7-\tfrac{1}{2}N^{14}$ (cf. Table LXXI). He^4 is obtained from the doublet D_2-He, using the average of the determinations of Aston and Bainbridge-Jordan. Ne^{20} comes directly from $O^{16}D_2-Ne^{20}$, Ne^{21} from $Ne^{20}H-Ne^{21}$.

The boron isotopes are the only ones for which the agreement between various determinations is not quite perfect. B^{10} is compared to nuclei already mentioned in two ways, *viz.* by means of the doublets

$$B^{10}H_2-C^{12}=28.74\pm0.14, \qquad (g)$$

$$B^{10}-\tfrac{1}{2}Ne^{20}=16.75\pm0.15. \qquad (h)$$

From these doublets and the masses of C^{12} and Ne^{20} as previously determined, we find

$B^{10}=10.016\ 46\pm0.000\ 18$ (from C^{12} and g),
$B^{10}=10.016\ 16\pm0.000\ 16$ (from Ne^{20} and h).

The average is

$$B^{10}=10.016\ 31,$$

TABLE LXX. *Masses from mass spectrograph.*

NUCLEUS	MASS	AUTHOR	ASTON MASS
H^1	1.008 13±0.000 017	B	1.008 12±0.000 04
H^2	2.014 73±0.000 02	B	2.014 71±0.000 07
He^4	4.003 89±0.000 07	B+A	4.003 91±0.000 16
Li^7	7.018 18±0.000 12	B	
Be^9	9.015 16±0.000 2	B	
B^{10}	10.016 31±0.000 20	B	10.016 1 ±0.000 3
B^{11}	11.012 92±0.000 16	B	
C^{12}	12.003 98±0.000 09	B	12.003 55±0.000 15
C^{13}	13.007 61±0.000 15	B	
N^{14}	14.007 50±0.000 08	B	14.007 3 ±0.000 5
N^{15}	15.004 89±0.000 2	B	
O^{16}	16.000 000		
O^{18}	18.003 69±0.000 20	M	18.005 7 ±0.000 2*
F^{19}	19.004 52±0.000 3	A	19.004 5 ±0.000 6
Ne^{20}	19.998 81±0.000 11	B	19.998 6 ±0.000 6
Ne^{21}	20.999 68±0.000 23	B	
Ne^{22}	21.998 64±0.000 36	B	
Si^{28}	27.986 8 ±0.000 6	A	27.986 3 ±0.000 7
Si^{29}	28.986 6 ±0.000 7	A	28.986 4 ±0.000 8
P^{31}	30.984 1 ±0.000 5	A	30.983 6 ±0.000 6
S^{32}	31.982 3 ±0.000 3	A	31.982 3 ±0.000 3
Cl^{35}	34.981 3 ±0.000 7	A	34.980 0 ±0.000 8
Cl^{37}	36.978 8 ±0.000 8	A	36.977 5 ±0.000 8
A^{36}			35.978 0 ±0.001 0*
A^{40}	39.975 04±0.000 26	B	39.975 4 ±0.001 4

A = Aston
B = Bainbridge and Jordan
M = Mattauch
* Added in proof. (A21a)

which is just within the experimental error of the two determinations mentioned. Aston's determination of the $B^{10}-\frac{1}{2}Ne^{20}$ doublet (16.84) gives better agreement with the average. For B^{11}, we have then again two determinations, one in terms of C^{12} through the doublet $B^{11}H-C^{12}$ and one in terms of B^{10} through $B^{10}H-B^{11}$. The results for the mass are 11.012 99 and 11.012 84, respectively; the average was taken in Table LXX. Finally, there are again two determinations for Be^9, from the doublets Be^9H-B^{10} and $Be^9H-\frac{1}{2}Ne^{20}$: They agree almost perfectly, giving 9.015 18 and 9.015 14, respectively, for the mass of Be^9.

A^{40} was found by averaging the "direct" determination $OD_2-\frac{1}{2}A^{40}$ with the "indirect" OD_2-Ne^{20} plus $Ne^{20}-\frac{1}{2}A^{40}$; Ne^{22} from $B^{11}-\frac{1}{2}Ne^{22}$. The other nuclei ($C^{13}$ N^{15} O^{18} F^{19} Si^{28} Si^{29} P^{31} S^{32} Cl^{35} Cl^{37}) appear in just one "doublet" each (cf. Table LXXI), so that their determination is straightforward, inserting for the "standards" to which these nuclei are compared ($C^{12}H$, $N^{14}H$, etc.) the values obtained from the foregoing analysis. The masses determined in this way are listed in Table LXX, together with those given by Aston.

The masses given in Table LXX were adopted for the final mass table (LXXIII) and used as a basis for obtaining additional masses from disintegration data (§108), with the exception of Be^9, Si^{28}, P^{31}, Cl^{35} and Cl^{37}. For Be^9, the disintegration data are very good and give consistently lower results for the Be^9 mass, *viz.* 9.015 04 instead of 9.015 16. Si^{28} and P^{31} are connected by the well-investigated reaction $Si^{28}+He^4=P^{31}+H^1$ whose observed reaction energy (−2.23 MV) does not agree completely with that calculated from spectrograph masses (−1.45 MV); the discrepancy was distributed on the masses of Si^{28} (0.2 MV) and of P^{31} (0.2 MV) and on the reaction energy (0.4 MV). For Cl^{35}

TABLE LXXI. *Measured mass-spectrograph "doublets." (In thousandths of a mass unit.)*

DOUBLET	AUTHOR	OBSERVED	CALCUL.	DIFF.
H_2-D	B	1.53±0.04	1.53	*
	A	1.52±0.04	1.53	0.01
D_2-He	B	25.61±0.04	25.56	0.05Δ
	A	25.51±0.08	25.56	0.05Δ
Be^9H-B^{10}	B	6.96±0.20	6.86	0.10
$B^{10}H-B^{11}$	B	11.60±0.10	11.52	0.08Δ
$D_3-\frac{1}{2}C^{12}$	B	42.19±0.05	42.20	*
	A	42.36±0.18	42.20	0.16
$B^{10}H_2-C^{12}$	B	28.75±0.20	28.59	0.16Δ
$B^{11}H-C^{12}$	B	17.14±0.10	17.07	0.07Δ
$C^{12}H-C^{13}$	B	4.5 ±0.1	4.51	*
$Li^7-\frac{1}{2}N^{14}$	B	14.43±0.1	14.43	*
$C^{12}H_2-N^{14}$	B	12.74±0.08	12.74	0.00Δ
	A	12.45±0.07	12,74	0.29
$C^{12}H_3-N^{15}$	M	23.82±0.08	23.48	0.34
$N^{14}H-N^{15}$	B	10.74±0.2	10.74	*
$C^{12}H_4-O^{16}$	B	36.49±0.08	36.50	*
	A	36.01±0.24	36.50	0.49
$N^{14}H_2-O^{16}$	B	23.69±0.15	23.76	0.07Δ
$N_2^{14}-C^{12}O^{16}$	B	11.17±0.20	11.02	0.15Δ
$O^{16}H_2-O^{18}$	M	12.57±0.18	12.57	*
$O^{16}DH-F^{19}$	A	18.33±0.26	18.33	*
$Be^9H-\frac{1}{2}Ne^{20}$	B	23.91±0.20	23.77	0.14
$B^{10}-\frac{1}{2}Ne^{20}$	B	16.75±0.15	16.91	0.16Δ
	A	16.84±0.15	16.91	0.07
$O^{16}D_2-Ne^{20}$	B	30.65±0.10	30.65	*
	A	30.82±0.40	30.65	0.17
$Ne^{20}H-Ne^{21}$	B	7.26±0.20	7.26	*
$B^{10}H-\frac{1}{2}Ne^{22}$	B	25.1 ±0.5	25.12	0.02
$B^{11}-\frac{1}{2}Ne^{22}$	B	13.60±0.15	13.60	*
$C^{12}O^{16}-Si^{28}$	A	17.2 ±0.6	17.4	0.2Δ
$B^{10}F^{19}-Si^{29}$	A	34.2 ±0.6	34.2	*
$C^{12}F^{19}-P^{31}$	A	24.4 ±0.5	24.2	0.2Δ
$O_2^{16}-S^{32}$	A	17.7 ±0.3	17.7	*
$C_3^{12}-Cl^{35}H$	A	22.5 ±0.7	23.4	0.9
$C_3^{12}H-Cl^{37}$	A	41.2 ±0.7	42.1	0.9Δ
$O^{16}D_2-\frac{1}{2}A^{40}$	B	41.89±0.20	41.94	0.04Δ
$N_e^{20}-\frac{1}{2}A^{40}$	B	11.30±0.20	11.29	0.01Δ
	A	10.88±0.3	11.29	0.41

A = Aston
B = Bainbridge and Jordan
M = Mattauch
* used as standard to calculate one of the masses involved.
Δ used in combination with other data to calculate masses.

TABLE LXXII. *Energy evolution in important nuclear disintegrations.*
A. Reactions produced by deuterons and protons and yielding charged particles.

Reaction	Reference	Energy Inc. Part. MV	Obs. Range cm	Straggling and Thick Target Corrections: Straggling % Range	Straggling % Angle	β	Corr. cm	Mica Corr. cm	Obliquity Corr. cm	Mean Range cm	Energy Prod. Part. MV	Q MV	Q Calc. MV
$H^2+H^2=H^3+H^1$	O8	0.20	14.70±0.05	2.07	2.58	2.7	0.36	0.00_5	0.02_5	14.37 ±0.10	3.04 ±0.01_2	3.98±0.02	3.98*
$Li^6+H^1=He^4+He^3$	N4	0.12	1.19 M	for He^3†			+0.03†			1.22 ±0.04	2.17$_5$±0.04	3.72±0.08	3.76
			0.82 M	for He^4†			+0.03†			0.85 ±0.04	1.62 ±0.08	3.72±0.18	‡‡
$Li^6+H^2=2He^4$	O8	0.19	12.70±0.05	1.05	1.36	4.32	0.18	0.00_5	0.02	12.50 ±0.07	11.05$_5$±0.03_6	22.07±0.07	22.17*
$Li^6+H^2=Li^7+H^1$	C25	0.500	30.5±0 6	1.96	1.31	0.82	0.35	0.34		30.5 ±0.8	4.71 ±0.10	5.02±0.12	4.92*
$Li^7+H^1=2He^4$	O8	0.20	8.40±0.03	1.10	1.13	1.82	0.09			8.31 ±0.04	8.63$_5$±0.03	17.13±0.06	17.25
$Be^9+H^1=Li^6+He^4$	K16	0.12	0.74 M†				+0.02†			0.76 ±0.04	1.43 ±0.08	2.28±0.13	2.25
$Be^9+H^1=Be^8+H^2$	O9	0.20	0.74 M	2.2	1.45	0.26	+0.01			0.75 ±0.06	0.51 ±0.06	0.46±0.08	0.49
$Be^9+H^2=Li^7+He^4$	O9	0.20	‡	1.22	1.31	1.46	0.00					7.19±0.12	7.17*
$Be^9+H^2=Be^{10}+H^1$	O9	0.20	25.6		large			0.2		25.8 ±1.0	4.32 ±0.10	4.59±0.11	4.59*
$B^{10}+H^2=Be^8+He^4$	C28	0.55	14.75±0.07	1.03_5	1.89	2.26	0.22	0.08		14.61 ±0.10	12.11$_5$±0.05	17.76±0.08	17.90
$B^{10}+H^2=B^{11}+H^1$	C28	0.55	90.7 ±0.6	1.81	1.20	1.66	1.25	1.9_5		91.4 ±1.0	8.79 ±0.05	9.14±0.06	9.30
			58.5 ±0.7	1.86	1.34	1.36	0.8	1.0		58.7 ±1.0	6.83 ±0.07	7.00±0.08	—
			30.7 ±0.3	1.96	0.83	0.88	0.32	0.35		30.7 ±0.5	4.72$_5$±0.04_5	4.71±0.05	—
$B^{11}+H^1=Be^8+He^4$	O9	0.20	4.40±0.06 M	1.15	0.79	1.28	+0.03_5		−0.02	4.41$_5$±0.08	5.83 ±0.07	8.60±0.11	8.60*
$B^{11}+H^2=Be^9+He^4$	C28	0.55	4.60±0.07	1.15	2.30	1.07	0.06	−0.01		4.53 ±0.09	5.92 ±0.08	8.13±0.12	8.11*
$C^{12}+H^2=C^{13}+H^1$	C29	0.563	13.85±0.12	2.08	1.73	0.72	0.17	0.08		13.76 ±0.12	2.95$_5$±0.017	2.71±0.05§	2.76
$C^{13}+H^2=B^{11}+He^4$	C29	0.55	2.70±0.05	1.24	2.23	0.76	0.03	−0.01		2.66 ±0.05	4.17 ±0.05	5.24±0.11	5.14
$N^{14}+H^2=C^{12}+He^4$	C29	0.575	11.37±0.10	1.06	1.54	1.17	0.12	0.04		11.29 ±0.18	10.41 ±0.10	13.40±0.15	13.37
			6.20±0.10	1.11_5	1.75	1.28	0.07	0.00		6.13 ±0.10	7.17 ±0.065	9.08±0.09	—
$N^{14}+H^2=N^{15}+H^1$	C29	0.575	85.1 ±1.0	1.81	0.91	1.74	1.1	1.75		85.7_5 ±1.3	8.48 ±0.07	8.55±0.08	8.57
			18.24±0.3	2.04	1.41	0.82	0.20	0.13		18.17 ±0.3	3.48 ±0.03_3	3.11±0.04	—
$O^{16}+H^2=N^{14}+He^4$	C29	0.575	1.59±0.05	1.25	2.30	0.26	0.01	−0.01		1.57 ±0.07	2.81$_5$±0.09$_5$	3.13±0.13	3.11
$O^{16}+H^2=O^{17}+H^1$	C29	0.575	9.22±0.07	2.15	1.45	0.62	0.10	0.02		9.14 ±0.07	2.32 ±0.01	1.95±0.06	1.95*
			4.35±0.12	2.30	1.72	0.40	0.04_5	−0.01		4.59_5±0.15	1.54 ±0.03	1.12±0.07	—
$F^{19}+H^1=O^{16}+He^4$	H22	1.69‖	6.95±0.15	1.11	2.06	0.92	0.02			6.93 ±0.15	7.72 ±0.10	8.15±0.12¶	8.14
$Na^{23}+H^2=Ne^{21}+He^4$	L15	2.15	6.5±0.2**	1.1	2.75	0.15	0.13			6.44 ±0.2	7.39 ±0.14	6.85±0.20	6.76*
$Na^{23}+H^2=Na^{24}+H^1$	L15	2.15	53.1±4††	1.89	1.6	0.29	0.4	1.5		55.4 ±4	6.61 ±0.27	4.92±0.30	4.94*
$Al^{27}+H^2=Mg^{25}+He^4$	Mc5	2.20	6.37±0.2**				0.05			6.32 ±0.2	7.31 ±0.14	6.46±0.14	6.46*
$Al^{27}+H^2=Al^{28}+H^1$	Mc5	2.20	67.2 ±4				0.5	2.2		68.9 ±4	7.50 ±0.3	5.79±0.3	5.79*

M = Mean range. The straggling and thick target corrections must be *added* instead of subtracted.
* Used for calculation of masses.
† Mean range measured in cloud chamber. The average depth in the target at which the reaction occurs was estimated (0.03 and 0.02 cm for Li^6 $p\alpha$ and Be^9 $p\alpha$, respectively) from the Gamow disintegration function, and added to the observed mean range.
‡ Range not given by authors, but only reaction energy (7.21 MV). The straggling correction applied by Oliphant, Kempton and Rutherford (range straggling only) is exactly equal to that calculated from our scheme. The only correction to be made is thus the change in the range-energy relation.
§ Average of five determinations at different deuteron energies.
‖ The energy of the protons was deduced by the authors from the range and given as 1.63 MV. The change in the range-energy relation increases this figure to 1.69 MV.
¶ Average of six determinations at different proton energies.
** The ranges were given by the authors for air at 20°C. The value given here is corrected to the standard temperature of 15°C.
†† The stopping power of Al was assumed to be 4.4 cm air of 15°C per mil of Al rather than 4.0 cm air of 20°C as assumed by the authors.
‡‡ Used for determining the range-energy relation.

the mass was determined from the reaction $S^{32}+He^4=Cl^{35}+H^1$. Cl^{37} was obtained by assuming that it differs from the value given by Aston by the same amount (+0.4 unit) as Cl^{35}.

The masses obtained in this way are given in Table LXXIII, §108, together with estimated errors. The latter are based on the estimates given by the respective authors and are believed to be rather larger (about by a factor two) than the mean errors. Table LXXI gives, for each measured doublet, besides the observed value also the one calculated from the adopted masses in Table LXXIII. The agreement is gratifying.

§108. Masses from Disintegration Data

As is well known, disintegration data gave the first indication of an error in the then accepted nuclear mass values (B11, O9). The extent of the error has since been found to be greater than had been supposed at first (mass of He^4 according to old scale 4.002 16; suggested by Bethe in 1935, 4.003 36; new value, 4.003 89). Subsequently, improved disintegration masses were given by Cockcroft and Lewis (C29) and by Bonner and Brubaker (B40), both of them in substantial agreement with the now accepted masses. With the improvement of mass spectrograph technique, it seems that the mass spectrograph determinations are now superior to the disintegration values, especially for comparing atoms of widely different mass such as *D* and *C*. The chief value of the disintegration data consists now in four points:

1. To provide a check of the mass spectrograph data.

2. To deduce the masses of radioactive nuclei and of nuclei too rare to be measured in the mass spectrograph.

TABLE LXXII*B*. *Reactions of the α-p type.*

REACTION	REF.	α-PART. ENERGY MV	ANGLE BETWEEN α AND PART.	PROTON RANGE CM	MICA CORRECTION	PROTON ENERGY MV	RECOIL ENERGY MV	*Q* MV	*Q* CALC. MV
$(B^{10}+He^4=C^{13}+H^1$	M16	5.30	0°	82	1.8	8.37	0.22	3.29 }	4.15)
		5.30	90°	61	1.1	7.06	1.54	3.30 }	
$N^{14}+He^4=O^{17}+H^1$	P9	8.36	45°	48	0.7	6.15	1.05	−1.16	−1.16‡
$F^{19}+He^4=Ne^{22}+H^1$	C4	5.30	0°	56	0.8	6.71	0.17	1.58	1.53
$(Ne^{20}+He^4=Na^{23}+H^1$	P9	8.36	45°	32.5	0.4	4.92	0.90	−2.54	−1.42)
$Na^{23}+He^4=Mg^{26}+H^1$	K21	4.44	0°	49	0.7	6.22	0.13	1.91	1.9
$Mg^{24}+He^4=Al^{27}+H^1$†	D19	7.68	0°	39.5	0.5	5.49	0.37	−1.82	−1.6
$Mg^{25}+He^4=Al^{28}+H^1$†	D19	7.68	0°	50	0.8	6.30	0.33	−1.05	−0.6
$Al^{27}+He^4=Si^{30}+H^1$	D19	7.68	0°	107	2.5	9.74	0.20	2.26	2.26*
$Si^{28}+He^4=P^{31}+H^1$	H19	8.78	75°	38.0	0.5	5.48	1.07	−2.23	−1.8*
$(P^{31}+He^4=S^{34}+H^1$	M11	7.68	75°	62	1.1	7.13	0.88	0.31	1.9)
$S^{32}+He^4=Cl^{35}+H^1$	H19	8.78	75°	42.5	0.6	5.73	0.95	−2.10	−2.1*
$(Cl^{35,\ 37}+He^4=A^{38,\ 40}+H^1$	P8	8.36	0°	88	1.8	8.71	0.23	0.16	?)
$K^{39}+He^4=Ca^{42}+H^1$	P8	8.36	0°	70	1.6	7.65	0.24	−0.89	?
$Ca^{40}+He^4=Sc^{43}+H^1$	P9	8.36	45°	19	—	3.59	0.60	−4.27	?

( ) Parentheses indicate that the longest proton group has probably not yet been observed.
* Used for calculating masses.
† Concerning the assignment of the proton groups to the nuclei Mg^{24} Mg^{25}, cf. §99A.
‡ Standard reaction for evaluating effective angle in experiments of Pollard and Brasefield.

TABLE LXXII*C*. *Reactions producing neutrons.*

REACTION	REF.	ENERGY OF INCID. PART.	NEUTRON ENERGY GIVEN (MV)	STOPPING POWER OF GAS	CORRECTIONS TO ENERGY (MV)			CORRECTED NEUTRON ENERGY	*Q* MV	*Q* CALC. MV
					Stopp. Power	Range-En. Rel.	Straggl., Obliquity etc.			
$H^2+H^2=He^3+n^1$	B38	0.50	2.53	0.960‡	+0.02	−0.03	−0.01	2.51	3.18	*
$Li^7+H^2=Be^8+n^1$	B37	0.85	13.5	0.906‡	0†	−0.01	0.03	13.5	14.55	14.91
$Be^9+H^2=B^{10}+n^1$	B40	0.9	4.52	0.934‡	−0.05	−0.02	+0.02	4.47	4.20	4.18
$B^{10}+H^2=C^{11}+n^1$	B40	0.9	6.35	0.918‡	−0.13	−0.02	+0.05	6.25	6.08	6.34
$B^{11}+H^2=C^{12}+n^1$	B40	0.9	13.2	0.896‡	−0.17†	−0.01	+0.05	13.07	13.4	13.68
$C^{12}+H^2=N^{13}+n^1$	C29	0.32	Threshold of reaction					0	−0.28	*
$O^{16}+H^2=F^{17}+n^1$	N6	1.95	" " "					0	−1.7	*
$O^{18}+H^1=F^{18}+n^1$	D28	2.7	" " "					0	-2.5_5	*

* Used as standard for computing masses.
† Part of the path is in mica, part in the gas.
‡ Assumed = 0.950 by Bonner and Brubaker.

3. To find excited levels in nuclei (§109) and, most of all,

4. To establish and confirm the interpretation of nuclear reactions.

A. Computation of energy evolution

The method for deriving accurate values of the energy evolved in a nuclear reaction was described in Chapter XVI. The results for all reactions in which the ranges of the produced particles were measured, were given in the tables at the end of §§99–102. In Table LXXII, we have listed the most important nuclear reactions and given an account of how the energy evolution *Q* was calculated. The first column gives the reaction, the second the reference to the paper in which the observations were reported, the third the energy of the incident particles. In all reactions listed in part *A* of Table LXXII, the observation of the range recorded in the fourth column was at right angles to the incident beam and the geometry was "good" in the sense of §§96, 97. The following columns in Table LXXII*A* give the ordinary (range) straggling (§97*A*) and the angle straggling (§96*b*) in percent, the quantity β determining the thick target correction (§97*C*), the difference between extrapolated and mean range deduced from straggling and thick target correction in cm, the mica correction (§95*E*) where necessary, and the obliquity correction (§96*b*) which was only computed for the most accurate experiments. With

the three last named corrections applied to the observed range, the corrected mean range is obtained; from this the corresponding energy of the produced particles is calculated with the help of the range-energy relations of Figs. 29, 30. This energy corresponds to emission exactly at right angles, so that the energy evolution Q follows from (768). This "observed" energy evolution and the energy evolution calculated from the masses of Table LXXIII are listed in the last two columns.

In Table LXXII*B*, we have listed some of the more important α-p-reactions. In these cases, the geometry is necessarily poor because of the low intensity. It was customary in experimental papers to assume that the particles of maximum range observed are emitted at the most forward angle permissible by the experimental arrangement. This is certainly not the case (§§96, 97) because so few particles will have this maximum possible energy that they cannot be observed. We have therefore estimated a probable angle which we believe to correspond approximately to the fastest disintegration products observed. This angle was estimated from the given geometrical arrangement in all cases except for the experiments of Pollard and Brasefield. For these, the estimate was based on the reaction $N^{14}+He^4=O^{17}+H^1$ whose reaction energy is very exactly known from mass-spectrograph data combined with the reaction energy of $O^{16}+H^2=O^{17}+H^1$. The N^{14}-α-p reaction was measured by Pollard and Brasefield with the same apparatus as were the reactions with heavier targets. Therefore we computed the "probable angle" so that P. and B.'s measurements gave the correct answer for the N^{14} reaction, and used this value throughout. In all cases, only the data for the longest proton group were given.

In Table LXXII*C*, we have given the most reliable data on reactions in which neutrons are produced. All these data are based on cloud chamber measurements of the ranges of recoil protons emitted within a small angle about the direction of the neutrons. In column 4 we have listed the neutron energy given by the authors (Bonner and Brubaker). In the next column the stopping power of the gas used in the cloud chamber is given; this was a mixture of 85.1 percent CH_4, 13.5 percent C_2H_6 and 1.4 percent N_2. Bonner and Brubaker assumed a stopping power of 0.950 for this mixture; the correction caused by the difference between this figure and the actual stopping power is given in column 6. The range-energy relation used by Bonner and Brubaker was that given by Mano (M6); the necessary correction is listed in column 7. The following column gives all other corrections, for straggling, for thick target and for the fact that

TABLE LXXIII. *Atomic masses.*

NUCLEUS	MASS	ERROR IN 10^{-5} M.U.	SOURCE
n^1	1.008 97	6	$H^2+\gamma=H^1+n^1$
H^1	1.008 13	2	B
H^2	2.014 73	2	B
H^3	3.017 05	7	$H^2+H^2=H^3+H^1$
He^3	3.017 07	12	$H^2+H^2=He^3+n^1$
He^4	4.003 89	7	B and A
He^5	5.013 7	40	$Li^7+H^2=He^5+He^4$
He^6	6.020 8	50	$He^6=Li^6+\epsilon^-$
Li^6	6.016 86	20	$Li^6+H^2=2He^4$ $Li^6+H^2=Li^7+H^1$
Li^7	7.018 18	18	B
Li^8	~8.025 1	100	$Li^7+H^2=Li^8+H^1$
Be^8	8.007 92	28	$B^{11}+H^1=Be^8+He^4$
Be^9	9.015 04	25	$Be^9+H^2=Li^7+He^4$ $B^{11}+H^2=Be^9+He^4$
Be^{10}	10.016 71	30	$Be^9+H^2=Be^{10}+H^1$
B^{10}	10.016 31	25	B
B^{11}	11.012 92	17	B
B^{12}	<12.019 9 >12.018 6		$B^{11}+H^2=B^{12}+H^1$
C^{11}	11.015 26	35	$C^{11}=B^{11}+\epsilon^+$
C^{12}	12.003 98	10	B
C^{13}	13.007 61	15	B
C^{14}	14.007 67	12	$N^{14}+n^1=C^{14}+H^1$
N^{13}	13.010 04	13	$C^{12}+H^2=N^{13}+n^1$
N^{14}	14.007 50	8	B
N^{15}	15.004 89	20	B
N^{16}	~16.011	200	$F^{19}+n^1=N^{16}+He^4$
O^{15}	15.007 8	40	$O^{15}=N^{15}+\epsilon^+$
O^{16}	16.000 000		Standard
O^{17}	17.004 50	7	$O^{16}+H^2=O^{17}+H^1$
O^{18}	18.003 69	20	M
F^{17}	17.007 6	30	$O^{16}+H^2=F^{17}+n^1$
F^{18}	18.005 6	40	$O^{18}+H^1=F^{18}+n^1$
F^{19}	19.004 52	17	A
F^{20}	<20.009 2 >20.004 2		$F^{19}+H^2=F^{20}+H^1$ $F^{20}=Ne^{20}+\epsilon^-$
Ne^{20}	19.998 81	11	B
Ne^{21}	20.999 68	23	B
Ne^{22}	21.998 64	36	B
Na^{22}	22.000 2	50	$Na^{22}=Ne^{22}+\epsilon^+$
Na^{23}	22.996 1	35	$Na^{23}+H^2=Ne^{21}+He^4$
Na^{24}	23.997 4	45	$Na^{23}+H^2=Na^{24}+H^1$
Mg^{24}	23.992 4	60	$Na^{24}=Mg^{24}+\epsilon^-$
Mg^{25}	24.993 8	90	$Al^{27}+H^2=Mg^{25}+He^4$
Mg^{26}	25.989 8	50	$Na^{23}+He^4=Mg^{26}+H^1$
Mg^{27}	26.992 1	150	$Mg^{27}=Al^{27}+\epsilon^-$
Al^{26}	25.992 9	200	$Al^{26}=Mg^{26}+\epsilon^+$
Al^{27}	26.989 9	80	$Al^{27}+H^2=Al^{28}+H^1$
Al^{28}	27.990 3	70	$Al^{28}=Si^{28}+\epsilon^-$
Al^{29}	28.990 4	200	$Al^{29}=Si^{29}+\epsilon^-$
Si^{27}	26.993 1	150	$Si^{27}=Al^{27}+\epsilon^+$
Si^{28}	27.986 6	60	A, and $Si^{28}+He^4=P^{31}+H^1$
Si^{29}	28.986 6	60	A
Si^{30}	29.983 2	90	$Al^{27}+He^4=Si^{30}+H^1$
Si^{31}	30.986 2	60	$Si^{31}=P^{31}+\epsilon^-$
P^{30}	29.988 2	150	$P^{30}=Si^{30}+\epsilon^+$
P^{31}	30.984 3	50	A, and $Si^{28}+He^4=P^{31}+H^1$
P^{32}	31.984 1	50	$P^{32}=S^{32}+\epsilon^-$
S^{32}	31.982 3	30	A
S^{34}	33.978	200	$P^{31}+He^4=S^{34}+H^1$ (estimate)
Cl^{34}	33.981	300	$Cl^{34}=S^{34}+\epsilon^+$
Cl^{35}	34.980 3	60	$S^{32}+He^4=Cl^{35}+H^1$
Cl^{37}	36.977 9	120	A (comparison with Cl^{35})
Cl^{38}	37.981	300	$Cl^{38}=A^{38}+\epsilon^-$ (Raa $+\gamma$)
A^{38}	37.974	250	$Cl^{35}+He^4=A^{38}+H^1$ (estimate)
A^{40}	39.975 04	30	B

A = Aston
B = Bainbridge
M = Mattauch

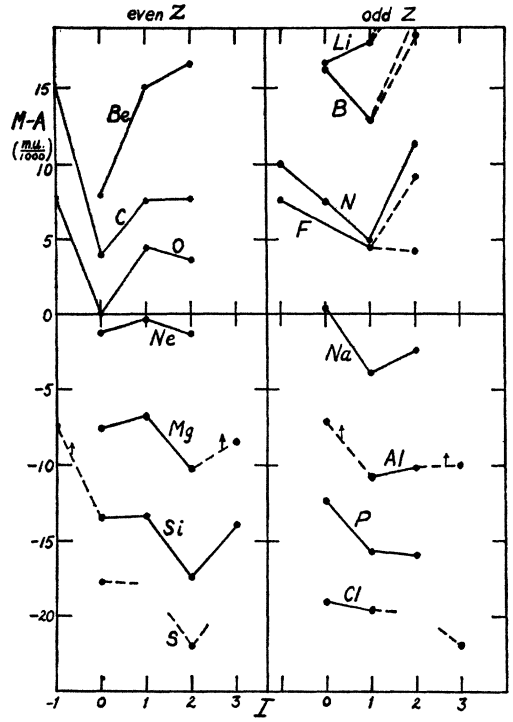

FIG. 50. The mass excess of the lighter atoms. Abscissa: isotopic number. Ordinate: Difference between exact atomic mass and mass number in thousandths of a mass unit. The lines join isotopes of the same element. Left-hand part, even nuclear charge; right-hand side, odd charge. The diagram shows clearly the minima for even number of neutrons. The general trend of the curves shows a minimum at or near zero isotopic number for small nuclear charge which shifts to larger I for the heavier nuclei.

the recoil proton does not move exactly in the same direction as the neutron and therefore does not have quite the full energy. The neutron energy thus corrected is given next, and the energy evolution is calculated (second last column) assuming the neutron to be emitted exactly at right angles to the incident deuteron. The last column gives, as in parts *A* and *B*, the energy evolution calculated from the nuclear masses of Table LXXIII.

B. Agreement of disintegration data with mass spectrograph and with each other

The agreement with the mass spectrograph values is good to excellent for all reactions for which exact determinations are available (cf. Table LXXII). Among the less favorable agreements would be the reactions involving Be^9, either as target or as product, if we took the spectrograph mass of that atom which is 0.11 MV higher than the adopted disintegration mass. With the latter, the agreement is almost perfect for all beryllium reactions.—The agreement for the two reactions involving Li^7, *viz.* Li^7-*p*-α and Li^6-*d*-*p*, is also not quite as good as might be expected in view of the excellent disintegration data and might be improved by adopting a slightly lower mass for Li^7. For most other reactions, the agreement is within the limits of error of mass spectrograph and disintegration measurements.

Of special interest are the reactions connecting the nuclei C^{12}, N^{14} and O^{16} with respect to which the mass spectrograph results of Bainbridge and Jordan and those of Aston disagree seriously. The disintegration data are decidedly in favor of Bainbridge and Jordan, *viz.*

$N^{14}+H^2=C^{12}+He^4+13.40$ MV observed,
13.41 MV using all masses from Bainbridge and Jordan,
13.37 MV using the adopted masses,
13.59 MV using Aston's masses throughout,
13.64 MV using Aston's doublet CH_2-N combined with adopted masses for H, D and He^4.

$O^{16}+H^2=N^{14}+He^4+3.13$ MV observed,
3.14 MV Bainbridge-Jordan,
3.11 MV adopted masses,
3.26 MV Aston.

Of importance is also the very good agreement in the case of C^{12}-*d*-*p* because it showed that in this reaction the C^{13} nucleus is formed in the ground state (B1), a matter which had been in question before (C25, B11, C29, H4).

The internal agreement is best shown by "cycles" involving three or more reactions. The oldest example is

I
$Li^7+H^1=2He^4+17.13$ MV, (a)
$Li^6+H^2=2He^4+22.07$, (b)
$Li^6+H^2=Li^7+H^1+5.02$. (c)

The agreement between $(a)+(c)$ and (b) is satisfactory (difference 0.08 MV). Other examples are

II
$Be^9+H^1=Li^6+He^4+2.28$ MV,
$Be^9+H^2=Li^7+He^4+7.19$,
$Li^6+H^2=Li^7+H^1+5.02$.

Difference = 0.11

II $Be^9+H^1=Be^8+H^2+0.46$ MV,
$B^{11}+H^1=Be^8+He^4+8.70$,
$B^{11}+H^2=Be^9+He^4+8.13$.

Difference: 0.11

III $N^{14}+He^4=O^{17}+H^1-1.26$ MV,
$O^{16}+H^2=N^{14}+H^4+3.13$,
$O^{16}+H^2=O^{17}+H^1+1.95$.

Difference: 0.08

The most notable disagreements among light nuclei are the reactions

$B^{10}+He^4=C^{13}+H^1$,
$B^{10}+n^1=Li^7+He^4$ (slow neutrons, cf. Table LXI).

In both cases, the energy evolution is much less (by 0.85 and 0.55 MV, respectively) than is expected from masses. This discrepancy cannot be due to an error in the B^{10} mass, not only because this mass is well established by many cross checks with the mass spectrograph (§107) but also by the reactions

$B^{10}+H^2=B^{11}+H^1$,
$B^{10}+H^2=Be^8+He^4$,

which both check with the masses.

C. Determination of additional masses

Table LXXIII gives all the atomic weights derived from both mass-spectrograph (§107) and disintegration data. After each element, we have indicated whether its mass was derived from the mass spectrograph or from disintegrations, and, in the latter case, which nuclear reaction was used. For many nuclei, one single reaction is sufficient to express the mass of the nucleus in terms of masses already determined. (Examples: n^1, H^3, Be^8, Be^{10} etc.) When the masses of these nuclei are known, it is possible to express others in terms of them, such as He^3 which is produced in the reaction $H^2+H^2=He^3+n^1$ and is therefore determinable from the energy evolution in this reaction and the neutron mass.

A longer chain of reactions is needed to calculate the masses of heavier nuclei. There is no reliable mass spectrograph measurement between neon and silicon; therefore, all the intermediate nuclei must be obtained from disintegration data. The chain of reactions connecting Ne^{21} to Si^{28} is the following:

$Na^{23}+H^2=Ne^{21}+He^4$, I (L15)
$Na^{23}+H^2=Na^{24}+H^1$, II (L15)
$Na^{24}=Mg^{24}+\epsilon^-$, III (K33)
$Mg^{24}+He^4=Al^{27}+H^1$, IV (D19)
$Al^{27}+H^2=Al^{28}+H^1$, V (Mc5)
$Al^{28}=Si^{28}+\epsilon^-$. VI (C34)

Of these six reactions, the most accurately measured ones are I, II, III. In all these cases the measurement of the range of the produced particle is straightforward and the geometry satisfactory. The only correction necessary is for the stopping power of the Al used for measuring the proton range in II and V: In accord with the considerations in §95*E*, we assumed one mil of Al to be equivalent to 4.4 cm air of 15°C rather than 4.0 cm of 20°C as assumed by Lawrence and McMillan (L15, Mc5).

The β-transformations III and VI involve the well-known uncertainty regarding the validity of the Konopinski-Uhlenbeck or the inspection limit. Moreover, in both cases the β-decay is accompanied by γ-rays: Na^{24} emits β-particles of 1.9 MV (inspection limit) and γ-rays of 2.9, 0.95 and 1.93 MV. It seems reasonable to assume that the β-transformation leads always to a state of 2.9 MV excitation, which may go over into the ground state either by emission of one quantum of 2.9 MV or two of 0.95 and 1.93 MV. This would mean a total energy evolution of 4.6 MV which fits in fairly well with similar nuclei (N^{16}, F^{20}, Al^{28} etc., cf. Table LII). Al^{28} emits β-rays of 3.3 MV and γ-rays of 2.3 MV: Here it is possible to assume that the β-spectrum is complex, leading either to the ground state (emission of 3.3 MV betas) or to a state with 2.3 MV excitation energy (1.0 MV betas). Although such a complexity is not apparent in the β-spectra, it may very well be present since it is quite possible that only a fairly small fraction of the β-processes lead to the excited states. The main argument is again the comparison of the energy evolution of the analogous nuclei F^{20}, Na^{24}, Al^{28}, P^{32}, K^{40}: The energy evolution in this series decreases in a regular way with increasing mass, as should be

TABLE LXXIV. *Nuclear excitation levels.*

Nucleus	Level No.	Energy MV	Width kv	Nuclear Mass	Spectr. Symbol	Class	Source	γ-rays
Li^7	1	0.44	—	7.018 65	$^2P_{1/2}$ *u*	*A*	Li^6-*d*-*pP*	~0.4 Li^7-α-α
Be^8	1	2.9	780	8.011 1		*A*	B^{11}-*p*-αP, B^{10}-*d*-αP	
	2	~4.8	~1400	8.013 1	$^1D_2$ *g*	*B*	Li^8-ϵ^--αP	17.5 MV 4→0
	3	6–12	Large	8.014–20		*C*	B^{10}-*d*-αP, Li^8-ϵ^--αP	10–14 MV 4→1, 2
	4	17.50	9	8.026 72	1 *u*	*A*	Li^7-*p*-γR	(from Li^7-*p*-γ)
	5	17.86	Large	8.027 11		*B*	Li^7-*p*-γR	(from Li^7-*p*-γ)
Be^{10}	1	2.4	Small	10.019 3	^1D *g* ?	*C*	Be^9-*d*-*pP* ?	
B^{10}	1	0.5	"	10.016 9	*S g* ?	*B*	Be^9-*d*-*nP*	
	2	2.0	"	10.018 5	*D g* ?	*B*	"	
	3	3.3	"	10.019 8	*D g* ?	*B*	"	
	4	7.28	Large	10.024 13		*B*	Be^9-*p*-γR	(from Be^9-*p*-γ)
B^{11}	1	2.14	Small	11.015 22	*D u* ?	*A*	B^{10}-*d*-*pP*	
	2	4.43	"	11.017 68	F *u* ?	*B*	"	
C^{12}	1	4.3	"	12.008 6	$^1D_2$ *g*	*B*	N^{14}-*d*-αP, B^{11}-*d*-*nP* Be^9-α-*nP* ?	2.7 MV 2→1 (Be^9-α-*n*, B^{11}-α-*n*)
	2	7.0	Small	12.011 5	1 *u* ?	*B*	Be^9-α-*nP*, B^{11}-*d*-*nP* ?	4.3 MV 1→0 (Be^9-*d*-*n*, B^{11}-*d*-*n*, N^{14}-*d*-α)
	3	9.5	?	12.014 2		*D*	B^{11}-*d*-*nP* ?	7.0 MV 2→0(Be^9-α-*n*, B^{11}-*d*-*n*, N^{14}-*d*-α)
	4	16.07	~10	12.021 25	1 *u* ?	*A*	B^{11}-*p*-αR, B^{11}-*p*-γR	15 MV 4→0 (B^{11}-*p*-γ)
C^{13}	1	0.8	Small	13.008 5	$^1P_{3/2}$?	*B*	B^{10}-α-*pP*	
	2	3.6	"	13.011 5	$^2F_{3/2}$?	*B*	"	
	3	4.0	"	13.011 9	$^2F_{5/2}$?	*C*	"	
	4	4.9	"	13.012 9		*B*	"	
	5	6.0	?	13.014 1		*B*	"	
	6	12.9	300	13.021 5		*B*	Be^9-α-*nR*	
N^{13}	1	2.25	~20	13.012 46		*A*	C^{12}-*p*-γR	2 MV 1,2→0 (C^{12}-*p*-γ)
	2	2.32	~20	13.012 56		*A*	C^{12}-*p*-γR	
N^{14}	1	0–4	Small	several levels		*D*	B^{11}-α-*nP*	4.0 MV 2→0 (C^{13}-*d*-*n*)
	2	4.0	"	14.011 8		*C*	C^{13}-*d*-*n*γ	
	3	14.8	500	14.023 4		*B*	B^{10}-α-*pR*	
N^{15}	1	5.42	Small	15.010 72		*A*	N^{14}-*d*-*pP*	
	2	13.4	~400	15.019 2		*D*	B^{11}-α-*nR*	
O^{16}	1	10.7	700	16.011 5		*B*	C^{12}-α scatt. *R*	
O^{17}	1	0.82	Small	17.005 38		*A*	O^{16}-*d*-*pP*	
	2	4.6	"	17.009 4		*D*	Ne^{20}-*n*-αP	
F^{18}	1	8.2	~150	18.014 4		*D*	N^{14}-α-*pR*	
Ne^{20}	1	7.2	?	20.006 5		*A*	F^{19}-*p*-γP	6.0 MV 2→1 (F^{19}-*p*-γ)
	2	13.20	<4	20.012 98		*A*	" *R*	
	3	13.5	Large	20.013 3		*B*	" *R*	
	4	13.73	<12	20.013 56		*A*	" *R*	
	5	13.78	<15	20.013 59		*A*	" *R*	
	6	14.22	Small	20.014 08		*B*	" *R*	
	7	14.85	?	20.014 44		*D*	" *R*	
Ne^{22}	1	0.6	Small	21.999 3		*B*	F^{19}-α-*pP*	
	2	1.5	"	22.000 3		*B*	"	
	3	3.5	"	22.002 4		*B*	"	
	4	4.6	"	22.003 6		*B*	"	
Na^{22}	1	1.3	"	22.001 6		*C*	F^{19}-α-*nP*	
	2	1.6	"	22.001 9		*C*	"	
Na^{23}	1	14.5	100	23.011 7		*B*	F^{19}-α-*pR*	
	2	14.8	130	23.012 0		*B*	"	
Na^{24}	1	3.20	Small	24.000 8		*A*	Na^{23}-*d*-*pP*	
Mg^{24}	1	1.0 or 2.0	Small	23.993 5 or 9945		*B*	Na^{24}-$\epsilon^-\gamma$	0.95 MV 1→0 or 2→1
	2	2.9	"	23.995 4		*B*	"	1.93 MV 2→1 or 1→0
	3	12.2	Large	24.005 5		*B*	Na^{23}-*p*-γR	2.9 MV 2→0 (Na^{24}-ϵ^-)
Mg^{25}	1	0.7	Small	24.994 6		*A*	Al^{27}-*d*-αP	
Mg^{26}	1	2.3	"	25.992 3		*B*	Na^{23}-α-*pP*	
	2	4.0	"	25.994 1		*B*	"	
	3	5.0	"	25.995 2		*B*	"	
Al^{27}	1	0.98	"	26.991 0		*B*	Mg^{24}-α-*pP*	1.3 MV by absorp. meth. (Mg^{27}-ϵ^-)
Al^{28}	1	0.68	"	27.991 0		*A*	Al^{27}-*d*-*pP*	
	2	2.69	"	27.993 2		*A*	"	
	3	3.67	"	27.994 2		*A*	"	
	4	5.15	"	27.995 8		*A*	"	

TABLE LXXIV.—*Continued.*

Nucleus	Level No.	Energy MV	Width kv	Nuclear Mass	Spectr. Symbol	Class	Source	γ-rays
Si^{28}	1	2.3	Small	27.989 1		*B*	Al^{28}-$\epsilon^-\gamma$	2.3 MV 1→0 (Al^{28}-ϵ^-)
	2	12.0	"	27.999 5		*B*	Al^{27}-*p*-γR	
	3	13.7	100	28.001 3		*C*	Mg^{24}-α-*pR*	
	4	14.2	130	28.001 9		*C*	"	
Si^{30}	1	2.3	Small	29.985 7		*B*	Al^{27}-α-*pP*	
	2	3.6	"	29.987 1		*B*	"	
	3	4.8	"	29.988 4		*B*	"	
P^{31}	1	1.05	"	30.985 4		*B*	Si^{28}-α-*pP*	
	2	1.7	"	30.986 1		*B*	"	
	3	12.0	~100	30.997 2		*B*	Al^{27}-α-*pR*	
	4	12.4	~100	30.997 6		*B*	Al^{27}-α-*pR*	
	5	12.7_5	80	30.998 0		*B*	"	
	6	13.1	130	30.998 4		*B*	"	
	7	13.5_5	~120	30.998 9		*B*	"	
	8	14.3	~120	30.999 7		*B*	"	
S^{34}	1	*x*	Small	33.980 2		*C*	P^{31}-α-*pP*	
	2	*x*+1.3	"	33.981 6		*C*	"	
	3	*x*+2.8	"	33.983 2		*C*	"	
	4	*x*+4.8	"	33.985 3		*C*	"	
Cl^{35}	1	0.6	Small	34.981 0		*B*	S^{32}-α-*pP*	
	2	1.5	"	34.982 0		*B*	"	
A^{38}	1	2.1	"	37.976 1		*C*	Cl^{38}-$\epsilon^-\gamma$, Cl^{35}-α-*pP*	2.0 MV 1→0
	2	4.5	"	37.978 7		*C*	Cl^{38}-ϵ^-P, Cl^{35}-α-*pP*	2.5 MV 2→1
	3	6.2	"	37.980 5		*C*	Cl^{35}-α-*pP*	β-groups with en. diff. of 4.6 MV

expected theoretically (W18), therefore it seems highly improbable that it should increase between Na^{24} and Al^{28} from 5.0 to 5.6 MV. This forces us to the conclusion that the total energy evolution in VI is equal to the β-energy, i.e. 3.3 MV. The agreement finally obtained (see below) confirms this decision.

The remaining reaction IV is complicated by the fact that magnesium represents a mixed element and it is not known to which isotope a given proton group should be attributed. The observed proton groups from Mg-α-*p* correspond to energy evolutions $Q=-1.04$, -1.82 and -2.80 MV. The longest group ($Q=-1.04$ MV) is weak compared to the two others. The isotopes of Mg which may be responsible for these groups, are Mg^{24} and Mg^{25} while Mg^{26} is excluded because the energy evolution would in this case be -4.4 MV. The calculated energy evolution for Mg^{25} is -0.6 MV which agrees sufficiently with the observed Q for the longest group. This group might still be a superposition of protons from Mg^{24} and Mg^{25} although this is unlikely in view of the small intensity of the group. The main reason against assigning the longest group to Mg^{24} is again the analogy to other nuclei of the $4n$-type: For Ne^{20}-α-*p*, the Q calculated from masses is -1.4 MV, for Si^{28}, the observed energy evolution is -2.2, for S^{32} also -2.2. A Q value of -1.8 for the Mg^{24}-α-*p* reaction would fit in very well with this sequence, while -1.0_5 would definitely not. Therefore we decided to accept -1.82 MV for the energy evolution in reaction IV.

With the energy evolutions in I to VI thus determined, the mass difference between Si^{28} and Ne^{21} comes out about 0.5 MV too great which must be considered as a very good agreement in view of the many uncertain data involved. For the determination of the masses, we "distributed" the error among the reactions I to VI, assuming the observed reaction energy to be 0.1 MV too high in I, 0.1 MV too low in III and VI, and 0.2 MV too low in IV, the general experience being that α-*p* reactions give generally too low energy evolutions owing to small intensity and poor geometry.

With the main chain thus established, it is easy to link additional masses to it such as Mg^{25} by the Al^{27}-*d*-α reaction etc. For the elements heavier than silicon, reaction energies have been used in some cases to correct the mass spectroscopic values which have a rather large probable error: Thus, e.g. Si^{28} and P^{31} have both been measured

TABLE LXXV. *Binding energies of neutrons, protons and α-particles, in thousandths of a mass unit.*

A. NEUTRONS

Z	I=0			I=1			I=2			I=3		
	N	odd	even		odd	even		odd	even		odd	even
1	H^2	2.37		H^3		6.65						
2	He^4		22.15	He^5	<0.8		He^6		1.9			
3				Li^7		7.65	Li^8	~2				
4				Be^9	1.85		Be^{10}		7.30			
5				B^{11}		12.36	B^{12}	~3				
6	C^{12}		20.25	C^{13}	5.34		C^{14}		8.91			
7	N^{14}	11.51		N^{15}		11.58	N^{16}	~3				
8	O^{16}		16.8	O^{17}	4.47		O^{18}		9.8			
9	F^{18}	11.0		F^{19}		10.1	F^{20}	~6				
10				Ne^{21}	8.10		Ne^{22}		10.0			
11				Na^{23}		13.1	Na^{24}	7.7				
12				Mg^{25}	7.6		Mg^{26}		13.0	Mg^{27}	6.7	
13				Al^{27}		12.0	Al^{28}	8.6		Al^{29}		8.9
14	Si^{28}		15.5	Si^{29}	9.0		Si^{30}		12.4	Si^{31}	6.0	
15				P^{31}		12.9	P^{32}	9.2				

B. PROTONS

N	I=2			I=1			I=0			I=−1		
	Z	odd	even		odd	even		odd	even		odd	even
1							H^2	2.37				
2							He^4		21.29	He^3		5.79
3				Li^7	10.7		Li^6	4.9				
4				Be^9		~18	Be^8		18.39			
5				B^{11}	11.92		B^{10}	6.86				
6				C^{13}		~20	C^{12}		17.07	C^{11}		9.18
7				N^{15}	10.91		N^{14}	8.24		N^{13}	2.07	
8				O^{17}		15	O^{16}		13.02	O^{15}		7.8
9				F^{19}	7.30		F^{18}	7.0		F^{17}	0.5	
10				Ne^{21}		16	Ne^{20}		13.84			
11				Na^{23}	10.7		Na^{22}	7.6				
12				Mg^{25}		11.7	Mg^{24}		11.8			
13	Al^{28}	9.9		Al^{27}	8.0		Al^{26}	9.0				
14	Si^{30}		15.3	Si^{29}		11.8	Si^{28}		11.4			
15				P^{31}	7.0		P^{30}	6.5				
16							S^{32}		10.1			

C. α-PARTICLES

Z	I=−1		0		1		2		3		
3			Li^6	1.76	Li^7	2.76					
4			Be^8	−0.14	Be^9	2.5	Be^{10}	8.0			
5			B^{10}	4.44	B^{11}	9.15	B^{12}	~10			
6			C^{12}	7.83	C^{13}	11.32	C^{14}	12.93			
7			N^{14}	12.70	N^{15}	11.92	N^{16}	~12			
8	O^{15}	11.3	O^{16}	7.87	O^{17}	7.00	O^{18}	7.87			
9	F^{17}	6.4	F^{18}	~5.8	F^{19}	4.26	F^{20}	~ 8			
10			Ne^{20}	5.08	Ne^{21}	8.71	Ne^{22}	8.94			
11			Na^{22}	9.3	Na^{23}	12.3	Na^{24}	~14			
12			Mg^{24}	10.3	Mg^{25}	9.8	Mg^{26}	12.8			
13			Al^{26}	11.2	Al^{27}	10.1	Al^{28}	11.0			
14			Si^{28}	9.7	Si^{29}	11.1	Si^{30}	10.5	Si^{31}	9.8	
15			P^{30}	8.6	P^{31}	9.5	P^{32}	10.1			
16			S^{32}	8.2			S^{34}	~9			
17			Cl^{34}	~11	Cl^{35}	7.9					
18							A^{38}	~8			

TABLE LXXVI. *Energy difference between isobars (weight of nucleus with lower charge minus that with higher charge in thousandths of a mass unit).*

$I=+1/-1$		$I=2/0$				$I=1/3$	
		Z and N odd		even			
n^1-H^1	+0.84	He^6-Li^6	3.9	Li^8-Be^8	17	$Mg^{27}-Al^{27}$	2.2
H^3-He^3	−0.02	$Be^{10}-B^{10}$	0.40	$B^{12}-C^{12}$	∼15	$Al^{29}-Si^{29}$	3.8
$B^{11}-C^{11}$	−2.34	$C^{14}-N^{14}$	0.17	$N^{16}-O^{16}$	∼11	$Si^{31}-P^{31}$	1.9
$C^{13}-N^{13}$	−2.34	$O^{18}-F^{18}$	−1.9	$F^{20}-Ne^{20}$	∼8		
$N^{15}-O^{15}$	−2.9	$Ne^{22}-Na^{22}$	−1.6	$Na^{24}-Mg^{24}$	5.0		
$O^{17}-F^{17}$	−3.1	$Mg^{26}-Al^{26}$	−3.1	$Al^{28}-Si^{28}$	3.7		
		$Si^{30}-P^{30}$	−5.0	$P^{32}-S^{32}$	1.8		
		$S^{34}-Cl^{34}$	−3??	$K^{40}-Ca^{40}$	0.8		

in the mass spectrograph and are also connected by the reaction $Si^{28}+He^4=P^{31}+H^1$; the observed reaction energy is 0.8 MV less than that obtained from the masses; it was therefore assumed that the spectrograph masses of Si^{28} and P^{31} are 0.2 units too high and too low, respectively, and the actual energy evolution in the reaction is 0.4 MV higher than the observed one. Cl^{35} has been based entirely on the reaction $S^{32}+He^4=Cl^{35}+H^1$ which reduces the probable error considerably since the mass of S^{32} is very accurately known.

§109. Excited States of Nuclei

The evidence for excited states of nuclei is obtained from three sources, *viz.*

(1) groups of outgoing particles from nuclear reactions,

(2) γ-rays emitted by the residual nucleus,

(3) resonance effects.

From (3), only states above the dissociation energy may be obtained, from (2), primarily states below the dissociation energy, because the higher states will ordinarily disintegrate with emission of particles rather than γ-rays. The particle groups (1) give evidence of high as well as low states.

The evidence is reported and discussed together with the various reactions in chapter XVII, that on resonance levels also in Tables XXXIX and XXXX (§§81, 82). In Table LXXIV, we give a summary of the excited levels for which there is experimental evidence. In the first column, the nucleus is given, in the second, the number of the excitation level, in the third, the excitation energy in MV above the ground state; then follows the width of the level, and the mass of the nucleus in that particular state (which may be useful for comparing the levels of isobars and other similar nuclei). The following column gives the probable spectroscopic character of the level according to the theory of Feenberg and Wigner. Where it is reasonably certain the full spectroscopic character is given, e.g. $^2P_{\frac{1}{2}}$, sometimes only the orbital momentum (S, P, D level etc.) or the total angular momentum (e.g., 1). The parity of the term is indicated by g (even) or u (odd). The "class" A, B, C, D denotes the reliability of the evidence about the level, A denoting the most reliable. The next column gives the reaction from which the evidence is obtained; the letter P means that the evidence comes from a group of outgoing particles, γ that it comes from γ-rays, and R that the level is a resonance level. The last column indicates the γ-ray transitions observed, giving first the quantum energy of the γ-ray, then the transition to which it is ascribed (using the numbers of the levels introduced in the second column) and finally the nuclear reaction in which the γ-rays are produced.

It need hardly be pointed out that practically each of the nuclei listed will have many more levels than are known at present.

§110. Discussion

The masses given in Table LXXIII show, with greater precision than earlier mass tables, the often-discussed features of nuclear masses: For very light nuclei, we have the well-known periodicity with the period 4, with the "multiples of α-particles" having an especially low mass. For higher atomic weight, this periodicity becomes

TABLE LXXVII. *Stable isotopes of the elements.**

Element	Z	A	Relative Abundance	Element	Z	A	Relative Abundance	Element	Z	A	Relative Abundance	Element	Z	A	Relative Abundance
H	1	1	99.98	Zn	30	64	50.9	Cd	48	111	13.0	Gd	64	155	21
		2	0.02			66	27.3			112	24.2			156	23
		3	$\sim 10^{-8}$			67	3.9			113	12.3			157	17
He	2	4	—			68	17.4			114	28.0			158	23
Li	3	6	7.9			70	0.5			116	7.3			160	16
		7	92.1	Ga	31	69	61.2	In	49	113	4.5	Tb	65	159	—
Be	4	9	—			71	38.8			115	95.5	Dy	66	161	22
B	5	10	20.6	Ge	32	70	21.2	Sn	50	112	1.1			162	25
		11	79.4			72	27.3			114	0.8			163	25
C	6	12	99			73	7.9			115	0.4			164	28
		13	~ 1			74	37.1			116	15.5	Ho	67	165	—
N	7	14	99.7			76	6.5			117	9.1	Er	68	166	36
		15	0.3	As	33	75	—			118	22.5			167	24
O	8	16	99.76	Se	34	74	0.9			119	9.8			168	30
		17	0.04			76	9.5			120	28.5			170	10
		18	0.20			77	8.3			122	5.5	Tm	69	169	—
F	9	19	—			78	24.0			124	6.8	Yb	70	171	9
Ne	10	20	90.00			80	48.0	Sb	51	121	56			172	24
		21	0.27			82	9.3			123	44			173	17
		22	9.73	Br	35	79	50.7	Te	52	120	<0.1			174	38
Na	11	23	—			81	49.3			122	2.9			176	12
Mg	12	24	77.4	Kr	36	78	0.42			123	1.6	Lu	71	175	—
		25	11.5			80	2.45			124	4.5	Hf	72	176	5
		26	11.1			82	11.79			125	6.0			177	19
Al	13	27	—			83	11.79			126	19.0			178	28
Si	14	28	89.6			84	56.85			128	32.8			179	18
		29	6.2			86	16.70			130	33.1			180	30
		30	4.2	Rb	37	85	72.7	I	53	127	—	Ta	73	181	—
P	15	31	—			87	27.3	Xe	54	124	0.08	W	74	182	22.6
S	16	32	97.0	Sr	38	84	0.5			126	0.08			183	17.3
		33	0.8			86	9.6			128	2.30			184	30.2
		34	2.2			87	7.5			129	27.13			186	29.9
Cl	17	35	76			88	82.4			130	4.18	Re	75	185	38.2
		37	24	Y	39	89	—			131	20.67			187	61.8
A	18	36	0.31	Zr	40	90	48			132	26.45	Os	76	186	1.0
		38	0.06			91	11.5			134	10.31			187	0.6
		40	99.63			92	22			136	8.79			188	13.4
K	19	39	93.2			94	17	Cs	55	133	—			189	17.4
		40	0.012			96	1.5	Ba	56	130	0.16			190	25.1
		41	6.8	Cb	41	93	—			132	0.015			192	42.5
Ca	20	40	96.76	Mo	42	92	14.2			134	1.72	Ir	77	191	38.5
		42	0.77			94	10.0			135	5.7			193	61.5
		43	0.17			95	15.5			136	8.5	Pt	78	192	0.8
		44	2.30			96	17.8			137	10.8			194	30.2
Sc	21	45	—			97	9.6			138	73.1			195	35.3
Ti	22	46	8.5			98	23.0	La	57	139	—			196	26.6
		47	7.8			100	9.8	Ce	58	136	<1			198	7.2
		48	71.3	Ma	43	—	—			138	<1	Au	79	197	—
		49	5.5	Ru	44	96	5			140	89	Hg	80	196	0.15
		50	6.9			98	—			142	11			198	10.1
V	23	51	—			99	12	Pr	59	141	—			199	17.0
Cr	24	50	4.9			100	14	Nd	60	142	36			200	23.3
		52	81.6			101	22			143	11			201	13.2
		53	10.4			102	30			144	30			202	29.6
		54	3.1			104	17			145	5			204	6.7
Mn	25	55	—	Rh	45	101	0.1			146	18	Tl	81	203	30.5
Fe	26	54	6.5			103	99.9			148	<1			205	69.5
		56	90.2	Pd	46	102	0.8			150	<1	Pb	82	204	1.50
		57	2.8			104	9.3	—	61	—	—			206	28.3
		58	0.5			105	22.6	Sm	62	144	3			207	20.1
Co	27	57	0.2			106	27.2			147	17			208	50.1
		59	99.8			108	26.8			148	14	Bi	83	209	—
Ni	28	58	67.2			110	13.5			149	15	Th	90	232	—
		60	27.0	Ag	47	107	52.5			150	5	U	92	235	<1
		61	~ 1			109	47.5			152	26			238	>99
		62	3.8	Cd	48	106	1.4			154	20				
		64	~ 1			108	1.0	Eu	63	151	50.6				
Cu	29	63	68			110	12.8			153	49.4				
		65	32												

* Main reference: Rasetti, *Nuclear Physics*, pp. 157–160 (R3a, M10a). Other references: A, Zn, Cd (N8); Co (S2); Ni (D27a); Ga, Ba (S3a); Br (S28); Rh, Pd, Ir, Pt (S3); Hg, Pb (N9).

less pronounced, and the minimum mass shifts gradually to nuclei containing more neutrons than protons.

Figure 50 shows the mass excess of the nuclei contained in Table LXXIII. Each curve corresponds to a certain value of Z, and gives the mass excess as a function of the isotopic number I. The general tendency of the mass excess to decrease with increasing mass number is apparent. The curves in the left-hand half of Fig. 50 refer to even, those in the right-hand half to odd Z. All curves, but especially those for even Z, have minima for even number of neutrons, maxima for odd number of neutrons. These maxima and minima are most pronounced for very light nuclei. Apart from this period of two, the curves have a minimum for equal number of neutrons and protons for light nuclei, and a general trend to fall off towards the right for heavier nuclei. The latter effect is, of course, due to the Coulomb forces.

Another useful representation of nuclear masses was given by Bothe and Maier-Leibnitz (B47a). They plot the mass excess of nuclei of the same isotopic number $I=-1$, 0, 1 and 2 against the atomic weight. For odd isotopic number, smooth curves are obtained, while for even isotopic number the nuclei with even Z lie much lower than those with odd Z, each group forming again a smooth curve.

Table LXXV gives the binding energies of neutrons, protons and α-particles in nuclei. The nuclei are listed according to their isotopic number ($I=-1$ to $+3$), and, in the case of neutrons (protons), the binding energies are listed in separate columns for even and odd number of neutrons (protons). It is evident from these tables that the binding energy of "even" neutrons and protons is much greater than of "odd" ones, the difference being, in the average, of the order of 5 units. This difference is an effect of the Pauli principle (cf. §10, and F10, W17). The binding energies of neutrons (protons) decrease from the left to the right of the tables, i.e. with increasing number of neutrons (protons) already present in the nucleus, which is also primarily an effect of the Pauli principle (§6, W8, W17). In each column, the binding energy of protons decreases generally with increasing size of the nucleus (due to Coulomb forces, §8). The binding of neutrons decreases steadily for isotopic number 0 while for $I=1$ the binding energy increases at first up to a maximum near Mg and decreases afterwards. For $I=2$ the maximum binding energy occurs approximately at the end of the table. This behavior is again a consequence of the competition between nuclear and electric forces: There is a general tendency towards a higher binding energy of neutrons for higher atomic weight, but when the nuclei become less stable because of the Coulomb forces, their density will become smaller and therefore the binding energy of neutrons will decrease slowly.

The binding energies of α-particles do not show such marked trends as those of neutrons and protons but stay in general fairly constant except for an increase in the beginning and, perhaps, a very slight decrease at the end. This absence of trends makes it easier to recognize fluctuations such as the minimum in the binding energies at the fluorine isotopes: This minimum is evidence for the completion of a neutron-proton shell at O^{16} (cf. §33).[22a]

Table LXXVI contains the mass differences between some pairs of isobars. The weight of the isobar containing more protons has been subtracted from that containing more neutrons. In accordance with general rules (Coulomb forces!), the figures decrease with increasing atomic number in practically all instances. Some irregularities are apparent, but unfortunately many experimental data are still very uncertain.

[22a] The effect of the completion of the shell, though noticeable, is much less marked than would be expected on the grounds of the elementary individual particle-picture. According to that picture, the energy difference between subsequent levels of an individual particle, is about 5×10^{-3} mass units near O^{16}. This would make the difference in the binding energy of an α-particle before and after completion of the shell 20 units instead of, at the best, the 8 units observed.

References

The following list of references is not intended to be a complete list. It does contain all papers referred to explicitly in the text, both in Part B and in Part C. The references are arranged alphabetically and are denoted by a letter indicating the initial of the primary author and a number representing the position in the alphabetical list. The paragraphs in which the references appear are indicated.

A1. Alichanian, Alichanow and Dzelepow, Physik. Zeits. Sowjetunion **10**, 78 (1936). (§87, 99, 101 105)

A2. Alichanow, Alichanian and Dzelepow, Nature **133**, 871 (1934). (§99, 105)

A2a. Alichanow, Alichanian and Dzelepow, Nature **133**, 950 (1934). (§99)

A3. Alichanow, Alichanian and Dzelepow, Nature **135**, 393 (1935). (§102, 105)

A4. Allen, Phys. Rev. **51**, 182 (1937). (§100)

A5. Allison, Proc. Camb. Phil. Soc. **32**, 179 (1936). (§81)

A6. Alvarez, McMillan and Snell, Phys. Rev. **51**, 148 (1937). (§92)

A7. Amaldi, D'Agostino, Fermi, Pontecorvo, Rasetti and Segrè, Proc. Roy. Soc. **149**, 522 (1935). (§57, 59, 65, 101, 102, 105)

A8. Amaldi, Nuovo Cimento **12**, 223 (1935). (§57, 102, 105)

A9. Amaldi and Fermi, Ricerca Scient. **1**, 56 (1936). (§57)

A10. Amaldi and Fermi, Ricerca Scient. **1**, 310 (1936). (§57)

A11. Amaldi and Fermi, Phys. Rev. **50**, 899 (1936). (§58, 59, 60, 61, 62, 92, 101, 102, 105)

A11a. Amaldi, Hafstad and Tuve, Phys. Rev. **51**, 896 (1937). (§102)

A12. Anderson and Neddermeyer, Phys. Rev. **50**, 263 (1936). (§104)

A13. Andersen, Nature **137**, 457 (1936). (§102, 105)

A14. Andersen, Zeits. f. physik. Chemie **32**, 237 (1936). (§102, 105)

A15. Andersen, Nature **138**, 76 (1936). (§102, 105)

A16. Arsenjewa-Heil, Heil and Westcott, Nature **138**, 462 (1936). (§60)

A17. Aston, Nature **135**, 541 (1935). (§107)

A18. Aston, *Mass Spectra and Isotopes* (E. Arnold, 1933). (§107)

A19. Aston, Nature **137**, 357 (1936). (§107)

A20. Aston, Nature **137**, 613 (1936). (§107)

A21. Aston, Nature **138**, 1094 (1936). (§107)

A21a. Aston, Nature **139**, 922 (1937). (§107)

A22. Aoki, Nature **139**, 372 (1937). (§65)

B1. Bainbridge and Jordan, Phys. Rev. **49**, 883 (1936). (§107)

B2. Bainbridge and Jordan, Phys. Rev. **51**, 384 (1937). (§101, 107)

B2a. Bainbridge and Jordan, Phys. Rev. **50**, 282 (1936). (§107)

B3. Banks, Chalmers and Hopwood, Nature **135**, 99 (1935). (§103)

B4. Bardeen, Phys. Rev. **51**, 799 (1937). (§53)

B4a. Barnes, DuBridge, Wiig, Buck, and Strain, Phys. Rev. **51**, 775 (1937). (§100, 105)

B5. Bayley, Curtis, Gaerttner and Goudsmit, Phys. Rev. **50**, 461 (1936). (§63)

B5a. Bayley and Crane, Phys. Rev. **51**, 1012 (1937). (§101, 105)

B6. Beams and Trotter, Phys. Rev. **45**, 849 (1934). (§92)

B6a. Bennet, Proc. Roy. Soc. **155**, 419 (1936). (§95)

B7. Bernardini, Zeits. f. Physik **85**, 555 (1933). (§82, 99)

B7a. Bernardini, Ricerca Scient. **8**, 33 (1937). (§99)

B7b. Bernardini and Bocciarelli, Accad. Lincei, Atti. **24**, 132 (1936). (§99)

B8. Bethe, Ann. d. Physik **5**, 325 (1930). (§95)

B9. Bethe and Heitler, Proc. Roy. Soc. **146**, 83 (1934). (§93)

B10. Bethe and Peierls, Int. Conf. Phys., London (1934). (§103)

B11. Bethe, Phys. Rev. **47**, 633 (1935). (§99, 101, 107)

B12. Bethe, Phys. Rev. **47**, 747 (1935). (§57, 65, 102)

B13. Bethe, Phys. Rev. **50**, 332 (1936). (§52)

B14. Bethe, Phys. Rev. **50**, 977 (1936). (§101)

B15. Bethe and Placzek, Phys. Rev. **51**, 450 (1937). (§52, 54, 61, 71, 91, 102)

B16. Bethe, *Handbuch der Physik*, Vol. 24, 273 (1933). (§51, 95)

B17. Bethe, Phys. Rev. to be published shortly. (§80)

B18. Bethe, Phys. Rev. **51**, 1004 (1937). (§79, 80)

B19. Bethe, Zeits. f. Physik **76**, 293 (1932). (§95)

B20. Birge, Phys. Rev. **37**, 1669 (1931). (§101)

B21. Bjerge and Westcott, Nature **134**, 286 (1934). (§102, 105)

B22. Bjerge and Westcott, Nature **134**, 177 (1934). (§102)

B23. Bjerge, Nature **137**, 865 (1936). (§102)

B24. Bjerge and Broström, Nature **138**, 400 (1936). (§102, 105)

B24a. Bjerge, Nature **139**, 757 (1937). (§102)

B25. Blackett and Lees, Proc. Roy. Soc. **134**, 658 (1932). (§95)

B26. Blackett, Proc. Roy. Soc. **135**, 132 (1932). (§95)

B27. Blackett and Champion, Proc. Roy. Soc. **130**, 380 (1931). (§74)

B28. Blewett, Phys. Rev. **49**, 900 (1936). (§87, 105)

B29. Bloch, Ann. d. Physik **16**, 285 (1933). (§95)

B30. Bloch and Gamow, Phys. Rev. **50**, 260 (1936). (§87)

B31. Bloch, Zeits. f. Physik **81**, 363 (1933). (§95)

B32. Bohr, Nature **137**, 344 (1936). (§51, 57, 100, 102)

B33. Bohr and Kalckar, Kgl. Dansk Acad. (1939). (§51–56, 77, 79, 81–90)

B33a. Bohr, Phil. Mag. **25**, 10 (1913). (§95)

B34. Bohr, Phil. Mag. **30**, 581 (1915). (§97)

B35. Bonner and Mott-Smith, Phys. Rev. **46**, 258 (1934). (§99)

B36. Bonner and Brubaker, Phys. Rev. **48**, 469 (1935). (§102)
B37. Bonner and Brubaker, Phys. Rev. **48**, 742 (1935). (§85, 97, 101)
B38. Bonner and Brubaker, Phys. Rev. **49**, 19 (1936). (§97, 101)
B39. Bonner and Brubaker, Phys. Rev. **49**, 778 (1936). (§102, 105)
B40. Bonner and Brubaker, Phys. Rev. **50**, 308 (1936). (§74, 85, 97, 99, 101, 108)
B41. Bonner and Brubaker, Phys. Rev. **50**, 781 (1936). (§65, 95, 102)
B42. Born, Zeits. f. Physik **58**, 306 (1929). (§66)
B43. Bothe and Becker, Zeits. f. Physik **66**, 289 (1930). (§99)
B44. Bothe and Frãnz, Zeits. f. Physik **49**, 1 (1928). (§95)
B45. Bothe and Baeyer, Gött. Nachr. **1**, 195 (1935). (§94)
B46. Bothe, Physik. Zeits. **36**, 776 (1935). (§99)
B47. Bothe, Zeits. f. Physik **100**, 273 (1936). (§99, 101)
B47a. Bothe and Maier-Leibnitz, Niturwiss. **25**, 25 (1937). (§110)
B47b. Bothe and Gentner, Naturwiss. **25**, 90 (1937). (§91, 103)
B47c. Bothe and Gentner, Naturwiss. **25**, 126 (1937). (§91, 103)
B47d. Bothe and Gentner, Naturwiss. **25**, 191 (1937). (§91, 103)
B47e. Bothe and Gentner, Naturwiss. **25**, 284 (1937). (§103)
B47f. Bothe and Gentner, Zeits. f. Physik **106**, 236 (1937). (§102)
B47g. Bothe and Gentner, Zeits. f. Physik **104**, 685 (1937). (§100)
B48. Brasch, Naturwiss. **21**, 82 (1933). (§92)
B49. Brasch, Lange, Waly, Banks, Chalmers, Szilard and Hopwood, Nature **134**, 880 (1934). (§92)
B50. Brasefield and Pollard, Phys. Rev. **50**, 296 (1936). (§99)
B51. Breit and Wigner, Phys. Rev. **49**, 519 (1936). (§52, 57, 86, 100, 102)
B52. Breit and Condon, Phys. Rev. **49**, 904 (1936). (§103)
B53. Breit, Condon and Present, Phys. Rev. **50**, 825 (1936). (§72)
B53a. Breit, R. S. I. **8**, 95 (1937). (§99)
B54. Breit, Phys. Rev. **51**, 248, 778 (1937). (§84)
B54a. Breit and Wigner, Phys. Rev. **51**, 593 (1937). (§105)
B55. Briggs, Proc. Roy. Soc. **114**, 313 (1927). (§97)
B56. Briggs, Proc. Roy. Soc. **114**, 341 (1927). (§96)
B57. Briggs, Proc. Roy. Soc. **118**, 549 (1928). (§95)
B58. Briggs, Proc. Roy. Soc. **139**, 638 (1933). (§95)
B59. Briggs, Proc. Roy. Soc. **143**, 604 (1934). (§95)
B60. Briggs, Proc. Roy. Soc. **157**, 183 (1936). (§92)
B61. Brillouin, Comptes rendus **183**, 24 (1926). (§66)
B62. Brown and Mitchell, Phys. Rev. **50**, 593 (1936). (§105)
B63. Burcham and Goldhaber, Proc. Camb. Phil. Soc. **32**, 632 (1936). (§102)
B64. Blau, J. de phys. et rad. **61** (1934). (§99)
B65. Bruche and Scherzer, *Geometrische Elektronenoptik* (J. Springer, 1934). (§106)
B66. Brubaker and Pollard, Phys. Rev. **51**, 1013 (1937). (§99)
B67. Buck, Strain, and Valley, Phys. Rev. **51**, 1012 (1937). (§100, 105)
B68. Burhop, Proc. Camb. Phil. Soc. **32**, 643–7 (1936). (§92, 100, 101)
C1. Carlson and Oppenheimer, Phys. Rev. **51**, 220 (1937). (§104)
C2. Chadwick and Bieler, Phil. Mag. **42**, 923 (1921). (§76)
C3. Chadwick, Proc. Roy. Soc. **128**, 114 (1930). (§74)
C4. Chadwick and Constable, Proc. Roy. Soc. **135**, 48 (1931). (§82, 99)
C5. Chadwick, Proc. Roy. Soc. **136**, 692 (1932). (§99)
C6. Chadwick, Nature **129**, 312 (1932). (§99)
C7. Chadwick, Proc. Roy. Soc. **142**, 1 (1933). (§82, 99)
C8. Chadwick, Feather and Davies, Proc. Camb. Phil. Soc. **30**, 357 (1934). (§85, 112)
C9. Chadwick and Goldhaber, Nature **134**, 237 (1934). (§91, 92)
C10. Chadwick and Feather, Int. Conf. Phys., London (1934). (§82, 99)
C11. Chadwick, Phil. Mag. **40**, 734 (1920). (§70)
C12. Chadwick and Goldhaber, Nature **135**, 65 (1935). (§102)
C13. Chadwick, Constable and Pollard, Proc. Roy. Soc. **130**, 463 (1931). (§82)
C14. Chadwick and Goldhaber, Proc. Roy. Soc. **151**, 479 (1935). (§93, 103)
C15. Chadwick, Phil. Mag. **2**, 1056 (1926). (§99)
C16. Chadwick and Goldhaber, Proc. Camb. Phil. Soc. **31**, 612 (1935). (§57, 102)
C16a. Chang, Goldhaber and Sagane, Nature **139**, 962 (1937). (§102, 103)
C17. Coates, Phys. Rev. **46**, 542 (1934). (§104)
C18. Cockcroft and Walton, Proc. Roy. Soc. **129**, 477 (1930). (§92)
C19. Cockcroft and Walton, Proc. Roy. Soc. **137**, 229 (1932). (§92, 100)
C20. Cockcroft and Walton, Nature **129**, 242 (1932). (§95)
C21. Cockcroft and Walton, Nature **129**, 649 (1932). (§100)
C22. Cockcroft and Walton, Proc. Roy. Soc. **136**, 619 (1932). (§92)
C23. Cockcroft and Walton, Nature **131**, 23 (1933). (§100)
C24. Cockcroft, Gilbert and Walton, Nature **133**, 328 (1934). (§100, 105)
C25. Cockcroft and Walton, Proc. Roy. Soc. **144**, 704 (1934). (§92, 96, 101)
C26. Cockcroft, Int. Conf. Phys., London (1934). (§96, 100, 101)
C27. Cockcroft, Gilbert and Walton, Proc. Roy. Soc. **148**, 225 (1935). (§92, 101)
C28. Cockcroft and Lewis, Proc. Roy. Soc. **154**, 246 (1936). (§85, 96, 101)

C29. Cockcroft and Lewis, Proc. Roy. Soc. **154**, 261 (1936). (§85, 96, 101, 107)
C30. Collie, Nature **137**, 614 (1936). (§93, 102)
C31. Condon and Breit, Phys. Rev. **49**, 229 (1936). (§59)
C32. Condon and Gurney, Phys. Rev. **33**, 127 (1929). (§66, 92)
C33. Cooksey and Lawrence, Phys. Rev. **49**, 866 (1936). (§101)
C34. Cork, Richardson and Kurie, Phys. Rev. **49**, 208 (1936). (§101, 105)
C35. Cork and Lawrence, Phys. Rev. **49**, 788 (1936). (§79, 84, 85, 101, 105)
C36. Cork and Thornton, Phys. Rev. **51**, 59 (1937). (§79, 85, 92, 101, 105)
C36a. Cork and Thornton, Phys. Rev. **51**, 608 (1937). (§101, 105)
C37. Crane, Lauritsen and Soltan, Phys. Rev. **44**, 514 (1933). (§101)
C38. Crane, Lauritsen and Soltan, Phys. Rev. **44**, 692 (1933). (§78, 101)
C39. Crane and Lauritsen, Phys. Rev. **45**, 497 (1934). (§81, 100, 105)
C40. Crane and Lauritsen, Phys. Rev. **45**, 430 (1934). (§101, 105)
C41. Crane, Lauritsen and Soltan, Phys. Rev. **45**, 507 (1934). (§101)
C42. Crane, Delsasso, Fowler and Lauritsen, Phys. Rev. **46**, 531 (1934). (§100)
C43. Crane and Lauritsen, Int. Conf. Phys., London (1934). (§99)
C44. Crane, Delsasso, Fowler and Lauritsen, Phys. Rev. **46**, 1109 (1934). (§99, 101)
C45. Crane, Delsasso, Fowler and Lauritsen, Phys. Rev. **47**, 782 (1935). (§100, 101)
C46. Crane, Delsasso, Fowler and Lauritsen, Phys. Rev. **47**, 887 (1935). (§101, 105)
C47. Crane, Delsasso, Fowler and Lauritsen, Phys. Rev. **48**, 484 (1935). (§100, 101)
C48. Crane, Delsasso, Fowler and Lauritsen, Phys. Rev. **47**, 971 (1935). (§101, 105)
C49. Crane, Delsasso, Fowler and Lauritsen, Phys. Rev. **48**, 100 (1935). (§101)
C50. Crane, Delsasso, Fowler and Lauritsen, Phys. Rev. **48**, 102 (1935). (§81, 90, 100)
C51. Crane, Delsasso, Fowler and Lauritsen, Phys. Rev. **48**, 125 (1935). (§90, 94, 100)
C52. Crane, Phys. Rev. **52**, 11 (1937). (§92)
C53. Curie and Joliot, J. de phys. et rad. **5**, 153 (1934). (§94)
C54. Curie and Joliot, Comptes rendus **198**, 254 (1934). (§99, 105)
C55. Curie and Joliot, Comptes rendus **197**, 237 (1933). (§99)
C56. Curie and Joliot, J. de phys. et rad. **4**, 21 (1933). (§99)
C57. Curie and Joliot, J. de phys. et rad. **4**, 494 (1933). (§105)
C58. Curie and Joliot, Comptes rendus **198**, 559 (1934). (§105)
C59. Curie and Joliot, J. de phys. et rad. **4**, 278 (1933). (§99)
C60. Curie, Halban and Preiswerk, J. de phys. et rad. **7**, 361 (1935). (§102, 105)
C61. Curie and Preiswerk, Comptes rendus **203**, 787 (1936). (§102)
D1. Dahl, Hafstad and Tuve, R. S. I. **4**, 373 (1933). (§94)
D2. Danysz, Rotblat, Wertenstein and Zyw, Nature **134**, 970 (1934). (§65)
D3. Danysz and Zyw, Acta Phys. Polonica **3**, 485 (1934). (§99)
D3a. Darling, Curtis and Cork, Phys. Rev. **51**, 1010 (1937). (§101, 105)
D4. Darrow, Bell S. Tech. J. **10**, 628 (1931). (§99, 105)
D5. Darrow, R. S. I. **5**, 66 (1934). (§99)
D6. Dee and Walton, Proc. Roy. Soc. **141**, 733 (1933). (§100, 101)
D7. Dee, Nature **133**, 564 (1934). (§101)
D8. Dee and Gilbert, Proc. Roy. Soc. **149**, 200 (1935). (§101)
D9. Dee and Gilbert, Proc. Roy. Soc. **154**, 279 (1936). (§85, 100, 101)
D10. Delbruck and Gamow, Zeits. f. Physik **72**, 492 (1931). (§87)
D11. Delsasso, Fowler and Lauritsen, Phys. Rev. **48**, 848 (1935). (§101)
D12. Delsasso, Fowler and Lauritsen, Phys. Rev. **50**, 389 (1936). (§100)
D13. Delsasso, Fowler and Lauritsen, Phys. Rev. **51**, 391 (1937). (§81, 90, 100)
D14. Delsasso, Fowler and Lauritsen, Phys. Rev. **51**, 527 (1937). (§90, 100)
D15. Dolch, Zeits. f. Physik **100**, 401 (1936). (§84)
D16. Doolittle, Phys. Rev. **49**, 779 (1936). (§84, 100)
D17. Döpel, Zeits. f. Physik **91**, 796 (1934). (§100)
D18. Duncanson, Proc. Camb. Phil. Soc. **30**, 102 (1934). (§95)
D19. Duncanson and Miller, Proc. Roy. Soc. **146**, 396 (1934). (§82, 99)
D20. Dunning and Pegram, Phys. Rev. **45**, 295 (1934). (§92)
D21. Dunning, Phys. Rev. **45**, 586 (1934). (§59, 85, 99)
D22. Dunning, R. S. I. **5**, 387 (1934). (§94)
D23. Dunning, Pegram, Fink and Mitchell, Phys. Rev. **48**, 265 (1935). (§57, 58, 60, 62, 63, 74)
D24. Dunning, Pegram, Fink and Mitchell, Phys. Rev. **47**, 970 (1935). (§102)
D25. Dunning, Pegram, Fink and Mitchell, Phys. Rev. **48**, 704 (1935). (§60)
D26. Dunning, Fink, Pegram and Segrè, Phys. Rev. **49**, 199 (1936). (§60)
D27. Dempster, Phys. Rev. **11**, 316 (1918). (§106)
D27a. Dempster, Phys. Rev. **50**, 98 (1936). (§107)
D28. DuBridge, Barnes and Buck, Phys. Rev. **51**, 995 (1937). (§100, 105)
D29. Dyer, *The Long Death* (Chas. Scribner's Sons, 1937). (§92)
E1. Ehrenberg, Nature **136**, 870 (1935). (§65, 102)
E2. Ellis, Int. Conf. Phys., London (1934). (§69)

E3. Ellis and Mott, Proc. Roy. Soc. **139**, 369 (1933). (§69)
E4. Ellis, Proc. Roy. Soc. **136**, 396 (1932). (§69)
E5. Ellis and Henderson, Nature **135**, 429 (1935). (§99, 101, 105)
E6. Ellis and Henderson, Nature **136**, 755 (1935). (§105)
E7. Ellis, Proc. Roy. Soc. **138**, 318 (1932). (§88)
E8. Ellis, Proc. Roy. Soc. **143**, 350 (1934). (§69, 103)
E9. Ellis and Aston, Proc. Roy. Soc. **129**, 180 (1930). (§88)
E10. Ellis and Henderson, Proc. Roy. Soc. **156**, 358 (1936). (§99, 105)
E11. Evans and Livingston, Rev. Mod. Phys. **7**, 229 (1935). (§98)
F1. Fahlenbrach, Zeits. f. Physik **96**, 503 (1935). (§99, 105)
F2. Farkas and Farkas, *Ortho-hydrogen, Para-hydrogen and Heavy hydrogen.* (§101)
F3. Fay, Phys. Rev. **50**, 560 (1936). (§65)
F4. Fea, Nuovo Cimento **12**, 368 (1935). (§101)
F5. Feather, Proc. Roy. Soc. **136**, 709 (1932). (§102)
F6. Feather, Nature **130**, 257 (1932). (§102)
F7. Feather, Proc. Roy. Soc. **141**, 194 (1933). (§95)
F8. Feather, Proc. Roy. Soc. **142**, 689 (1933). (§93, 94, 102)
F9. Feather, Nature **136**, 468 (1935). (§103)
F9a. Feenberg, Phys. Rev. **49**, 328 (1936). (§84)
F10. Feenberg and Wigner, Phys. Rev. **51**, 95 (1937). (§81, 83, 89, 99, 101, 110)
F11. Feenberg and Phillips, Phys. Rev. **51**, 597 (1937). (§110)
F12. Fermi, Ric. Sci. **2**, 12 (1933). (§102, 105)
F13. Fermi, Amaldi, D'Agostino, Rasetti and Segrè, Proc. Roy. Soc. **146**, 483 (1934). (§57, 65, 94, 102, 105)
F14. Fermi, Nature **133**, 757 (1934). (§102)
F15. Fermi, Pontecorvo and Rasetti, Ricerca Scient. **2** (1934). (§105)
F16. Fermi and Rasetti, Nuovo Cimento **12**, 201 (1935). (§105)
F17. Fermi, Ric. Sci. **7**, 13 (1936). (§59, 102)
F18. Fermi, *Zeeman Jubilee* (1935), p. 128. (§59)
F19. Fink, Dunning, Pegram and Mitchell, Phys. Rev. **49**, 103 (1936). (§60, 61)
F20. Fink, Phys. Rev. **50**, 738 (1936). (§59)
F21. Fischer-Colbrie, Ak. W. Wien, **145**, 283 (1936). (§99)
F22. Fisk, Schiff and Shockley, Phys. Rev. **50**, 1090 (1936). (§59)
F23. Fisk and Morse, Phys. Rev. **51**, 54 (1937). (§59)
F24. Fleischmann and Gentner, Zeits. f. Physik **100**, 440 (1936). (§102, 103)
F25. Fleischmann, Zeits. f. Physik **103**, 113 (1936). (§57, 90, 102)
F26. Flügge, and Krebs, Physik. Zeits. **36**, 466 (1935). (§101)
F26a. Flügge and Krebs, Physik. Zeits. **38**, 13 (1937). (§101)
F27. Fomin and Houtermans, Physik. Zeits. Sowjetunion **9**, 273 (1936). (§102, 105)
F28. Fowler, Delsasso and Lauritsen, Phys. Rev. **49**, 561 (1936). (§101, 105)
F28a. Fowler and Lauritsen, Phys. Rev. **51**, 1103 (1937). (§101)
F29. Fox and Rabi, Phys. Rev. **48**, 746 (1935). (§101)
F30. Frenkel, Physik. Zeits. Sowjetunion **9**, 533 (1936). (§53)
F31. Frisch, Nature **133**, 721 (1934). (§99, 101, 105)
F32. Frisch, Nature **136**, 220 (1935). (§99, 105)
F33. Frisch and Placzek, Nature **137**, 357 (1936). (§58, 61, 102)
F33a. Fünfer, Ann. d. Physik **29**, 1 (1937). (§102)
F34. Furry, Phys. Rev. **51**, 592 (1937). (§59)
G1. Gaerttner, Turin and Crane, Phys. Rev. **49**, 793 (1936). (§105)
G2. Gaerttner and Crane, Phys. Rev. **51**, 58 (1937). (§100)
G3. Gaerttner and Crane, Phys. Rev. **51**, 49 (1937). (§100)
G4. Gamow, Nature **133**, 833 (1934). (§87, 105)
G5. Gamow, Phys. Rev. **49**, 946 (1936). (§65)
G6. Gamow, Physik. Zeits. **32**, 651 (1931). (§69)
G7. Gamow, Zeits. f. Physik **52**, 510 (1929). (§66, 92)
G8. Gamow, Nature **122**, 805 (1929). (§66)
G9. Gamow, *Atomic Nuclei and Radioactivity* (Cambridge, 1937). (§68)
G10. Gamow and Houtermans, Zeits. f. Physik **52**, 496 (1929). (§66, 68)
G11. Geiger, Proc. Roy. Soc. **83**, 492 and 505 (1910). (§95)
G12. Geiger, *Handbuch der Physik*, Vol. 24 (1927), 137. (§95)
G13. Geiger and Nuttall, Phil. Mag. **22**, 613 (1911). (§68)
G13a. Gentner, Naturwiss. **25**, 12 (1937)
G14. Gerthsen and Reusse, Physik. Zeits. **34**, 478 (1933). (§95)
G14a. Giarratana and Brennecke, Phys. Rev. **49**, 35 (1936). (§84)
G15. Goldhaber, Proc. Camb. Phil. Soc. **30**, 560 (1934). (§83, 101)
G16. Goldsmith and Cohen, Phys. Rev. **45**, 850 (1934). (§102)
G17. Goldsmith and Rasetti, Phys. Rev. **50**, 328 (1936). (§58, 60, 61)
G18. Goldsmith and Manley, Phys. Rev. **51**, 382 (1937). (§58, 60)
G18a. Goldsmith and Manley, Phys. Rev. **51**, 1022 (1937). (§60)
G18b. Goloborodko and Rosenkewitsch, Physik. Zeits. Sowjetunion **11**, 78 (1937). (§103)
G19. Goudsmit, Phys. Rev. **49**, 406 (1936). (§59)
G20. Goudsmit, Phys. Rev. **51**, 64 (1937). (§53)
G21. Gray, Proc. Camb. Phil. Soc. **27**, 103 (1931). (§93)
G22. Greinacher, Zeits. f. Physik **36**, 364 (1926). (§94)
G23. Griffiths and Szilard, Nature **139**, 323 (1937). (§90)
G24. Gurney, Nature **123**, 565 (1929). (§99)
G25. Güttinger and Pauli, Zeits. f. Physik **67**, 743 (1931). (§83)
G26. Gentner, Naturwiss. **25**, 12 (1937). (§100)

G27. Grahame, Seaborg and Gibson, Phys. Rev. **51**, 590 (1937). (§65)
G28. Gibson, Seaborg and Grahame, Phys. Rev. **51**, 370 (1937). (§65)
H1. Hafstad, Tuve and Brown, Phys. Rev. **45**, 746 (1934). (§101)
H2. Hafstad and Tuve, Phys. Rev. **47**, 506 (1935). (§92, 100)
H3. Hafstad and Tuve, Phys. Rev. **47**, 507 (1935). (§100)
H4. Hafstad and Tuve, Phys. Rev. **48**, 306 (1935). (§81, 92, 100, 105)
H5. Hafstad, Heydenburg and Tuve, Phys. Rev. **49**, 866 (1936). (§92, 100)
H6. Hafstad, Heydenburg and Tuve, Phys. Rev. **50**, 504 (1936). (§56, 81, 84)
H7. Hahn and Meitner, Naturwiss. **23**, 320 (1935). (§65, 85)
H8. von Halban and Preiswerk, Nature **137**, 905 (1936). (§58, 60)
H9. von Halban and Preiswerk, Helv. Phys. Acta **9**, 318 (1936). (§58, 60)
H10. von Halban and Preiswerk, J. de phys. et rad. **8**, 29 (1937). (§60)
H11. Hall, Phys. Rev. **49**, 401 (1936). (§103)
H11a. Halpern, Lueneburg and Clark, Phys. Rev., in press. (§59)
H12. Harkins, Gans, Newson, Phys. Rev. **44**, 529 (1933). (§102)
H13. Harkins and Gans, Phys. Rev. **46**, 397 (1934). (§102)
H14. Harkins, Gans and Newson, Phys. Rev. **47**, 52 (1935). (§102)
H15. Harkins, Kamen, Newson and Gans, Phys. Rev. **50**, 980 (1936). (§59)
H16. Hartree, Proc. Roy. Soc. **139**, 311 (1933). (§95)
H17. Haxel, Zeits. f. Physik **83**, 323 (1933). (§99)
H18. Haxel, Zeits. f. Physik **93**, 400 (1935). (§99)
H19. Haxel, Physik. Zeits. **36**, 804 (1935). (§99)
H19a. Haxel, Zeits. f. Physik **104**, 540 (1937). (§102)
H20. Henderson, M. C., Phys. Rev. **43**, 98 (1935). (§84)
H21. Henderson, Livingston and Lawrence, Phys. Rev. **45**, 428 (1934). (§100, 101, 105)
H22. Henderson, Livingston and Lawrence, Phys. Rev. **46**, 38 (1934). (§78, 100)
H23. Henderson, Phys. Rev. **48**, 480 (1935). (§78, 80)
H24. Henderson, Phys. Rev. **48**, 855 (1935). (§101, 105)
H24a. Henderson, W. J., Ridenour, White and M. C. Henderson, Phys. Rev. **51**, 1107 (1937). (§99)
H24b. Henderson and Ridenour, Phys. Rev. **52**, 40 (1937). (§99)
H25. Henneberg, Zeits. f. Physik **83**, 555 (1933). (§51)
H26. Henneberg, Zeits. f. Physik **86**, 592 (1933). (§95)
H27. Herb, Parkinson and Kerst, Phys. Rev. **48**, 118 (1935). (§84, 100)
H28. Herb, Parkinson and Kerst, Phys. Rev. **51**, 75 (1937). (§92)
H28a. Herb, Kerst and McKibben, Phys. Rev. **51**, 691 (1937). (§100)
H29. Hevesy and Levi, Nature **135**, 580 (1935). (§102, 105)
H30. Hevesy and Levi, Nature **136**, 103 (1935). (§102, 105)
H31. Hevesy and Levi, Nature **137**, 185 (1936). (§60, 62, 102, 105)
H31a. Hevesy and Levi, Kgl. Danske Acad. (1936). (§102)
H32. Hevesy, Nature **135**, 1051 (1935). (§102, 105)
H33. Heyn, Nature **138**, 723 (1936). (§85, 102, 105)
H33a. Heyn, Physica **4**, 160 (1937). (§65, 102)
H33b. Heyn, Nature **139**, 842 (1937). (§102)
H34. Hoffman and Bethe, Phys. Rev. **51**, 1021 (1937). (§61)
H35. Hönl, Zeits. f. Physik **84**, 1 (1933). (§95)
H36. Hopwood and Chalmers, Nature **135**, 341 (1935). (§93)
H37. Horsley, Phys. Rev. **48**, 1 (1935). (§74)
H38. Horvay, Phys. Rev. **50**, 897 (1936). (§59)
H38a. Hulme, McDougall, Buckingham and Fowler, Proc. Roy. Soc. **149**, 131 (1935). (§93)
H39. Hulme, Mott, Oppenheimer and Taylor, Proc. Roy. Soc. **155**, 315 (1936). (§88)
H39a. Hurst and Walke, Phys. Rev. **51**, 1033 (1937). (§99, 101, 102)
I1. Inglis, Phys. Rev. **50**, 783 (1936). (§83)
J1. Jaeckel, Zeits. f. Physik **96**, 151 (1935). (§102)
J2. Johnson and Hamblin, Nature **138**, 504 (1936). (§102, 105)
J3. Johnson and Johnson, Phys. Rev. **50**, 170 (1936). (§94)
J4. Jordan and Bainbridge, Phys. Rev. **49**, 883 (1936). (§107)
J5. Jordan and Bainbridge, Phys. Rev. **50**, 98 (1936). (§107)
J6. Jordan and Bainbridge, Phys. Rev. **51**, 385 (1937). (§107)
K1. Kapitza, Proc. Roy. Soc. **106**, 602 (1924). (§95)
K2. Kempton, Browne and Maasdorp, Proc. Roy. Soc. **157**, 372 (1936). (§83, 85, 101)
K3. Kempton, Browne and Maasdorp, Proc. Roy. Soc. **157**, 386 (1936). (§84, 85, 101)
K4. Kikuchi, Aoki and Husimi, Proc. Phys. Math. Soc. Japan **17**, 369 (1935). (§57)
K5. Kikuchi, Husimi and Aoki, Proc. Phys. Math. Soc. Japan **18**, 35 (1936). (§57, 89)
K6. Kikuchi, Aoki and Husimi, Nature **137**, 186 (1936). (§102)
K7. Kikuchi, Aoki and Husimi, Nature **137**, 398 (1936). (§65)
K8. Kikuchi, Aoki and Husimi, Nature **137**, 745 (1936). (§102)
K9. Kikuchi, Aoki and Husimi, Proc. Phys. Math. Soc. Japan **18**, 115 (1936). (§57, 65)
K10. Kikuchi, Husimi and Aoki, Nature **137**, 992 (1936). (§57)
K11. Kikuchi, Husimi and Aoki, Proc. Phys. Math. Soc. Japan **18**, 188 (1936). (§57, 102)
K12. Kikuchi, Aoki and Husimi, Nature **138**, 84 (1936). (§102)
K12a. Kikuchi, Aoki and Husimi, Proc. Phys. Math. Soc. Japan **18**, 727 (1936). (§65)
K12b. Kikuchi, Husimi and Aoki, Zeits. f. Physik **105**, 265 (1937). (§102)

K13. Kinsey, Phys. Rev. **50**, 386 (1936). (§92, 104)
K14. Kirchner, Ergeb. d. exact. Naturwiss. **13**, 57 (1934). (§101)
K15. Kirchner and Neuert, Physik. Zeits. **35**, 292 (1934). (§85, 100)
K16. Kirchner and Neuert, Physik. Zeits. **36**, 54 (1935). (§95, 100)
K17. Klarmann, Zeits. f. Physik **95**, 221 (1935). (§102)
K18. Klarmann, Zeits. f. Physik **87**, 411 (1933). (§94)
K19. Klein and Nishina, Zeits. f. Physik **52**, 853 (1928). (§93)
K20. Knol and Veldkamp, Physica **3**, 145 (1936). (§102, 105)
K21. Konig, Zeits. f. Physik **90**, 197 (1934). (§99)
K22. Konopinski and Uhlenbeck, Phys. Rev. **48**, 7 (1935). (§105)
K23. Konopinski and Bethe, Phys. Rev., to be published shortly. (§78)
K23a. Konopinski and Bethe, Phys. Rev. **51**, 1004 (1937). (§54).
K24. Kramers, Zeits. f. Physik **39**, 828 (1926). (§66)
K25. Kraus and Cork, Phys. Rev. **51**, 383 (1937). (§101, 105)
K26. Kruger and Green, Phys. Rev. **51**, 699 (1937). (§92)
K26a. Kruger, Shoupp and Stallmann, Phys. Rev. **51**, 1021 (1937). (§59)
K26b. Kruger and Green, Phys. Rev. **52**, 247 (1937). (§101)
K27. Kurie, R. S. I. **3**, 655 (1932). (§94)
K28. Kurie, Phys. Rev. **43**, 771 (1933). (§102)
K29. Kurie, Phys. Rev. **43**, 1056 (1933). (§59)
K30. Kurie, Phys. Rev. **45**, 904 (1934). (§102)
K31. Kurie, Phys. Rev. **47**, 97 (1935). (§65, 102)
K32. Kurie, Richardson and Paxton, Phys. Rev. **48**, 167 (1935). (§105)
K33. Kurie, Richardson and Paxton, Phys. Rev. **49**, 368 (1936). (§99, 101, 105)
K34. Kurtchatov, Kurtchatov, Myssowsky and Roussinow, Comptes rendus **200**, 1201 (1935). (§87, 102, 105)
K35. Kurtschatow, Nemenow and Selinow, Comptes rendus **200**, 2162 (1935). (§102, 105)
K36. Kurtschatow, Latyschew, Nemenow and Selinow, Physik. Zeits. Sowjetunion **8**, 589 (1935). (§102, 105)
K37. Kronig, Physica **4**, 171 (1937). (§85)
L1. Ladenburg, Roberts and Sampson, Phys. Rev. **48**, 467 (1935). (§92)
L1a. Ladenburg and Kanner, Phys. Rev. **51**, 1022 (1937). (§105)
L1b. Laporte, Phys. Rev., in press (§61)
L2. Laslett, Phys. Rev. **50**, 388 (1936). (§101, 105)
L3. Latimer, Hull and Libby, J. Am. Chem. Soc. **57**, 781 (1935). (§102, 105)
L4. Laue, Zeits. f. Physik **52**, 726 (1929). (§66)
L5. Lauritsen and Crane, Phys. Rev. **45**, 493 (1934). (§85, 101)
L6. Lauritsen and Crane, Phys. Rev. **45**, 63 (1934). (§100)
L7. Lauritsen and Crane, Phys. Rev. **45**, 345 (1934). (§94, 101)
L8. Lauritsen and Crane, Phys. Rev. **45**, 550 (1934). (§101)
L9. Lauritsen and Crane, Phys. Rev. **32**, 850 (1928). (§92)
L10. Lawrence, Phys. Rev. **46**, 746 (1934). (§101)
L11. Lawrence, Livingston and White, Phys. Rev. **42**, 150 (1932). (§92)
L12. Lawrence, Livingston and Lewis, Phys. Rev. **44**, 56 (1933). (§101)
L13. Lawrence and Livingston, Phys. Rev. **45**, 220 (1934). (§101)
L14. Lawrence and Livingston, Phys. Rev. **45**, 608 (1934). (§92)
L15. Lawrence, Phys. Rev. **47**, 17 (1935). (§101, 105)
L16. Lawrence, McMillan and Henderson, Phys. Rev. **47**, 273 (1935). (§96, 101)
L17. Lawrence, McMillan and Thornton, Phys. Rev. **48**, 493 (1935). (§80, 101)
L18. Lawrence and Cooksey, Phys. Rev. **50**, 1131 (1936). (§92)
L19. Lea, Proc. Roy. Soc. **150**, 637 (1935). (§65, 83, 102)
L20. Lewis, G. N., and Macdonald, J. Chem. Phys. **1**, 341 (1933). (§101)
L21. Lewis, G. N., Livingston and Lawrence, Phys. Rev. **44**, 55 (1933). (§101)
L22. Lewis, G. N., Livingston and Lawrence, Phys. Rev. **44**, 317 (1933). (§101)
L23. Lewis, W. B. and Wynn-Williams, Proc. Roy. Soc. **136**, 349 (1932). (§69, 92)
L24. Lewis, W. B., Burcham and Chang, Nature **139**, 24 (1937). (§101, 105)
L25. Livingood and Snell, Phys. Rev. **48**, 851 (1935). (§92, 104)
L26. Livingood, Phys. Rev. **50**, 425 (1936). (§101, 105)
L27. Livingood and Seaborg, Phys. Rev. **50**, 435 (1936). (§101, 105)
L27a. Livingood, Seaborg and Fairbrother, Phys. Rev. **52**, 135 (1937). (§101, 102, 105)
L27b. Livingood and Seaborg, Phys. Rev. **52**, 135 (1937). (§101, 102, 105)
L28. Livingston, Henderson and Lawrence, Phys. Rev. **44**, 316 (1933). (§100)
L29. Livingston, Henderson and Lawrence, Phys. Rev. **46**, 325 (1934). (§102)
L30. Livingston and McMillan, Phys. Rev. **46**, 437 (1934). (§101)
L31. Livingston, R. S. I. **7**, 55 (1936). (§92)
L32. Livingston and Hoffman, Phys. Rev. **50**, 401 (1936). (§102)
L33. Livingston and Hoffman, Phys. Rev. **51**, 1021 (1937). (§61)
L34. Livingston, Genevese and Konopinski, Phys. Rev. **51**, 835 (1937). (§95)
L35. Lyford and Bearden, Phys. Rev. **45**, 743 (1934). (§68)
L36. Lyman, Phys. Rev. **51**, 1 (1937). (§105)
L37. Lukirsky and Careva, Comptes rendus (U.S.S.R.) **3**, 411 (1936). (§102)
L38. Li, Proc. Roy. Soc. **158**, 571 (1937). (§88)
M1. Madsen, Nature **138**, 722 (1936). (§102, 105)

M2. Manley and Millman, Phys. Rev. **51**, 19 (1937). (§83)
M2a. Manley, Goldsmith and Schwinger, Phys. Rev. **51**, 1022 (1937). (§61)
M3. Mano, Comptes rendus **197**, 47 (1933). (§95)
M4. Mano, Ann. d. Physik **1**, 407 (1934). (§95)
M5. Mano, Comptes rendus **194**, 1235 (1932). (§95)
M6. Mano, J. de phys. et rad. **5**, 628 (1934). (§95)
M7. Marsh and Sugden, Nature **136**, 102 (1935). (§102, 105)
M8. Massey and Mohr, Proc. Roy. Soc. **148**, 206 (1935). (§74)
M9. Massey and Burhop, Phys. Rev. **48**, 468 (1935). (§51)
M10. Mattauch, Phys. Rev. **50**, 617, 1089 (1936). (§107)
M10a. Mattauch, Physik. Zeits. **35**, 567 (1934). (§107)
M10b. Mattauch, Naturwiss. **25**, 156 (1937). (§107)
M10c. Mattauch, Naturwiss. **25**, 170 (1937). (§107)
M11. May and Vaidyanathan, Proc. Roy. Soc. **155**, 519 (1936). (§99)
M12. Meitner and Philipp, Naturwiss. **20**, 929 (1932). (§102)
M13. Meitner and Philipp, Zeits. f. Physik **87**, 484 (1934). (§102)
M14. Meitner, Naturwiss. **22**, 420 (1934). (§99, 105)
M15. Meitner and Hahn, Naturwiss. **24**, 158 (1936). (§65, 85, 105)
M15a. Meitner, Ann. d. Physik **29**, 246 (1937). (§105)
M16. Miller, Duncanson and May, Proc. Camb. Phil. Soc. **30**, 549 (1934). (§82, 99, 105)
M17. Mitchell, A. C. G., and Murphy, Phys. Rev. **47**, 881 (1935). (§58, 63)
M18. Mitchell, A. C. G., and Murphy, Phys. Rev. **48**, 653 (1935). (§58, 63)
M19. Mitchell, A. C. G., Murphy and Langer, Phys. Rev. **49**, 400 (1936). (§58, 63)
M20. Mitchell, A. C. G., Murphy and Whitaker, Phys. Rev. **50**, 133 (1936). (§58, 63)
M20a. Mitchell, A. C. G., Phys. Rev. **51**, 995 (1937). (§102, 105)
M20b. Mitchell, A. C. G. and Langer, Phys. Rev. **52**, 137 (1937). (§105)
M21. Mitchell, D. P., Phys. Rev. **49**, 453 (1936). (§93, 102)
M22. Mitchell, D. P., Rasetti, Fink and Pegram, Phys. Rev. **50**, 189 (1936). (§91, 103)
M23. Mitchell, D. P., and Powers, Phys. Rev. **50**, 486 (1936). (§60)
M24. Mohr and Pringle, Nature **137**, 865 (1936). (§74)
M25. Møller, Ann. d. Physik **14**, 531 (1932). (§95)
M26. Moon and Tillman, Proc. Roy. Soc. **153**, 476 (1936). (§57, 102)
M28. Morse, Fisk and Schiff, Phys. Rev. **50**, 748 (1936). (§59)
M29. Morse, Fisk and Schiff, Phys. Rev. **51**, 706 (1937). (§59)
M30. Marsden and Taylor, Proc. Roy. Soc. **88**, 443 (1913). (§95)
M31. Mott, Proc. Roy. Soc. **126**, 259 (1929). (§74)
M32. Mott and Massey, *Theory of Atomic Collisions* (Oxford, 1933). (§51, 59, 70)
M33. Mott, Proc. Camb. Phil. Soc. **27**, 553 (1931). (§95)
M34. Mott-Smith and Bonner, Phys. Rev. **45**, 554 (1934). (§92)
Mc1. McLennan, Grimmett and Read, Nature **135**, 147 (1935). (§102, 105)
Mc2. McLennan, Grimmett and Read, Nature **135**, 505 (1935). (§102)
Mc3. McLennan and Rann, Nature **136**, 831 (1935). (§102, 105)
Mc4. McMillan, Phys. Rev. **46**, 868 (1934). (§93, 100, 101)
Mc5. McMillan and Lawrence, Phys. Rev. **47**, 343 (1935). (§101)
Mc6. McMillan and Livingston, Phys. Rev. **47**, 452 (1935). (§94, 101, 105)
Mc7. McMillan, Phys. Rev. **49**, 875 (1936). (§101, 102, 105)
N1. Nahmias and Walen, Comptes rendus **203**, 71 (1936). (§102, 105)
N2. Naidu and Siday, Proc. Phys. Soc. London **48**, 330 (1936). (§105)
N3. Naidu, Nature **137**, 578 (1936). (§102, 105)
N4. Neuert, Physik. Zeits. **36**, 629 (1935). (§95, 100)
N4a. Neuert, Physik. Zeits. **38**, 122 (1937). (§100, 101)
N5. Newson, Phys. Rev. **48**, 482 (1935). (§101, 105)
N6. Newson, Phys. Rev. **48**, 790 (1935). (§96, 99, 105)
N7. Newson, Phys. Rev. **49**, 208 (1936). (§101)
N7a. Newson, Phys. Rev. **51**, 620 (1937). (§101)
N7b. Newson, Phys. Rev. **51**, 624 (1937). (§101, 105)
N8. Nier, Phys. Rev. **50**, 1041 (1936). (§107)
N9. Nier, Phys. Rev. **51**, 1007 (1937). (§107)
O½. Oeser and Tuck, Nature **139**, 1110 (1937). (§102)
O1. Oliphant, Shire and Crowther, Proc. Roy. Soc. **146**, 922 (1934). (§100, 101)
O2. Oliphant and Rutherford, Proc. Roy. Soc. **141**, 259 (1933). (§85, 92, 100)
O3. Oliphant, Kinsey and Rutherford, Proc. Roy. Soc **141**, 722 (1933). (§78, 85, 100, 101)
O4. Oliphant, Shire and Crowther, Nature **133**, 377 (1934). (§101)
O5. Oliphant, Harteck and Rutherford, Nature **133**, 413 (1934). (§101)
O6. Oliphant, Int. Conf. Phys., London (1934). (§84, 100, 101)
O7. Oliphant, Harteck and Rutherford, Proc. Roy. Soc. **144**, 692 (1934). (§92, 101)
O8. Oliphant, Kempton and Rutherford, Proc. Roy. Soc. **149**, 406 (1935). (§96, 100, 101)
O9. Oliphant, Kempton and Rutherford, Proc. Roy. Soc. **150**, 241 (1935). (§85, 96, 100, 101)
O10. Oppenheimer, Phys. Rev. **43**, 380 (1933). (§101)
O11. Oppenheimer and Phillips, Phys. Rev. **48**, 500 (1935). (§80, 101)
O12. Oppenheimer and Serber, Phys. Rev. **50**, 391 (1936). (§53)
O13. Ortner and Stetter, Zeits. f. Physik **54**, 449 (1929). (§94)
O14. Ostrofsky, Breit and Johnson, Phys. Rev. **49**, 196 (1936). (§84)
O15. Ostrofsky, Breit and Johnson, Phys. Rev. **49**, 22 (1936). (§84, 100)

O16. Ostrofsky, Bleick and Breit, Phys. Rev. **49**, 352 (1936). (§84)
P1. Paton, Phys. Rev. **46**, 229 (1934). (§99)
P1a. Paneth and Lollett, Nature **136**, 950 (1935). (§99)
P2. Paton, Zeits. f. Physik **90**, 586 (1934). (§82)
P3. Paton, Phys. Rev. **47**, 197 (1935). (§99)
P4. Paxton, Phys. Rev. **49**, 206 (1936). (§101)
P5. Peierls, Proc. Roy. Soc. **149**, 467 (1935). (§105)
P6. Perrin and Elsasser, J. de phys. et rad. **6**, 194 (1935). (§57)
P6a. Polanyi and Wigner, Zeits. f. physik. Chemie **139**, 439 (1928). (§51)
P7. Pollard, Proc. Leeds Phil. Lit. Soc. **2**, 324 (1932). (§99)
P8. Pollard and Brasefield, Phys. Rev. **50**, 890 (1936). (§99)
P9. Pollard and Brasefield, Phys. Rev. **51**, 8 (1937). (§99)
P10. Pollard, Schultz and Brubaker, Phys. Rev. **51**, 140 (1937). (§99)
P11. Pool and Cork, Phys. Rev. **51**, 383 (1937). (§101, 105)
P11a. Pool and Cork, Phys. Rev. **51**, 1010 (1937). (§101, 105)
P11b. Pool, Cork and Thornton, Phys. Rev. **51**, 890 (1937). (§102, 105)
P11c. Pool, Cork and Thornton, Phys. Rev. **52**, 41 (1937). (§102, 105)
P11d. Pool, Cork and Thornton, Phys. Rev. **52**, 239 (1937). (§102, 105)
P12. Pose, Physik. Zeits. **30**, 780 (1929). (§99)
P13. Pose and Diebner, Zeits. f. Physik **90**, 773 (1934). (§74)
P14. Powers, Fink and Pegram, Phys. Rev. **49**, 650 (1936). (§61, 62)
P15. Preiswerk and Halban, Comptes rendus **201**, 722 (1935). (§102, 105)
R1. Rabi, Phys. Rev. **43**, 838 (1933). (§65)
R2. Rasetti, Zeits. f. Physik **78**, 165 (1932). (§99)
R3. Rasetti, Zeits. f. Physik **97**, 64 (1935). (§57, 90, 93, 94, 102)
R4. Rasetti, Segrè, Fink, Dunning and Pegram, Phys. Rev. **49**, 104 (1936). (§58, 61, 102)
R5. Rasetti, Mitchell, Fink and Pegram, Phys. Rev. **49**, 777 (1936). (§58, 60)
R5a. Rasetti, *Elements of Nuclear Physics* (Prentice Hall, 1936). (§69, 88)
R6. Richardson, Phys. Rev. **49**, 203 (1936). (§105)
R6a. Richardson and Emo, Phys. Rev. **51**, 1014 (1937). (§103)
R7. Richardson and Kurie, Phys. Rev. **50**, 999 (1936). (§101, 105)
R7a. Ridenour, Henderson, Henderson and White, Phys. Rev. **51**, 1013 (1937). (§99)
R7b. Ridenour and Henderson, Phys. Rev. **51**, 1102 (1937). (§99)
R7c. Ridenour and Henderson, Phys. Rev. **52**, 139 (1937). (§99)
R8. Riezler, Proc. Roy. Soc. **134**, 154 (1932). (§75)
R9. Riezler, Ann. d. Physik **23**, 198 (1935). (§75)
R9a. Risser, Phys. Rev. **51**, 1013 (1937). (§102, 105)
R10. Rose and Bethe, Phys. Rev. **51**, 205 (1937). (§83)
R10a. Rose and Bethe (Errata), Phys. Rev., in press. (§91)
R11. Rose, Phys. Rev. **51**, 1024 (1937). (§90)
R12. Rosenblum and Chamie, Comptes rendus **194**, 1154 (1932). (§69)
R13. Rosenblum, Ann. d. Physik **10**, 408 (1928). (§95)
R14. Rosenblum, Comptes rendus **202**, 1274 (1936). (§69)
R14a. Rosenblum, Guillot and Perey, Comptes rendus **204**, 175 (1937). (§69)
R15. Rotblat, Nature **136**, 515 (1935). (§102, 105)
R16. Rotblat, Nature **138**, 202 (1936). (§102)
R16a. Rotblat, Nature **139**, 1110 (1937). (§102).
R17. Ruark and Fussler, Phys. Rev. **48**, 151 (1935). (§68)
R17a. Ruben and Libby Phys. Rev. **51**, 776 (1937). (§60)
R18. Rüchardt, Ann. d. Physik **71**, 377 (1923). (§95)
R19. Rumbaugh and Hafstad, Phys. Rev. **50**, 681 (1936). (§101)
R19a. Rumbaugh, Roberts and Hafstad, Phys. Rev. **51**, 1106 (1937). (§101)
R20. Rusinow, Physik. Zeits. Sowjetunion **10**, 219 (1936). (§65, 85, 102)
R21. Rutherford, Chadwick and Ellis, *Radiations from Radioactive Substances* (1930). (§94, 99)
R21a. Rutherford, Phil. Mag. **47**, 277 (1924). (§95)
R22. Rutherford, Lewis, Bowden, Proc. Roy. Soc. **142**, 347 (1933). (§69, 95)
R23. Rutherford, Wynn-Williams, Lewis and Bowden, Proc. Roy. Soc. **139**, 617 (1933). (§69, 92, 95)
R24. Rutherford and Chadwick, Phil. Mag. **42**, 809 (1921). (§99)
R25. Rutherford and Chadwick, Phil. Mag. **4**, 605 (1927). (§74)
R26. Rutherford, Phil. Mag. **21**, 669 (1911). (§70)
S1. Sagane, Phys. Rev. **50**, 1141 (1936). (§101, 105)
S2. Sampson, Ridenour and Bleakney, Phys. Rev. **50**, 382 (1936). (§105)
S3. Sampson and Bleakney, Phys. Rev. **50**, 732 (1936). (§105)
S3a. Sampson and Bleakney, Phys. Rev. **50**, 456 (1936). (§107)
S4. Savel, Comptes rendus **198**, 368 (1934). (§99)
S5. Savel, Ann. d. Physik **4**, 88 (1935). (§99)
S6. Savel, Comptes rendus **198**, 1404 (1934). (§99)
S7. Schnetzler, Zeits. f. Physik **95**, 302 (1935). (§99)
S8. Schüler, Zeits. f. Physik **66**, 431 (1930). (§83)
S8a. Schultz, Phys. Rev. **51**, 1023 (1937). (§99)
S9. Segrè, Nuovo Cimento **12**, 232 (1935). (§94)
S10. Sexl, Zeits. f. Physik **81**, 163 (1933). (§66)
S11. Sexl, Zeits. f. Physik **56**, 62 and 72: **59**, 579 (1929). (§66)
S11a. Shepherd, Haxby and Williams, Phys. Rev. **52**, 247 (1937). (§100, 101)
S12. Sizoo and Koene, Physica **3**, 1053 (1936). (§105)
S13. Sloan and Coates, Phys. Rev. **46**, 539 (1934). (§92, 104)
S14. Sloan, Phys. Rev. **47**, 62 (1935). (§92)
S15. Snell, Phys. Rev. **49**, 555 (1936). (§101, 105)
S16. Snell, Phys. Rev. **51**, 142 (1937). (§101, 105)
S16a. Snell, Phys. Rev. **51**, 1011 (1937). (§99, 101, 105)

S17. Soden, Ann. d. Physik **19**, 409 (1934). (§51)
S18. Sosnowski, Comptes rendus **200**, 391 (1935). (§101)
S19. Sosnowski, Comptes rendus **200**, 1027 (1935). (§105)
S20. Sosnowski, Comptes rendus **200**, 922 (1935). (§102, 105)
S21. Stegmann, Zeits. f. Physik **95**, 72 (1935). (§99)
S22. Stetter, Zeits. f. Physik **100**, 652 (1936). (§99)
S23. Steudel, Zeits. f. Physik **77**, 139 (1932). (§99)
S24. Stone, Livingston, Sloan and Chaffee, Radiology **24**, 153 (1935). (§92)
S25. Sugden, Nature **135**, 469 (1935). (§102, 105)
S26. Szilard and Chalmers, Nature **134**, 494 (1934). (§92, 103)
S27. Szilard and Chalmers, Nature **134**, 462 (1934). (§94)
S28. Szilard and Chalmers, Nature **135**, 98 (1935). (§87, 105)
S29. Szilard, Nature **136**, 950 (1935). (§57, 102)
T1. Taylor and Goldhaber, Nature **135**, 341 (1935). (§94)
T2. Taylor, Proc. Phys. Soc. London **47**, 873 (1935). (§102)
T3. Taylor and Dabholkar, Proc. Phys. Soc. London **48**, 285 (1936). (§102)
T4. Taylor and Mott, Proc. Roy. Soc. **142**, 215 (1933). (§88)
T5. Taylor and Mott, Proc. Roy. Soc. **138**, 665 (1932). (§88)
T6. Taylor, Proc. Roy. Soc. **136**, 605 (1932). (§73, 74)
T7. Taylor, Proc. Roy. Soc. **134**, 103 (1931). (§74)
T8. Teller, Phys. Rev. to be published shortly? (§78)
T9. Thomson and Saxton, Phil. Mag. **23**, 241 (1937). (§104)
T10. Thornton, Phys. Rev. **49**, 207 (1936). (§101, 105)
T10a. Thornton, Phys. Rev. **51**, 893 (1937). (§101)
T11. Thornton and Cork, Phys. Rev. **51**, 383 (1937). (§101, 105)
T12. Traubenberg, Eckardt and Gebauer, Naturwiss. **21**, 26 (1933). (§92, 100)
T13. Traubenberg, Eckardt and Gebauer, Zeits. f. Physik **80**, 557 (1933). (§100)
T14. Tuve and Hafstad, Phys. Rev. **45**, 651 (1934). (§101)
T15. Tuve and Hafstad, Phys. Rev. **48**, 106 (1935). (§101)
T16. Tuve, Hafstad and Dahl, Phys. Rev. **48**, 315 (1935). (§92)
U1. Urey, Brickwedde and Murphy, Phys. Rev. **40**, 1 (1932). (§101)
U2. Urey and Teal, Rev. Mod. Phys. **7**, 34 (1935). (§101)
V1. Van Atta, Northrup, Van Atta and Van de Graaff, Phys. Rev. **49**, 761 (1936). (§92)
V2. Van Atta, Van de Graaff and Barton, Phys. Rev. **43**, 158 (1933). (§92)
V3. Van de Graaff, Compton and Van Atta, Phys. Rev. **43**, 149 (1933). (§92)
V4. Van de Graaff, Phys. Rev. **38**, 1919 (1931). (§92)
V5. Van Vleck, Phys. Rev. **48**, 367 (1935). (§57)
V6. Van Voorhis, Phys. Rev. **49**, 889 (1936). (§101, 105)
V7. Van Voorhis, Phys. Rev. **50**, 895 (1936). (§101, 105)
V8. Veldkamp and Knol, Physica **4**, 166 (1937). (§102, 105)
W1. Walke, Phys. Rev. **51**, 439 (1937). (§99, 101, 102, 105)
W1a. Walke, Phys. Rev. **51**, 1011 (1937). (§99, 101, 102, 105)
W2. Ward, Wynn-Williams and Cave, Proc. Roy. Soc. **125**, 715 (1929). (§94)
W3. Waring and Chang, Proc. Roy. Soc. **157**, 652 (1936). (§99)
W4. Webster, Proc. Roy. Soc. **136**, 428 (1932). (§99)
W5. Weekes, Livingston and Bethe, Phys. Rev. **49**, 471 (1936). (§58, 102)
W6. Weisskopf and Wigner, Zeits. f. Physik **63**, 54 (1930). (§52)
W7. Weisskopf, Phys. Rev., in press. (§54, 56, 65, 79)
W8. Weizsäcker, Zeits. f. Physik **96**, 431 (1935). (§110)
W9. Weizsäcker, Naturwiss. **24**, 813 (1936). (§87)
W10. Wentzel, Zeits. f. Physik **38**, 518 (1926). (§66)
W11. Wenzel, Zeits. f. physik. Chemie **90**, 754 (1934). (§75)
W12. Wertenstein, Nature **133**, 564 (1934). (§99, 105)
W13. Wheeler, Phys. Rev., to be published shortly, (§73)
W13a. White, Henderson, Henderson and Ridenour, Phys. Rev. **51**, 1012 (1937). (§99)
W14. Whitmer and Pool, Phys. Rev. **47**, 795 (1935). (§104)
W15. Wick, Phys. Rev. **49**, 192 (1936). (§59)
W16. Wigner and Breit, Phys. Rev. **50**, 1191 (1936). (§101)
W17. Wigner, Phys. Rev. **51**, 106 (1937). (§87, 110)
W18. Wigner, Phys. Rev. **51**, 947 (1937). (§105, 110)
W19. Wilson, Phil. Trans. Roy. Soc. **193**, 289 (1913). (§94)
W20. Williams, E. J., Proc. Roy. Soc. **135**, 108 (1932). (§51, 97)
W21. Williams, J. H., and Wells, Phys. Rev. **50**, 187 (1936). (§100)
W21a. Williams, J. H., Wells, Tate and Hill, Phys. Rev. **51**, 434 (1937). (§100)
W21b. Williams, J. H., Shepherd and Haxby, Phys. Rev. **51**, 1011 (1937). (§101)
W21c. Williams, J. H., Shepherd and Haxby, Phys. Rev. **51**, 888 (1937). (§101)
W22. Wright, Proc. Roy. Soc. **137**, 677 (1932). (§72)
W23. Wynn-Williams, Proc. Roy. Soc. **132**, 295 (1931). (§94)
Y1. Yost, D. M., Ridenour and Shinohara, J. Chem. Phys. **3**, 133 (1935). (§101)
Y2. Yost, F. L., Wheeler and Breit, Phys. Rev. **49**, 174 (1936). (§72)
Z1. Zeleny, Brasefield, Bock and Pollard, Phys. Rev. **46**, 318 (1934). (§92, 104)
Z1a. Zahn, Phys. Rev., in press. (§61)
Z2. Zinn and Seeley, Phys. Rev. **50**, 1101 (1936). (§92, 101)
Z3. Zyw, Nature **134**, 64 (1934). (§99, 105)

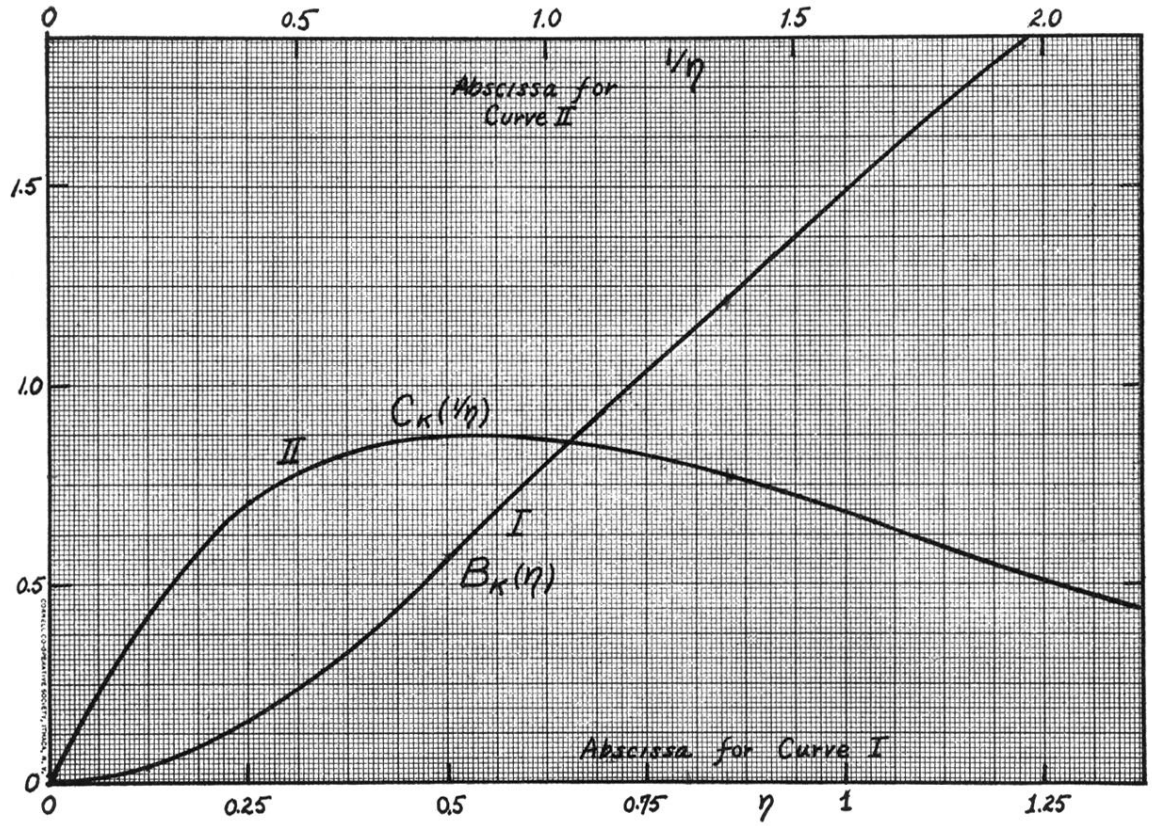

FIG. 28. Curve I: Contribution B_K of the K shell to the "stopping number" B (cf. (749a)). Abscissa: η = (velocity of the incident particle/velocity of a K electron)^2 = (electron mass × energy of the incident particle)/(particle mass × "ideal" ionization potential Z^2 Ry of the K shell). Curve II: Correction C_K to the high energy stopping number for K electrons against $1/\eta$. From C_K, the stopping number of K electrons can be obtained using (756), or the stopping number of the complete atom from (758).

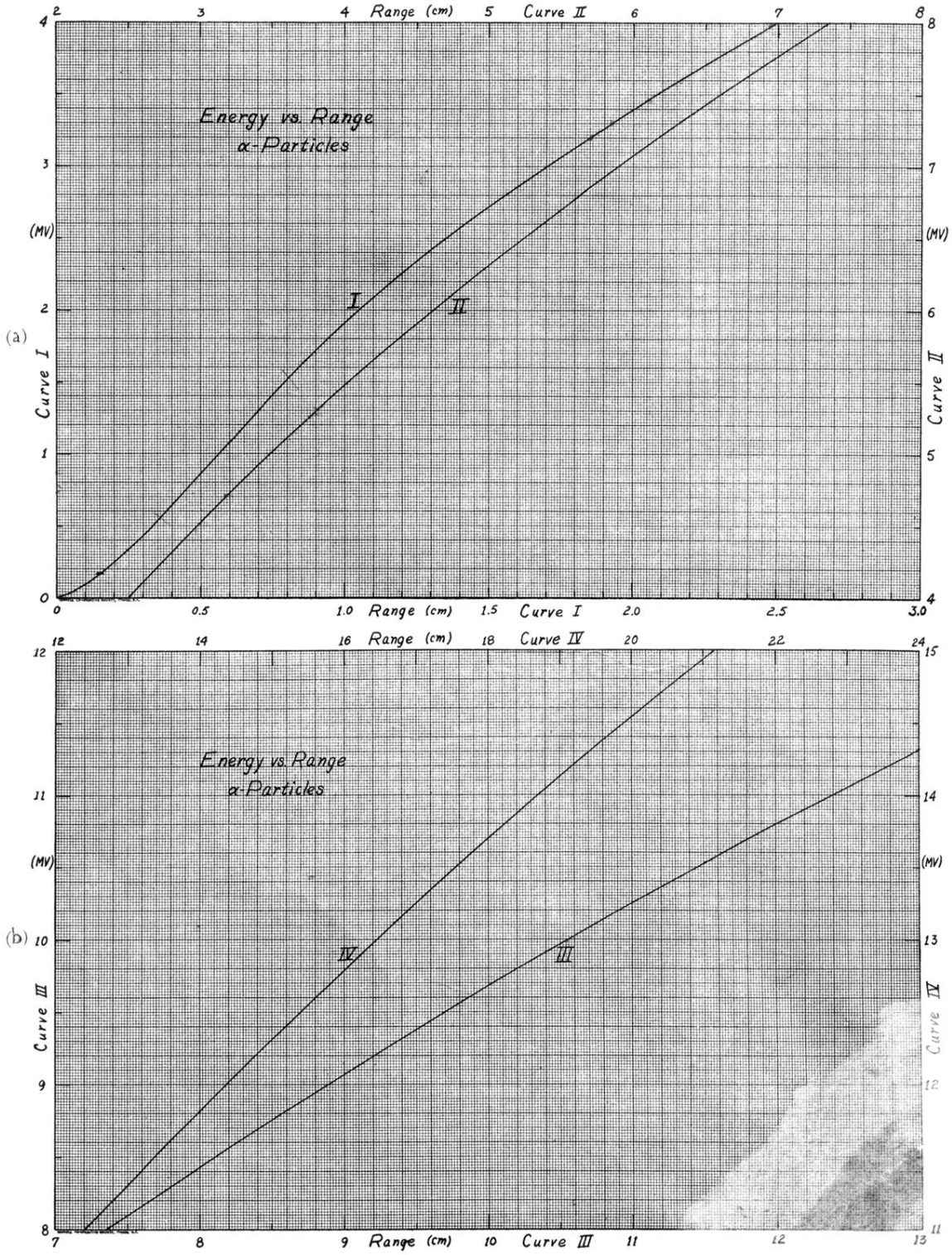

FIG. 29. Range-energy relation for α-particles. Abscissa: Range in air of 15°C and 760 mm pressure in cm. Ordinate: Energy in MV. (a) From 0 to 8 MV. (b) From 8 to 15 MV.

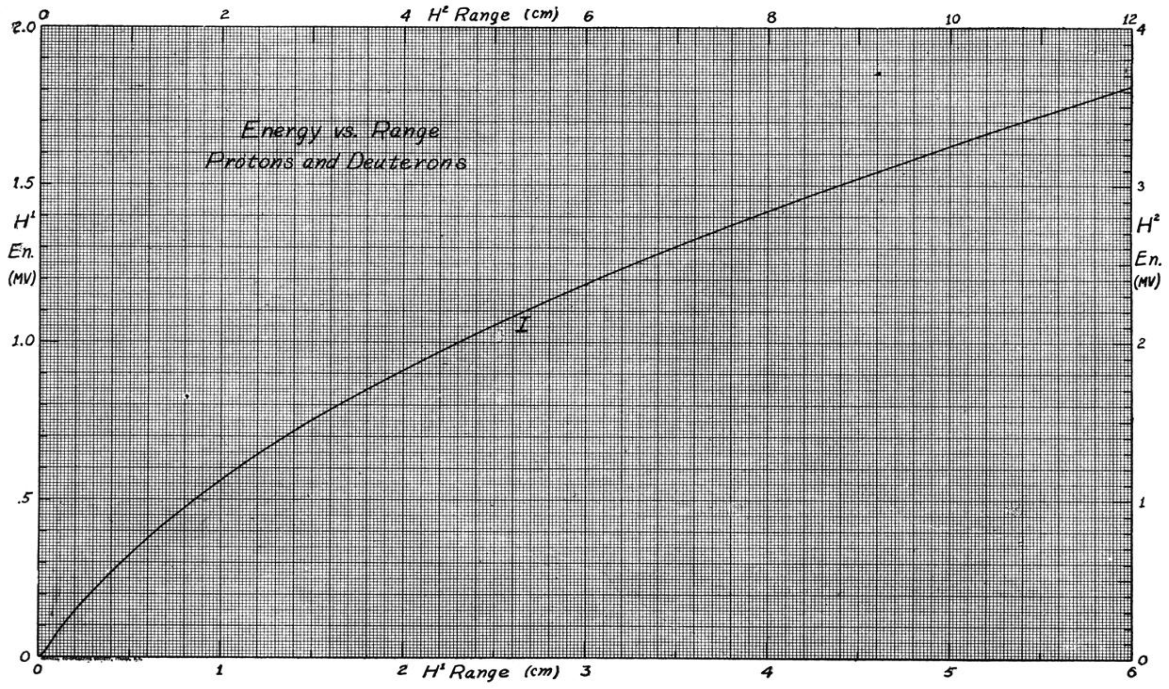

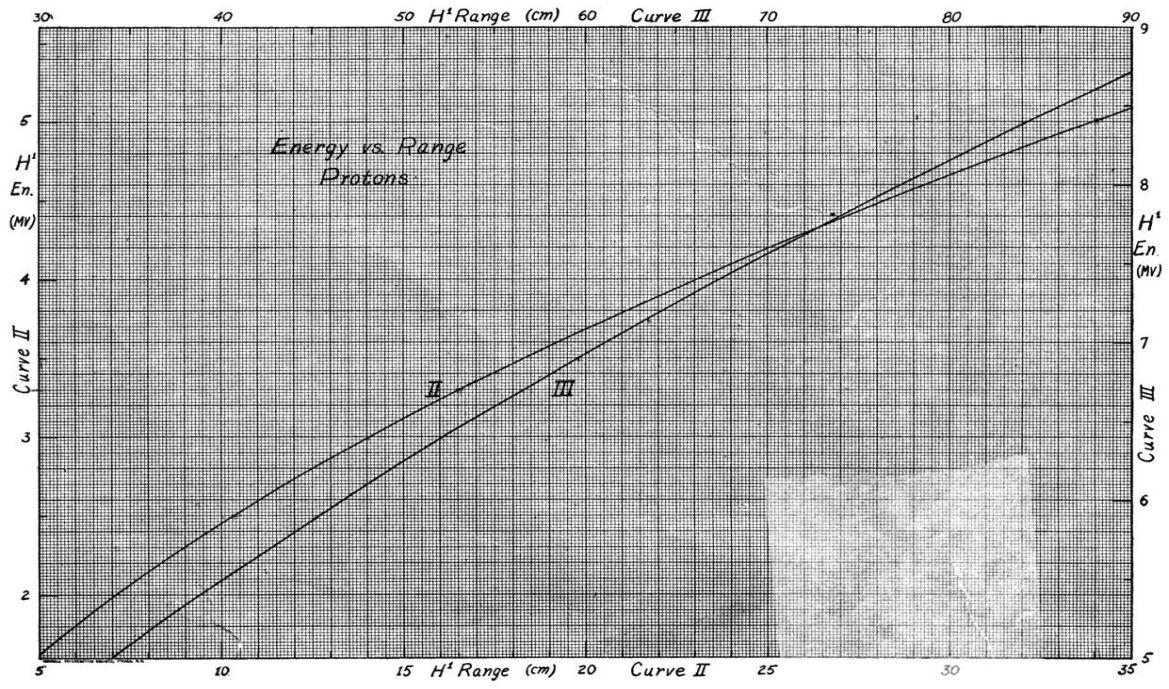

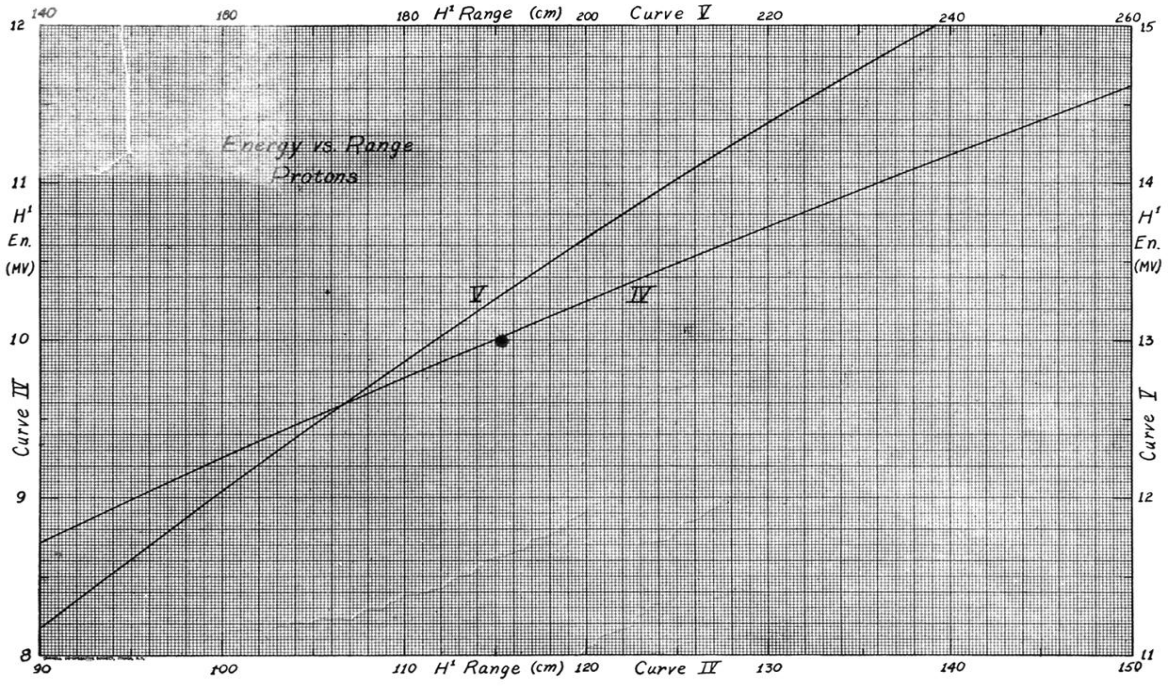

FIG. 30. (a) (b) (page 268) (c) (above) Range-energy relation for protons. (For deuterons, the ranges and the energies should be multiplied by 2.)

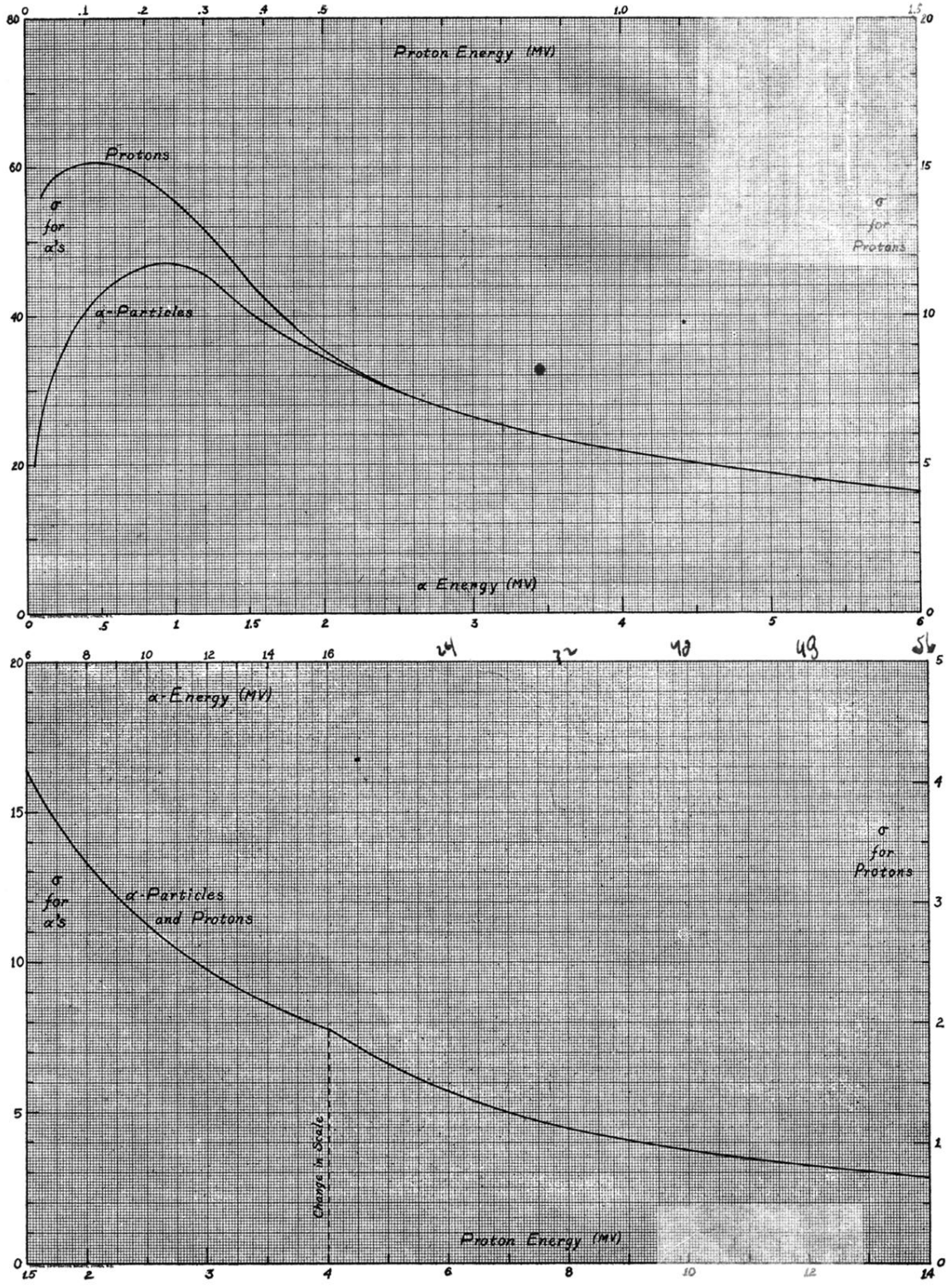

FIG. 31. Cross section for energy loss in 10^{-15} cm^2 volt. Scale for α-particles on left, for protons on right hand side. Abscissa: energy (different scale for protons and α-particles!). (a) (top) Up to 1.5 MV proton (6 MV alpha) energy. (b) (lower) From 1.5 to 14 MV proton energy, with a break of scale at 4 MV.

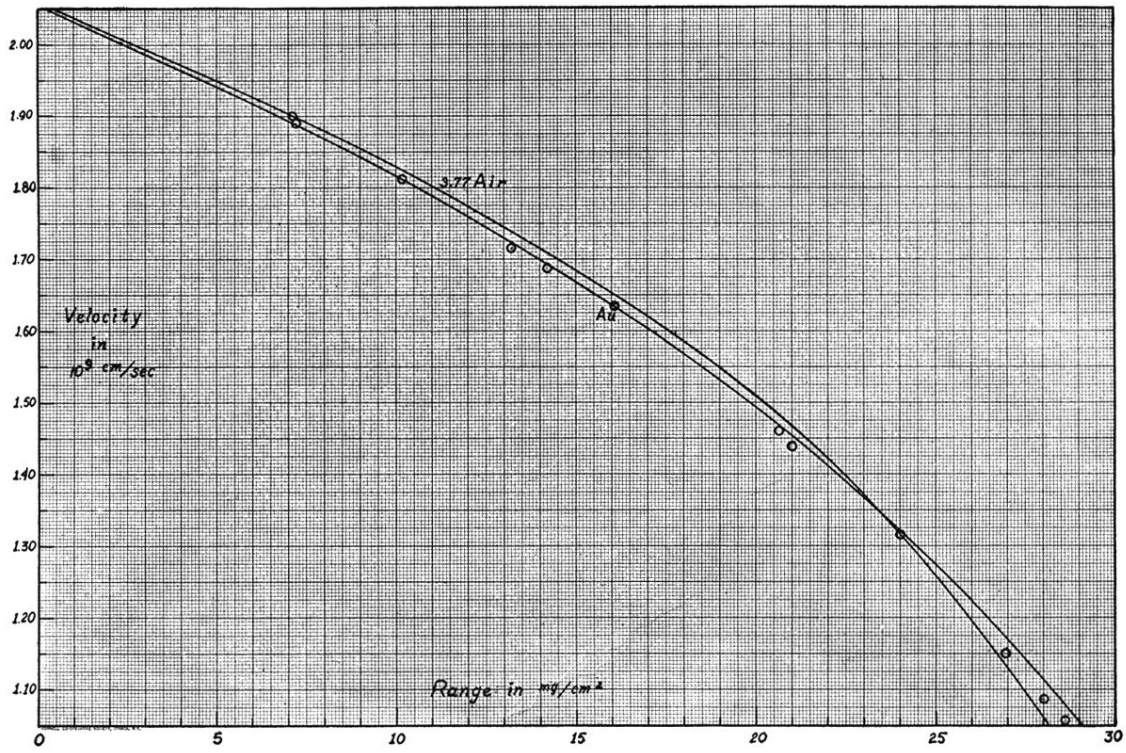

FIG. 32. Range-velocity relation of gold. Abscissa: thickness of gold absorber in mg/cm². Ordinate: velocity of α-particles in 10^9 cm/sec. The curve marked "Au" gives the theoretical range-velocity relation for Au. The curve marked "3.77 air" is computed assuming that 3.77 mg/cm² of Au are equivalent to 1 cm of air. The circles represent experimental points of Rosenblum. They fall closely on the Au curve except at the end where the N electrons of the Au will cease to follow the elementary theory of stopping. The figure shows the variation with velocity of the stopping power of gold relative to air.

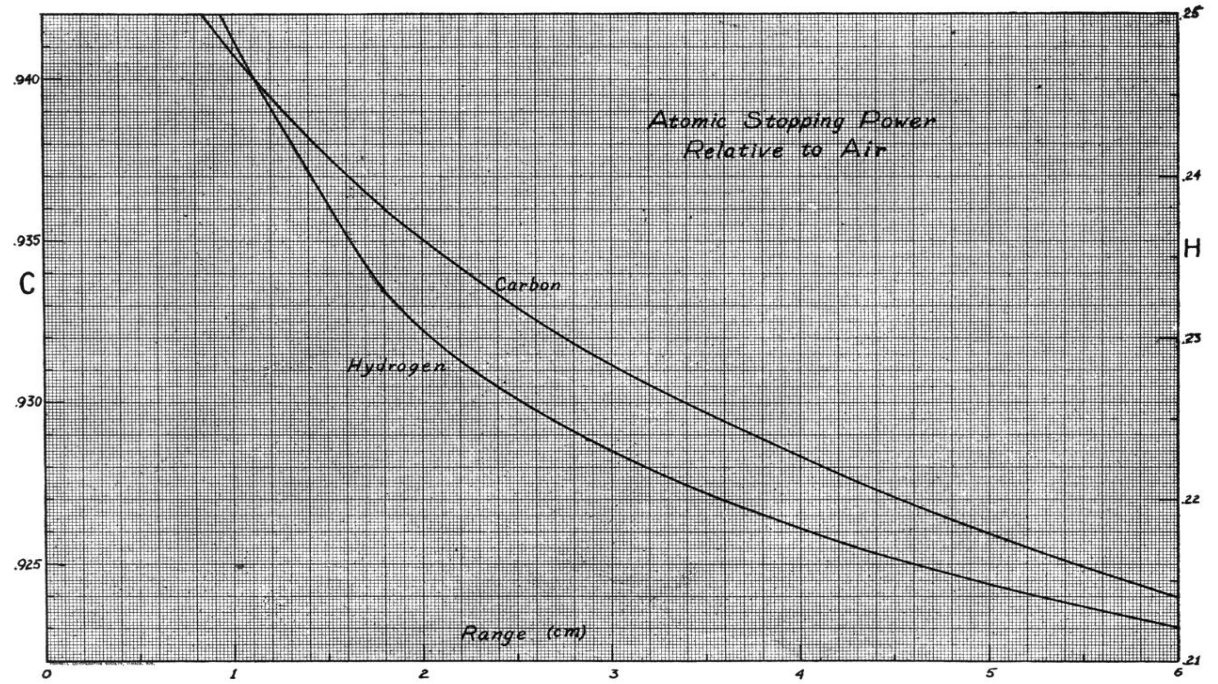

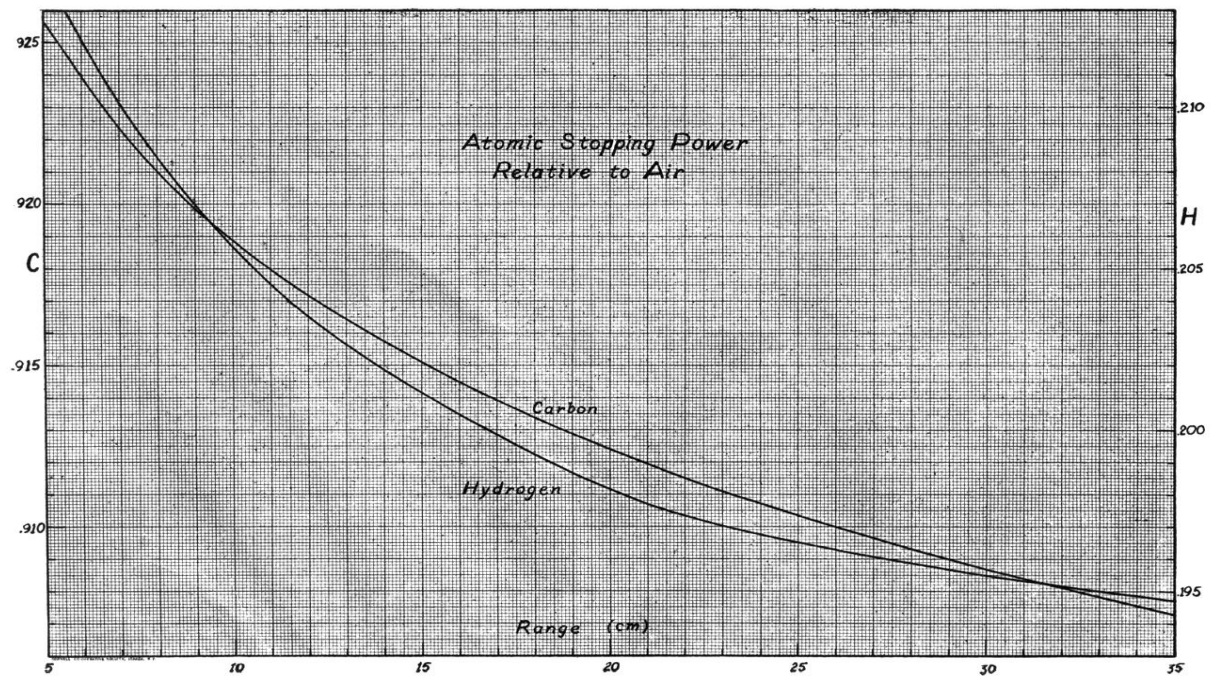

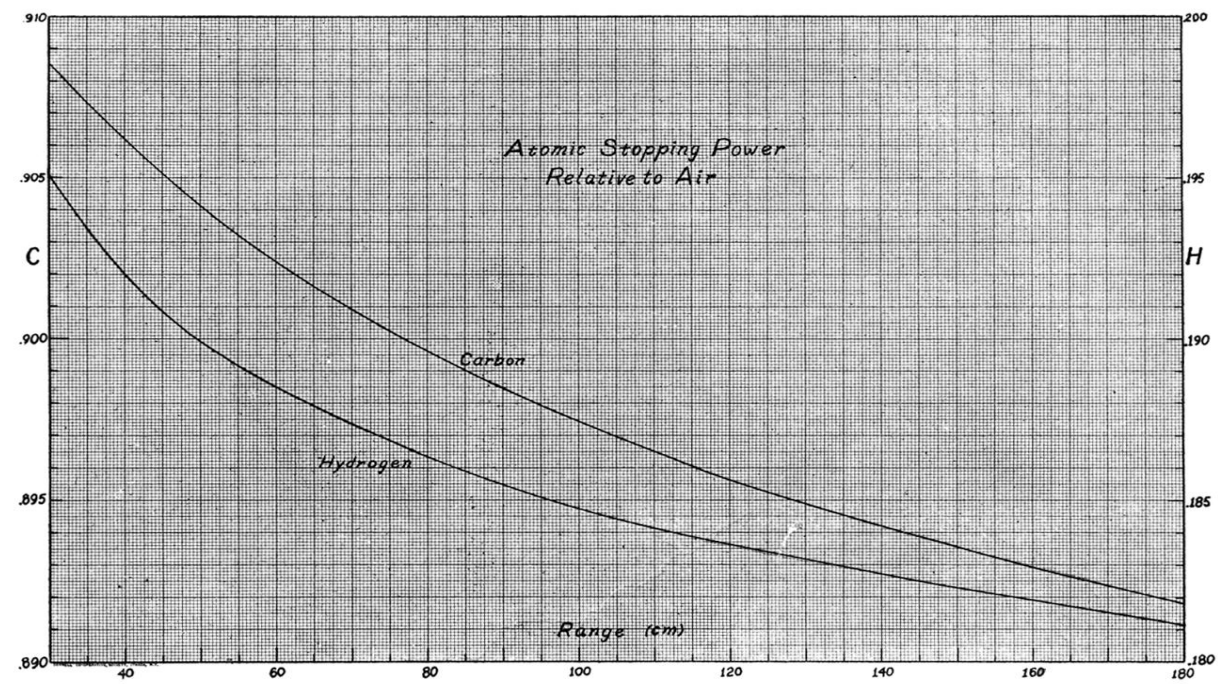

FIG. 33. (a) (b) (page 274) (c) (above) Stopping power of carbon and hydrogen. Abscissa: Range of particles in air. Ordinate: stopping power per atom relative to air. The curve is intended for the evaluation of experiments with hydrogen or methane filled cloud chambers. It is valid for α-particles and protons.

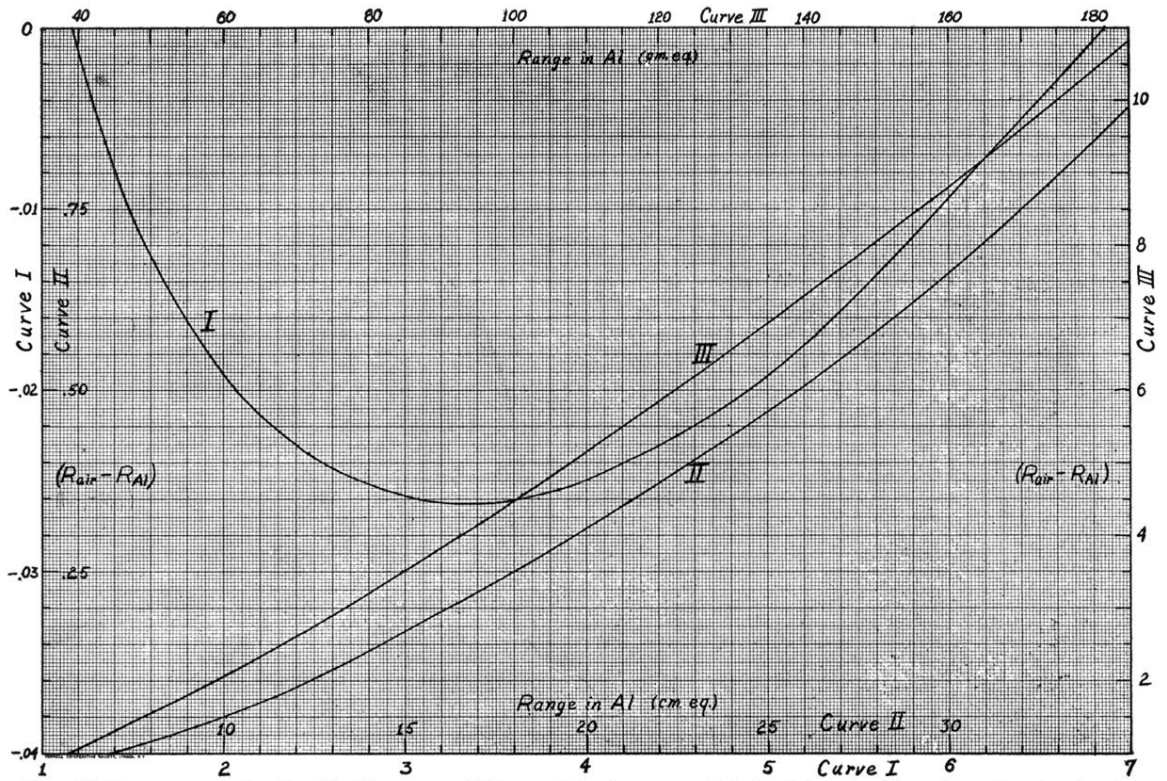

FIG. 34. Range correction for Al. The range of the particles is supposed to be determined by absorption in aluminum foils whose air equivalent has been measured beforehand using natural α-particles for calibration or using a suitable conversion factor (e.g., 1.52 mg/cm^2 Al = 1 cm air). For any value of the equivalent range in air thus obtained (abscissa), the curve gives the correction to be applied for the variation of the stopping power of Al with velocity (ordinate). For mica, one-half the correction should be applied. Curve valid for protons and α-particles.

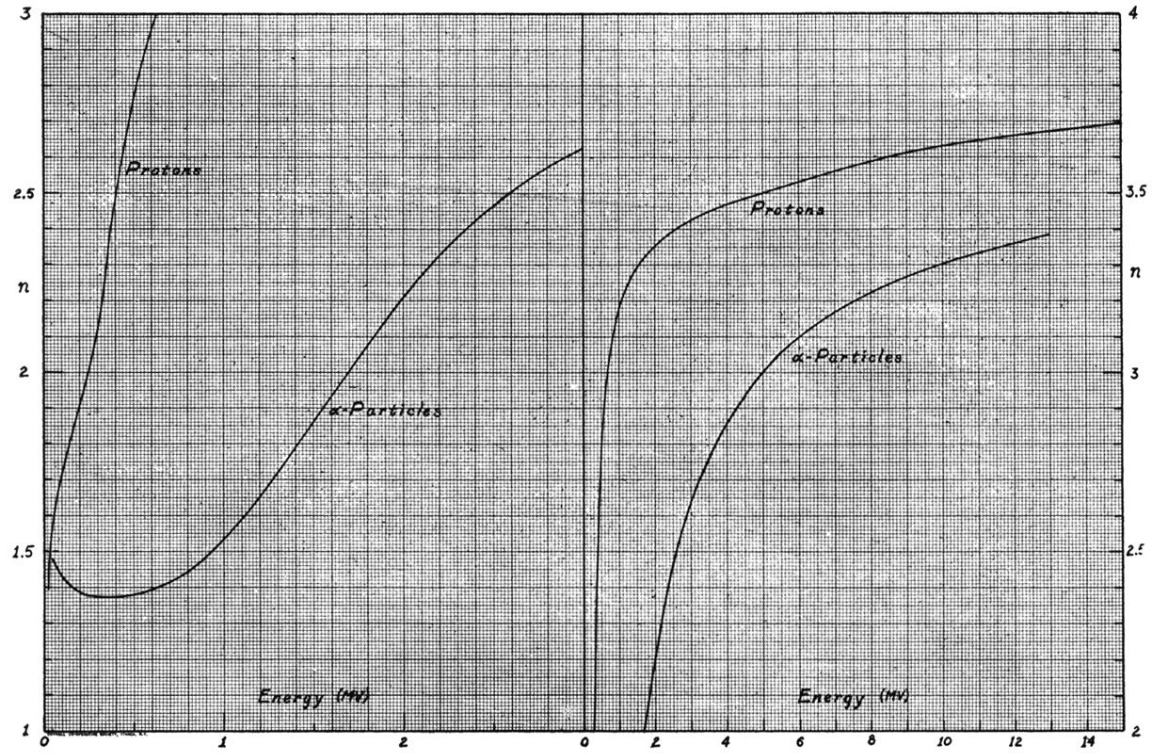

FIG. 35. Range exponent n for protons and α-particles. Over small regions, the range is proportional to the nth power of the velocity. Analytical definition: $n = 2\ d \log R/d \log E$. The large deviations from Geiger's law ($n = 3$) are apparent. The range exponent is important for thick target correction, angular straggling etc. (§§ 96, 97.)